VIRUSES IN CORAL REEF SPONGES

Thesis submitted by Cecília Pascelli Sant'Ana Santos in October 2019

for the degree of Doctor of Philosophy

College of Science and Engineering

James Cook University, Townsville, Queensland

THESIS DECLARATION

This thesis has been substantially accomplished during enrolment in this degree.

This thesis does not contain material which has been submitted for the award of any other degree or diploma in my name, in any university or other tertiary institution.

In the future, no part of this thesis will be used in a submission in my name, for any other degree or diploma in any university or other tertiary institution without the prior approval of James Cook University and where applicable, any partner institution responsible for the joint-award of this degree.

This thesis does not contain any material previously published or written by another person, except where due reference has been made in the text and, where relevant, in the Authorship Declaration that follows.

This thesis does not violate or infringe any copyright, trademark, patent, or other rights whatsoever of any person.

This thesis contains published work and/or work prepared for publication, some of which has been co-authored.

18/02/2020

STATEMENT OF CONTRIBUTION OF OTHERS

Assistance	Contribution	Contributor
Intellectual support	Writing and editing	Nicole Webster Patrick Laffy Marcus Sheaves
	Statistical support	Murray Logan Guilherme Longo
Financial support	Stipend	CAPES AIMS@JCU
	Research	AIMS@JCU Australian Research Council Future Fellowship FT120100480
	Travel	AIMS@JCU
Research assistance	Field work	Holly Bennett Muhammad Azmi Abdul Wahab Blake Ramsby Marija Kupresanin
	Lab work	Emmanuele Botté Marija Kupresanin Pedro Frade Merle Schlawinsky

AUTHORSHIP DECLARATION OF PUBLISHED OR PREPARED FOR PUBLICATION THESIS CHAPTERS

This thesis contains published work and/or work prepared for publication, some of which has been co-authored.

Thesis title: Viruses in coral reef sponges **Name of the Candidate:** Cecília Pascelli Sant'Ana Santos			
Chapter	**Publication / under review / in preparation for publication reference**	**Intellectual input of each author**	**I confirm the candidate's contribution to this paper and consent to the inclusion of the paper in this thesis**
2	Pascelli, C., Laffy, P. W., Kupresanin, M., Ravasi, T. and Webster, N. S. (2018). Morphological characterization of virus-like particles in coral reef sponges. *PeerJ* 6:e5625 https://doi.org/10.7717/peerj.5625	C.P., N.W. and P.L. designed the study. C.P. and M.K collected the data, C.P. analysed the data. C.P. wrote the manuscript with significant contributions from N.W., P.L., T.R. and M.K.	Nicole Webster Signature: Patrick Laffy Signature:
3	Pascelli, C., Laffy, P. W., Webster, N. S., Botté, E., Kupresanin, M., Rattei, Thomas, Lurgi, M., Ravasi, T. Webster, N. S. Under review in *Microbiome*.	C.P., N.W. and P.L. designed the study. C.P. and M.K collected the samples. C.P. undertook the	Nicole Webster Signature: Patrick Laffy

		laboratory work. C.P. and P.L. processed the sequence data. C.P., P.L., N.W. and M.L. analysed the results. C.P. wrote the manuscript with significant contributions from N.W., P.L., E.B., M.L., M.K, T.Rattei. and T.Ravasi.	Signature:
4	Pascelli, C., Laffy, P. W., Schlawinsky, M., Webster, N. S. The impacts of thermal stress on the virome of the marine sponge *Carteriospongia foliascens.* In preparation for publication.	C.P., N.W. and P.L. planed the experiment. C.P. and M.S. performed the experiment. C.P. and P.L. analysed the data, C.P., wrote the manuscript with significant contributions from N.W and P.L.	Nicole Webster Signature: Patrick Laffy Signature:

ACKNOWLEDGEMENTS

It is with immense gratitude that I acknowledge the support of my supervisors Dr. Nicole Webster, Dr. Patrick Laffy and Dr. Marcus Sheaves, thank you for being always helpful. Nicole, thank you for giving me this amazing opportunity to investigate viruses in sponges, for always keeping faith on my work and for your kind words in difficult times. Patrick, thank you for the countless explanations on bioinformatics and for being so thorough in your comments, I have learned so much with you. Marcus, thank you for always being present whenever I needed your help, for your great advises and positive words.

I thank CAPES foundation for creating a life opportunity for thousands of Brazilian students through Science Without Borders and for funding my PhD at James Cook University.

I thank the support for AIMS@JCU, Lauren, Melanie you are amazing professionals and persons that have inspired and encouraged me so much. Libby, I would never thank you enough for everything you have done for me. For being so understanding, kind and for fighting hard so I could keep working on my thesis with dignity and perseverance. You make the difference in this world.

I thank my collaborators, Dr. Thomas Rattei, Miguel Lurgi, Timothy Ravasi for contributing with my work. Thank you Marija Kupresanin for the lab and field assistance in KAUST and for your friendship.

It was an honour to work with the best professionals at AIMS. Mannue, this thesis wouldn't be possible without your impar lab training. Brett, Sara, Jason, thank you for your help in PC2 lab. All the amazing people at SeaSim for your prompt assistance during my experiments. Robert, Emerson, Peter, thank you for all the advises and for the pleasant lunch company. All the great front desk and IT team, the AIMS canteen and cleaning staff, you are amazing! Merle, thank you for saving my last chapter with your lab assistance and your great company! To all the sponge team, it was a true pleasure sharing my days with you at AIMS!

To all my friends that helped me in the field, in the lab, with the writing and giving me love and emotional support. Thank you Catia, you are an angel that saved me when I needed most.

Thank you, Pedro, for all your help with my work and for being an amazing friend. Ellie, my adorable sister, no words to thank all your love and care during these years in Townsville. Paul, Jose, best housemates ever!

I owe my deepest gratitude to my parents and sister for your unconditional love and support. My amazing partner who taught me so much during these years, for supporting me in difficult times and for sharing with me the great joy of being Kai's parents. Finally, I thank you my beautiful son Kai, for raising love to a new level, making my life brighter and happier. I love you!

GENERAL ABSTRACT

Sponges constitute a diverse and functionally important element of coral reef systems. They are holobionts hosting a diverse array of macro and micro symbionts. The high symbiotic complexity in sponges makes them an ideal model for studying host-viral interactions. Viruses are ubiquitous entities that regulate diverse biological processes in marine ecosystems. Despite their high abundance and ecological relevance, there is limited knowledge about the role of viruses in sponges. The aim of this thesis was to understand the impact and function of viruses in coral reef sponge holobionts. Specifically, the objectives of this thesis were to 1) morphologically characterize viral-like particles (VLPs) associated with coral reef sponges, 2) assess the diversity and function of viruses inhabiting sponge species from two coral reef ecosystems, the Great Barrier Reef (GBR, Australia) and the Red Sea (RS, Saudi Arabia), 3) assess how host-specific factors (microbial abundance, presence of photosymbionts, sponge morphology and geographic location) correlated with viral community composition and function, and 4) investigate how the virome of a phototrophic sponge responded to heat-stress.

Viruses are ubiquitous in marine holobionts, and until recently there had only been a single visualization of VLPs in sponges and this occurred over 40 years ago. Chapter 2 of this thesis represents the first comprehensive visualisation of VLPs in sponges, showing that coral reef sponges associate with a diverse array of VLPs, dominated by bacteriophages. Amongst the eight GBR and seven RS sponge species investigated, 50 different VLP morphologies were visualized within sponge cells, extracellular mesohyl matrices, ectoderm and within/on sponge-associated microbes. The findings from this chapter confirmed that sponges harbour diverse communities of viruses, which interact with both prokaryotic and eukaryotic components of the sponge holobiont.

Viruses have been proposed to play key roles in modulating the microbial community of marine holobionts, contributing to the host ecology through viral encoded auxiliary metabolic genes (AMGs). Chapter 3 of this thesis addresses some of the knowledge gaps regarding the roles of viruses in sponge holobionts, investigating whether the sponge viromes are influenced by the host strategy for microbial symbiosis or whether sponge-viral communities and functions respond to geographic variation. Metaviromic sequencing of 15 representative sponge species from the GBR and RS coral reefs established that the sponge metaviromic community and functional profiles are influenced by the following factors: host species

specificity, site specificity, host sponge microbial abundance and the presence of photosymbionts within the host sponge. The metaviromic approach reinforced the TEM results, showing that the sponge virome is dominated by bacteriophages of the order Caudovirales, but also contain representatives from the nucleocytoplasmic large DNA virus families. This chapter also revealed that sponge-viral functional profiles had several AMGs, including those associated with herbicide resistance, heavy metal resistance and nylon degradation which may provide competitive advantage for the host environmental acclimatisation.

Future climate scenarios are forecast to shift the community structure of coral reefs. In this context, sponges have been proposed as potential 'winners', since several species are more tolerant than reef building corals to climate change related stressors, including ocean warming (OW). The role of viruses in the thermal tolerance of sponges is poorly understood. In order to address this knowledge gap, a heat-stress experiment was conducted on *Carteriospongia foliascens* to assess sponge-viral responses to short (3 days) and long (21 days) term heat-stress (31 °C, representing a sub-lethal/stress temperature for *C. foliascens*). Metaviromic analysis revealed that the viral community of *C. foliascens* is influenced by elevated seawater temperature. Specifically, after 21 days exposure to 31 °C an increase in *Inovirus* was detected, correlating with bleaching of *C. foliascens.* Functional differences between control and heat stressed sponges included a reduction in genes associated with heavy metal resistance and an increase of virulence-related genes in the viral communities of sponges exposed to 31 °C. These results indicate that viral infections may play a role in *C. foliascens* thermal sensitivity, particularly in sponges displaying a phenotypic bleaching response.

This thesis has shown that viruses are diverse and ubiquitous components of sponge holobionts, are host-species and site-specific, correlating with the associated microbial communities and respond to changes in ambient environmental conditions. This thesis also revealed that coral reef sponge viruses carry AMGs, including those associated with herbicide resistance, heavy metal resistance, nylon degradation and antimicrobial activity, all of which may assist the sponge host or associated microbiome in acclimatizing to its surrounding environment.

TABLE OF CONTENTS

LIST OF FIGURES

LIST OF TABLES

SUPPLEMENTARY TABLE LINKS

Supplementary Table 3.1 available in https://tinyurl.com/y3q9uu8b

Supplementary Table 3.2 available in https://tinyurl.com/y2cc2yox

Supplementary Table 3.3 available in https://tinyurl.com/y6rnmc5m

Supplementary Table 4.1 available in https://tinyurl.com/yy7fubz3

Supplementary Table 4.2 available in https://preview.tinyurl.com/y4jzwk44

Chapter 1. GENERAL INTRODUCTION

1.1. CORAL REEF ECOSYSTEMS

Coral reefs are among the most diverse ecosystems on Earth and although their area is less than 0.2 % of the worlds ocean, they are home to 35 % of the all marine species (Reaka-Kudla, 2005). These marine ecosystems are ecologically, culturally and economically relevant, being an important source of goods and services (Hoegh-Guldberg, 2011) representing a value over 350,000 US$ ha^{-1} $year^{-1}$ (Glynn & Ault, 2000). Furthermore, the Great Barrier Reef is valued at $56 billion as an Australian economic, social an iconic asset, contributing with over 64,000 direct and indirect jobs (O'Mahony et al., 2017). Coral reefs also play key roles in oceanic nutrients cycling (Rädecker et al., 2015), atmospheric gas fixing (Wiebe, Johannes & Webb, 1975) and provide shelter for millions of marine species (Moran & Reaka, 1988). There is an increasing concern of coral reefs declining due to overexploitation, habitat destruction, impacts of pollutants and anthropogenic climate change (Hughes, 2003). Over recent years, several studies have been carried out whose goals were to understand the functioning of coral reefs, investigating the ecological roles of macro and microscopic communities (Webster & Reusch, 2017; Stuart-Smith et al., 2018; Weynberg, 2018) in an effort to identify new management and restoration strategies which may mitigate the impacts of these stressors on these important ecosystems.

Sponges constitute an abundant and functionally important component of coral reef system (Diaz & Rützler, 2001; Bell, 2008). They can be found in distinct habitats, including intertidal zones, shallow, mesophotic and deep reefs (Roberts & Davis, 1996; Barnes, 1999; Olson & Mccarthy, 2005) and are often resistant to extreme conditions of temperature, salinity, current, radiation and pollutants (Richelle-Maurer et al., 1994; Barnes, 1999; Taylor et al., 2007a). Additionally, it has been demonstrated that several sponge species are more tolerant than corals to climate change impacts and have been proposed as potential "winners" in future coral reefs scenarios (Bell et al., 2018). Several sponge biological functions, including nutrition, defence and development, can be partially attributed to their associated microorganisms (Richelle-Maurer et al., 1994; Shieh & Lin, 1994; Walters & Pawlik, 2005; Taylor et al., 2007a; Webster & Taylor, 2012), which may influence the way sponges respond to environmental shifts. The roles prokaryotes play in marine sponges have been extensively

studied (Thomas et al., 2010; Webster & Thomas, 2016; Lurgi et al., 2019), however, there is still a big knowledge gap on the roles of viruses within marine sponges. Describing the sponge-viral association in coral reefs is the core of this thesis, which adds to what is known about viruses in coral reef organisms and characterises how viruses contribute to the sponge response to environmental disturbances.

1.2. CORAL REEF SPONGES

Sponges (phylum Porifera) are conspicuous and biodiverse members of marine benthic communities (Rützler, 2001) and the most primitive extant metazoan group, comprising approximately of 8500 known species (Van Soest et al. 2012). Sponges perform many ecological roles that structure biological communities from polar to tropical regions, in both shallow and deep waters (Bell, 2008; Van Soest et al., 2012). Most sponge species are suspension filter feeders with a complex aquiferous system composed of channels and chambers that enable the filtration of large volumes of seawater (Figure 1.1.), in some instances, sponge species can filter more than a thousand times their own volume per day (Patterson et al., 1997). A unidirectional (ostia-chamber-atrium-oscula) water flow is driven by flagellated choanocyte cells that are also responsible for capturing and retaining small particles (<0.1 µm) with high efficiency (Thomassen & Riisgård, 1995). In a study investigating the role of sponges in coral reef nutrients cycling, de Goeij and colleagues (2013) suggested that sponges can make dissolved organic matter available to other reef species via rapid cellular turnover and expulsion of detritus, in a process termed the “sponge-loop”. While this flux of energy and nutrients has been experimentally demonstrated, the mechanisms of the rapid cell turnover have not been clarified, although it was suggested that sponge symbionts play a role in this process. These filter feeders are also notable for their remarkable efficiency in removing microbial and viral particles from seawater (Hadas et al., 2006). In addition to digesting and metabolizing seawater filtrate, sponges also incorporate foreign organisms in their structure and harbor a diverse community of microbial symbionts, and are usually defined as ‘holobionts’.

The term ‘holobiont’ was coined in 1993 by the scientist Lynn Margulis to define the entire organism comprised of various *bionts* living in symbiogenesis (Margulis, 1981). Holobiont has been commonly used to refer to coral reef organisms, including marine sponges, since they

often host a wide diversity and abundance of Bacteria, Archaea and unicellular Eukaryotes in their mesohyl (collagenous matrix within the sponge). These microorganisms can comprise up to half of the sponge biomass (Cuvelier et al., 2014), and play a variety of roles in marine sponges with established symbiotic relationships ranging from mutualism to commensalism and parasitism (Webster & Taylor, 2012). Among those interactions, nutritional functions, such as contributions by nitrogen-fixing bacteria and autotrophic symbionts (Wilkinson & Fay, 1979; Shieh & Lin, 1994), are particularly important. It is estimated that 80% of intertidal sponge species benefit nutritionally from compounds produced directly by photosynthetic symbionts (Steindler, Beer & Ilan, 2002). In addition, sponge symbionts provide UV protection, protein recycling and production of photosynthates (Wilkinson, 1980; Arillo et al., 1993; Steindler, Beer & Ilan, 2002; Yahel et al., 2003; Taylor et al., 2007a). Sponges also rely on microbes for production of secondary metabolites, often used in defence mechanisms against predation and competition pressure (Walters & Pawlik, 2005), and have hence been a major focus of bioactivity studies (Taylor et al., 2007a; Perdicaris, Vlachogianni & Valavanidis, 2013). Symbiotic relationships are so intrinsically linked that it has been suggested the holobiont genomic repertoire (or hologenome) is a unit of natural selection and evolution (Rosenberg et al., 2007). The intimacy of sponge-microbial relations is also reflected in their life strategies, where sponges with microbial densities 2–4 orders of magnitude greater than that of surrounding seawater are referred to as 'high-microbial abundance (HMA) sponges', whereas those with microbial densities similar to seawater as 'low-microbial abundance (LMA) sponges' (Wilkinson, 1978; Hentschel, Usher & Taylor, 2006).

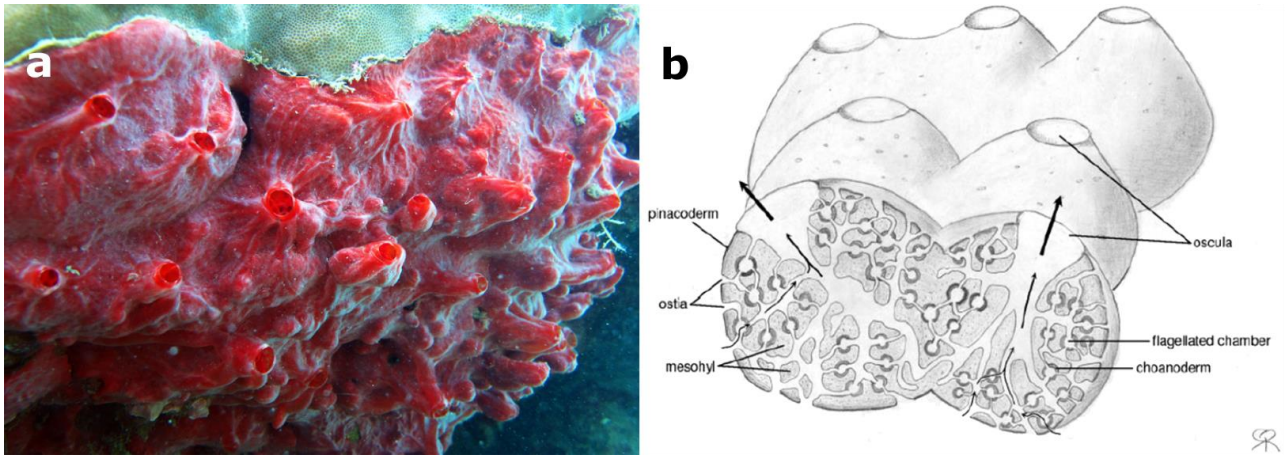

Figure 1.1 (a) Photo and (b; adapted from Taylor et al 2007) schematic representation of a Demospongiae. Arrows indicate water direction inside the sponge.

Despite the dedicated effort to determine the ecological role that microorganisms play within marine sponges, there is a substantial knowledge gap with respect to the interaction of sponges with viruses; the most abundant biological agents in marine ecosystems.

1.3. VIRUSES IN MARINE ECOSYSTEMS

Just over 70 years ago, viruses were acknowledged as natural components of aquatic ecosystems (Kriss & Rukina, 1947), but it wasn't until the early 90's that their widespread impact was understood, once their high abundancy and key roles in structuring marine planktonic communities was revealed (Borsheim, Bratbak & Heldal, 1990; Fuhrman & Suttle, 1993; Proctor, 1997). From that time, studies in this field have attempted to characterize marine viral diversity, distribution and interactions with a targeted focus on oceanic seawater (e.g., Jover et al. 2014; Danovaro et al. 2008; Gregory et al. 2019). Viruses are the most abundant biological entities in marine environments, with up to 10^{10} viruses per l^{-1} of seawater and 10^{10} per g^{-1} dry weight of marine sediment (Monier et al. 2008; Danovaro et al. 2011). Marine virus communities are notably diverse, with over 195,728 known viral populations (Gregory et al., 2019). Viruses are small (20-100 nm) intracellular obligate parasites, consisting of DNA or RNA based genetic material (both single or double stranded), and surrounded by a protein coat (Gelderblom, 1996). Viruses do not self-propel, respire or grow outside a host environment and to survive, they must infect a host cell (Fuhrman, 1999; Wommack & Colwell, 2000; Danovaro et al., 2008; Rohwer & Thurber, 2009; Breitbart et al.,

2018). They have several infection strategies (Roberts & Compans, 1998; Steward, Culley & Wood-Charlson, 2013) including: lytic, chronic and lysogenic life stages (Howard-Varona et al., 2017). In the lytic cycle, viruses inject the nucleic acid into a host's cell, taking over regular cellular processing, and prioritising the production of numerous virions (infectious particles produced inside the host) that are released upon the bursting of host cells. In the chronic life cycle, produced viral copies are extruded from the cell by a non-lethal exclusion. In the lysogenic cycle, the viral nucleic acid stays inside the host cell and reproduces as genetic material during normal cell division processes, without releasing virions. Eventually, either spontaneously or trigged by environmental shifts, lysogenic viruses can switch to a lytic or chronic phase, releasing virions (Hobbs & Abedon, 2016). Moreover, viruses can remain in a free virion state (i.e., not associated with a host cell) (Allers et al., 2013) and drift across ecosystems with notable stability for extended periods (Pirtle & Beran, 1991).

Viruses play several important roles in marine ecosystems affecting: biogeochemical cycles, microbial community composition, horizontal gene transfer between cells and metabolic reprogramming of the host. Viral infections are responsible for the death of 20% of total marine microbial biomass each day (Suttle, 2007), converting and trapping the biomass into particulate and dissolved organic carbon, and inorganic nutrients in a process called the 'viral shunt'. This process is responsible for cycling these organic and inorganic nutrients, making this matter available to other organisms (Middelboe & Lyck, 2002; Suttle, 2005; Shelford et al., 2012). Thus, viruses are key organisms in the microbial loop, directly affecting the flux of matter and energy in marine food webs (Azam, Fenchel & Field, 1983; Bratbak, Thingstad & Heldal, 1994). In marine oligotrophic ecosystems, such as coral reefs, this process is particularly relevant, as a major source of organic compounds (Dell'Anno, Corinaldesi & Danovaro, 2015; Thurber et al., 2017). In addition, this viral-induced mortality can be selective, thereby determining host community composition and acting as an important bottom-up ecological driver of microbial community composition (Bouvier & Del Giorgio, 2007; Hewson & Fuhrman, 2007). An example of how viruses can manipulate microbial community composition was presented by Lehahn and colleagues (2014) showing that viruses likely regulate algal blooms by infecting coccolithophore cells, highlighting the environmental relevance of viruses as mortality agents (Lehahn et al., 2014).

Another role of viruses is their capacity to reprogram the metabolism of their host by the introduction of viral-encoded auxiliary metabolic genes (AMGs) (Jiang & Paul, 1998; Hurwitz, Brum & Sullivan, 2015). The acquisition of genes from their hosts can influence the way host genes are expressed, modifying the host metabolism, often redirecting the host energy and resources to optimise viral production (Thompson et al., 2011). For instance, it has been suggested that 'Bacterial-like' genes found in cyanophages, produce the energy needed for cyanophage DNA replication (Lindell et al., 2007). Nevertheless, it has been proposed that the combination of viral and host genes during infection may concomitantly benefits the hosts by boosting its metabolism (Breitbart et al., 2007; Paul, 2008; Rosario & Breitbart, 2011; Crummett et al., 2016). For example, it has been suggested that phages (ie. microbe-infecting viruses) that infect *Synechococcus* and *Prochlorococcus* bacteria can help to maintain the host's photosynthetic activity during infection through genes coding for photosystem proteins (psbA, hliP) (Lindell et al., 2004; Sullivan et al., 2005). Likewise, 34 microbial gene families encoding different energy metabolism pathways (such as electron transport, photosystem and carbohydrate metabolism genes) were detected within the 452 viral Global Ocean Survey assembled viral genomic scaffolds, suggesting that marine phages can influence their host fitness by translation and post-translation control (Sharon et al., 2011). Another comprehensive study on global ocean viromes (viral genome) identified 243 viral-encoded AMGs, revealing that viruses may manipulate nitrogen and sulfur cycling in the epipelagic ocean (Roux et al., 2016). In lysogenic cells, the expression of viral genes have shown to promote host fitness, enabling antibiotic resistance, toxin production and immunity responses (Williamson, McLaughlin & Paul, 2001; Howard-Varona et al., 2017; Tsao et al., 2018). Thus, most of the suggestions of the viral impact on host metabolism still lack validation through experimental studies (Warwick-Dugdale et al., 2019).

Viruses are found everywhere, and a recent study divided viral communities into five ecological zones (Arctic, Antarctic, temperate and tropical epipelagic (1-150 m), mesopelagic (150-1000 m), and bathypelagic (>2000 m)), each forming a discrete genotypic cluster, with tropical surface waters being a hotspot of viral diversity (Gregory et al., 2019). It has also been demonstrated that viral and microbial distribution cluster together , suggesting that physicochemical structuring of marine microbial communities is the main factor structuring marine viral communities (Gregory et al., 2019). Furthermore, it has also been suggested that

viral assemblages show higher richness at lower latitudes, caused by the proportions of different taxa found in these locations rather than by their presence /absence at particular sites (Angly et al., 2006). Given coral reefs are highly diverse ecosystems, viruses may play an important role in maintaining their complexity by influencing the structure of prokaryotic and eukaryotic populations, regulating the composition, diversity and functions of these communities, modulating their interactions (Rohwer & Thurber, 2009; Thurber & Correa, 2011; Levin et al., 2017; Sweet & Bythell, 2017; Weynberg, 2018). Considering that viruses potentially infect all living cells (Fuhrman, 1999), the high diversity of symbionts in sponges make them an ideal model for characterising the role of viruses in marine holobionts. Sponges are also a relevant model to investigate viral functions, due to their unique ability in promoting benthic-pelagic coupling in the ocean through seawater filtration.

1.4. SPONGE-VIRAL INTERACTIONS

The most common viral-host interaction in marine environments is assumed to occur between prokaryotes and phages (Breitbart, Miyake & Rohwer, 2004; Weinbauer, 2004; Flores, Valverde & Weitz, 2013; Perez Sepulveda et al., 2016), as prokaryotes represent about 90% of the biomass in the ocean (Worden, 2006). Examples of marine phage-prokaryote interactions have been extensively described and these studies have highlighted that phages influence prokaryote abundance, diversity and evolution (Proctor & Fuhrman, 1990; Noble & Fuhrman, 1998; Prangishvili, Forterre & Garrett, 2006; Weitz & Wilhelm, 2012). Phage-prokaryote interactions can be highly specific with the same virus species infecting only one prokaryote genus, species or strain (Brussaard, 2004a; Duffy, Burch & Turner, 2007; Atabekov, 2011). However, some phage have also been shown to infect multiple distinct prokaryote types in natural environments (Holmfeldt et al., 2007; Malki et al., 2015; Kauffman et al., 2018), forming a complex host range web pattern (Flores, Valverde & Weitz, 2013). The phage-prokaryote interaction patterns can be influenced by several factors, such as geographic variations (Flores, Valverde & Weitz, 2013), seasonal fluctuations (Parsons et al., 2012), temporal dynamics (Winget & Wommack, 2008), nutrient concentrations (Bratbak et al., 1996; Jover et al., 2014; Finke et al., 2017) or temperature and photic regimes (Coutinho et al., 2017). However, characterizing these interactions at large scales is challenging since phage and prokaryote communities are extremely dynamic (Breitbart, 2012) and such studies

would require a massive sampling effort (Weitz et al., 2013). A possible way of minimizing this effort would be to investigate the phage-prokaryote interactions within macro-organisms (eukaryotes), which are relatively closed systems, with structural stability, and are often subjected to distinct environmental conditions.

Virus-eukaryote association in marine ecosystems have been reported from numerous species including sponges, corals, molluscs, arthropods, echinoderms, and urochordates (Table 1.1.). The majority of studies investigating viral-eukaryote interactions describe viruses associated with commercially important taxa (Shapiro, 2003; Suttle, 2007; Abdullah et al., 2017; Arzul et al., 2017; Doan et al., 2017; Flowers et al., 2018). One of the most frequently studied eukaryotic viral pathogen is the White Spot Syndrome Virus, a *Nimaviridae* that typically infects shrimp, and has substantially impacted the aquaculture industry worldwide (Sánchez-Paz, 2010; Bir et al., 2017). *Herpesviridae* is a viral family commonly associated with diseases in marine eukaryotes and have been correlated with high mortality rates in the maricultured abalone *Haliotis* spp. (Pen et al., 2005; Bai et al., 2019) and the oyster *Crassostrea gigas* (Sauvage et al., 2009; {Merging Citations} et al., 2014; Fuhrmann et al., 2016; Nguyen, Alfaro & Merien, 2018). Viral diseases have also been described for uncultured marine species. Multiple studies have suggested that coral diseases, including black band disease and white plague disease, as well as physiological disfunctions including bleaching, may involve viral infection as a part of disease pathogenesis (Soffer et al., 2014; Yvan et al., 2014; Sweet & Bythell, 2017). Additionally, recent experiments revealed *Parvovirus* as the etiological agent of sea-star wasting disease, which is responsible for mass mortalities of *Asteroides* sp. (Hewson et al., 2014).

Table 1.1 Families of viruses associated with marine organisms. Taxa for which marine isolates have been described are labelled with *.

Host Type	Marine Host	Genome Type	Taxonomy of major associated viral groups	Reference
Bacteria	Cyanobacteria	dsDNA	*Caudovirales** *(Myoviridae, Podoviridae, Siphoviridae)*	(Suttle & Chan, 1993; Perez Sepulveda et al., 2016)
	Bacteria	dsDNA	*Caudovirales** *(Myoviridae, Podoviridae, Siphoviridae)* *Corticoviridae**, *Plasmaviridae* *Tectiviridae, Corticoviridae*	(Casjens, 2005) (McDaniel et al., 2002) (Leigh et al., 2018) (Proctor, 1997) (Breitbart et al., 2004)

Bacteria Protist	Cyanobacteria	ssDNA	*Inoviridae*, Microviridae* (Gokushovirinae),*	(Roux et al., 2019) (Roux et al., 2012)
	Bacteria Heterotrophic protist Microalgae	ssRNA	*Leviviridae*	(Bollback & Huelsenbeck, 2001)
		dsDNA	*Mimiviridae*, Marseilleviridae**	(Monier, Claverie & Ogata, 2008) (Boyer et al., 2009)
		dsDNA	*Phycodnaviridae* Reoviridae* (Sedoreovirinae) Picornavirales*	(Correa, Welsh & Vega Thurber, 2013) (Schroeder et al., 2002)
Plantae Invertebrate	Macroalgae		*Phycodnaviridae*	(Wilson, Van Etten & Allen, 2009)
	Sponge	dsDNA	Caudovirales *(Myoviridae, Podoviridae, Siphoviridae), Mimiviridae, Phycodnaviridae, Ascoviridae, Baculoviridae, Herpesviridae, Irdoviridae, Marseilleviridae, Poxviridae*	(Laffy et al., 2018)
Plantae	Macroalgae	ssDNA	*Microviridae, Circoviridae, Macroviridae, Parvoviridae, Nidoviridae, Potyviridae*	(Laffy et al., 2018)
Invertebrate Vertebrate	Cnidarians	dsDNA	Caudovirales *(Myoviridae, Podoviridae, Siphoviridae) Mimiviridae, Phycodnaviridae, Parvoviridae, Inviridae, Herpesviridae*	(Laffy et al., 2018) (Weynberg et al., 2017a) (Thurber et al., 2017) (Grasis et al., 2014)
		ssDNA	*Circoviridae, Bidnaviridae*	(Laffy et al., 2018) (Weynberg et al., 2017a) (Thurber et al., 2017)
	Cnidarians Molluscs	dsRNA	*Totiviridae*	(Gudenkauf & Hewson, 2016)
		dsDNA	*Papovaviridae, Birnaviridae, Herpesviridae*, Malacoherpesviridae*, Papillomaviridae*	(Renault & Novoa, 2004) (Meyers et al., 2010) (Meyers, 1981) (Sauvage et al., 2009)
		dsRNA	*Birnaviridae Reoviridae**	(Renault & Novoa, 2004) (Meyers, 1979) (Kitamura et al., 2002)
	Molluscs Echinoderms	ssRNA	*Picornaviridae, Togaviridae*	(Renault & Novoa, 2004) (Rasmussen, 1986)
		dsDNA	Caudovirales *(Myoviridae, Podoviridae, Siphoviridae), Asfaviridae, Iridoviridae, Parvoviridae**	(Gudenkauf & Hewson, 2016) (Hewson et al. 2014)
		ssDNA	*circular* rep*-encoding single-stranded (CRESS)*	(Jackson et al., 2016)

	Arthropods	dsDNA	Caudovirales *(Myoviridae, Podoviridae, Siphoviridae), Baculoviridae, Nimaviridae**	(Clark, 2016) (Gudenkauf & Hewson, 2016) (Sánchez-Paz, 2010; Bir et al., 2017)
		ssDNA	*Circoviridae*	(Dunlap et al., 2013)
	Arthropods Urochordates	ssRNA	*Arteriviridae*	(Gudenkauf & Hewson, 2016)
		dsDNA	Caudovirales *(Myoviridae, Podoviridae, Siphoviridae), Nimaviridae*	(Gudenkauf & Hewson, 2016)
		ssDNA	*Circoviridae*	(Gudenkauf & Hewson, 2016)
	Fish	dsDNA	*Iridoviridae*, Herpesviridae**,	(Crane & Hyatt, 2011)
		dsRNA	*Birnaviridae**	(Wolf et al., 1960)
Vertebrate	Fish Reptiles Mammals	ssRNA	*Nodaviridae, Orthomyxoviridae*, Togaviridae*,Rhabdoviridae*, Paramyxoviridae*, Picornaviridae*	(Glazebrook, Heasman & Beer, 1990) (Mori et al., 1992) (Alavandi & Poornima, 2012) (Fichtner et al., 2013)
		dsDNA	*Herpesviridae*, Papillomaviridae*	(Jones et al., 2016) (Herbst et al., 2009)
		dsDNA	*Herpesviridae*, Papillomaviridae*, Poxviridae*	(Ng et al., 2015) (Varsani et al., 2014) (Colegrove et al., 2010)
	Reptiles	ssRNA	*Togaviridae*, Orthomyxoviridae*, Astroviridae*, Caliciviridae*, Paramyxoviridae**	(Van Bressem, Van Waerebeek & Raga, 1999) (La Linn et al., 2001) (Lvov et al., 1978) (Rivera et al., 2010) (Di Guardo et al., 2005)
	Sea birds	ssRNA	*Orthomyxoviridae*, Flaviviridae, Coronaviridae*	(Chastel et al., 1985) (Lebarbenchon et al., 2015) (Traavik, Mehl & Kjeldsberg, 1977)

Recent metaviromic (viral metagenomic) studies have shown that viruses are important components of coral reef organisms, potentially interfering in their host functions through AMGs (Levin et al., 2017; Weynberg et al., 2017a; Laffy et al., 2018). However, only a few studies have described sponge viruses. The first report of viruses associated with sponges was

published 40 years ago, demonstrating isometric particles similar to adenoviruses in cells of the sponge *Verongia cavernicola*, through Transmission electron microscopy (TEM) analysis (Vacelet & Gallissian, 1978). Recently, metagenomic studies have provided compelling evidence that viruses are important components of the sponge holobiont (Laffy et al., 2016, 2018, 2019).The sponge virome has demonstrated to be notably diverse, species-specific and greatly represented by bacteriophage groups (Laffy et al., 2018; Jahn et al., 2019). Additionally, sponge-viruses possess genes that encode host auxiliary metabolic functions, such as herbicides resistance genes (Laffy et al., 2018) and ankyrin repeat protein, which have been proposed to aid bacterial hosts in evading eukaryotic immune responses within sponge holobionts (Jahn et al., 2019). However, even though the first insights regarding sponge-virome roles have been revealed, many facets of the association remain unknown. For instance, how does the sponge virome vary under distinct geographic locations and across different sponge-microbial association strategies? Moreover, since viruses are key organisms in modulating marine communities (Rohwer & Thurber, 2009; Mojica & Brussaard, 2014), it is important to understand how sponge viromes respond the acute anthropogenic impacts that substantially threaten marine ecosystems worldwide.

Sponges are a noteworthy taxa to investigate the role of viruses in holobiont communities (Claverie et al., 2009) as they are ecologically important, evolutionary significant and they host a diverse array of macro- and micro-symbionts (Thomas et al., 2016). The ecological role of sponges and their associated viruses is likely to influence marine biogeochemical cycling as they have both been characterised to contribute to the cycling of organic and inorganic matter in seawater (Wilkinson & Fay, 1979; Shieh & Lin, 1994; Fuhrman, 1999; Steindler, Beer & Ilan, 2002).

1.5. SPONGE HOLOBIONT UNDER HEAT-STRESS

In a global context, coral reef ecosystems have been increasingly compromised by climate change and deterioration in water quality (Doney et al., 2012). Shifts in seawater temperature, circulation, stratification and nutrient content, have all led to alterations in physiological tolerances, population dynamics, species interactions and disease susceptibility in coral reef species (Doney et al., 2012). Rising seawater temperatures are one of the most significant and direct impacts of climate change (Levitus, Antonov & Boyer, 2005; Lyman et

al., 2010). Increases in accumulated heat stress events have resulted in massive coral bleaching (Skirving et al., 2019), and during the period from 2014–2017 coral reefs experienced the most severe, widespread and longest-lasting global-scale bleaching event ever recorded (Eakin, Sweatman & Brainard, 2019). During this time, it was reported that bleaching had occurred on 91% of the reefs within the Great Barrier Reef (GBR), following heat-stress events that occurred in 2016 (Hughes et al., 2017).

The effects of ocean warming and heat-stress events have been extensively investigated in marine sponges (Webster et al., 2011; Lesser et al., 2016; Bennett et al., 2017; Bell et al., 2018) and although most of the species have shown to be negatively affected by higher temperatures (Rubio-Portillo et al., 2016; Bennett et al., 2017; Carballo & Bell, 2017), others could tolerate or even benefit from a heat stress condition (Vicente, 1990; Carballo et al., 2013; Kelmo, Bell & Attrill, 2013; Marlow et al., 2018). The adaptative advantage of certain sponge species over other reef-building organisms has lead to the proposal that sponges may dominate coral reefs in future climate change scenarios (Bell et al., 2018). The effects of thermal stress in sponges can be reflected on their physiology (Bennett et al., 2017), gene expression (López-Legentil et al., 2008; Webster et al., 2013b), feeding ecology (Massaro et al., 2012), and microbial symbiosis (Webster, Cobb & Negri, 2008; Strand et al., 2017). Additionally, thermal stress can trigger disease-like syndromes, such as necrosis, bleaching (Fan et al., 2013; Bennett et al., 2017; Whalan, 2018), and also promote an imbalance in the holobiont community structure (Lemoine et al., 2007; López-Legentil et al., 2008; Webster, Cobb & Negri, 2008), which has been suggested to lead to opportunistic infections in marine sponges (Pita et al., 2018a). The occurrence of diseases and disease-like syndromes in sponges is often associated with shifts in their microbial community (Blanquer et al., 2016; Luter et al., 2017; Whalan, 2018), however, the etiological agents of these diseases have not been elucidated, with exception of pathogenic *Pseudoalteromonas agarivorans* strain isolated from infected *Rhopaloeides odorabile* (Webster et al., 2002; Choudhury et al., 2015). Specific bacterial clades are rarely identified as etiological agents of disease (Mouchka, Hewson & Harvell, 2010), indicating that other contributing factors are driving these dynamics (Littman, Willis & Bourne, 2011). As viruses are considered important disease drivers in marine ecosystems (Patten, Seymour & Mitchell, 2006; Suttle, 2007; Thurber et al., 2009b; Sánchez-

Paz, 2010; Crane & Hyatt, 2011; Jones et al., 2016), it is necessary to also investigate the role of viruses in sponge stress responses, including thermal-stress events.

Despite our current understanding of how sponge microbial communities are influenced by environmental stressors, only one study has focused so far on the description of the sponge-viral responses to a heat-stress event, where it was demonstrated that thermal stress can promote shifts in viral population associated with the marine sponge *R. odorabile*, including an enrichment in endogenous retro-transcribing viruses (Laffy et al., 2019). As different sponge species exhibit unique responses to environmental stressors (Bennett et al., 2017), there is a need to better characterise the role that viruses may be playing in thermally stressed sponges, and it is important investigate distinct species, particularly those whom exhibit a clear physiological responses to the heat stress.

1.6. METHODOLOGICAL APPROACHES TO STUDYING SPONGE-VIRAL INTERACTIONS

Substantial efforts have been made to improve and standardize the techniques that can be used to describe viruses in marine ecosystems (Weinbauer 2004). However, there are still many technical challenges that hinder our ability to obtain a comprehensive picture of sponge-viral communities (Hurwitz et al., 2013). The different approaches for characterizing viral communities all have inherent strengths and limitations and can often be complementary. Currently, sponge-virus interactions have been observed using two complementary techniques: Transmission electron microscopy (TEM) and metagenomics.

1.6.1. Transmission electron microscopy

Viruses are generally structurally simple, primarily composed of genetic material surrounded by a protein coat and this lack of distinct morphological variations between viruses means it is often difficult to characterize of these biological entities (Perez Sepulveda et al., 2016). Historically, the morphology of sponge viruses was characterised using the most common, and time-consuming method to assess viral diversity in aquatic ecosystems: transmission electron microscopy (TEM) (Wommack & Colwell, 2000). Viral classification is largely based on capsid morphology and size, and TEM is a powerful tool for visualization and putative identification of viruses, with TEM providing the first evidence of high viral abundance and diversity in marine systems (Bergh et al., 1989), revealing the morphological diversity and relative abundance of virus-like particles in marine hosts (Borsheim, Bratbak & Heldal, 1990;

Wilson & Chapman, 2001; Patten, Harrison & Mitchell, 2008; Pollock et al., 2014; Hewson et al., 2014). Interpretation of TEM analyses can be hindered by technical issues including the frequent low representation of samples, uneven staining, removal of viruses during washing steps, low detection limits and lack of recognition of non-typical viruses (Weinbauer & Suttle, 1997; Bettarel et al., 2000).

The following TEM preparation methods have been used to assess viruses associated with marine hosts: i) density gradient purification and isolation (Weynberg et al., 2014); ii) direct ultracentrifugation of samples in liquid medium onto Formvar-coated electron microscopy grids (Pollock et al. 2014; Borsheim et al. 1990), iii) filtration method (Wommack et al., 2010) and iv) preparation of ultrathin sections from the host tissue (Wilson & Chapman, 2001). The first two methods allow the concentration of VLPs, which increase visualization rates via TEM, but can be problematic in tissue sections, as they can provide an inaccurate and incomplete viral representation. Initial filtering steps within the first three methods often exclude specific viral groups and mask relationships between the virus and host. The most successful way to identify direct viral-host interactions (including host specificity and reproductive mode) is through analysis of histological sections (Wilson et al., 2005). Thus, it is important to use multiple isolation methods in order to have a broad description of host virus relationships.

1.6.2. Metagenomic analysis of viral assemblages

Metaviromics is the study of viral genome communities obtained directly from environmental samples by viral purification and subsequent shotgun sequencing (Kim, Whon & Bae, 2013). The metaviromic approach is an important tool to describe viruses, considering that many viral hosts are not amenable to cultivation (Edwards & Rohwer, 2005) and that viruses do not contain a universal marker gene to facilitate identification (Rohwer & Edwards, 2002; Rohwer & Thurber, 2009). The use of molecular approaches, combined with advances in Next Generation Sequencing (NGS) technologies has greatly reduced the cost of obtaining genomic data, accelerating the development of viral community sequence-based studies (Wommack, Bhavsar & Ravel, 2008). Metaviromics was first used to describe marine viruses in 2002 (Breitbart et al., 2002) and was considerably impactful on viral diversity exploration, quadruplicating the number of known sequenced viral genomes (Roux, 2019). However, the analysis and interpretation of metaviromic data can be challenging, due to the high diversity of viruses in natural environments (Rosario & Breitbart, 2011) and the limited number of viral

genomes present within reference databases (Kim, Whon & Bae, 2013). Thus, the use of appropriate bioinformatic tools is an essential component in interpreting metaviromic sequencing datasets.

Holovir is an effective pipeline to assess the taxonomic composition and function of metaviromic data, specifically designed to characterize viral metagenomes from host-associated holobiont communities (Laffy et al., 2016). As a part of this computational workflow, the taxonomic assignment of the metaviromic data is performed utilising BLAST analysis to search for homology between predicted gene data and known viral reference sequence within the NCBI RefSeq database (Pruitt, Tatusova & Maglott, 2007). Taxonomic assignment is then performed using a lowest common ancestor scoring system based on the best significant matches to viral reference database. To perform functional analysis of the metaviromic data, this pipeline utilises BLASTP sequence similarity searches of predicted genes against the Swiss-Prot manually curated UniprotKB protein database (The UniProt Consortium, 2015), and assigns Swiss-Prot Keywords based on the best significant BLASTP match. Furthermore, potential cellular contamination of these host associated viromic communities is performed to evaluate sample purity.

Metaviromics has greatly expanded our understanding of the diversity and function of viruses associated with marine hosts (Willner & Hugenholtz, 2013; Laffy et al., 2016). Additionally, the improvement of techniques used to isolate and purify the viral nucleic acid has been fundamental in the generation of good quality viromes associated with marine holobionts (Weynberg et al., 2014; Wood-Charlson et al., 2015). A key benefit of utilising this methodology is the capacity to isolate viromes associated with both eukaryotic and prokaryotic components of marine holobionts, expanding the understanding of the viral roles within these host associated communities. Several studies have validated the use of these viral purification techniques and have utilised the Holovir protocol in describing the diversity and function of viruses within marine holobionts (Laffy et al., 2016, 2018, 2019, Weynberg et al., 2017a,b; Weynberg, 2018). Thus, these methodological approaches would greatly complement the TEM analysis in efforts to characterize viruses and their roles in coral reef sponges.

1.7. THESIS OUTLINE

Our limited knowledge of host-viral association in marine communities has hindered our broader understanding of oceanic dynamics and our ability to predict ecological responses to environmental change. Marine sponges represent an ecologically important model for exploring host-viral dynamics as they are ancient metazoans with a wide geographic distribution and host dense, diverse and stable microbial symbiont communities. With recent developments in sequencing technologies, computational pipelines and microscopy, we are now well placed to explore the diversity and function of sponge viruses and determine how they influence host health in a rapidly changing climate.

This thesis aims to characterise viral communities of coral reef sponge species that utilize distinct symbiotic strategies, collected from different biogeographic regions, and to determine the effect of ocean warming on sponge-associated viral communities. This thesis is organized in three data chapters, presenting a 1) morphological characterization of sponge viruses, 2) a molecular description and characterisation of multiple sponge viromes, and 3) an experimental work revealing the impacts of heat-stress events on viral community composition and function within a phototrophic sponge species.

Chapter 2 reports on three transmission electron microscopy (TEM) preparation methods that provide the first morphological characterization of viruses associated with 15 different coral reef sponge species, validating the spatial localization of these VLPs within the sponge holobiont.

In Chapter 3, comparative analyses of the viromes associated with the same 15 sponge species that underwent TEM analysis were explored. Variations in the viral communities and their associated functions have been correlated with the sponge species, geographic location, host nutritional modes (photosymbionts vs no photosymbionts) and strategies for microbial symbiosis (high microbial abundant vs low microbial abundant sponges).

Chapter 4 investigate the sponge virome response to elevated temperatures, describing two experiments where the photosynthetic sponge *Carteriospongia foliascens* was exposed to a short (3 days) and longer term (21 days) heat-stress event. A metaviromic approach was used to assess the shifts in the community and functional composition across these treatments.

Finally, Chapter 5 presents and discusses the main findings of this thesis and gives suggestions on the future direction of sponge-viral research.

Chapter 2. MORPHOLOGICAL CHARACTERIZATION OF VIRUS-LIKE PARTICLES IN CORAL REEF SPONGES

2.1. ABSTRACT

Marine sponges host complex microbial consortia that vary in their abundance, diversity and stability amongst host species. While our understanding of sponge-microbe interactions has dramatically increased over the past decade, little is known about how sponges and their microbial symbionts interact with viruses, the most abundant entities in the ocean. In this study, we employed three transmission electron microscopy (TEM) preparation methods to provide the first comprehensive morphological assessment of sponge-associated viruses. The combined approaches revealed 50 different morphologies of viral-like particles (VLPs) represented across the different sponge species. VLPs were visualized within sponge cells, within the sponge extracellular mesohyl matrix, on the sponge ectoderm and within sponge-associated microbes. Non-enveloped, non-tailed icosahedral VLPs were the most commonly observed morphotypes, although tailed bacteriophages, brick-shaped, geminate and filamentous VLPs were also detected. Visualization of sponge-associated viruses using TEM has confirmed that sponges harbor not only diverse communities of microorganisms but also diverse communities of viruses.

2.2. INTRODUCTION

Sponges are abundant and ecologically important members of marine benthic communities (Van Soest et al., 2012). Most sponges are suspension filter feeders (Thomassen & Riisgård, 1995), with complex aquiferous systems capable of manipulating the seawater composition at both macro and micro scales (Vacelet & Boury-Esnault, 1995; Patterson et al., 1997; de Goeij et al., 2013a). A unidirectional (ostia-chamber-atrium-oscula) water flow driven by flagellated choanocyte cells is responsible for capturing and retaining small eukaryotes, prokaryotic cells and viral particles (Hadas et al., 2006). Sponge filtration of large quantities of seawater represents an important nutrient link between the pelagic and benthic environments (Pile & Young, 2006), especially in oligotrophic ecosystems such as coral reefs (de Goeij et al., 2013b).

Sponges form intimate partnerships with diverse microbial consortia, and these relationships range from mutualism to commensalism to parasitism (Webster & Taylor, 2012; Thomas et al., 2016). The sponge microbiome is often highly conserved across individuals of the same sponge species but varies considerably across species (Thomas et al., 2016). It is because of these functionally important symbiotic partnerships that sponges are considered a typical example of a marine 'holobiont', an organism comprised of various 'bionts', living in symbiogenesis (Margulis & Fester, 1991; Webster & Thomas, 2016). However, while the symbiotic association between sponges and their bacterial / archaeal symbionts has been extensively studied (Maldonado 2007; Thomas et al. 2016; Pita et al. 2018), the role of viruses in the sponge holobiont remain largely unknown, despite TEM images from the 1970s alluding to viral-infected sponge cells (Vacelet & Gallissian, 1978), a demonstration of phage infection in a sponge-associated bacterium (Lohr, Chen & Hill, 2005), and a few recent metagenomic studies providing insights into sponge virus diversity and function (Butina et al., 2015; Laffy et al., 2016, 2018).

Viruses are the most abundant biological agents in marine ecosystems, with about 10^{10} viruses per liter of surface seawater and 10^{10} per gram dry weight of marine sediment (Suttle, 2007; Danovaro et al., 2011). Importantly, viruses have the ability to regulate the prokaryotic and eukaryotic populations responsible for maintaining metabolic cycling in complex ecosystems such as coral reefs (Seymour et al., 2005; Thurber & Correa, 2011; Mojica & Brussaard, 2014). Viruses modulate microbial-driven processes through mortality, horizontal gene transfer and metabolic reprogramming by viral-encoded auxiliary metabolic genes (AMGs) (Bergh et al., 1989; Thurber et al., 2009b; Danovaro et al., 2011; Hurwitz et al., 2014; Breitbart et al., 2018). Recent years have seen an increased focus on the diversity and function of viruses associated with reef invertebrates including sea anemones (Wilson & Chapman, 2001); starfish (Hewson et al., 2014); scleractinian corals and their associated microbial communities (Patten, Harrison & Mitchell, 2008; Weynberg et al., 2014, 2017b; Laffy et al., 2018). However, while viruses have been described as essential components of coral reef ecosystems, capable of controlling microbial community dynamics, playing a role in coral bleaching / disease, and mediating reef biogeochemical cycling (Thurber et al., 2017), there is a paucity of research exploring viruses associated with ecologically important reef sponges.

Metagenomic analysis of purified viral fractions (metaviromics) recently provided the first insights into the composition and function of viruses inhabiting reef sponges (Laffy et al., 2016, 2018). Consistent with the pattern reported for sponge-associated microbial communities, the viral communities were found to be highly conserved within each sponge species, and displayed functional repertoires clearly distinct from viruses inhabiting the surrounding seawater (Laffy et al., 2018). Sequence analysis revealed that the virome assignments were dominated by viromes from the order Caudovirales but also contained representatives of the Mimiviridae, Phycodnaviridae, Circoviridae, Parvoviridae, Bidnaviridae and Microviridae. Unique viral adaptations to specific host microenvironments were also evident, with viral auxiliary genes being differentially represented across sponge species (Laffy et al., 2018).

While molecular approaches have substantially improved our understanding of viral-host interactions (Breitbart et al., 2002; Rosario & Breitbart, 2011; Laffy et al., 2016), biases associated with DNA /RNA extraction methods (Wood-Charlson et al., 2015) and the limited genomic resources available for most environmental viruses (Roux et al., 2015a) can still constrain our understanding of host-associated viral ecology. Transmission electron microscopy (TEM) is a powerful approach that has helped to reveal the morphology and distribution of virus-like particles (VLPs) in many marine hosts as well as deciphering patterns of host-viral interactions (Wilson & Chapman, 2001; Patten, Harrison & Mitchell, 2008; Brum, Schenck & Sullivan, 2013; Pollock et al., 2014; Hewson et al., 2014; Weynberg et al., 2017a). Here we use TEM to provide the first morphological characterization of viruses associated with 15 different coral reef sponge species and confirm the spatial localization of these VLPs within the sponge holobiont.

2.3. METHODS

2.3.1. Sponge collection and identification

Sampling was conducted on coral reefs of Orpheus Island, Great Barrier Reef, Australia (18°35’34’’S, 146°28’53”E) and Al Fahal, Red Sea, Saudi Arabia (22°13’95”N, 39°01’81”E), between December 2015 and February 2016. Sampling in Australia was conducted under the Great Barrier Reef Marine Park Authority permit G12/35236.1, and sampling in Saudi

Arabia was authorized by the Saudi Arabian coastguard as the study did not involve endangered or protected species.

Triplicate specimens of 13 sponge species were collected by scuba diving between three and 15 meters depth. Two sponge species, *Stylissa carteri* and *Carteriospongia foliascens* were found at both locations, and sampling was performed in triplicate at both sites. Sponge specimens were photographed *in situ* before being individually placed within sterile Falcon® tubes and kept on ice until processing. All sampling materials were sterilized prior to and between each sampling. Morphological characterization of sponge species was performed as described in (Hooper & Van Soest, 2002) and DNA barcoding was additionally performed using mitochondrial cytochrome oxidase I (COI) gene primers and internal transcriber spacer 2 (ITS2) region of nuclear ribosomal DNA as described in (Erwin & Thacker, 2007; Andreakis, Luter & Webster, 2012; Wörheide et al., 2012). Sponge species are described in Table 2.1. and can be seen in Appendix 2 (Figure A2.1).

Three different sample preparation methods for TEM imaging of sponge-associated viruses were trialed: i) ultrathin sectioning of sponge tissue (Cheville & Stasko, 2014); ii) purification of viral fractions via density gradient ultracentrifugation (Lawrence & Steward, 2010; Weynberg et al., 2014) and iii) filtration of sponge mucus. All samples were examined using a Titan Cubed TEM and images were analysed on the Cs-corrected Titan™ 80-300 platform at the Imaging Characterization Core Lab in KAUST. TEM search time was standardized to 1 hr / sample.

Table 2.1 Collection details for all sponge species examined by TEM. GBR refers to the Great Barrier Reef collection site and RS refers to the Red Sea collection site.

Sponge Species	Location	Depth (m)
***Carteriospongia foliascens,* P.S. Pallas (1766)**	GBR, RS	3 – 10
***Stylissa carteri,* A. Dendi (1889)**	GBR, RS	10 – 15
***Xestospongia* sp.**	GBR	5 – 15
***Lamellodysidea herbacea,* C. Keller (1889)**	GBR	5 – 10
***Cymbastela marshae,* J.N.A.Hooper & P.R. Bergquist (1992)**	GBR	10 – 15
***Cinachyrella schulzei,* C. Keller (1891)**	GBR	3 – 7
***Pipestela candelabra*, B. Alvarez et al. (2008)**	GBR	7 – 15
***Echinochalina isaaci,* J.N.A. Hooper (1996)**	GBR	7 – 15
***Xestospongia testudinaria,* J.B.P. Lamarck (1815)**	RS	7 – 15
***Amphimedon ochracea,* C. Keller (1889)**	RS	7 – 15
***Hyrtios erectus,* C. Keller (1889)**	RS	5 – 15
***Crella (Grayela) cyathophora,* H.J. Carter (1869)**	RS	7 – 15
***Mycale* sp.**	RS	5 – 15

2.3.1.1 Preparation of ultrathin sections of sponge tissue

Histological sections were prepared from fresh sponge tissue based on standard procedures for TEM (Cheville & Stasko, 2014). Briefly, each fragment of approximately 1mm³ was fixed in 2.5% glutaraldehyde in 0.2M cacodylate buffer and kept at 4°C for 2-24 h. After fixation, samples were immersed in 1% osmium tetroxide in 100 mM phosphate buffer for 1-2 h, washed in distilled water and stained in the dark with 2% aqueous uranyl acetate for 2 h at 4°C. Stained tissue was dehydrated through a series of ethanol and propylene oxide then embedded in epoxy resin. Ectosome-choanosome oriented sections (about 65 nm thick) were prepared using a Leica EM UC7 ultramicrotome and placed on TEM copper grids.

2.3.1.2 Viral purification via density gradient solution

Viral purification was performed according to the fraction separation method by sedimentation in density gradients (Meselson, Stahl & Vinograd, 1957), following the pre-processing approach established to isolate viruses from coral and sponge tissue (Weynberg et al., 2014; Laffy et al., 2018). In order to eliminate contaminants present in the aquiferous

system, sponges were partially dried via repeated gentle squeezing alternated with rinses of filtered (0.02µm) seawater. Sponge tissue was then dissected into small pieces (~5 mm^3) and covered with 15 µL of 0.02 µm filter-sterilized (Anotop, Whatman) SM buffer (100 mM NaCl, 8 mM MgSO4, 50 mM Tris pH 7.5), then homogenized with a Craig's HS30E homogenizer (Witeg, Germany) for 5 to 10 minutes (min). Tissue homogenate was filtered through a Falcon® 100 µm Cell Strainer (Corning, USA), then centrifuged at 500 g for 15 min at 4°C to pellet the majority of cell debris. The supernatant was used to purify the VLP via centrifugation in Cesium Chloride solution, with density varying from 1.2 g/mL to 1.6 g/mL (Weynberg et al., 2014). After ultracentrifugation, sponge VLPs were collected from the fractions with densities between 1.2 g/mL and 1.5 g/mL. In order to exchange the buffer and remove CsCl salts, samples were loaded onto 30 KDa Amicon centrifugal spin columns (Millipore, EUA) and centrifuged at 4000 g for 30 min at 4°C. This process was repeated four–six times per sample. Filter- sterilized SM Buffer was added to the concentrate and all flow-through was discarded. The concentrate was fixed in 0.5% glutaraldehyde and kept at 4°C until TEM analysis. TEM preparation involved applying a droplet of sample onto a TEM Copper grid, rinsing with sterile water, staining with 1% uranyl acetate for one min, washing with sterile water, followed by removal of excess liquid from the grid by touching filter paper to the edge.

2.3.1.3 Viral purification via filtration of sponge mucus

To describe the VLPs associated with sponge mucus and the external ectoderm, the sponge surface was carefully scraped with a sterile scalpel blade followed by rinsing three times with filtered (0.02µm) seawater. This TEM preparation method was based on a viral purification method described for marine hydras (Grasis et al., 2014). Extracted mucus was added to filtered (0.02 µm) *Milli-Q*® water (1:4) and centrifuged at 4000g for 10 minutes. Mucus supernatant was filtered through 0.45 µm filters (EMD Millipore, EUA) and fixed in1.5% glutaraldehyde. TEM imaging of mucus preparations was performed as described above for CsCl purified samples.

2.4. RESULTS

2.4.1. Sponge associated viruses

TEM analysis revealed that viral particles are diverse constituents of the sponge holobiont. Fifty VLP morphotypes (Figs. 2.1-5; Table A2.1, Morphotypes: M-I – M-L) were found in association with eight coral reef sponge species from the Great Barrier Reef: *Carteriospongia foliascens*, *Stylissa carteri*, *Xestospongia* sp., *Pipestela candelabra*, *Lamellodysidea herbacea*, *Cymbastella marshae*, *Echinochalina isaaci* and *Cinachyrella schulzei*; and seven sponge species from the Red Sea: *Carteriospongia foliascens*, *Stylissa carteri*, *Xestospongia testudinaria*, *Hyrtios erectus*, *Mycale* sp., *Amphimedon ochracea* and *Crella cyathophora*. VLPs were observed within sponge cells, in the extracellular mesohyl matrix, in the mucus/surface biofilm and within sponge-associated microbes. A diverse range of viral morphologies were observed, including hexagonal (tailed and non-tailed), spherical, filamentous, brick-shaped, beaded and geminate VLPs. While we detected numerous viral morphotypes, most were rare and often obscured by vesicles, cell debris and particulate organic matter.

Most sponge-associated VLP morphotypes possessed an icosahedral/polyhedral symmetry (~75%), ranging from 60-205 nm in diameter (Fig. 2.1; 2; 3; 4a). Tails were evident on some VLPs, confirming the presence of viruses from the bacteriophage order Caudovirales. Tailed VLPs were tentatively assigned to the three Caudovirales families based on their capsid symmetry and tail size/shape. VLPs characteristic of the *Podoviridae* presented a short tail attached to a non-enveloped icosahedral capsid and these VLPs were observed in the sponges *C. foliascens* (Fig. 2.1a), *Xestospongia* sp. (Fig. 2.1b), *E. isaaci* (Fig. 2.1c) and *S. carteri* (Fig. 2.1d). VLPs characteristic of the *Siphoviridae* presented an icosahedral head with a long non-contractile tail and these VLPs were detected in the surface biofilm of *C. schulzei* (Fig. 2.1e). VLPs characteristic of the *Myoviridae* presented an icosahedral head and a long contractile tail and these VLPs were observed in the sponges *E. isaaci* (Fig. 2.1f, g), *S. carteri* (Fig. 2.1h) and *A. ochracea* (Fig. 2.1i).

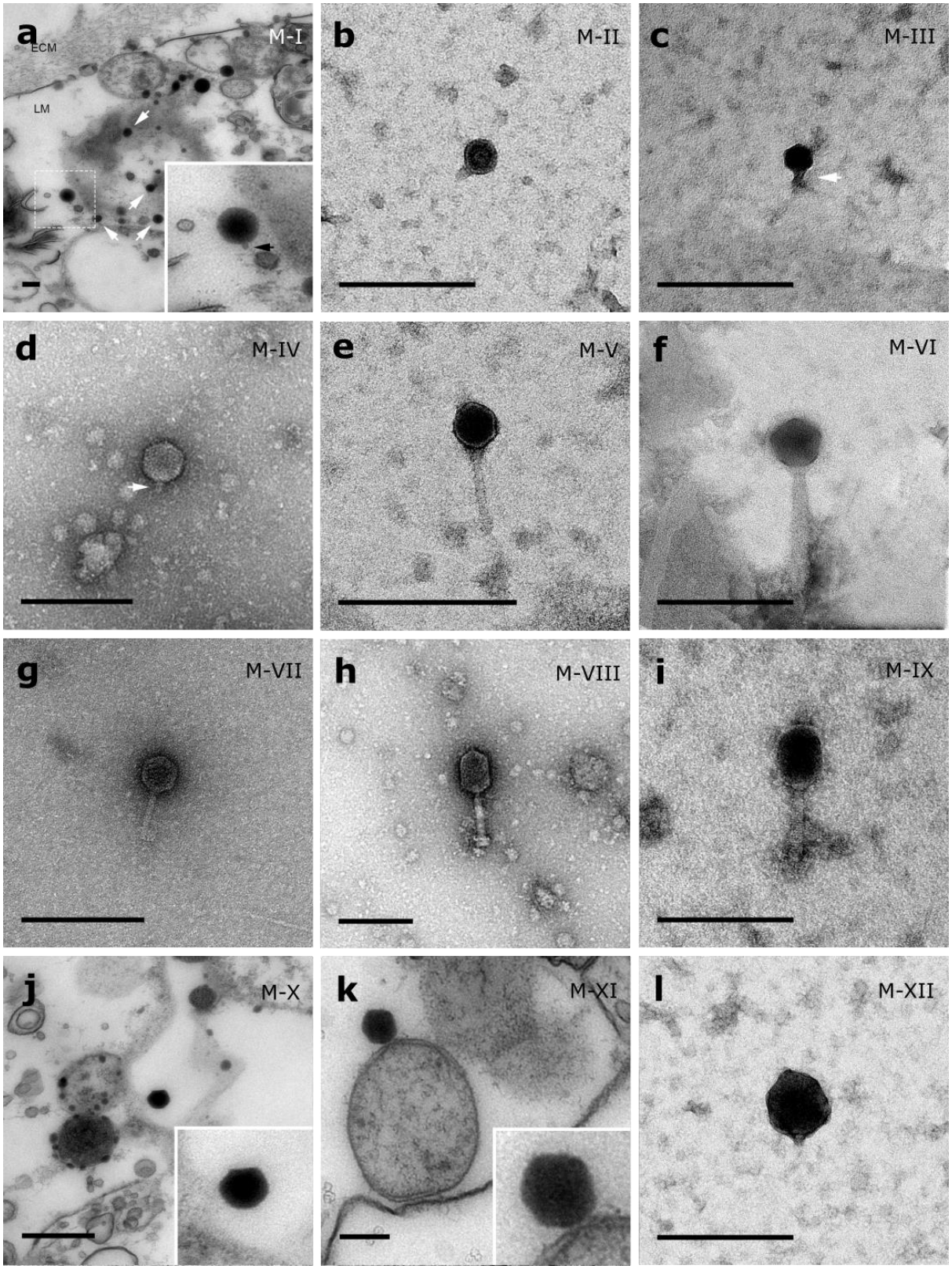

Figure 2.1 Representative morphotypes of virus-like particles associated with GBR and Red Sea sponges. GBR sponge species: (a, j, k, l) *C. foliascens*, (B) Xestospongia sp., (c, f, g) *E. isaaci*, (e) *C. schulzei*. Red Sea sponge species: (d, h) *S. carteri*, (k) *Amphimedon ochracea*. TEM preparation method: (a, j, k) ultrathin sections of sponge tissue, (b–i, l) viral purification via filtration of sponge mucus. Scale bar: 200 nm. Black arrows indicate the viral tail and white arrows indicate the VLPs.

Non-tailed icosahedral/polyhedral VLPs were observed using all three TEM preparation methods. Particle sizes ranged from 60 to 205 nm in diameter and some presented an electron dense core inside the viral capsid (35-124 nm in diameter). The majority of VLPs did not show an envelope outside the capsid, however an envelope was observed in association with a small proportion of VLPs (Fig. 2.2e; 3k-l; 5h). A typical example of an enveloped VLP was observed in *Hyrtios erectus* where a group of four virions were observed within a vacuole in the mesohyl matrix (Fig. 2.3l) and another free virion was captured merging its envelope into the cell membrane of the host (Fig. 2.3k).

In addition to the polyhedral VLPs, eight morphotypes of filamentous virus-like particles (FVLPs) were observed in the sponge mucus, mesohyl matrix, within sponge cells and associated with sponge-associated microorganisms (Fig. 2.4c-i; 5a). These morphotypes varied greatly in size (100-1300 nm length, 12-60 nm width) and shape. Rod-shaped FVLPs were detected in the CsCl purified viral fraction of *Xestospongia* sp. (Fig. 2.4c, d) and the mucus of *S. carteri* (Fig. 2.4i). Although similar, the *S. carteri* bacilliform VLPs were longer than those observed in *Xestospongia* sp. (230 nm long, 19 nm wide in *S. carteri*; 120-130 nm long, 18 nm wide in *Xestospongia* sp.). In *C. foliascens*, a FVLP was frequently observed attached to cyanobacteria and within the sponge mesohyl, (Fig. 2.4f-g). This FVLP resembled viruses of the family *Inoviridae* due to their shortened body (100-130 nm length, 50-60 nm width) and electron-translucent core with outer membrane structures consistent with a glycoprotein coat surrounding the entire membrane (Ploss & Kuhn, 2010). In *X. testudinaria*, a FVLP morphotype was observed within cells and dispersed throughout the mesohyl (Fig. 2.4j-l). This thin, elongated FVLP (340-1300 nm long and 15-30 nm wide) was observed at high abundance inside some choanocyte cells and lysed cells releasing virions were also evident (Fig. 2.4j-l). Another distinct FVLP morphotype was evident in the sponge mucus of *C. cyathophora* (Fig. 2.5a). It presented a tube-like shape indicating helical symmetry and size ranging from 150-154 nm in length and 22-25 nm in width.

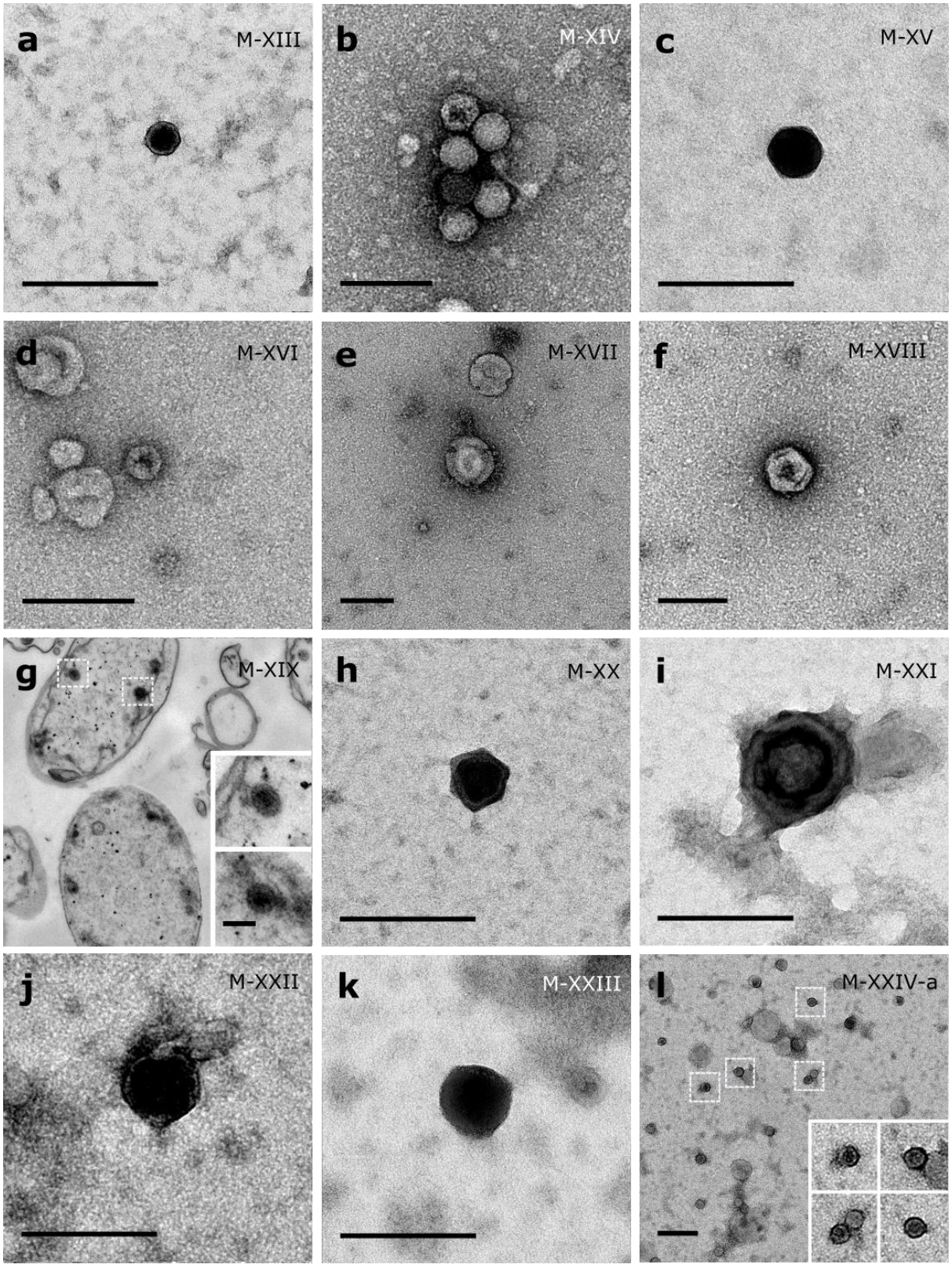

Figure 2.2 Representative morphotypes of virus-like particles associated with GBR sponges. Sponge species: (a) *C. foliascens*, (b, c) *S. carteri*, (d) Xestospongia sp., (e–h) *P. candelabra*, (i–k) *L. herbacea*, (l) *C. schulzei*. TEM preparation method: (a, h–k) viral purification via filtration of sponge mucus, (b–f, l) viral purification via CsCl gradient centrifugation, (g) ultrathin sections of sponge tissue. Scale bar: 200 nm.

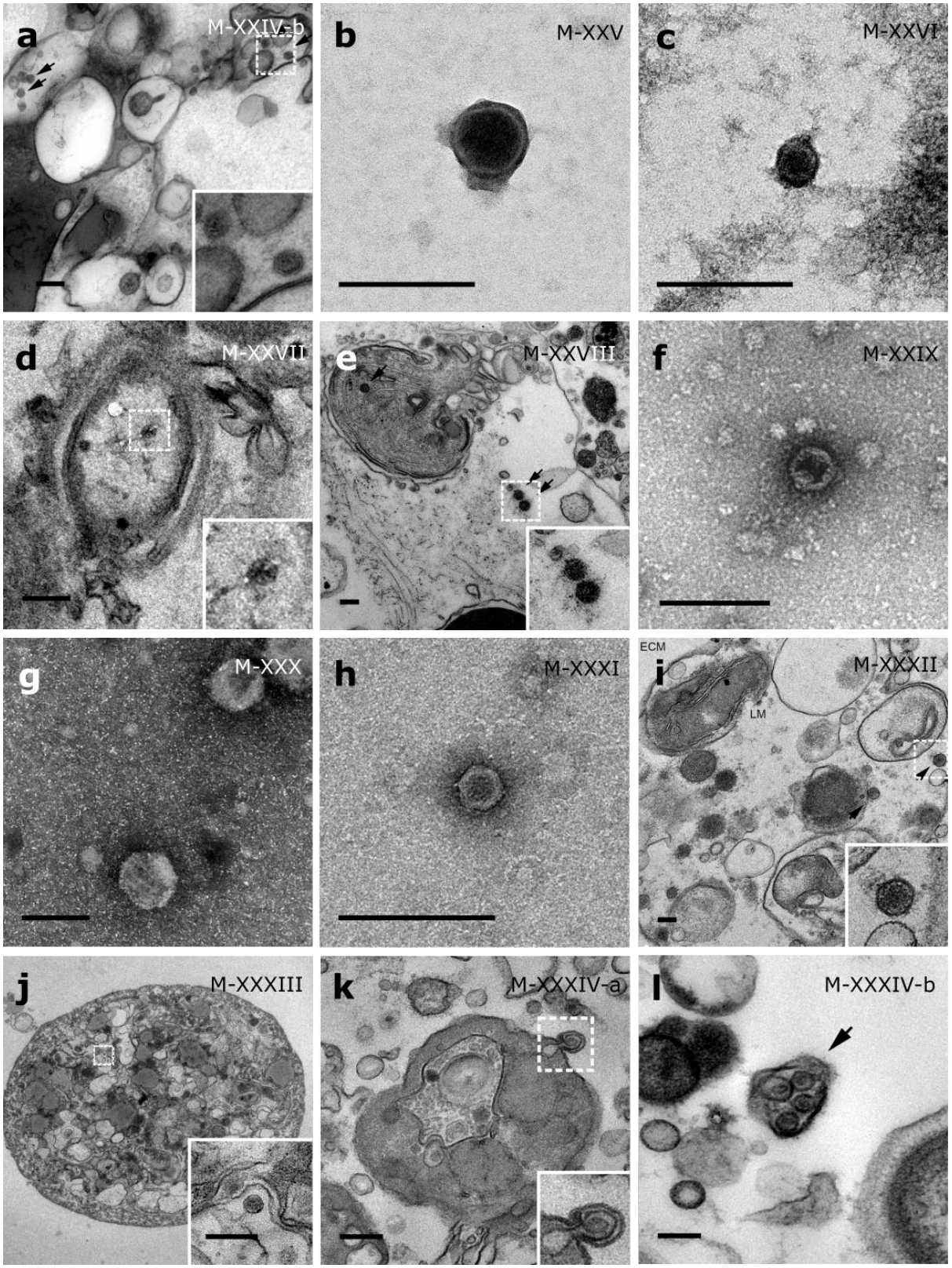

Figure 2.3 Representative morphotypes of virus-like particles associated with GBR and Red Sea sponges. GBR sponge species: (a, b) *C. schulzei*, (c) *C. marshae*. Red Sea sponge species: (d, e) *C. foliascens*, (f–h) *S. carteri*, (i) *X. testudinaria*, (j–l) *H. erectus*. TEM preparation method: (a, d–e, i–l) ultrathin sections of sponge tissue, (b, c, f–h) viral purification via filtration of sponge mucus. Scale bar: (a–c, e–l) 200 nm, (d) 500 nm. Black arrows indicate the VLPs.

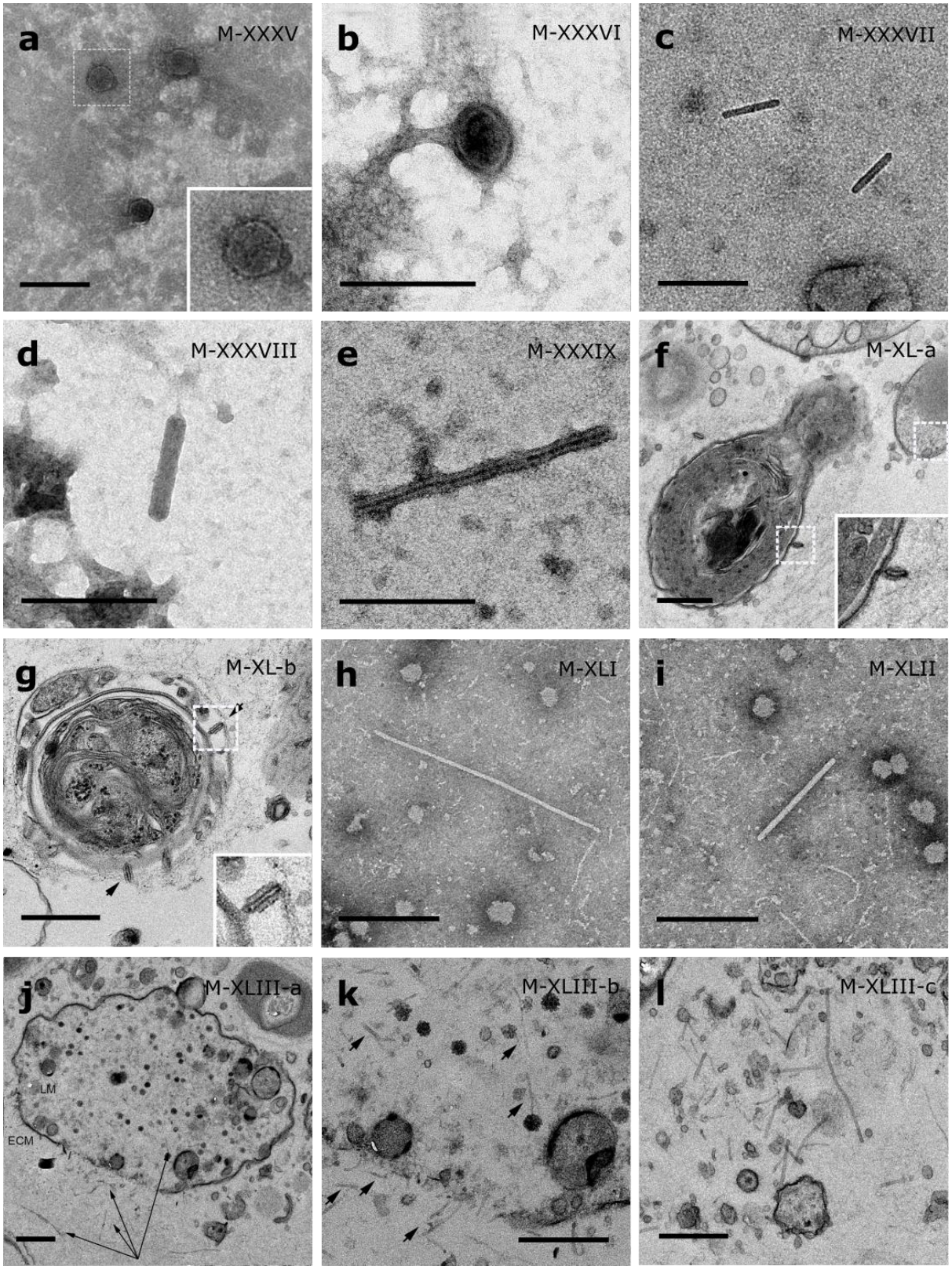

Figure 2.4 Representative morphotypes of virus-like particles associated with GBR and Red Sea sponges. GBR sponge species: (a) *Mycale* sp., (b) *C. foliascens*, (c, d) Xestospongia sp., (e) *C. schulzei*. Red Sea sponge species: (f, g) *C. foliascens*, (h, i) *S. carteri*, (j–l) *X. testudinaria*. TEM preparation method: (a, b, d, e, h, i) viral purification via filtration of sponge mucus, (c) viral purification via CsCl gradient centrifugation, (f, g, j–l) ultrathin sections of sponge tissue. Scale bar: (a–e, h, i) 200 nm, (f, g, j–l) 500 nm.

Geminate VLPs were observed in *C. cyathophora* mesohyl matrix (Fig. 2.5b), in *L. herbacea* mucus (Fig. 2.5c), and found infecting filamentous cyanobacteria associated with the sponge *A. ochracea* (Fig. 2.5d-g). The cyanobacteria associated VLPs shared morphological traits with viruses from the family Geminiviridae (Li, Ou & Zhang, 2013) and were typically twinned (81-95 nm long, 37-48 nm wide), comprising two quasi-isometric particles (34-45 nm length). The VLPs were spread across the cytoplasm, thylakoid lumen, and vacuoles of the cyanobacterial cells and were often at high abundance surrounding the stellar bodies (Fig. 2.5f).

A brick-shaped VLP morphotype, closely resembling viruses from the Poxviridae, was observed in sections of *Crella cyathophora* (Fig. 2.5h). This morphotype had a complex structure comprising a biconcave core encased within a double layer membrane with two lateral bodies surrounded by an ovoid envelope (Buller & Palumbo, 1991). Three representatives of this morphotype were observed within the sponge mesohyl matrix, and a single non-enveloped VLP was also observed in close proximity to a lysed sponge cell.

A beaded VLP was observed in sections of the sponges *C. foliascens* (Fig. 2.5i) and *H. erectus* (Fig. 2.5j-l). In *C. foliascens*, the branched VLP was 340 nm long, and was comprised of six beads, each measuring 30-35 nm in diameter. In *H. erectus*, the VLPs varied from 80 to 350 nm in length and were composed of 2-8 aligned beads with diameters ranging from 36-42 nm. This morphotype was observed as isolated VLPs, attached to extracellular vacuole membranes in the sponge mesohyl, and within intracellular vacuoles of archaeocyte cells.

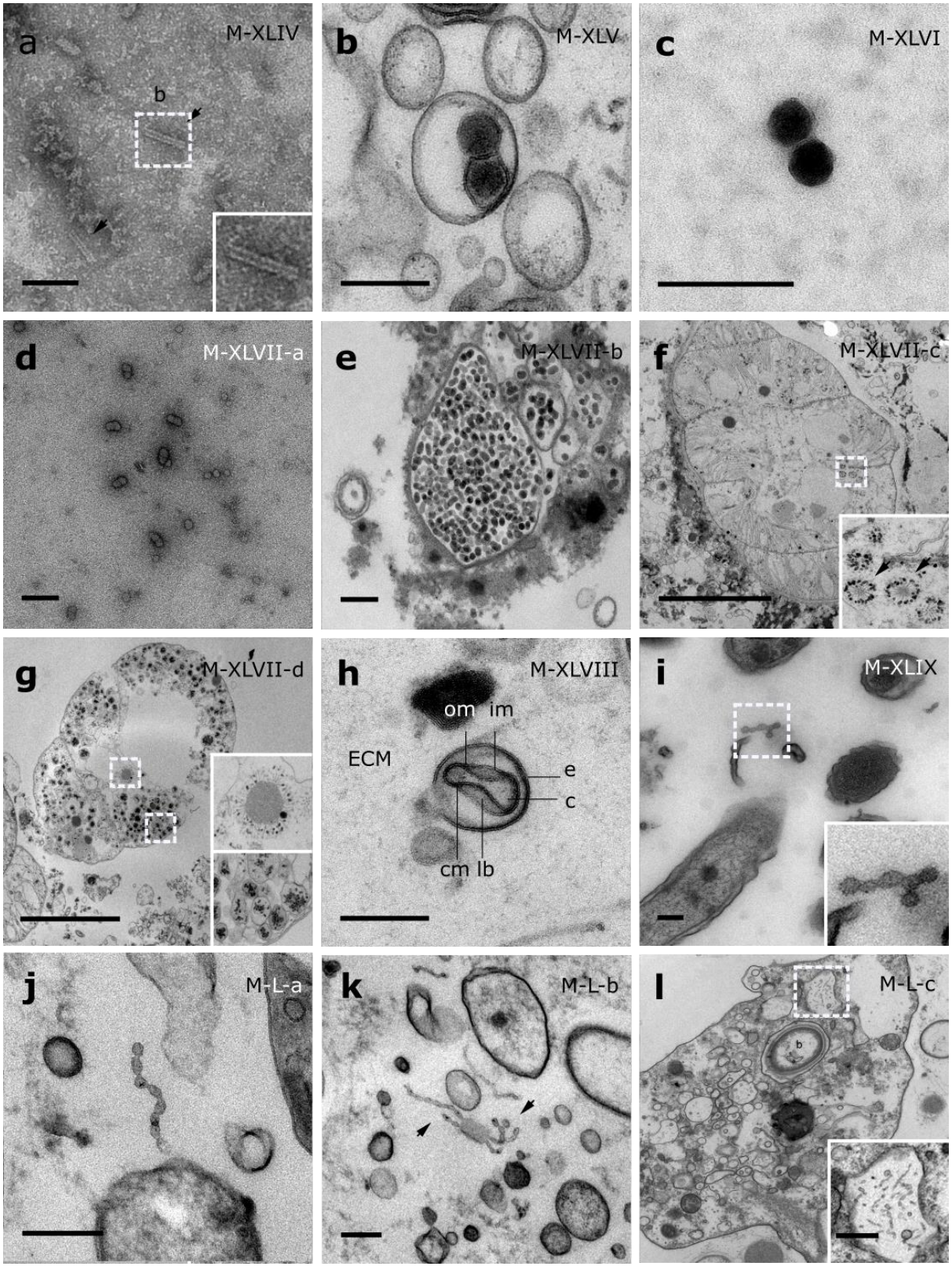

Figure 2.5 Representative morphotypes of virus-like particles associated with GBR and Red Sea sponges. GBR sponge species: (c) *L. herbacea*, (i) *C. foliascens*. Red Sea sponge species: (a, b, h) *C. cyathophora*, (d–g) *A. ochracea*, (j–l) *H. erectus*. TEM preparation method: (a, c, d) viral purification via filtration of sponge mucus, (b, e–l) ultrathin sections of sponge tissue. Scale bar: (d) 100 nm, (a–c, e, h–l) 200 nm, (f, g) 5 µm. ECM: External Cell Matrix, om: outer membrane, im: inner membrane, cm: core membrane, lb: lateral bodies; c: core, e: external membrane; b: bacterium. Black arrows indicate the VLPs.

2.5. DISCUSSION

Sponges are complex holobionts that host a diverse array of bacteria, archaea, and eukaryotic microorganisms (Fan et al., 2012, 2013; Webster & Thomas, 2016). Whilst previous publications have alluded to the potential importance of viruses in sponges (Claverie et al., 2009; Webster & Taylor, 2012; Laffy et al., 2016, 2018), including in sponge disease (Luter, Whalan & Webster, 2010), this study provides the first visual evidence that viruses are diverse components of the sponge holobiont. The broad range of VLP morphologies visualised across the 15 different sponge species is consistent with recent molecular data showing sponges harbour diverse communities of viruses.

The frequent detection of multiple viral morphotypes within a single sponge species most likely reflects the large number of potential hosts within the sponge holobiont (sponge cells, bacteria, archaea, microeukaryotes). However, it is also possible that multiple viruses infect the same host, as has been observed in some bacterioplankton (Holmfeldt et al., 2007) and corals (Thurber & Correa, 2011). Similarly, the same viral morphotype may infect multiple hosts within the holobiont, as recently highlighted from phage-bacteria network analyses (Flores et al., 2011; Flores, Valverde & Weitz, 2013). This is particularly relevant considering the role of viruses in lateral gene transfer between hosts and their subsequent effects on host metabolism (Breitbart et al., 2018). Observed viral morphotypes may also not be native to the holobiont, as some may have been extracted from the virioplankton by the sponge's aquiferous system. Although the isolation methods employed in this study unveiled a wide range of VLP morphotypes, no quantitative assessments were undertaken. To further our understanding of viral dynamics within the sponge holobiont, quantitative studies that count the number of VLPs per known tissue area, perform quantitative transmission electron microscopy (qTEM) (Brum, Schenck & Sullivan, 2013), flow cytometry (Brussaard, 2004b; Pollock et al., 2014) or fluorescent staining (Leruste, Bouvier & Bettarel, 2012; Pollard, 2012) should also be performed.

Morphology is an important feature for viral classification according the International Committee on Taxonomy of Viruses (ICTV). However, there are also some limitations associated with using TEM to identify viruses. For instance, many viral groups lack morphological structures that characterize them as typical viral particles by TEM. Also, as many viruses are small and simple they can be mistaken for non-viral particles such as cellular

vesicles or organelles. Although the assignment of viral-like particles in this study was made by comparison to morphologically characterised viruses, the possibility remains that some VLPs may not represent true viruses.

In this study, TEM analysis revealed a prevalence of polyhedral VLPs with characteristic bacteriophage morphology, consistent with what has been described for other marine invertebrates (Wilson et al., 2005; Davy et al., 2006; Davy & Patten, 2007; Patten, Harrison & Mitchell, 2008). The presence of *Caudovirales*-like morphotypes highlights the potential for these VLPs to target sponge symbionts and ultimately control microbial population dynamics within the sponge holobiont. Amongst them, a *Siphoviridae* VLP detected in the surface biofilm of *C. schulzei* presented similar morphology, although slightly smaller, to the previously described sponge-associated Phage ΦJL001 (Lohr, Chen & Hill, 2005).

Surprisingly, relatively few tailed bacteriophages were detected within the reef sponges, despite the dominance of *Caudovirales* within the assigned sponge viromes (Laffy et al., 2018). Although the dominance of tailed viruses in aquatic ecosystems is well characterised (Mizuno et al., 2013; Weynberg et al., 2017a; Thurber et al., 2017; Laffy et al., 2018), results from morphological analysis of uncultivated viruses vary with respect to the relative dominance of tailed (Cochlan et al., 1993; Colombet et al., 2006; Dutova & Drucker, 2013) versus non-tailed (Bergh et al., 1989; Wommack et al., 1992; Auguet, Montanié & Lebaron, 2006; Brum, Schenck & Sullivan, 2013) VLPs. The reduced number of tailed VLPs in morphological descriptions has been attributed to the destruction of the delicate VLP structures during centrifugation and TEM sample preparation (Cochlan et al., 1993; Proctor, 1997). However, Brum et al. (2013) have shown that sample preservation and preparation do not alter the morphological characteristics of seawater derived VLPs (Brum, Schenck & Sullivan, 2013) and non-tailed VLP have therefore been proposed as the dominant viral group in aquatic ecosystems (Brum, Schenck & Sullivan, 2013; Kauffman et al., 2018). Nevertheless, in this study, tailed VLPs were almost exclusively detected in samples purified via filtration of mucus or scraping of the external biofilm, the least disruptive of the three TEM preparation methods. This suggests that tailed VLPs are either more abundant on the external surface of the sponge or that TEM preparation method could bias the detection of tailed VLPs in sponges by mechanically damaging or distorting viral structures.

Filamentous viral-like particles (FVLP) were detected in both prokaryotic and eukaryotic cells within the sponge holobiont. In *C. foliascens*, multiple individual *Inoviridae*-like VLPs were observed attached to the surface of cyanobacteria, although no virions were observed inside the cells. The absence of intracellular FVLPs combined with the absence of a dense core in these morphotypes provides further support for their classification as putative *Inoviridae*, as the replication mechanism of this viral family often relies on the virus injecting its DNA into the host cell and getting extruded without inducing cell lysis (Bayer & Bayer, 1986; Russel, 1991; Ploss & Kuhn, 2010). A previous study demonstrated that temperate viruses are relatively less abundant within host cells at high density (McDaniel et al., 2002).

FVLPs with helicoidal symmetry resembling *Spiraviridae* were detected in the sponge *C. cyathophora*, with this viral family known to infect Archaea (Mochizuki et al., 2012). FVLPs were also observed infecting eukaryotic cells in *X. testudinaria*. Abundant elongated and flexible FVLPs were also detected in the archaeocytes and extracellular mesohyl matrix of *X. testudinaria* (Fig. 2.4j-l). The point of host cell lysis was captured with a recently burst cell releasing virions into the extracellular matrix (Fig. 2.4-k), characteristic of typical lytic viral infection (Dyson et al., 2015). Morphologically similar filamentous VLPs have been detected in coral mucus and associated *Symbiodinium* and were characterised as a coral-infecting RNA virus ((Davy et al., 2006; Weynberg et al., 2017b). There is a general lack of studies investigating filamentous viruses in marine invertebrates, although metaviromic sequencing recently detected sequences assigned as filamentous viruses of the family Inoviridae in Great Barrier Reef sponges (Laffy et al., 2018).

VLPs morphologically consistent with viruses from the family *Geminiviridae* were observed in association with cyanobacteria in the sponge *A. ochracea*. *Geminiviridae*-like viruses have been isolated from infected freshwater cyanobacteria (Li, Ou & Zhang, 2013), and, with the exception of being slightly smaller (79 ± 5 nm in length, 28 ± 3 nm in diameter), the geminate VLPs from *A. ochracea* were morphologically similar. Most infected cyanobacterial cells had dense populations of these VLPs (Fig. 2.5d-g), although no lysed cells or free geminate VLPs were observed in the sponge mesohyl. However, several extracellular vesicles containing VLPs were observed, indicating that VLPs could use cell extrusion as part of their reproductive cycle. A geminate VLP has previously been isolated from mucus secreted by scleractinian corals (Davy & Patten, 2007), however the morphology differs from the *A. ochracea* VLP, since

it is notably bigger (about 145 nm in length, 82nm width), with each isomer being wider than they are long, contrasting with the isomer dimensions in the *A. ochracea* VLP. Beaded VLPs were also detected in sponges and their non-isomeric particles comprising a flexible filament strongly resembled the beaded VLPs previously reported from scleractinian corals (Davy & Patten, 2007; Lawrence et al., 2015).

Brick-shaped VLPs closely resembling viral morphotypes from the family *Poxviridae* were observed within the mesohyl of *Crella cyathophora*, a (Fig. 2.5h). Typical of enveloped viruses, poxviruses use their envelopes to connect and fuse with their host membrane so that the viral capsid is injected directly into the host cell (Moss, 2012). Poxviruses are notable pathogens, infecting a wide host range among vertebrate and invertebrate taxa (Bracht et al., 2006; Haller et al., 2014; Grasis et al., 2014) In the marine environment, they have been reported associated with cetaceans and pinnipeds (Bracht et al., 2006) and more recently, analysis of sponge metaviromes detected sequences affiliated to *Poxviridae* in *Amphimedon queenslandica* and *Ianthella basta* (Laffy et al., 2018).

2.6. CONCLUSION

In this study we validated the efficacy of three different methods for TEM imaging of sponge-associated viruses: i) ultrathin sections of sponge tissue, ii) purification via density gradient ultracentrifugation and iii) ectoderm scraping and filtration of sponge mucus. While density gradient purification facilitated concentration and recovery of VLPs from different areas of the sponge holobiont, it also co-concentrated cellular debris, potentially masking many VLPs. Tissue sectioning enabled direct visualisation of spatial localisation and host-viral interactions but was labour intensive and some VLP structures were distorted during sectioning. Ectoderm scraping and collection of sponge mucus was most effective at preserving delicate viral structures and minimizing the amount of cellular debris, however, it was restricted to recovering VLPs associated with the sponge mucus or ectoderm.

This first morphological characterisation of sponge-associated viruses revealed a wide diversity of VLPs infecting both the sponge cells and symbiont compartments of the holobiont. By confirming that viruses are a significant component of the sponge holobiont, this work paves the way for future metaviromic and cell culturing analyses that can characterise the taxonomy and function of the sponge viral community.

Chapter 3. VIRAL ECOGENOMICS ACROSS THE PORIFERA

3.1. ABSTRACT

Viruses directly affect the most important biological processes in the ocean via their regulation of prokaryotic and eukaryotic populations. Marine sponges form stable symbiotic partnerships with a wide diversity of microorganisms and this high symbiont complexity makes them an ideal model for studying viral ecology. Here we used morphological and molecular approaches to illuminate the diversity and function of viruses inhabiting nine sponge species from the Great Barrier Reef and seven from the Red Sea. Metaviromic sequencing revealed host-specific and site-specific patterns in the viral assemblages, with all sponge species dominated by the bacteriophage order Caudovirales but also containing variable representation from the nucleocytoplasmic large DNA virus families *Mimiviridae, Marseilleviridae, Phycodnaviridae, Ascoviridae, Iridoviridae, Asfarviridae and Poxviridae*. While core viral functions related to replication, infection and structure were largely consistent across the sponge metaviromes, functional profiles varied significantly between species and sites largely due to differential representation of auxiliary metabolic genes (AMGs), including those associated with herbicide resistance, heavy metal resistance and nylon degradation. Furthermore, AMGs varied with the composition and abundance of the sponge-associated microbiome. For instance, AMGs associated with antimicrobial activity were enriched in low microbial abundance sponges, AMGs associated with nitrogen metabolism were enriched in high microbial abundance sponges and AMGs related to cellulose biosynthesis were enriched in species that host photosynthetic cyanobacteria. These results are consistent with our current understanding of sponge ecology and highlight the diverse functional roles that viruses can play in the marine sponge holobiont.

3.2. INTRODUCTION

Marine sponges (phylum Porifera) are an ecologically important component of the benthos, providing habitat for a diverse array of macro and microorganisms and mediating biogeochemical fluxes by filtering organic matter and facilitating the consumption and release of nutrients (Bell, 2008). As suspension feeders, sponges can filter up to 100, 000 times their own body volume in seawater every day (Weisz, Lindquist & Martens, 2008), which influences

the composition of the seawater at macro and micro scales (Thomassen & Riisgård, 1995; Patterson et al., 1997; Leys & Eerkes-Medrano, 2006). Sponges efficiently extract picoplankton, bacteria and archaea (Ribes, Coma & Gili, 1999), and can also retain viral-sized particles (Hadas et al., 2006). Moreover, most sponge species host diverse and stable communities of microbial symbionts, which contribute to a variety of host metabolic processes and produce a suite of secondary metabolites (Steindler, Beer & Ilan, 2002; Taylor et al., 2007b,a; Wilson et al., 2014). Although the complexity and composition of the microbiome varies across different sponge species, frequently enriched microbial phyla include the *Proteobacteria* (classes Alpha- and *Gammaproteobacteria*), *Actinobacteria*, *Chloroflexi*, *Nitrospirae* and *Cyanobacteria*, with *Thaumarchaea* being the major sponge-associated archaeal taxa (Thomas et al., 2016). Additionally, the microbiome of cosmopolitan sponges, such as *Carteriospongia foliascens* and *Xestospongia testudinaria,* often shows biogeographic distinctions, likely responding to environmental variations (Luter et al., 2015; Swierts, Cleary & de Voogd, 2018). Sponges and their complex communities of microbial symbionts are therefore a typical example of a 'meta-organism' or 'holobiont' (Margulis, 1981; Bosch & McFall-Ngai, 2011). However, while sponge-microbial interactions have been extensively studied over the past decades (Webster & Taylor, 2012; Gloeckner et al., 2014; Thomas et al., 2016; Lurgi et al., 2019), viruses represent the 'dark matter' in these ecologically important symbioses.

Viruses are recognised as the most abundant entity in marine environments, likely infecting all organisms in the ocean (Suttle, 2005; Thurber et al., 2009a) and directly affecting energy flux in marine food webs via their regulation of prokaryotic and eukaryotic populations (Fuhrman, 1999; Weinbauer, 2004; Roux et al., 2015b). Despite the critical role of viruses in marine ecosystems, we are only just beginning to describe their diversity and contributions to host ecology. This is particularly important considering the recently recognised role of phages in manipulating their bacterial hosts due to alteration of host metabolism via auxiliary metabolic genes (AMGs) (Breitbart et al., 2018).

Viral-like particles (VLPs) in sponges were first reported from transmission electron micrographs in 1978 (Vacelet & Gallissian, 1978), however it wasn't until 2016 that computational tools were optimised to explore sponge- associated viruses using metagenomic sequencing (Laffy et al., 2016). A subsequent comparative metagenomic

analysis of coral and sponge-associated viruses revealed high intra species similarity in the viromes of four sponge species, with communities dominated by dsDNA bacteriophages of the order Caudovirales, and a diverse community of ssDNA viruses of the family *Microviridae* (Laffy et al., 2018). Viruses belonging to the order Megavirales were also consistently observed, including members of the *Mimiviridae*, *Phycodnaviridae* and *Poxviridae* families (Laffy et al., 2018). AMGs involved in cobalamin biosynthesis and herbicide resistance were detected in the viromes of these reef sponges (Laffy et al., 2018). To assess the ubiquity of these patterns and investigate how these viruses contribute to host ecology, we undertook deep metaviromic sequencing of 15 representative sponge species (Fig. 3.1) from two coral reef ecosystems, the Great Barrier Reef and the Red Sea.

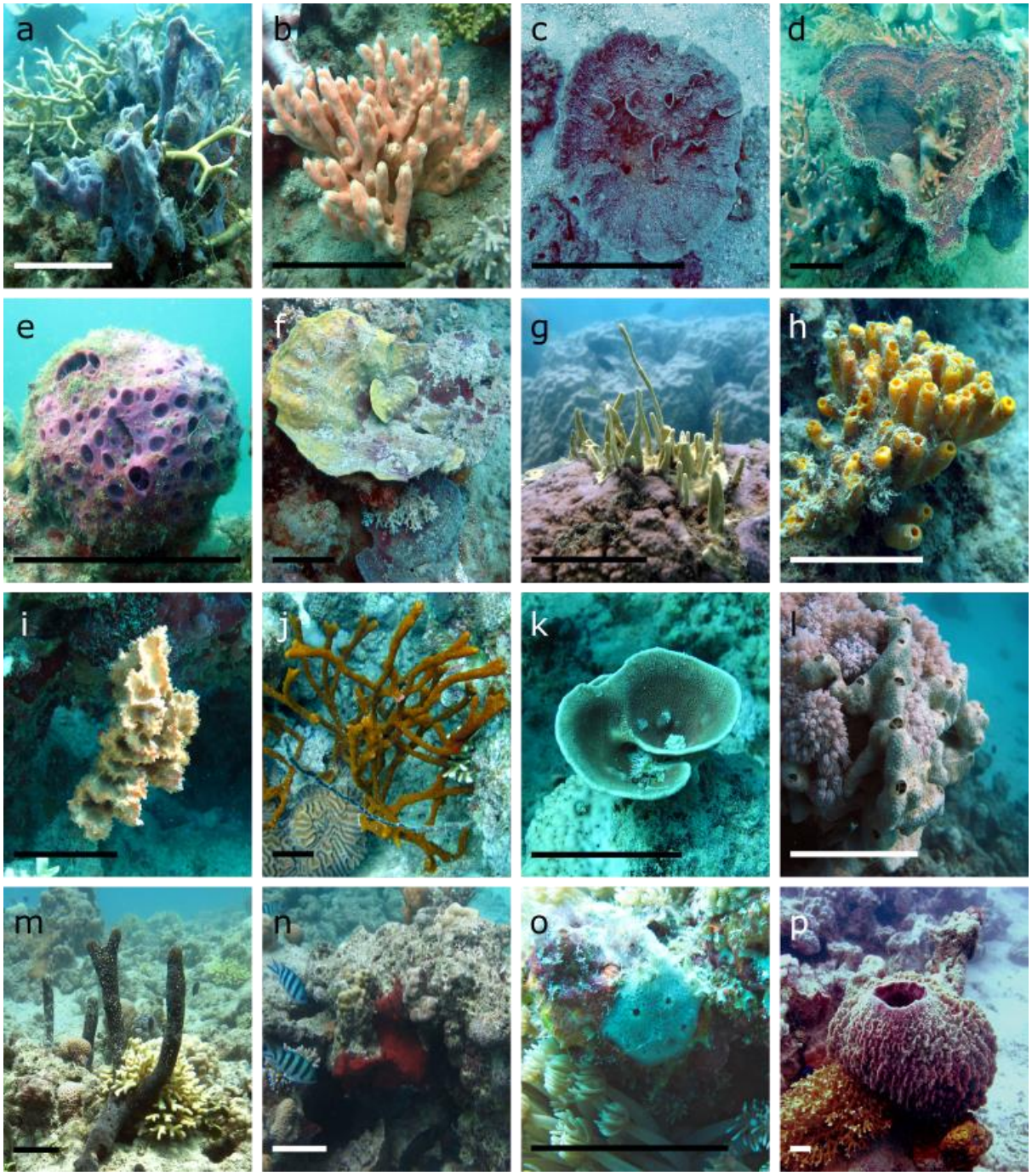

Figure 3.1 Sponge species used for metaviromic analysis in the GBR and Red Sea: GBR sponges included (a) *Callyspongia* sp., (b) *Echinochalina isaaci*, (c) *Carteriospongia foliascens*, (d) *Ianthella basta*, (e) *Cinachyrella schulzei*, (f) *Cymbastella marshae*, (g) *Lamellodysidea herbacea*, (h) *Pipestela candelabra*, (i) *Stylissa carteri*; and the Red Sea sponges included: (j) *Amphimedon ochracea*, (k) *Carteriospongia foliascens*, (l) *Crella cyathophora*, (m) *Hyrtios erectus*, (n) *Mycale* sp., (o) *Niphates* sp., (p) *Xestospongia testudinaria*. Scale bar = 10 cm.

3.3. METHODS

3.3.1. Sample collection

As sampling criteria, we opted for collecting sponge species that represented the dominant sponge fauna (Allen, 2008; Sonnewald & El-Sherbiny, 2017) (Hooper, Kennedy & Quinn, 2002; Ilan, Gugel & Van Soest, 2004) at two distinct biogeographical regions with varying levels of anthropogenic impact. Triplicate samples of nine coral reef sponges species - *Callyspongia* sp., *Carteriospongia foliascens*, *Cinachyrella schulzei*, *Cymbastella marshae*, *Echinochalina isaaci*, *Ianthella basta*, *Lamellodysidea herbacea*, *Pipestela candelabra*, *Stylissa carteri* were collected from Orpheus Island, Queensland, Australia (18°35'34''S, 146°28'53"E) and seven sponge species - *Amphimedon ochracea*, *Carteriospongia foliascens*, *Crella cyathophora*, *Hyrtios erectus*, *Mycale* sp., *Niphates rowi*, *Xestospongia testudinaria* were collected in Al Fahal, Saudi Arabia (22°13'95"N, 39°01'81"E), between December 2015 and February 2016 (Fig 3.1; Supplementary Table 3.1). Sponges were collected on SCUBA between three and fifteen meters depth. All specimens were photographed *in situ* before being individually placed in sterile tubes and immediately transferred on ice to the laboratory for purification of viral particles. A seawater sample was collected from each sampling location (n=1 x 20l) as a comparative reference for the sponge samples. Seawater was collected using sterile containers and stored at 4°C for 2-24 hours prior to being filtered through a 0.22 µm Sterivex polyethersulfone filter.

3.3.2. Viral concentration and purification

Isolation and purification of sponge viruses was performed using a modified version of the protocol designed to isolate VLP from culture lysates and coral tissue (Lawrence & Steward, 2010; Weynberg et al., 2014). Approximately 25 g of fresh sponge tissue was cut into small pieces (5 mm), covered with 15 µl of 0.02 µm filter-sterilized (Whatman Anotop, Merck, Darmstadt, Germany) SM buffer (100 mM NaCl, 8 mM $MgSO_4$, 50 mM Tris pH 7.5), and homogenized with a Craig's HS30E homogenizer (Witeg, Wertheim, Germany) for 5 to 10 minutes (min). Tissue homogenates were filtered through a Falcon 100 µm Cell Strainer (Corning, New York, NY, USA), then centrifuged at 500 g for 15 min at 4°C to pellet the majority of cellular debris. Supernatant density was brought to 1.2 g ml^{-1} with the addition of Cesium Chloride (CsCl). In parallel, different density CsCl solutions in 0.02 µm filtered SM Buffer, were layered in the ultracentrifuge tube (3 mL of 1.6 g ml^{-1} solution; 2.5 ml of 1.45 g ml^{-1} solution;

2.5 ml of 1.3 g ml^{-1} solution; 2 ml of 1.2 g ml^{-1} solution). A 7.5 ml aliquot of each sample was dispensed on top of three gradient tubes (2.5 ml per tube), and centrifuged (Beckman Coulter Ultracentrifuge, Brea, CA, USA) in a swinging-bucket rotor (SW 40 Ti) for 2h 40 min at 40,000 g, at 4°C. Following centrifugation, the tube content was fractionated by density into eighteen fractions. The density and nucleic acid concentration of each fraction was determined (Weynberg et al., 2014) and the fractions with density between 1.2 g/ml and 1.5 g/ml were pooled together and filtered (0.22 µm EMD Millipore filter, Merck) to remove any remaining cellular contamination. Buffer exchange was performed to remove the CsCl salt from the samples by loading each sample into a 30 KDa Amicon centrifugal spin column (Millipore), centrifuging at 4000 g for 30 min at 4°C, discarding the flow-through and repeating this operation four to six times to ensure complete exchange of CsCl into filter-sterilised SM buffer. A final centrifugation step resulted in the concentration of VLPs into a 600 µl solution of filter-sterilised SM buffer. In total, 200 µl of this solution was used for DNA extraction. Viruses were purified from seawater using Tangential Flow Filtration (30 kDa, Pall Corporation, New York, NY, USA) (Sun et al., 2014), by concentrating viruses from 20 l of pre-filtered (0.22 µm EMD Millipore filter) seawater into 20 ml seawater solution. Diafiltration was performed to replace seawater with SM buffer and samples were concentrated to a final volume of 500 µl using Amicon centrifugal spin columns (30kDa, Millipore) as described above.

3.3.3. Viral DNA extraction and amplification for sequencing.

To degrade any free nucleic acid residing outside the viral capsid, purified viral samples were treated with DNase and RNase (Ambion, Thermo Fisher Scientific, Waltham, MA, USA) prior to DNA extraction according to Manufacturer's instructions. DNA was extracted using the FastDNA SPIN Kit for Soil (MP Biomedicals, Santa Ana, CA, USA) following the Manufacturer's instructions. A modified Random Priming-mediated Sequence-Independent Single-Primer Amplification (RP-SISPA) approach was used to amplify viral DNA fragments (Weynberg et al., 2014). Briefly, viral DNA was converted to dsDNA using a Klenow Fragment (3'–5' exo-) using RP-SISPA primers with a 3' random hexamer sequence. Eight µl of DNA was added to 6 µl of reaction mix containing 1.5 µl of 10× NEB buffer (New England Biolabs. Ipswich, MA, USA); 1 µl of 2.5 mM dNTPs; 1.5 µl of primer FR26RV-N (GCCGGAGCTCTGCAGATATCNNNNNN, 10µM stock) and 2µl of DNase-free distilled water. Reactions were incubated at 94°C for 3 min,

placed on ice for 3 min (primer annealing) before 1 µl of Klenow Fragment was added to the mix and incubated at 37°C for 60 min. After incubation, 1 µl of dNTP and 1 µl of N primer was added to each tube, samples were incubated at 94°C for 3 min and placed on ice for 3 min. Lastly, 1 µl of Klenow was added to the solution and the reaction was incubated at 37°C for 60 min then terminated at 75°C for 20 minutes. Triplicate PCR amplifications were performed using the SISPA template. Two µl of template was added to 23 µl of reaction mix containing 2.5 µl of 10× reaction buffer, 4 µl of dNTP (2.5 mM stock), 2 µl of FR20RV primer (GCCGGAGCTCTGCAGATATC, 10µMstock) and 0.25 µl of TaKaRa LA HS Taq polymerase (5 U/µl, Scientifix, South Yarra, VIC, Australia). Reactions were incubated at 95°C for 10 min, followed by 30 amplification cycles (95°C for 30 sec, 60°C for 60 sec, 72°C for 90 sec) and a final hold at 72°C for 13 min to enable completion of complementary strand synthesis. PCR reactions were loaded onto a 0.8% agarose gel in 1×TAE at 100V for 30 min. Amplifications with no visible PCR product were repeated by diluting the SISPA template 10 or 100 times. A reconditioning PCR was performed after pooling triplicate reactions to avoid sequencing artifacts (Thompson, 2002). 10 µl of pooled template was added in 90 µl of mix containing 55.25 µl of PCR water, 10 µl 10× reaction buffer, 16 µl dNTP (2.5mM stock), 8 µl FR20RV primer (10µMstock) and 0.75 µl TaKaRa LA HS Taq. Reactions were incubated as per the PCR amplification protocol and cleaned using the MinElute PCR Purification Kit (Qiagen, Hilden, Germany). Samples were run on a 0.8% agarose gel in 1×TAE at 100V for 30 min and DNA quality (260:280 ratios) was assessed on a NanoDrop 2000 (Thermo Fisher Scientific).

3.3.4. Viral DNA sequencing and bioinformatic analysis

All purified viral DNA was sequenced using TruSeq SBS kit V4 s125 bp fragments paired-end sequencing (Illumina) at the Bioscience Core Lab at the King Abdullah University of Science and Technology- KAUST, Thuwal, Saudi Arabia.

Sequence data was analysed based on the HoloVir protocol (Laffy et al., 2016), a computational workflow designed for assigning taxonomy and function to host-associated viruses. Quality control (QC) was performed on raw sequence data using CLC Genomic Workbench version 9.0 (Cambridge, MA, USA), where library adaptors, ambiguous nucleotides (n=2) and low-quality bases (0.01) were trimmed and reads below 40 bp were discarded. Viral metagenomes were assembled from the trimmed sequences using the De Novo Assembly function in CLC Genomic Workbench. Contigs smaller than 500 bp in length

or with an average coverage-value below 3 were discarded. Gene prediction was performed on the contigs using MetaGeneAnnotator (Noguchi, Taniguchi & Itoh, 2008). Predicted genes were used for viral taxonomic assignment and functional annotation. Taxonomic assignment was performed using MEGAN6 (Huson et al., 2011), utilising BLAST analysis to search for homology between predicted gene data and the known viral reference genome within the NCBI RefSeq database (Pruitt, Tatusova & Maglott, 2007). MEGAN6 was run using a top-percent parameter of 80, min-support value of five reads and a bit score threshold value of 80. Assembled data was also compared to the HoloVir cellular and viral marker database to identify any cellular contamination (Laffy et al., 2016). Viral taxonomic classification was based on a lowest common ancestor scoring system using the best significant matches to viral reference sequences. However, it is important to acknowledge that mismatches may occur as a consequence of limited availability of adequate viral reference sequences.

Functional analysis of predicted genes was performed as described in the HoloVir protocol (Laffy et al., 2016), utilising BLASTP sequence similarity searches of predicted genes against the Swiss-Prot manually curated UniprotKB protein database (UniProt Consortium, 2015), using an *e*–value cutoff of 10^{-10} a cutoff range specifically chosen to capture and identify functional homology (Pearson, 2013). Swiss-Prot Keywords were assigned to each predicted gene based on the best significant BLASTP match. Overall keyword enrichment for each metavirome was calculated by adjusting for both contig coverage as well as keyword frequency within the Swiss-Prot database.

3.3.5. Data analyses

Permutational multivariate analysis of variance (PERMANOVA) was performed to identify significant differences in viral community composition and functional profiles between host species, sampling sites, host nutritional mode and microbial abundance. To visualise sample separation according to these host features, Non-metric Multidimensional Scaling (MDS) analyses were performed using Hellinger-transformed data to compare the viral community and viral function based on Bray-Curtis dissimilarity matrix using Primer v 6.1.7 (PRIMER-E Ltd., Plymouth, UK). Univariate tests to identify drivers of functional differences between each category were performed using the R package mvabund (Wang et al., 2012).

3.3.6. Data availability

The data that support the findings of this study are available on the GenBank website https://www.ncbi.nlm.nih.gov/genbank through the accession numbers SAMN09948703-SAMN09948748.

3.4. Results and Discussion

3.4.1. Community profile of the sponge virome

In total, 575,118 contigs were assembled and 1,162,879 genes were predicted (Table 1; Supplementary table 3.1). On average, 19.24% of all predicted genes were taxonomically assigned and 27.29% of all contigs contained at least one taxonomically assigned gene (Table 1; Supplementary Table 3.1). Cellular marker evaluation identified that an average of 0.25% of contigs contained cellular marker matches (Table 1; Supplementary Table 3.1), comparable to a previous study which reported that host-associated viromes with 0.1-0.3% of contigs containing cellular marker matches could be characterised as having negligible or low-level cellular contamination (Laffy et al., 2018).

Table 3.1 Summary of sampling locations, sequencing statistics and cellular contamination evaluation of virome datasets. N50 values for each dataset were calculated based on evaluation of unfiltered contigs. * The raw reads values are presented in million of reads.

Host species	Sampling site	# raw reads*	Contig N50	# contigs	Longest contig	# predicted genes	% Taxonomically assigned genes	% Taxonomically assigned contigs	% of contigs with cellular marker matches
***Callyspongia* sp. rep.1**	*GBR*	11.06	899	23,339	58,159	63,281	23.5	38.7	0.0
***Callyspongia* sp. rep.2**	*GBR*	9.36	932	20,309	172,832	56,308	23.6	38.5	0.0
***Callyspongia* sp. rep.3**	*GBR*	8.97	810	21,236	69,654	56,363	24.0	38.2	0.0
***C. foliascens* rep. 1**	*GBR*	4.92	675	33,078	24,096	57,288	13.2	18.7	0.4
***C. foliascens* rep. 2**	*GBR*	1.78	698	14,225	46,996	25,768	11.0	16.6	2.1
***C. foliascens* rep. 3**	*GBR*	15.28	624	45,237	23,964	76,516	13.0	18.5	0.8
***C. schulzei* rep. 1**	*GBR*	7.95	467	9,621	80,905	17,001	14.8	19.2	0.9
***C. schulzei* rep. 2**	*GBR*	8.23	571	12,170	81,025	26,002	17.5	24.2	1.3
***C. schulzei* rep. 3**	*GBR*	19.59	660	50,864	80,778	95,389	14.4	17.1	0.1
***C. marshae* rep. 1**	*GBR*	1.53	434	4,549	9,804	7,975	16.2	26.0	1.2
***C. marshae* rep. 2**	*GBR*	3.75	398	5,419	7,498	6,585	16.6	18.2	0.6
***C. marshae* rep. 3**	*GBR*	3.12	405	6,751	12,455	10,427	16.1	22.0	0.5
***E. isaaci* rep. 1**	*GBR*	4.20	566	11,349	31,106	21,794	22.5	34.7	0.3
***E. isaaci* rep. 2**	*GBR*	4.50	510	13,898	49,604	28,567	23.3	35.2	0.1
***E. isaaci* rep. 3**	*GBR*	1.26	694	4,752	42,237	11,022	21.8	34.7	0.1
***I. basta* rep. 1**	*GBR*	6.58	504	11,600	60,819	24,285	19.3	30.7	0.1

***I. basta* rep. 2**	*GBR*	4.63	495	12,591	39,149	23,850	22.2	34.1	0.0
***I. basta* rep. 3**	*GBR*	4.83	552	14,561	36,340	28,801	20.8	32.2	0.0
***L. herbacea* rep. 1**	*GBR*	7.96	457	11,693	43,955	21,907	20.2	31.4	0.1
***L. herbacea* rep. 2**	*GBR*	14.88	594	9,661	14,898	18,144	19.2	30.5	0.2
***L. herbacea* rep. 3**	*GBR*	3.02	504	16,931	43,769	30,283	20.2	30.5	0.2
***P. candelabra* rep. 1**	*GBR*	12.20	693	35,688	49,806	32,910	15.0	11.8	0.8
***P. candelabra* rep. 2**	*GBR*	7.74	557	27,010	58,681	48,732	14.4	20.0	1.2
***P. candelabra* rep. 3**	*GBR*	5.87	958	13,373	120,555	29,643	18.2	25.3	1.6
***S. carteri* rep. 1**	*GBR*	6.34	346	4,063	10,851	5,709	17.6	20.2	0.0
***S. carteri* rep. 2**	*GBR*	4.78	384	7,833	16,548	13,143	21.9	29.0	0.0
***A. ochracea* rep. 3**	Red Sea	3.38	720	7,706	26,892	18,040	25.6	40.9	0.7
***A. ochracea* rep. 1**	Red Sea	14.14	717	29,033	61,876	71,543	23.2	35.7	0.2
***A. ochracea* rep. 2**	Red Sea	2.79	694	7,692	20,756	10,981	21.1	15.8	0.4
***C. foliascens* rep. 1**	Red Sea	2.30	1,671	2,571	35,948	7,096	20.7	38.9	1.6
***C. foliascens* rep. 2**	Red Sea	1.64	1,135	3,913	49,410	10,708	19.7	33.6	1.7
***C. foliascens* rep. 3**	Red Sea	1.82	1,280	2,787	38,097	7,284	21.4	39.6	1.4
***C. cyathophora* rep. 1**	Red Sea	3.19	601	2,757	19,321	8,636	25.6	55.5	0.6
***C. cyathophora* rep. 2**	Red Sea	3.58	618	2,613	39,999	5,753	24.9	37.9	0.1
***C. cyathophora* rep. 3**	Red Sea	1.84	614	3,977	44,834	7,951	21.5	32.7	0.7
***H. erectus* rep. 1**	Red Sea	18.37	921	6,400	7,865	17,674	21.8	39.6	0.6
***H. erectus* rep. 2**	Red Sea	6.04	878	9,540	47,148	25,550	23.9	40.3	0.4
***Mycale* sp. rep. 1**	Red Sea	5.81	949	5,396	39,546	13,458	16.1	29.4	0.8
***Mycale* sp. rep. 2**	Red Sea	5.74	705	9,562	54,476	22,104	22.7	36.5	0.5
***Mycale* sp. rep. 3**	Red Sea	5.06	682	6,123	22,927	13,601	20.2	33.1	0.9
***N. rowi* rep. 1**	Red Sea	2.40	668	6,058	25,175	13,766	27.5	40.2	0.5
***N. rowi* rep. 2**	Red Sea	7.35	922	10,017	52,589	27,503	24.0	41.7	0.5
***X. testudinaria* rep. 1**	Red Sea	6.13	881	7,533	103,486	20,344	16.2	29.1	0.6
***X. testudinaria* rep. 2**	Red Sea	7.40	729	9,639	74,732	23,194	17.1	29.0	0.4
Sea water - GBR	GBR	21.64	406	11,008	20,625	19,950	22.0	32.2	1.2
Sea water - RS	Red Sea	9.51	523	10,568	52,589	36,395	35.1	75.1	0.1

Sponge-derived viral sequences predominantly matched dsDNA viruses (88%), with a lower relative abundance of matches to ssDNA viruses (9%) and retroviruses (3%) (Fig. 3.2; Supplementary Table 3.2). In particular, matches to the tailed bacteriophage order Caudovirales, including representatives of the *Podoviridae*, *Siphoviridae* and *Myoviridae*, accounted for more than 80% of total viral taxonomic assignments (Fig. 3.2; Supplementary Table 3.2). The Caudovirales infect a wide range of bacteria and archaea (Ackermann & Kropinski, 2007), are the most abundant viruses in marine environments (Breitbart, 2012), and have been reported to dominate the virome of numerous other coral reef species (Patten, Harrison & Mitchell, 2008; Wood-Charlson et al., 2015; Correa et al., 2016; Weynberg et al., 2017a; Thurber et al., 2017; Laffy et al., 2018). The predominance of bacteriophage matches

within the sponge metaviromes reflects the enormous abundance of microorganisms residing within the sponge holobiont, with as many as 10^9 symbiont cells per cm^3 of sponge tissue (Reiswig, 1981; Webster & Hill, 2001; Hoffmann et al., 2005). The detection of retroviruses is not uncommon in metaviromic studies targeting DNA viruses (Willner et al., 2009; Wood-Charlson et al., 2015; Correa et al., 2016; Laffy et al., 2018), and is possible because transcribed retroviral DNA can be present within retrovirus capsids, and this DNA can make up to 2.5% of the total virus nucleic acid (Byers et al., 1979).

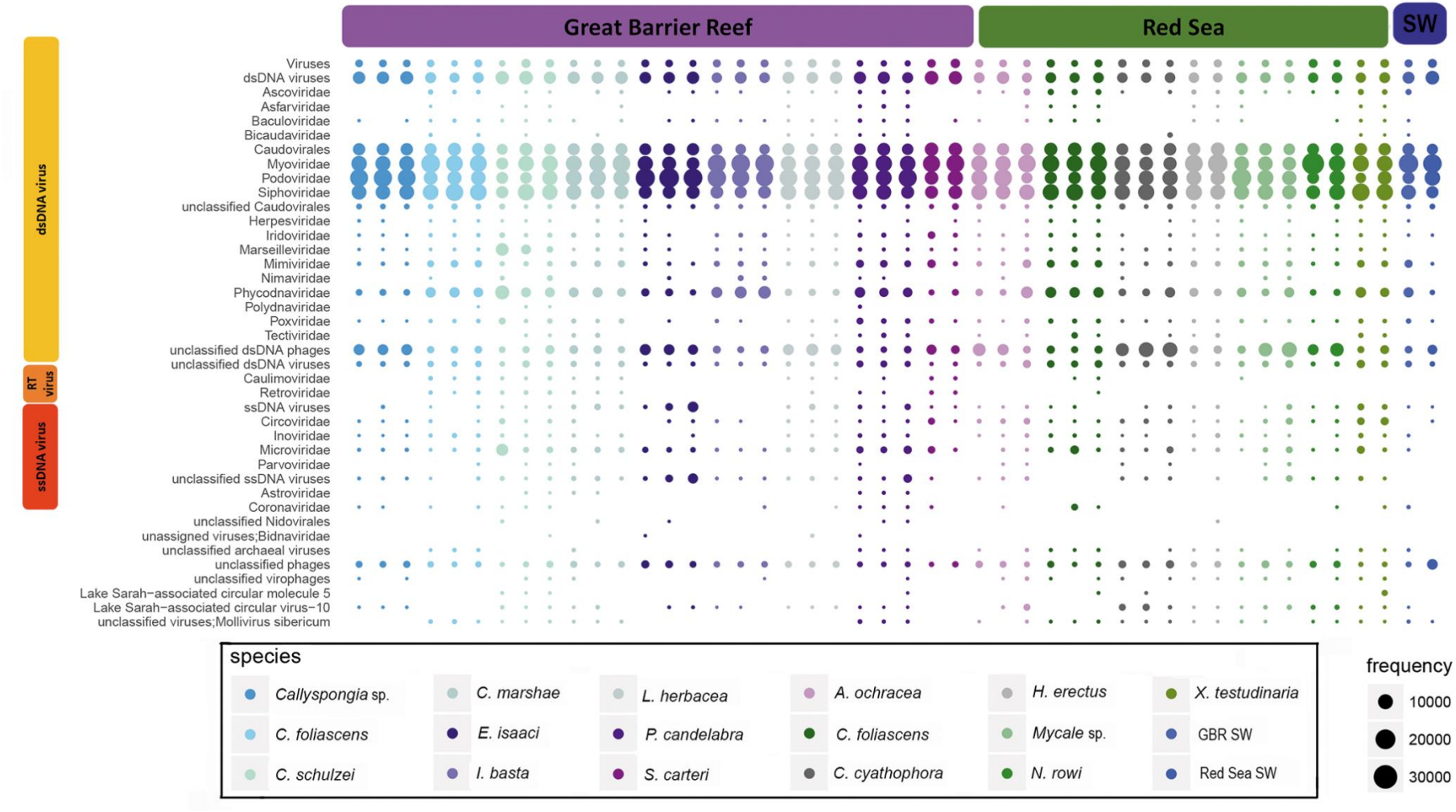

Figure 3.2 Taxonomic summary of the viral communities for fifteen sponge species from the Great Barrier Reef and the Red Sea. Taxonomy is summarised at the family level based on MEGAN6 LCA assignment using parameters defined in Laffy et al., 2016.

Contigs taxonomically assigned to viral families that typically infect eukaryotes were also prevalent in sponges, particularly representatives of the nucleocytoplasmic large DNA virus (NCLDV) families *Mimiviridae*, *Marseilleviridae*, *Phycodnaviridae*, *Ascoviridae*, *Iridoviridae*, *Asfarviridae* and *Poxviridae*. However, the presence and relative abundance of NCLDV assignments varied across sponge species (Fig. 3.2). *Mimiviridae* and *Marseilleviridae* are giant viruses that typically infect amoebae (Scola, 2003). While the sponge amoeba-like cells (amoebocytes and archaeocytes (Claverie et al., 2009)) may host these NCLDV, giant viruses also associate with marine cnidarians, echinoderms and protochordates that lack typical amoebocyte cells (Wegley et al., 2007; Thurber & Correa, 2011; Grasis et al., 2014; Wood-Charlson et al., 2015; Leigh et al., 2018; Laffy et al., 2018) . The high relative abundance of Mimiviruses in marine waters (Monier, Claverie & Ogata, 2008) combined with their large genome sizes (~1.2 Mbp) may explain their prevalence in the sponge metaviromes. Conversely, sponge-derived Mimivirus-like contigs have low diversity and high species-specificity (Laffy et al., 2018), suggesting that the giant virus signature in sponges does not originate from seawater.

Matches to *Phycodnaviridae* were consistently detected across all fifteen sponge species (Fig. 3.2). This viral family typically infects algae and cyanobacteria (Yau et al., 2011) and has been reported from cnidarian, arthropod, echinoderm and urochordate holobionts (Hingamp et al., 2013; Wood-Charlson et al., 2015; Weynberg et al., 2017a). In sponges, the *Phycodnaviridae* are likely targeting the associated photosymbionts, as cyanobacteria occur at high abundance in many of these sponge species (Webster et al., 2013a). Another NCLDV family detected in the viromes of all sponge species was the *Poxviridae* (Fig. 3.2). *Poxviridae* and the viral families *Ascoviridae*, *Iridoviridae* and *Asfarviridae* are associated with a wide range of invertebrate hosts (Bracht et al., 2006; Williams, 2008; Weynberg et al., 2014; Grasis et al., 2014; Gudenkauf & Hewson, 2016). The detection of *Poxviridae*-like viruses in marine sponges suggests an extension of their previously known host range, although cellular infection in sponges still needs to be validated. The NCLDV group of viruses pose considerable systematic and interpretative challenges due to horizontal gene transfer between different NCLDVs and their hosts, which can make taxonomic assignment hard to resolve (Iyer, Aravind & Koonin, 2001).

Matches to the ssDNA viral families *Microviridae*, *Circoviridae* and *Inoviridae* were evident in most sponge species whereas the *Parvoviridae* and *Bidnaviridae* had a more restricted distribution and lower intra-species similarity than other viral taxa (Fig. 3.2). The most prevalent ssDNA viral sequence assignments within the sponge metaviromes were to the *Microviridae*, which typically infect *Proteobacteria*, *Spiroplasma* and *Chlamydia* (Brentlinger et al., 2002; Ackermann & Kropinski, 2007). Proteobacteria are abundant and diverse symbionts of marine sponges (Pita et al., 2018b), likely explaining the high relative abundance and diversity of sequences assigned to these small ssDNA viruses in the sponge metaviromes as well as in viral communities from other reef invertebrates (Weynberg et al., 2017b; Laffy et al., 2018). The *Circoviridae* typically infect mammals and birds (Delwart & Li, 2012) but viruses from this family were also frequently detected in sponges. This group of viruses is characterised by their small circular genomes (~2 kb) and high genetic diversity, which has underpinned a rapid expansion in their host range (Li et al., 2010; Delwart & Li, 2012) to include cnidarians, urochordates and other invertebrates (Dunlap et al., 2013; Laffy et al., 2018). Retroviral sequences assigned to the families *Caulimoviridae* and *Retrovirdae* were also detected in just over one third of sponge species, including all replicates of the GBR sponges *C. foliascens*, *C. schulzei*, *C. marshae* and *S. carteri* (Fig. 3.2). Reverse-transcribing viruses infect a wide range of animal, algal and plant hosts (Bowser & Casey, 1993; Kim et al., 1994; Zaki, 2003) and have recently been reported within *Symbiodiniaceae* cultures from coral (Weynberg et al., 2017a,b).

3.4.2. Variation in the sponge viral community is driven by site-specific and host-specific features.

The composition of sponge-associated viral communities is strongly determined by host species and the geographical location of the host (Fig. 3.3a). A significant difference in viral community composition was found between the 15 sponge species (PERMANOVA, Pseudo-F value = 4.4534, df = 14, P-value = 0.001, Fig. 3.3a), consistent with previous reports of high intra-species similarity in the viral communities of sponges *Amphimedon queenslandica*, *Rhopaloiedes odorabile*, *Xestospongia testudinaria* and *Ianthella basta* (Laffy et al., 2018). Given the large volumes of seawater sponges filter to extract bacterioplankton and virioplankton, this species-specificity is particularly notable, and is likely attributed to the host-specificity of eukaryotic viruses (Drake, 1993; Duffy, Burch & Turner, 2007; Atabekov,

2011; Bandín & Dopazo, 2011; Chow et al., 2014; Grasis et al., 2014) and the high species-specificity of the sponge-associated microorganisms (Thomas et al., 2016) that host the bacteriophage component of the community. While viral communities were also significantly different between sampling sites (PERMANOVA, Pseudo-F value = 4.8483, df = 1, P-value = 0.001; Fig. 3.3a), this was not attributed to differences between seawater viromes from the GBR and the Red Sea. The geographic variation in sponge-associated viruses is consistent with findings by Brum and colleagues (Brum et al., 2015), who reported that marine viral communities can be locally structured by specific environmental conditions that affect host community structure.

Sponge populations contain a mixture of heterotrophic and phototrophic species as well as species with high (HMA) and low (LMA) microbial abundance (Moitinho-Silva et al., 2017). Microbial biomass in HMA sponges can comprise up to one third of the total sponge biomass, with microbial diversity generally being much higher than in sympatric LMA species (Hentschel, Usher & Taylor, 2006; Giles et al., 2013; Moitinho-Silva et al., 2017). Viral communities are more similar among sponges sharing similar traits in microbial ecology (Fig. 3.3b; Appendix 3 Table 3A.1), with permutation-based analysis of variance revealing significant differences in viral community composition between HMA and LMA sponges (PERMANOVA, Pseudo-F value = 2.4228, df = 1, P-value = 0.001) and between sponges with and without photosymbionts (PERMANOVA, Pseudo-F value = 2.1002, df = 1, P-value = 0.001). These results further support the role of the sponge-associated microbiome (abundance and composition) in structuring the virome.

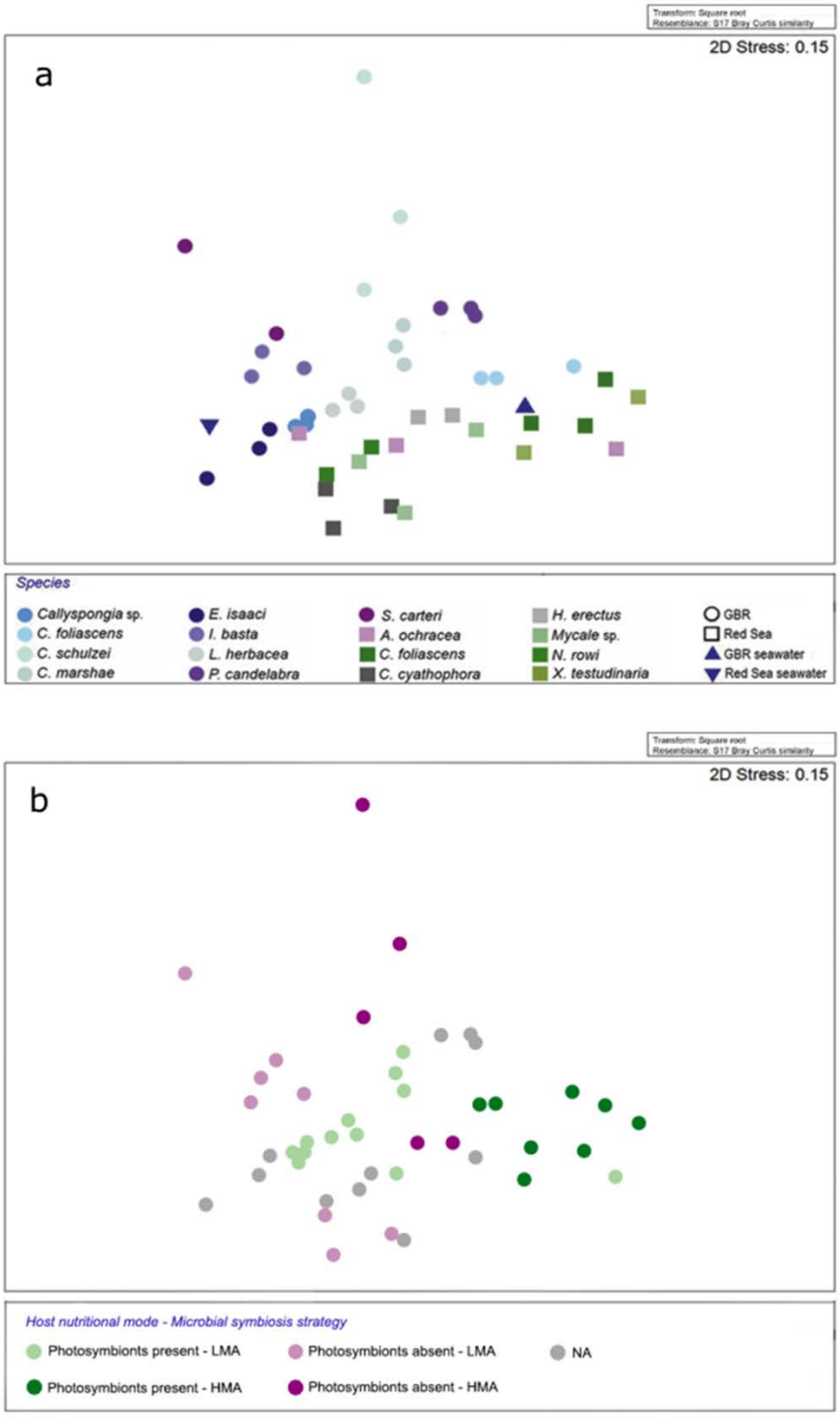

Figure 3.3 Endogenous and exogenous determinants of viral community composition within marine sponges. Non-metric multidimensional scaling plot based on Bray-Curtis similarity of genus-level taxonomy for predicted genes. Ordination displays similarities in the viral communities of the (a) fifteen sponge species (PERMANOVA, Pseudo-F value = 4.4534, df = 14, P-value = 0.001) from the Great Barrier Reef and the Red Sea (PERMANOVA, Pseudo-F value = 4.8483, df = 1, P-value = 0.001), and (b) discriminates between species classified as high microbial abundance (HMA) or low microbial abundance (LMA) (PERMANOVA, Pseudo-F value = 2.4712, df = 1, P-value = 0.001) and host nutritional modes, classified by the presence or absence of photosymbionts (PERMANOVA, Pseudo-F value = 2.1976, df = 1, P-value = 0.001).

3.4.3. Functional potential of the sponge virome

An average of 14.6% of predicted genes from the sponge viromes were assigned functional SwissProt keywords, based on BLASTP matches to the UniProt-KB database (Supplementary Table 3.1). Ordination analysis based on the relative frequency of Swiss-Prot keywords revealed both species-specific and site-specific clustering in gene function (Fig. 3.4.), consistent with taxonomic analyses (Fig. 3.3a). Permutational analysis of variance confirmed significant differences in functional gene repertoires across species (PERMANOVA, Pseudo-F value = 5.067, P-value = 0.001) and locations (PERMANOVA, Pseudo-F value = 6.9506, P-value = 0.001). Each sponge species showed a unique functional profile (Fig. 3.5), however of the 50 most enriched Swiss-Prot keywords, half were abundant across all sponge samples, while the remaining keywords were enriched only in specific sponge species (Fig. 3.5). Marked host specificity in functional genes reflected the distinct viral communities inhabiting each of the holobionts. For instance, the keyword for short tail ejection systems was particularly enriched in *E. isaaci* and it is notable that this species also hosted the highest relative abundance of the short tail bacteriophage family *Podoviridae* (Fig. 3.2).

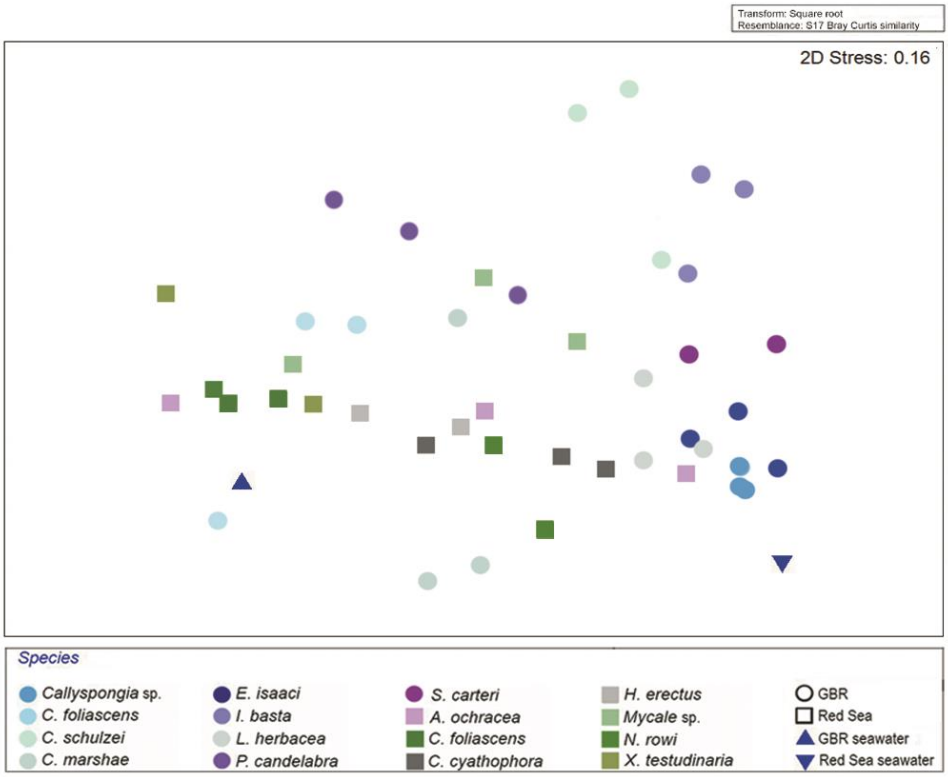

Figure 3.4 Non-metric multidimensional scaling plot based on Bray Curtis similarity of Swiss-Prot functional keyword assignment for predicted genes. Ordination displays similarities in the viral communities of the fifteen sponge species from the Great Barrier Reef and the Red Sea.

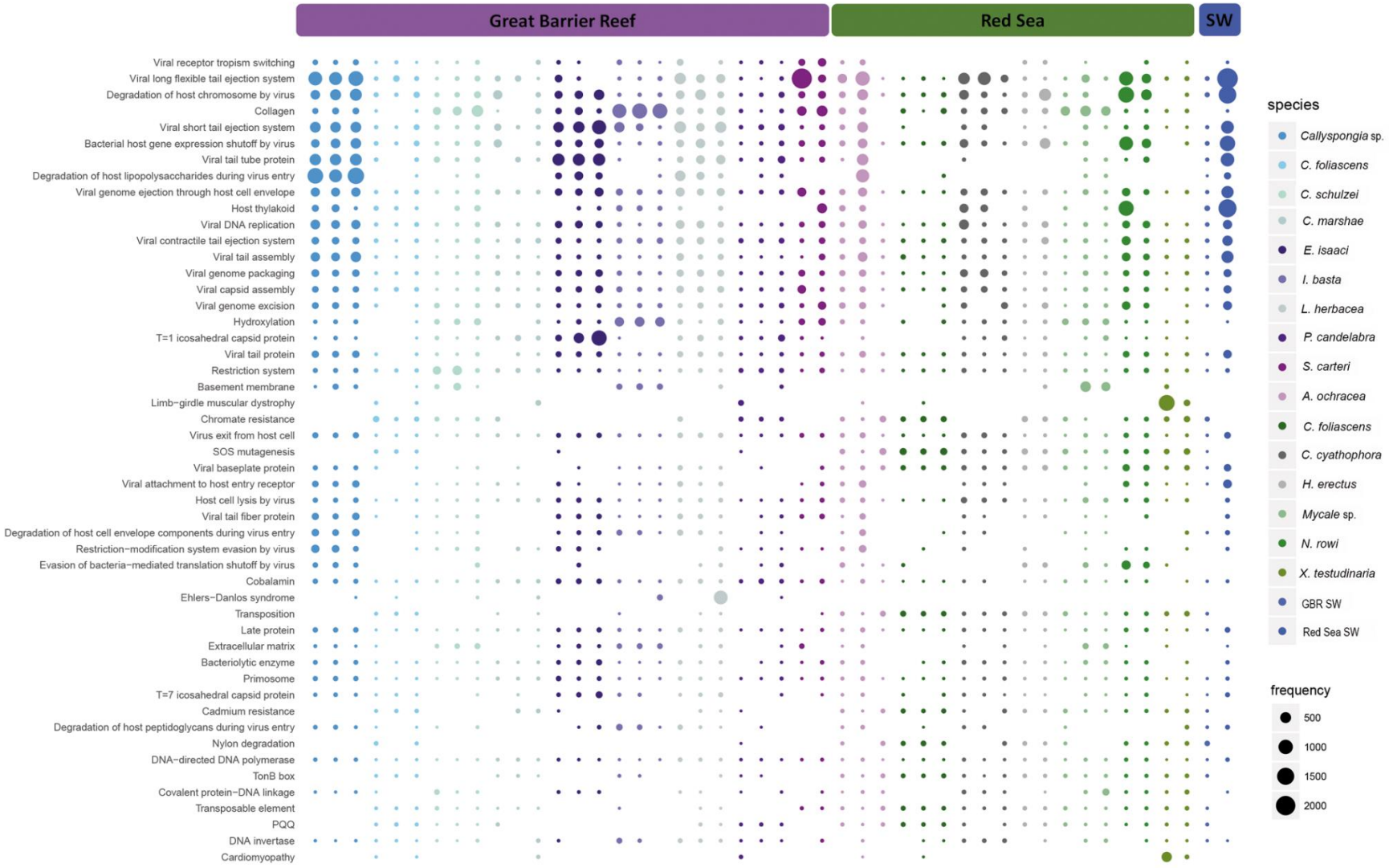

Figure 3.5 Swiss-Prot functional keyword assignment to predicted genes, normalised according to keyword frequency in the database *using parameters defined in Laffy* et al., *2016*. Keyword composition was further adjusted to account for the coverage of the source contig within the metavirome. The top 50 most abundant keywords across all datasets were identified based on UniProt-KB BLASTP analysis of sponge metaviromes and an e-value cutoff of $1e^{-1}$

Of the 50 most enriched viral keywords, 26% were associated with viral infection strategies including 'genome ejection through the host cell envelope', 'attachment to host entry receptor', 'long flexible tail ejection system' and 'exiting from the host cell' (Fig. 3.5). A further 22% were involved in viral structure, including 't=1 icosahedral capsid protein', 'collagen', 'tail assembly' and 'tail protein' (Fig. 3.5). Additionally, viral replication mechanisms comprised 20% of the top 50 keywords, including 'DNA replication', 'genome excision, 'genome packaging' and 'bacteriolytic enzymes' (Fig. 3.5). Finally, 6% of the 50 most enriched protein functions related to a suite of auxiliary metabolic genes (AMG), including 'chromate resistance', 'cadmium resistance', 'nylon degradation', 'SOS mutagenesis' and 'host thylakoid' (Fig. 3.5).

Significant differences in specific viral functions between host species (Fig. 3.6) and sampling sites (Fig. 3.7) were identified using mvabund analysis of the Swiss-Prot functional keyword profiles. This analysis provided further support for the significant variations in AMGs between sponge species and sampling locations. For instance, the 'host thylakoid' Swiss-Prot keyword which is attributed to a protein located in or on the host thylakoid of chloroplasts of green algae (Kieselbach et al., 1998), was particularly enriched in *Callyspongia* sp., *C. foliascens*, *C. schulzei*, *I. basta*, *S. carteri*, *C. cyathophora* and *N. rowi* (Fig. 3.7). The 'host thylakoid' genes were identified as Photosystem II D2 proteins, and the majority of contigs with this gene originated from *Synechococcus* phages within the family *Myoviridae* (Supplementary Table 3.3). While microbial community composition data is not available for all sponge species, both *C. foliascens* and *C. cyathophora* are known to host abundant populations of *Synechococcus* symbionts (Gao et al., 2014b, 2015; Luter et al., 2015). The enrichment of this keyword shows that viruses could potentially interfere with photosynthetic processes in their hosts. These auxiliary genes have also been observed in coral DNA viromes (Weynberg et al., 2017a) and, with the exception of *C. marshae*, *P. candelabra* and *X. testudinaria*, were present in all sponge species investigated (Fig. 3.6).

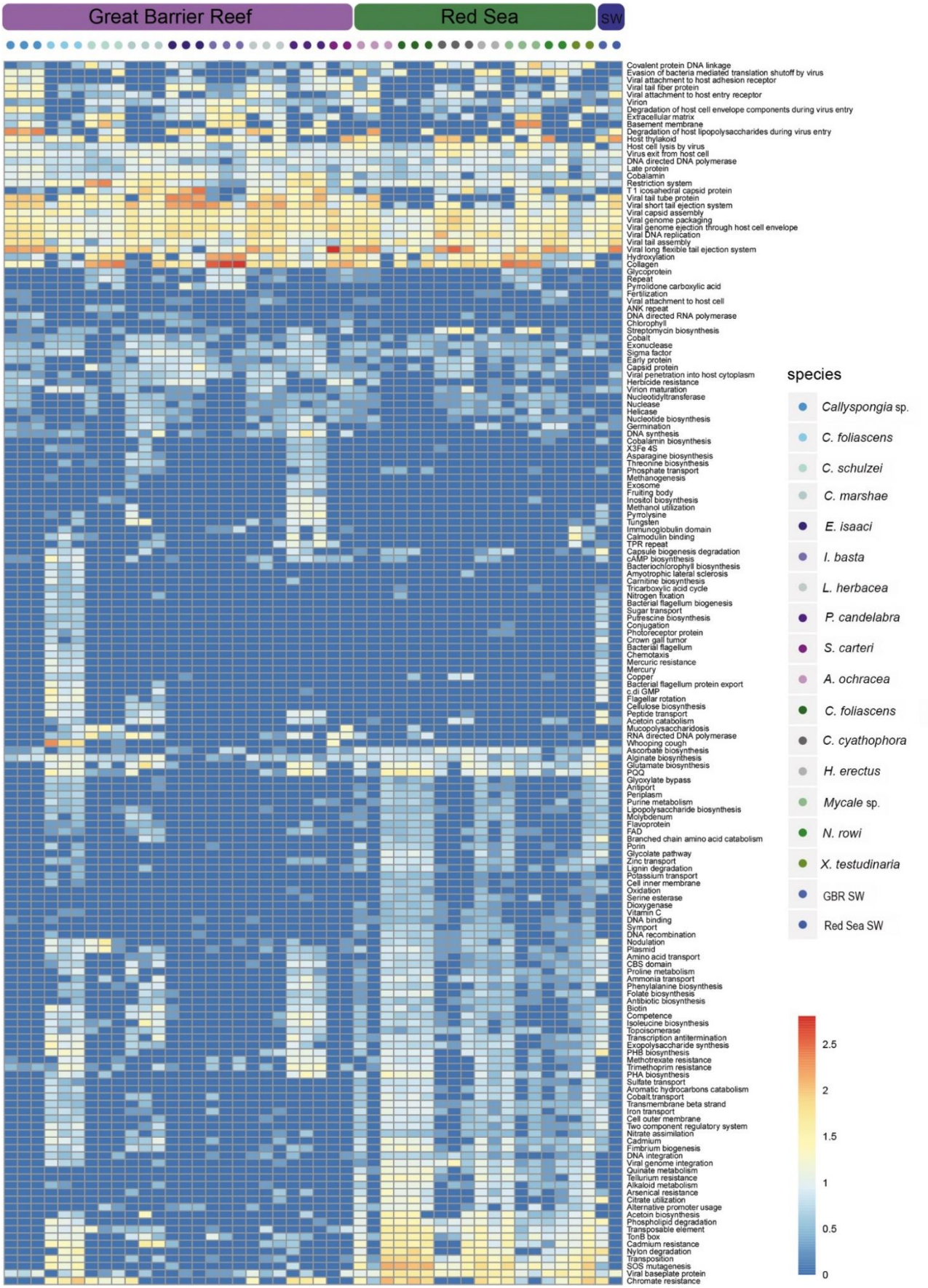

Figure 3.6 Viral functions that were significantly different between sponge species (P-value <0.02) from Swissprot Keyword abundance data from all samples, adjusted to account for coverage of the source contig within individual viromes using parameters defined in Laffy et al., 2016.

Figure 3.7 Viral functions that were significantly different between sampling sites (P-value <0.02) from Swissprot Keyword abundance data from all samples, adjusted to account for coverage of the source contig within individual viromes using parameters defined in Laffy et al., 2016.

Collagen was one of the most abundant SwissProt Keywords within the sponge viromes, being present in all sponge species (Fig. 3.5), and a significant driver of functional differences between host species (Fig. 3.6) and sampling locations (Fig. 3.7). A previous study also identified collagen as being an abundant component of sponge viromes, and a key driver of functional differences between sponge, coral and seawater viromes (Laffy et al., 2018). Contigs containing collagen proteins were consistently attributed to dsDNA viruses (Supplementary Table 3.3), and when assigned at the family level, they included members of the bacteriophage families *Myoviridae*, *Podoviridae* and *Siphoviridae*, the algal *Phycodnaviridae*, the crustacean-infecting *Nimaviridae* and the giant virus family *Mimiviridae* (Supplementary Table 3.3). Collagen is an integral structural component of the external capsid of members of the *Mimiviridae* (Shah et al., 2014) but is also used by sponges to form their skeletal structure (Simpson, 2011). While it is clear that collagen genes are an integral component of sponge-associated viruses, their functional role within the sponge virome remains unclear and warrants further investigation.

Genes coding for ankyrin repeat proteins (ARPs) were found on 60 contigs within the *C. schulzei* viromes, and 65% of these were taxonomically assigned to contigs matching dsDNA viruses (Supplementary Table 3.3). It is likely that these ARPs originated from a member of the Megavirales, as the only family level taxonomic assignments made to contigs containing ARPs were to contigs belonging to the *Phycodnaviridae*, *Iridoviridae*, *Mimiviridae* or *Poxviridae* (Supplementary Table 3.3). The ankyrin repeat is an amino-acid motif that can disrupt protein–protein interactions in cellular processes (Mosavi et al., 2004; Díez-Vives et al., 2017). In a recent publication Jahn and colleagues shown that sponge bacteriophages encodes ankyrins that, upon bacterial expression, reduce the eukaryotic immune response and phagocytosis of bacteria thereby influencing bacterial survival (Jahn et al., 2019). Phylogenetic analysis of sponge-bacterial ARPs shows they are highly divergent from known protein sequences and are most closely related to proteins found in bacteria living in association with eukaryotes (Reynolds & Thomas, 2016). Horizontal gene transfer of ARPs amongst diverse symbionts has been proposed as a possible mechanism explaining their widespread distribution in sponges (Reynolds & Thomas, 2016) and their enrichment in the virome of some sponge species indicates that this horizontal transfer may be viral-mediated.

Heavy metal resistance genes, including mercury, molybdenum, chromate, cadmium, tellurium and arsenic resistance were significantly enriched in *C. foliascens*, *X. testudinaria*, *C. schulzei*, *H. erectus* and *P. candelabra* and more broadly in sponges from the Red Sea sampling site (Figs. 3.6 and 3.7). While heavy metals occur naturally and can be accumulated by sponges in the absence of anthropogenic pressure (Negri et al., 2006), levels can also be exacerbated by inputs from mining and industrial production (Negri et al., 2006; Pan et al., 2011; Tchounwou et al., 2012). In comparison to elevated levels of heavy metal contamination in the Red Sea, largely attributed to industrial and human activities in the coastal area (Badr et al., 2009), levels in the GBR are generally low, particularly within the GBR Marine Park (Haynes & Johnson, 2000).

Arsenic is generally toxic to microbial communities (Tuulaikhuu, Romaní & Guasch, 2015), and genes associated with arsenic resistance (arsenite and arsenate reductase genes) were found to be significantly enriched in Red Sea sponges (Figs.3. 6 and 3.7), with the source contigs being almost exclusively assigned to bacteriophages (Supplementary Table 3.3). High levels of arsenic contamination has been identified in seawater, sediment and marine organisms from the Red Sea (El-Naggar & Al-Amoudi, 1989; El-Moselhy et al., 2014), and this has been primarily attributed to anthropogenic sources. Arsenic has also been shown to bioaccumulate in Red Sea sponges at levels exceeding 100 times the concentration in the surrounding environment (Mayzel, Aizenberg & Ilan, 2014). Arsenic tolerance in marine sponges has been attributed to a symbiotic bacterium, *Entotheonella* sp, that can mineralise the arsenic within intracellular vesicles (Keren et al., 2017). Tellurium resistance was also detected in all Red Sea sponges and was a significant driver of functional differences in the metaviromes between locations (Fig. 3.7). Tellurium resistance genes have previously been identified in yeast, fungi and bacteria (Ollivier et al., 2008; Tanaka et al., 2010; Boriová et al., 2014). Even though tellurium is usually present at low concentration in natural waters it is potentially harmful due to the recognised toxicity of some of its compounds and its association with anthropogenic sources (Belzile & Chen, 2015). Although there is no data available on the toxic effects of tellurium in the Red Sea, it has been hightlighted as an element of concern for the region (Ibrahim & Abdelmenam, 2015). Contigs carrying tellurium resistance genes were primarily assigned to the bacteriophage family *Myoviridae* (Supplementary Table 3.3).

With the exception of *C. cyathophora*, chromate resistance genes were significantly enriched in all Red Sea sponges, as well as in five of the nine GBR sponges. Analysis of fish collected near our Red Sea sampling site identified a 5-fold increase in chromate accumulation compared to fish at control sites (Mohamed et al., 2016), and a survey along the Saudi Arabian coast also identified elevated concentrations of chromate in several sponge species investigated here (*Callyspongia sp.*, *C. cyathophora*, *H. erectus* and *N. rowi*) (Pan et al., 2011). The 'chromate resistance' keyword was assigned to multiple genes included in operons containing both chromate and molybdite resistance (Nies, Nies & Silver, 1990; Juhnke et al., 2002) on contigs taxonomically assigned as Caudovirales (Supplementary Table 3.3). Similarly, cadmium resistance genes were significantly enriched in Red Sea sponges (Fig. 3.7), consistent with elevated cadmium levels reported in sponges sampled in the Red Sea off the coast of Israel (Mayzel, Aizenberg & Ilan, 2014). Cadmium is toxic to a wide range of bacteria and cyanobacteria (Trevors, Stratton & Gadd, 1986; Martelli et al., 2006). For the few contigs containing cadmium resistance genes that could be taxonomically assigned, matches were made to dsDNA viruses from the Caudovirales or *Phycodnaviridae* (Supplementary Table 3.3). Although cadmium accumulation in marine sponges is generally proportional to the concentration in the surrounding seawater (Müller et al., 1998), cadmium has also been detected in sponges from unpolluted environments where it can vary across sympatric sponge species (Patel, Balani & Patel, 1985). For this reason, without seawater chemistry from each collection site, it is not possible to unequivocally link the enrichment in cadmium resistance genes to anthropogenic cadmium contamination at the Red Sea sampling location.

Some sponge species appear to have an exceptionally high tolerance for heavy metals and can bioaccumulate them from comparatively low concentrations in the surrounding environment. For instance, *Tedania charcoti* can accumulate and tolerate extraordinarily high concentrations of cadmium, even when environmental exposure is low (Capon et al., 1993). In the present study, *C. foliascens* samples from both the Red Sea and the GBR were enriched in multiple heavy metal resistance genes, highlighting the importance of determining naturally occurring concentrations of heavy metals in this species. The enrichment of cadmium, arsenic, tellurium and chromate resistance genes in Red Sea sponge metaviromes (assigned to bacteriophage contigs), in comparison to their absence or low prevalence in most GBR sponges, suggests that viruses may be contributing heavy metal resistance to their host

microbes. These findings suggest that viral genes linked to heavy metal resistance are selected for by sponge holobionts living in polluted environments in an effort to mitigate the effects of environmental heavy metal contamination.

An enrichment of Swiss-Prot functional keywords for nylon degradation was also detected in the Red Sea sponge viromes. Pollution from synthetic plastic compounds has increased considerably in marine ecosystems (Worm et al., 2017), although surveys of surface water along the Arabian coast of the Red Sea reported lower levels of plastic contamination than what has been found in the Mediterranean Sea (Martí et al., 2017), despite detection of microplastics in the gastrointestinal tracts of Red Sea fish (Baalkhuyur et al., 2018). Genes and enzymes (carboxylesterases) associated with nylon degradation have previously been characterised from *Flavobacterium* and *Pseudomonas* species (Kinoshita et al., 1977; Tsuchiya et al., 1989; Negoro et al., 1992, 2005). The synthesis of nylon oligomer degradation enzymes from marine microbes can be particularly important for the biological removal or detoxification of the synthetic compounds released into the natural environment (Kakudo et al., 1993), therefore, the enrichment of nylon degradation genes in viruses associated with sponge microbes could improve host resistance to environmental contaminant exposure. Since viral transductions are important gene transfer processes in marine ecosystems, the enrichment of Nylon degradation in the sponge virome may possibly indicate a mechanism by which these genes are being acquired in oceanic microbiomes.

Although heavy metal resistance and nylon degradation genes are frequently characterised from operons located on plasmid DNA (Kinoshita et al., 1977; Tsuchiya et al., 1989; Nies, Nies & Silver, 1990; Goncharoff et al., 1991; Juhnke et al., 2002; Wang et al., 2009), a recent study investigating the presence of antibiotic and heavy metal resistance genes in aquatic viromes showed that 1-3% of viral genes derived from environmental samples were attributed to heavy metal resistance (Colombo et al., 2017). The enrichment of these genes in Red Sea sponge viromes, together with previous reports of heavy metal and plastic contamination at the coastal sampling site, suggests that viruses could help support host resistance to environmental contaminant exposure.

In contrast to the AMGs enriched in the Red Sea environment, herbicide resistance genes were significantly enriched in the GBR (Fig. 3.7), which could confer environmental tolerance to chemicals introduced to the reef ecosystem as a result of coastal agricultural activity.

Pesticides and herbicides associated with agricultural runoff can occur at high levels in coastal and lagoonal areas of the GBR (Jones & Kerswell, 2003; Lewis et al., 2009). Genes related to herbicide resistance were primarily assigned to contigs from *Synechococcus* phages (Supplementary Table 3.3). *Synechococcus* is the most abundant cyanobacterium in the ocean and a major contributor to the productivity of coastal seawater (Flombaum et al., 2013). The toxicological effects of herbicides on cyanobacterial populations is well documented (Linden et al., 1990; Weiner, DeLorenzo & Fulton, 2004; Singh et al., 2016), hence the presence of herbicide resistance genes in GBR sponges may provide a pathway for environmental acclimatisation of phototrophic species to agricultural runoff.

Analysis of how virome function reflected other aspects of host ecology revealed significant differences according to host nutritional mode (photosymbionts vs no photosymbionts; PERMANOVA, Pseudo-F value = 2.1976, df = 1, P-value = 0.001) and microbial abundance (HMA vs LMA; PERMANOVA, Pseudo-F value = 2.4712, df = 1, P-value = 0.001). Specific differences in viral functions were assessed by mvabund analysis of the Swiss-Prot keywords (Fig. 3.8, 3.9; Appendix 3 Table A3.1). For instance, the keyword 'antimicrobial' was significantly enriched in LMA sponges (Fig. 3.8). Currently, the mechanisms underpinning whether a sponge hosts high or low microbial abundance (which often translates to high and low microbial diversity, respectively (Moitinho-Silva et al., 2017)) are unknown. Within the LMA sponge viromes containing 'antimicrobial' genes, source contigs were assigned to member of the Caudovirales (Supplementary Table 3.3) and most were linked to hydrolytic enzymes (Supplementary Table 3.3). Endolysins digest bacterial cell walls to enable bacteriophage release from the cell (Oliveira et al., 2013), and are considered highly specific antimicrobial agents (Fischetti, 2005). Furthermore, in *P. candelabra*, the antimicrobial keyword was associated with a Pyocin-S2 gene, responsible for producing antimicrobial bacteriocins in *Pseudomonas aeruginosa* (Denayer, Matthijs & Cornelis, 2007). Sponges are renowned for their production of bioactive secondary metabolites, although, with a few notable exceptions (Mori et al., 2018), it is generally unknown whether these antimicrobial compounds originate from the host or the microbial symbionts. Hydrolytic enzymes with antimicrobial activities have previously been identified in a sponge microbial metagenome (Yung et al., 2011) and here we show a potential bacteriophage origin for at least some antimicrobial genes. While enrichment of antimicrobial genes in the viromes of LMA sponges

suggests viral AMGs could assist in maintaining the structure of the sponge microbiome, further work is still required to confirm and quantify their role in maintaining the density and diversity of sponge symbionts.

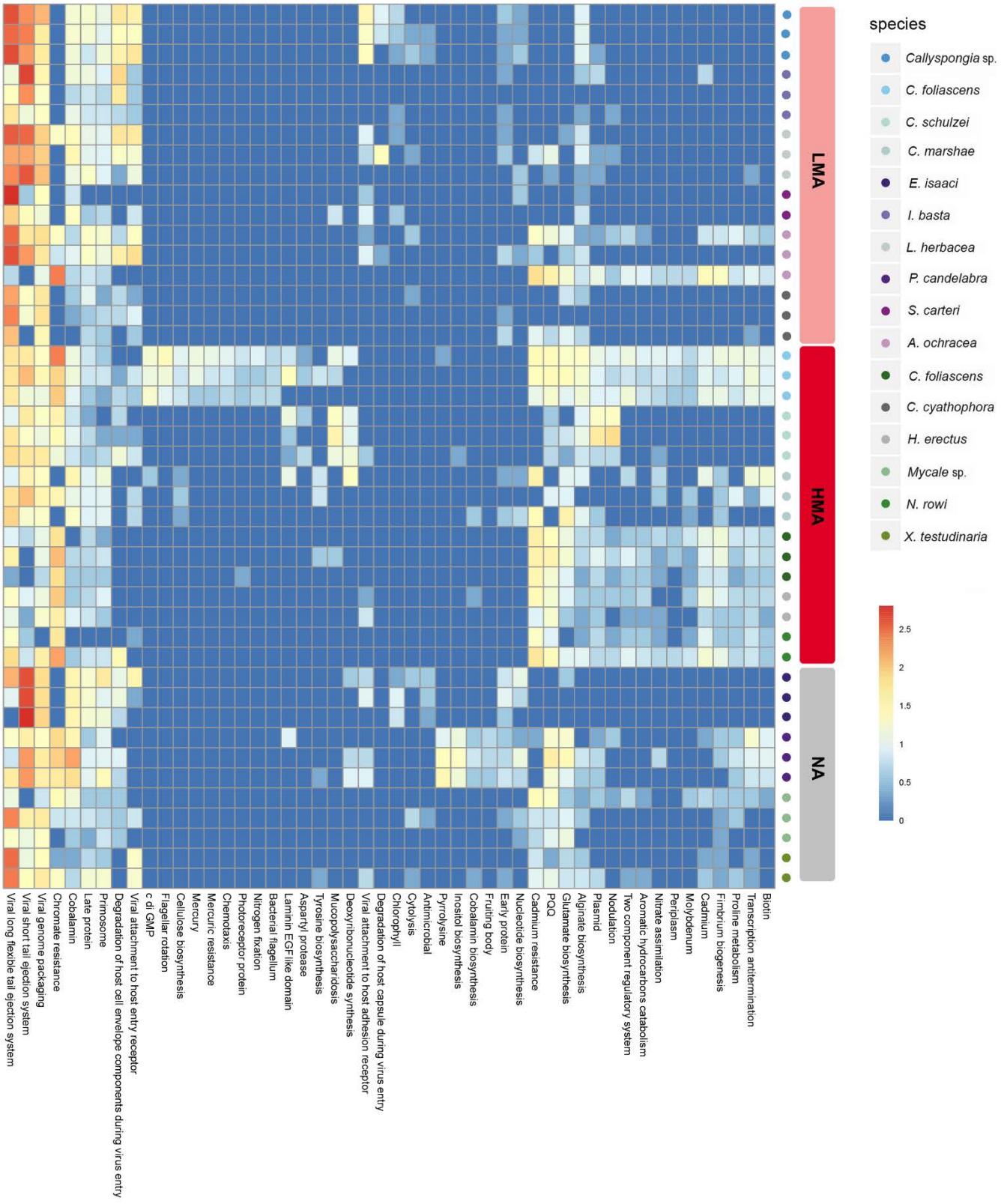

Figure 3.8 Heatmap of viral functions that were significantly different between HMA and LMA sponges. Mvabund was used to perform univariate tests on Swiss-Prot keywords abundance data using parameters defined in Laffy et al., 2016.

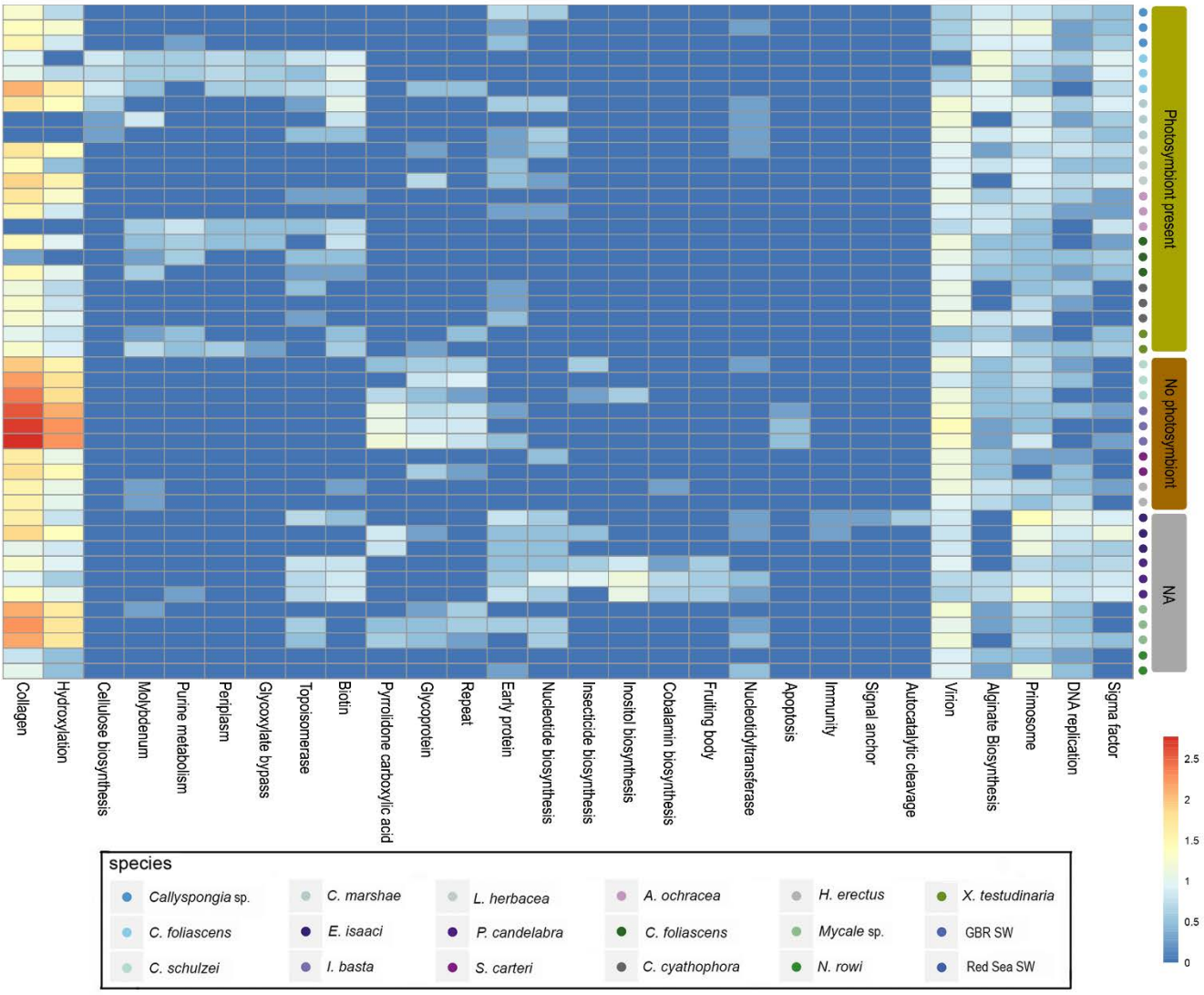

Figure 3.9 Heatmap of viral functions that were significantly different between sponges with or without photosymbionts. Mvabund was used to perform univariate tests on Swiss-Prot keywords abundance data using parameters defined in Laffy et al., 2016.

An enhanced potential for nitrogen metabolism is a key feature of the microbiome of most HMA sponge species (Webster & Thomas, 2016). Here we detected a significant enrichment of the Swiss-Prot keywords 'nitrate assimilation' and 'nitrogen fixation' in the HMA group (Fig. 3.8). Genes associated with nitrate assimilation included nitrate and nitrite reductases and associated transport genes, and genes associated with nitrogen fixation included glutamine synthetases and a large number of nitrogen fixation and regulation proteins (Supplementary Table 3.3). These genes occurred on contigs taxonomically assigned to *Myoviridae* and *Phycodnaviridae,* respectively. Interestingly, it has previously been shown that the HMA species *C. foliascens*, from which many of these nitrogen fixation genes were derived, gains considerable nutritional benefit from its nitrifying cyanobacterial symbionts (Wilkinson & Fay, 1979). These cyanobacterial symbionts likely play host to at least some of the *Myoviridae* (which includes a wide diversity of cyanophages) and *Phycodnaviridae* identified here. These results suggest that the virome may be contributing key genes involved in nitrogen metabolism in HMA sponges or that targeting the nitrogen metabolism pathway is part of the viral infection strategy in these species.

Significant differences in viral functional genes were also evident between the phototrophic and heterotrophic sponge species. For instance, the 'cellulose biosynthesis' keyword was significatively enriched in sponges hosting photosynthetic symbionts (Fig. 3.9), particularly in *C. foliascens* and *C. marshae* (Supplementary Table 3.3), which host *Synechoccoccus* and *Oscillatoria* respectively (Lemloh et al., 2009; Gao et al., 2014a). Associated with the cellulose biosynthesis keyword were genes related to cellulose synthase A (CesA) and probable diguanylate cyclase genes, which were both assigned to *Phycodnaviridae* and *Myoviridae* (Supplementary Table 3.3). CesA genes are involved in the formation of cellulose for cell walls in plants (Kumar & Turner, 2015) and cyanobacteria (Zhao et al., 2015) and it has been suggested that plant and cyanobacterial cellulose biosynthesis genes share common ancestry (Nobles, Romanovicz & Brown, 2001), and may indirectly contribute to photosynthesis in marine ecosystems (Delmer & Haigler, 2002; Boex-Fontvieille et al., 2014). It is possible that these CesA genes are contributing to cellulose metabolism in a select group of microoganisms, although further work is required to fully characterise the role of the CesA genes in the sponge holobiont.

3.5. CONCLUSION

Comparative analysis of viral communities from 15 sponge species collected from different geographic regions (GBR vs Red Sea), and representing different host nutritional modes (photosymbionts vs no photosymbionts) and strategies for microbial symbiosis (HMA vs LMA), has greatly expanded our understanding of viral ecology in marine sponges. dsDNA viruses spanning all three families of the Caudovirales as well as the NCLDV families *Mimiviridae*, *Marseilleviridae*, *Phycodnaviridae*, *Ascoviridae*, *Iridoviridae*, *Asfarviridae* and *Poxviridae* were present in sponges. ssDNA viruses from the *Microviridae*, *Circoviridae* and *Inoviridae*, as well as the *Retroviridae* were also prevalent, although their relative abundance was more variable across sponge species. While core viral functions related to replication, infection and structure were consistent across most sponge species, functional profiles varied significantly between species and sites, in part attributed by differential representation of AMGs associated with herbicide resistance, heavy metal resistance and nylon degradation. AMGs associated with antimicrobial activity were enriched in low microbial abundance species, while AMGs associated with nitrogen metabolism were enriched in high microbial abundance species and AMGs related to cellulose biosynthesis were enriched in sponge species hosting photosynthetic cyanobacteria. These results highlight the diverse suite of beneficial roles viral AMGs may play in the functional ecology of the sponge holobiont.

Chapter 4. THE IMPACTS OF THERMAL STRESS ON THE VIROME OF THE MARINE SPONGE *CARTERIOSPONGIA FOLIASCENS*

4.1. ABSTRACT

Ocean warming (OW) is causing irreversible damage in global coral reef communities. Future climate scenarios have forecast a shift in the reef structure as a result of environmental stressors, highlighting sponges as potential 'winners' due to their high environmental resilience. The role of viruses in the thermal tolerance of sponges remains largely unknown. Viruses are important components of the sponge holobiont and play diverse functional roles mediating metabolic processes in their host. In order to investigate how the sponge virome responds to elevated temperature, the photosynthetic sponge *Carteriospongia foliascens* was exposed to short (3 days) and longer term (21 days) heat-stress events. A metaviromic approach was used to assess the shifts in community and functional composition across treatments. No significant taxonomic variation was observed in the sponge viral metagenomes after three days exposure to 31 °C, however after 21 days a significant increase in temperate bacteriophages from the genus *Inovirus* was observed. This suggests that thermal stress in sponges may trigger *Inovirus* to switch from a dormant lysogenic to an active stage, facilitating the release of virions. Although no significant difference was observed in the overall functional profile of short or long term heat-stressed sponges, a significant reduction of genes associated with heavy metal resistance, together with an increase in virulence and stress-response related genes were detected in heat-stressed sponges, suggesting viruses may interfere with sponge-microbial infection or defence ability during a heat-stress event.

4.2. INTRODUCTION

Rising of atmospheric CO_2, largely attributed to the increased consumption of fossil fuels (Broecker et al., 1979), has been gradually increasing the Earth's temperature and is forecast to increase seawater temperatures by up to 4 °C by the end of this century (IPCC, 2014). Marine ecosystems are experiencing the impacts of Ocean Warming (OW), with coral reefs amongst the most vulnerable ecosystems (Hughes, 2003; Doney et al., 2012). Anthropogenic activities exacerbates natural warming events, increasing the frequency of seawater

temperature anomalies and directly impacting marine communities (Hughes et al., 2018). Mass-bleaching events are direct consequences of these temperature anomalies (Hughes et al., 2017; Harrison et al., 2018; Stuart-Smith et al., 2018) characterized by the loss of symbiotic dinoflagellates (zooxanthellae), photosynthetic bacteria and/or chlorophyll from a variety of hosts, including corals, algae and sponges (López-Legentil et al., 2008; McMurray et al., 2011; Zozaya-Valdes, Egan & Thomas, 2015). Over 300 severe bleaching episodes have been registered across 100 coral reefs worldwide between 1980 and 2016 (Hughes et al., 2018) and these events have impacted marine ecosystems by interrupting many biological processes, altering the overall fitness and survival of seawater organisms (Hoegh-Guldberg & Bruno, 2010; Nguyen et al., 2011; Hughes et al., 2017).

The impacts of OW on living marine organisms can be observed at the macroscopic level of whales (Leaper et al., 2006) down to the microscopic viruses (Danovaro et al., 2011; Laffy et al., 2019). While most coral reef organisms have been shown to be negatively impacted by OW (Przeslawski et al., 2008; Stuart-Smith et al., 2018), some sponge species were found to be more resilient compared to other benthic groups, such as coral or macroalgae (Bell et al., 2018). Different sponge species present varied responses to OW, and even though most of the investigated sponge species were negatively impacted by temperature increases, others could benefit from this disturbance, usually as a result of declining competitor abundance (Bell et al., 2018). The high tolerance of some sponge species to other environmental disturbances, including ocean acidification (Bell et al., 2018), sedimentation (Bell et al., 2015; Schönberg, 2015) and pollution (Richelle-Maurer et al., 1994; Carballo, Naranjo & García-Gómez, 1996), indicate that these animals are relevant models to investigate resilience of coral reefs to anthropogenic threats.

Sponges are biodiverse members of marine benthic communities (Hooper & Van Soest, 2002). They play important roles in coral reefs by linking pelagic and benthic environments (Pile & Young, 2006), and contributing to the flux of energy and nutrients in oligotrophic systems (de Goeij et al., 2013b). Members of the sponge phylum Porifera are considered the most primitive extant metazoans, and have historically established diverse and targeted symbiotic relationships with microorganisms (Webster & Taylor, 2012). This complex host-microbial aggregation exists as a unique meta-organism referred to as a holobiont (Margulis & Fester, 1991). Microbes can constitute up to half of the sponge holobiont biomass (Cuvelier et al.,

2014), and play important metabolic functions that support their host's nutrition, defence and development (Peters et al., 2010; Freeman & Thacker, 2011; Whalan & Webster, 2014; Webster & Thomas, 2016). Additionally, microbial symbionts have been suggested to mediate the sponge holobiont capacity to acclimatize and adapt to environmental stressors, although the mechanisms that underpin this mediation remain largely unknown (Pita et al., 2018b). Given the fundamental importance of microbes to host health (Webster & Taylor, 2012), several studies have been conducted which investigate sponge-holobiont response to OW events (Cebrian et al., 2011; Webster et al., 2011; Strand et al., 2017). While these studies have focussed on how the host or bacterial communities respond to thermal stress, only one previous study has focused on understanding the role viruses play within the sponge holobiont during a heat-stress event (Laffy et al., 2019).

Viruses are ubiquitous biological entities and play significant roles regulating natural processes in marine environments (Suttle, 2007; Danovaro et al., 2011). They also play a key role in the maintenance of complex ecosystems, including coral reefs (Davy et al., 2006; Thurber & Correa, 2011; Weynberg, 2018), as they influence the structure of prokaryotic and eukaryotic populations, regulating community composition and diversity (Suttle, 2007; Rohwer & Thurber, 2009; Breitbart et al., 2018). Viruses are a diverse component of the sponge holobiont and are mostly comprised of bacteriophages from the order Caudovirales (Laffy et al., 2018; Pascelli et al., 2018). Sponge viruses have also been shown to carry auxiliary metabolic genes involved in many host metabolic processes, including herbicide resistance genes (Laffy et al., 2018) (Chapter 3) and ankyrin repeat proteins (Jahn et al., 2019), the latter encoded by bacteriophage that, upon expression within host bacteria, reduce the eukaryotic immune response and phagocytosis of bacteria (Jahn et al., 2019).

Environmental stressors can directly affect viral communities (Danovaro et al., 2011; Lara et al., 2013) and interfere with viral-host interactions (Jacquet & Bratbak, 2003). Environmental stressors may also induce changes in the viral reproductive cycle (Howard-Varona et al., 2017), promoting shifts in viral population dynamics, as observed in the marine sponge *Rhopaloeides odorabile* where an enrichment in endogenous retro-transcribing viruses was observed following a thermal stress event (Laffy et al., 2019). As different sponge species exhibit unique responses to environmental stressors (Bennett et al., 2017), the high microbially diverse and photosynthetic sponge *Carteriospongia foliascens* was chosen to

further investigate the role of viruses in the thermal stress response of the sponge holobiont. This globally distributed sponge species was identified as having a higher mortality rate at elevated temperature and pCO_2 compared to other sponges (Bennett et al., 2017). Observed *C. foliascens* physiological responses to OW, include increases in the levels of tissue necrosis and bleaching, elevated respiration rates and decreasing photosynthetic rates (Bennett et al., 2017).

In order to characterise the role that viruses may be playing in the thermal stress response of *C. foliascens*, two controlled experiments were conducted, exposing the photosynthetic sponge to short (3 days) and longer term (21 days) heat-stress events. Experimental conditions based on previous studies (Bennett et al., 2017) determined 31 °C as a sub-lethal/stress temperature and 28.5 °C as the average ambient/control temperature for *C. foliascens* from the Great Barrier Reef. Following experimental exposure, viral nucleic acid was isolated from control and thermally stressed sponge tissue, sequenced and bioinformatically analysed to identify the viral taxonomic and functional changes associated with each thermal stress treatment. Additionally, host morpho-physiological responses to thermal stress were examined, and correlations were made between bleaching / necrosis and taxonomic / functional variations in the sponge virome.

4.3. METHODS

4.3.1. Experimental design

Two experiments were conducted in order to investigate how sponge associated viral communities and their corresponding functional potential responded to heat-stress. Experiment 1 (exp 1) was a short heat-stress exposure, where viral taxonomy and function were investigated after three days at 31 °C and Experiment 2 (exp. 2) was a longer heat-stress exposure, where metaviromics taxonomy and function were investigated after 21 days heat-stress exposure. Experiments were performed within the National Sea Simulator at the Australian Institute of Marine Science (AIMS). Temperature treatments were created by mixing streams of 22 and 36 °C 0.04 µm filtered seawater. In both experiments, sponges were exposed to two temperature treatments, the ambient, 28.5 °C (control), based on the present-day average ocean temperature on the Great Barrier Reef (GBR)(IPCC, 2014) and the sublethal, 31 °C (heat-stress treatment), based on mortality-inducing temperature thresholds

previously described for this species (Bennett et al., 2017). Specimens of *C. foliascens* were collected from Davies Reef- GBR (18°820S, 147°650E) between April and May of 2017. After collection, sponges were maintained in holding tanks at 27 °C for one week to reduce any effects of collection. Following acclimation, individual sponges were transferred to experimental tanks, initially kept at 27 °C and gradually increased (0.5 °C per day) to a final temperature of 28.5 °C in the control tanks and 31 °C in the treatment tanks. Acclimation and ramping took 8 days before time zero (T0) conditions were reached. In both experiments, four sponge replicates were placed within each of the three control tanks and three sponge replicates were kept in each of the three treatment tanks (n=21). One individual within each control tank was processed for viral purification at T0, and the others processed after 3 days (T3) or 21 days (T21), resulting in nine replicates per treatment in each experiment (exp. 1: n = 21 (T0, n = 3; T3 ambient, n = 9; T3 sublethal, n = 9); exp. 2: n = 21 (T0, n = 3; T21 ambient, n = 9; T21 sublethal, n = 9)). To assess gross physiological and morphological changes in the sponge host throughout the experiment, photographs were taken before (T0) and after (T-end) experimental exposure. ImageJ software (IMAGEJ; US National Institutes of Health, Bethesda, Md, USA) was used to determine whether sponge tissue was affected by necrosis and bleaching. Ten litres of seawater were collected in each tank at T0 and processed for comparative metaviromic analysis.

4.3.2. Virus extraction and purification for metagenomic analysis

Sponge-viral extraction and purification methods were optimized based on a protocol used to isolate VLPs from culture lysates and coral tissue (Lawrence & Steward, 2010; Weynberg et al., 2014). Approximately 10 g of fresh sponge tissue was homogenized, first by cutting the sponge into small pieces (5 mm), covering with 15 µL of 0.02 µm filter-sterilized (Anotop, Whatman) SM buffer (100 mM NaCl, 8 mM $MgSO_4$, 50 mM Tris pH 7.5), then processing with a Craig's HS30E homogenizer (Witeg, Germany) for 5 to 10 min. Tissue homogenate was filtered through a Falcon® 100 µm Cell Strainer (Corning, USA), and centrifuged at 500 g for 15 min at 4 °C to pellet cell debris. Supernatant was transferred to a new Falcon® tube (Fisher Scientific, USA) where Cesium Chloride (CsCl) was added to bring the solution to a final density of 1.2 g mL^{-1}. In parallel, CsCl solutions of varying densities, diluted in 0.02 µm filtered SM Buffer, were layered in an ultracentrifuge tube, with the greatest density at the bottom and reducing as layers were added (3 mL of 1.6 g mL^{-1} solution; 2.5 mL of 1.45 g mL^{-1} solution; 2.5

mL of 1.3 g mL^{-1} solution; 2 mL of 1.2 g mL^{-1} solution). After layering the gradients, 7.5 mL of each sample was added to the top of three gradient tubes (3x2.5 mL per tube), and centrifuged (Beckman Coulter Ultracentrifuge, USA) at 4 °C in a swinging-bucket rotor (SW 40 Ti) for 2h 40 min at 40,000 g. Following centrifugation, eighteen 0.7 mL fractions were pulled from the gradient into separate Eppendorff tubes. Density and nucleic acid concentration of each fraction was determined (Weynberg et al., 2014) and fractions with density between 1.2 g/mL and 1.5 g/mL were pooled together and filtered (0.22 µm EMD Millipore filter, EUA) to remove any remaining contaminating bacteria. A diafiltration method was used to change the buffer, removing the CsCl salt from the samples and concentrating the viral particles in solution. Samples were centrifuged in 30 KDa Amicon centrifugal spin columns (Millipore, EUA) at 4,000 g for 30 min at 4°C, between four and six times adding filter-sterilized SM Buffer and discarding the flow-through (additional times were required when larger volumes of solution remained in the tube after centrifugation). Samples were concentrated to a final volume of 600 µl. In total, 200 µL of the solution was used for DNA extraction and the remaining eluate was frozen at -80°C at the Australian Institute of Marine Science for any subsequent analyses. These protocols were based on the findings of Chapter 3.

4.3.3. Viral DNA extraction and amplification for sequencing

Viral purified samples were treated with DNase and RNase (Ambion, CA) to degrade free nucleic acid from the outside of the viral capsid prior to DNA extraction. DNA was extracted using FastDNA SPIN Kit for Soil (MP Biomedicals) following manufacturer's instructions. A modified Random Priming-mediated Sequence-Independent Single-Primer Amplification (RP-SISPA) approach was used to amplify the viral DNA fragments (Weynberg et al., 2014). Briefly, all virus DNA was converted to dsDNA using a Klenow Fragment (3'–5' exo-) using RP-SISPA primers with a 3' random hexamer sequence. For each reaction, 8 µL of DNA was added to 6 µl of reaction mix containing 1.5 µl of 10× NEB buffer (New England Biolabs Buffer 2); 1 µl of 2.5 mM dNTPs; 1.5 µl of primer FR26RV-N (GCCGGAGCTCTGCAGATATCNNNNNN, 10µM stock) and 2µl of DNase-free distilled water. Reactions were incubated at 94 °C for 3 min, placed on ice for 3 min (primer annealing) before 1 µl of Klenow Fragment was added to the mix and incubated at 37 °C for 60 min. After incubation 1 µl of dNTP and 1 µl of N primer was added to each tube, incubated again at 94°C for 3 min and placed on ice for 3 min. Finally, 1 µl of Klenow fragment was added to the solution and the reaction was incubated at 37 °C for

60 min then terminated at 75 °C for 20 minutes. Triplicate PCR amplifications were performed using the SISPA template. Two µl of template was added to 23 µl of reaction mix containing 2.5 µl of 10× reaction buffer, 4 µl of dNTP (2.5 mM stock), 2 µl of FR20RV primer (GCCGGAGCTCTGCAGATATC, 10 µM stock) and 0.25 µl of TaKaRa LA Taq™ HS polymerase (5 U/µl, Scientifix). The reaction was incubated at 95 °C for 10 min, followed by 30 thermal cycles (95 °C for 30 sec, 60 °C for 60 sec, 72 °C for 90 sec). At the end of the cycles the samples were held at 72 °C for 13 min to allow the completion of complementary strand synthesis. PCR reactions were loaded on a 0.8 % agarose gel in 1×TAE and underwent electrophoretic separation at 100V for 30 min. Amplifications with no visible PCR product were repeated using a dilution of the SISPA template (1:10 or 1:100). A reconditioning PCR was performed after pooling triplicate reactions. A volume of 10 µl of pooled template was added to 90 µl of master mix containing 55.25 µl of PCR grade water, 10 µl 10× reaction buffer, 16 µl dNTP (2.5mM stock), 8 µl FR20RV primer (10 µM stock) and 0.75 µl TaKaRa LA Taq™ HS polymerase. The reaction was cycled as per the PCR amplification described above. Reactions were cleaned using the MinElute PCR Purification Kit® following the Manufacturers protocol. Samples were run on a 0.8 % agarose gel in 1×TAE at 100V for 30 min and DNA quality (260:280 ratios) was checked using a NanoDrop 2000 spectrophotometer (Thermo Scientific, USA).

4.3.4. Viral DNA sequencing and bioinformatic analysis

Purified viral DNA was sent for sequencing in samples containing 20 µL of template concentrated at 20 ng / µL. Genomic DNA was sequenced using NextSeq500 platform, which produced paired-end 125 bp fragments at the Ramaciotti Centre for Genomics, University of New South Wales, Australia.

Sequencing datasets were analysed using the HoloVir protocol (Laffy et al., 2016), a computational workflow designed to assign taxonomy and function to host-associated viral metagenomes. Quality Control (QC) analysis and genome assembly was performed on raw sequence reads using CLC Genomic Workbench (version 9.0). Library adaptors, ambiguous nucleotides (n=2) and low-quality bases (error probability cutoff 0.01) were trimmed and reads below 40 base pairs were discarded. Viral contigs were assembled from the trimmed sequences using the *De Novo* Assembly function in CLC Genomic Workbench. Contigs smaller than 500bp or those that had average coverage-values below 3 were discarded (Laffy et al., 2016). Gene prediction was performed on the remaining contigs using MetaGeneAnnotator

(Noguchi, Taniguchi & Itoh, 2008), and in accordance with the HoloVir protocol, predicted genes were used for viral taxonomic assignment and functional annotation. Taxonomic assignment was performed using MEGAN6 (Huson et al., 2011) utilising a lowest common ancestor strategy based on best significant matches to viral RefSeq database BLASTP analysis (Pruitt, Tatusova & Maglott, 2007). MEGAN6 was run using a top-percent parameter of 80, min-support value of five reads and a bit score threshold value of 80. Assembled data was also compared with the HoloVir cellular and viral marker database, identifying potential cellular contaminants in the samples (Laffy et al., 2016).

Functional analysis of the predicted genes was also performed as described in the HoloVir protocol (Laffy et al., 2016), utilising BLASTP sequence similarity searches of predicted genes against the UniProtKB/Swiss-Prot protein database (UniProt Consortium, 2015), using an *e*–value cutoff of 10^{-10}. Swiss-Prot Keywords were assigned to predicted genes based on the best significant blast match and overall keyword enrichment for each metaviromic community was calculated, adjusting for both contig coverage as well as keyword frequency within the SwissProt database. The 50 most enriched Swissprot keywords were identified across samples. Analysis of deviance for multivariate generalized linear models for abundance data (anova.manyglm function) was performed using the R package mvabund (Wang et al., 2012) in order to identify the major drivers of difference between ambient and sublethal temperatures. MultiDimensional Scaling (MDS) analysis was performed to compare viral community composition and function based on Bray-Curtis dissimilarity matrix, and PERMANOVA analysis was used to attest for significant differences amongst different treatments and tank replicates. SIMPER analysis was used to identify viral taxa that contributed to dissimilarities between treatments, while canonical correspondence analysis (CCA) was employed to correlate viral taxa that contributed to the dissimilarity between the following factors; temperature, bleaching and necrosis. MDS, SIMPER, CCA and PERMANOVA analyses were performed using the software Primer (v 6.1.7).

4.4. RESULTS

4.4.1. Analysis of overall community profile of *C. foliascens* virome

In total, 693,342 contigs were assembled and 1,284,021 genes were predicted from all *C. foliascens* samples (Table 4.1). On average, 15 % of all predicted genes were taxonomically assigned and 20 % of all contigs contained at least one taxonomically assigned gene (Table 4.1). Cellular marker evaluation identified that an average of 1.3 % of contigs contained cellular marker matches (Table 4.1), which is higher than the observed percentage of contigs containing cellular marker genes in previous studies (0.1-0.3 % (Laffy et al., 2018); an average of 0.25 % (Chapter 3)). An additional contig filtration step was tested in an effort to improve the data quality and minimise the effect of cellular contamination, and the details and analysis of this approach is provided in Appendix 4 (Table A4.1, Fig. A4.1). However, this contig filtration step did not substantially improve the data quality, generating similar number and size of contigs as well as taxonomic assignments (Table A4.1, Fig. A4.1), hence this filtered output was not used in final analyses.

Viral metagenomes derived from *Carteriospongia foliascens* in the control treatment followed the same patterns previously described for *C. foliascens* samples from the GBR (Chapter 3), predominantly matching dsDNA viruses (90 ± 1.1 % (Chapter 4); 90 ± 1.9 % (Chapter 3)), with a lower relative abundance of matches to ssDNA viruses (5 ± 0.9 % (Chapter 4); 9 ± 2 % (Chapter 3)) and retroviruses (3 ± 0.4 % (Chapter 4); 1 ± 0.2 % (Chapter 3)). The order Caudovirales (tailed bacteriophages) was prevalent within the dsDNA viral matches, accounting for more than half (53 ± 1.5 %) of total viral taxonomic assignments (Supplementary Table 4.1). *Myoviridae* was the dominant Caudovirales family observed (24 ± 0.8 %) followed by *Siphoviridae* (18 ± 1.2 %) and *Podoviridae* (5 ± 0.4 %) (Supplementary Table 4.1). *Inoviridae* (2 ± 0.6 %) and *Microviridae* (2 ± 0.5 %) made up most of the non-tailed bacteriophages associated with *C. foliascens* (Supplementary Table 4.1). Contigs taxonomically assigned to the nucleocytoplasmic large DNA viral (NCLDV) families *Mimiviridae*, *Marseilleviridae*, *Phycodnaviridae*, *Ascoviridae*, *Iridoviridae*, *Asfarviridae* and *Poxviridae* were also associated with *C. foliascens* (Fig. 4.1). Within the NCLDV, *Phycodnaviridae* were present in a higher proportion of samples (11 ± 0.7 %) followed by *Mimiviridae* (5 ± 0.3 %). A complete table of viral taxonomic assignments is presented in Supplementary Table 4.1.

Analysis of viral metagenome composition revealed that the viral families *Myoviridae*, *Podoviridae*, *Siphoviridae*, *Mimiviridae*, *Phycodnaviridae* and *Poxviridae* were found in all sponge and seawater samples (Fig. 4.1). Matches to members of the *Ascoviridae* and *Inoviridae* were also found in all sponge and seawater samples, whereas matches to retro-transcribing viruses were exclusively found in sponge samples (Fig. 4.1).

Table 4.1 Summary of assembly statistics, taxonomic assignment and cellular contamination evaluation of virome datasets *from control and thermally stressed C. foliascens*. N50 values for each dataset were calculated based on evaluation of unfiltered contigs. * the number of days in the aquarium after period of acclimation. NA stands for not applicable.

Experiment	Samples	Samples nature	Time* (days)	Tank	Temp (°C)	Contig N50	# contigs	Longest contig	# predicted genes	% Taxonomically assigned genes	% Taxonomically assigned contigs	% of contigs with cellular marker matches	Presence (1) absence (0) of bleaching	Presence (1) absence (0) of necrosis
Short heat-stress exposure	E1_T0_1-1_43	Sponge	0	A1	28.5	398	6125	17212	8225	8.64%	10.94%	1.2%	0	0
	E1_T0_1-2_39	Sponge	0	A2	28.5	611	6041	218069	13387	13.32%	16.50%	1.0%	0	0
	E1_T0_1-4_32	Sponge	0	A3	28.5	692	7579	302902	17842	13.39%	15.13%	1.8%	0	0
	E1_T72_1-1_18	Sponge	3	A1	28.5	668	10271	567948	22952	13.01%	16.31%	1.6%	0	0
	E1_T72_1-1_7	Sponge	3	A1	28.5	1046	5219	50164	11343	12.81%	20.29%	2.2%	0	0
	E1_T72_1-1_50	Sponge	3	A1	28.5	525	5781	9176	9029	11.24%	16.55%	1.9%	0	0
	E1_T72_1-2_37	Sponge	3	A2	28.5	493	10235	158313	18541	11.60%	12.62%	1.3%	0	0
	E1_T72_1-2_74	Sponge	3	A2	28.5	456	8316	297818	16087	11.86%	9.76%	1.1%	0	0
	E1_T72_1-2_41	Sponge	3	A2	28.5	435	7099	8568	9529	8.86%	11.26%	1.2%	0	0
	E1_T72_1-4_17	Sponge	3	A3	28.5	478	18388	27146	26622	9.13%	10.63%	1.2%	0	0
	E1_T72_1-4_24	Sponge	3	A3	28.5	540	8288	17034	13757	11.46%	16.40%	1.7%	0	0
	E1_T72_1-4_57	Sponge	3	A3	28.5	545	7044	83157	13974	12.26%	16.43%	1.7%	0	0
	E1_T72_3-1_12	Sponge	3	S1	31	434	9870	164377	16210	9.86%	10.24%	1.3%	0	0
	E1_T72_3-1_29	Sponge	3	S1	31	2234	2527	297553	8523	15.09%	22.83%	2.1%	0	0
	E1_T72_3-1_16	Sponge	3	S1	31	498	5411	72447	10733	3.37%	6.36%	0.6%	0	0
	E1_T72_3-2_4	Sponge	3	S2	31	466	8462	12238	2522	57.69%	6.39%	0.8%	0	0
	E1_T72_3-2_45	Sponge	3	S2	31	388	3942	13838	4927	27.64%	21.49%	2.6%	0	0
	E1_T72_3-2_36	Sponge	3	S2	31	429	2080	17094	11373	8.47%	43.22%	5.4%	0	0
	E1_T72_3-4_9	Sponge	3	S3	31	547	7621	135589	13340	12.17%	12.74%	1.5%	0	0
	E1_T72_3-4_1	Sponge	3	S3	31	538	5909	228242	12602	12.94%	15.32%	1.8%	0	0
	E1_T72_3-4_54	Sponge	3	S3	31	8112	2195	415356	9262	2.07%	8.47%	0.6%	0	0
	SW_E1_T0_1-1	Seawater	0	A1	28.5	621	17595	85432	45454	11.24%	17.53%	0.4%	NA	NA
	SW_E1_T72_1-1	Seawater	3	A1	28.5	2342	14240	288572	13564	65.98%	42.97%	0.9%	NA	NA
	SW_E1_T72_1-2	Seawater	3	A2	28.5	1308	11277	70089	30431	7.61%	11.36%	2.0%	NA	NA
	SW_E1_T72_1-4	Seawater	3	A3	28.5	1669	4869	111115	13656	34.62%	63.63%	2.8%	NA	NA
	SW_E1_T72_3-1	Seawater	3	S1	31	933	13639	408481	33346	6.71%	10.40%	1.9%	NA	NA
	SW_E1_T72_3-2	Seawater	3	S2	31	705	11169	630162	27494	18.88%	29.09%	2.0%	NA	NA

	SW_E1_T72_3-4	Seawater	3	S3	31	967	17882	82144	44192	9.40%	14.34%	1.9%	NA	NA
Long heat-stress exposure	E2_T0_1-1_D4	Sponge	0	A1	28.5	534	29843	41722	45611	10.81%	13.77%	1.2%	0	0
	E2_T0_1-2_D39	Sponge	0	A2	28.5	482	19336	49146	25808	8.80%	9.78%	1.0%	0	0
	E2_T0_1-4_D64	Sponge	0	A3	28.5	583	23637	70431	41333	12.31%	17.74%	1.6%	0	0
	E2_T3W_1-1_D17	Sponge	21	A1	28.5	687	11603	78496	21230	9.14%	13.90%	1.9%	0	0
	E2_T3W_1-1_D37	Sponge	21	A1	28.5	604	14163	66906	23278	11.20%	14.54%	1.6%	0	0
	E2_T3W_1-1_D9	Sponge	21	A1	28.5	513	15990	50363	22438	22.43%	25.96%	1.0%	0	0
	E2_T3W_1-2_D72	Sponge	21	A2	28.5	563	17256	27249	27882	2.76%	4.04%	1.3%	0	0
	E2_T3W_1-2_D22	Sponge	21	A2	28.5	543	9048	21246	15952	16.54%	23.44%	1.6%	0	0
	E2_T3W_1-2_D65	Sponge	21	A2	28.5	450	6752	12339	8800	21.92%	23.96%	1.0%	0	0
	E2_T3W_1-4_D32	Sponge	21	A3	28.5	513	23307	56861	32998	12.29%	14.19%	1.0%	0	0
	E2_T3W_1-4_D16	Sponge	21	A3	28.5	567	14018	49368	25540	12.98%	19.43%	1.7%	0	0
	E2_T3W_1-4_D3	Sponge	21	A3	28.5	521	22787	38783	27763	11.58%	11.24%	0.8%	0	0
	E2_T3W_3-1_D51	Sponge	21	S1	31	486	26115	68406	33944	9.22%	9.99%	0.9%	1	1
	E2_T3W_3-1_D52	Sponge	21	S1	31	643	18511	30427	30164	9.18%	12.38%	1.5%	1	1
	E2_T3W_3-1_D57	Sponge	21	S1	31	477	9776	16535	12680	25.62%	29.64%	0.8%	1	1
	E2_T3W_3-2_D53	Sponge	21	S2	31	556	21379	19133	11373	28.30%	12.44%	0.5%	0	0
	E2_T3W_3-2_D55	Sponge	21	S2	31	647	7111	64655	12244	7.87%	12.64%	1.8%	1	0
	E2_T3W_3-2_D24	Sponge	21	S2	31	566	19013	76225	29971	3.35%	5.18%	1.8%	1	0
	E2_T3W_3-4_D19	Sponge	21	S3	31	351	5459	6131	6323	20.04%	21.08%	0.6%	0	0
	E2_T3W_3-4_D2	Sponge	21	S3	31	471	13607	27806	16552	8.95%	9.37%	0.7%	1	1
	E2_T3W_3-4_D23	Sponge	21	S3	31	2774	10155	104607	31244	1.50%	4.05%	1.8%	0	0
	SW_E2_T0_1-1	Seawater	0	A1	28.5	939	16288	102801	40318	17.10%	29.51%	1.6%	NA	NA
	SW_E2_T3W_1-2	Seawater	21	A2	28.5	907	9601	47617	22551	14.30%	25.29%	2.1%	NA	NA
	SW_E2_T3W_1-4	Seawater	21	A3	28.5	1112	19774	102658	47988	15.69%	25.86%	2.0%	NA	NA
	SW_E2_T3W_3-1	Seawater	21	S1	31	973	30937	131573	80757	15.99%	27.57%	1.8%	NA	NA
	SW_E2_T3W_3-2	Seawater	21	S2	31	727	10352	87708	21982	15.99%	24.23%	1.9%	NA	NA
	SW_E2_T3W_3-4	Seawater	21	S3	31	680	38450	102535	88380	15.89%	26.41%	1.3%	NA	NA

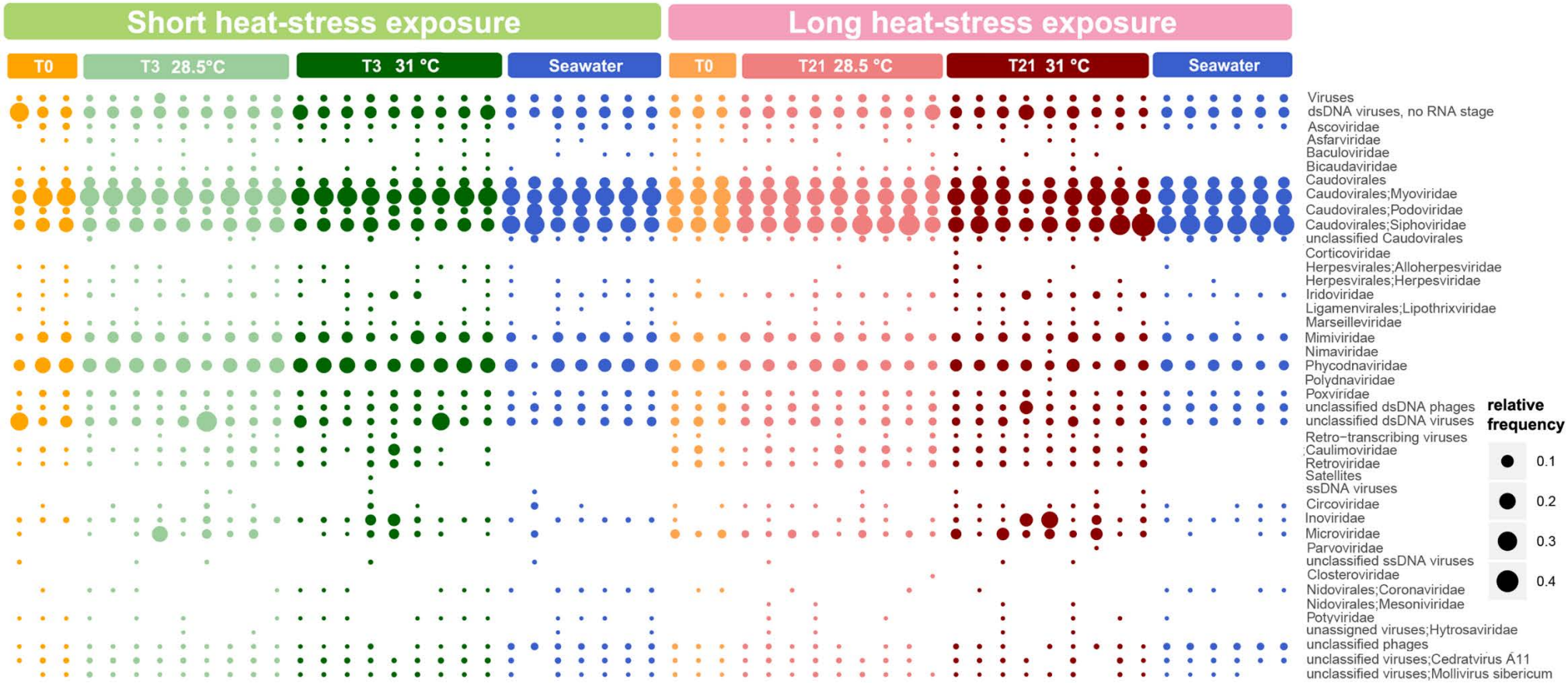

Figure 4.1 Taxonomic summary of the viral community associated with *C. foliascens* subjected to a short and long heat-stress experiment, with column headings denoting the number of days samples were exposed to heat stress (T0, T3, T21), the temperature treatment (28.5° C and 31° C) and seawater control samples. Taxonomy is summarised at the family level based on MEGAN6 LCA taxonomic assignment using parameters defined in Laffy et al., 2016.

4.4.2. Effect of temperature on the *C. foliascens* viral community

Comparison of viral communities in samples exposed to experimental treatments for 3 days, identified a higher number of samples with *Coronaviridae* matches in heat-stressed sponges (6) compared to control treatments (4), as well as fewer heat-stressed samples showing matches with *Iridoviridae* (8 in control, 6 in sub-lethal treatment) and *Circoviridae* (4 control, 2 in sub-lethal treatment) (Table 4.2). However, ordinate and variance analysis based on Bray-Curtis similarity of genus-level taxonomic assignment for predicted genes showed no significant difference in the overall viral community composition between ambient and sublethal temperature treatments following short term exposure (Table 4.2). In contrast, significant differences were evident between temperature treatments in the longer-term exposure (Fig 4.2; Table 4.2). Additionally, there was no significant difference between tank replicates and there was no difference between ambient samples across time (Table 4.2).

Table 4.2 PERMANOVA pairwise comparisons of predicted viral genes from *C. foliascens* based on viral RefSeq taxonomic assignments (genus level) from two experiments: short heat-stress exposure (3 days) and long heat-stress exposure (21 days), each profiling sponge associated viral metagenomes from sponges exposed to ambient (28.5 °C) and sublethal (31 °C) temperatures. Multivariate permutational analysis of variance (PERMANOVA) (Primer6/PERMANOVA+ v1.0.2, Plymouth, UK) was used to compare taxonomic differences in the viral communities amongst replicates from different tanks, time and temperature treatments. For each heat-stress experiment there were three ambient treatment tanks (A1, A2, A3) and three elevated temperature tanks (S1, S2, S3), each containing three sponge replicates. Differences between day zero (T0), day 3 (T3) and day 21 (T21) were measured within ambient conditions. Samples with significant p-values from pairwise tests (≤0.05) are highlighted with an asterix (*). Student's t-test are indicated by the letter "t" and "Unique perms" indicates how many unique-values of the test statistic were obtained under permutation.

Experiment	Factors	Groups	t	p	Unique perms
3 d Exposure	Tank (28.5 °C)	A1-A2	0.981	0.424	473
		A1-A3	1.302	0.212	473
		A2-A3	0.508	0.928	465
	Tank 31 °C)	S1-S2	0.813	0.785	10
		S1-S3	0.508	1	10
		S2-S3	0.782	0.703	10
	Time (28.5 °C)	T0-T3	0.831	0.653	59
	Temperature	28.5 °C-31 °C	1.267	0.204	10
21 d Exposure	Tank (28.5 °C)	A1-A2	0.889	0.611	470
		A1-A3	0.942	0.494	465
		A2-A3	1.147	0.268	468
	Tank (31 °C)	S1-S2	1.221	0.194	10
		S1-S3	1.325	0.313	10
		S2-S3	1.276	0.195	10
	Time (28.5 °C)	T0-T21	1.146	0.34	59
	Temperature	28.5 °C-31 °C	1.2041	0.001*	10

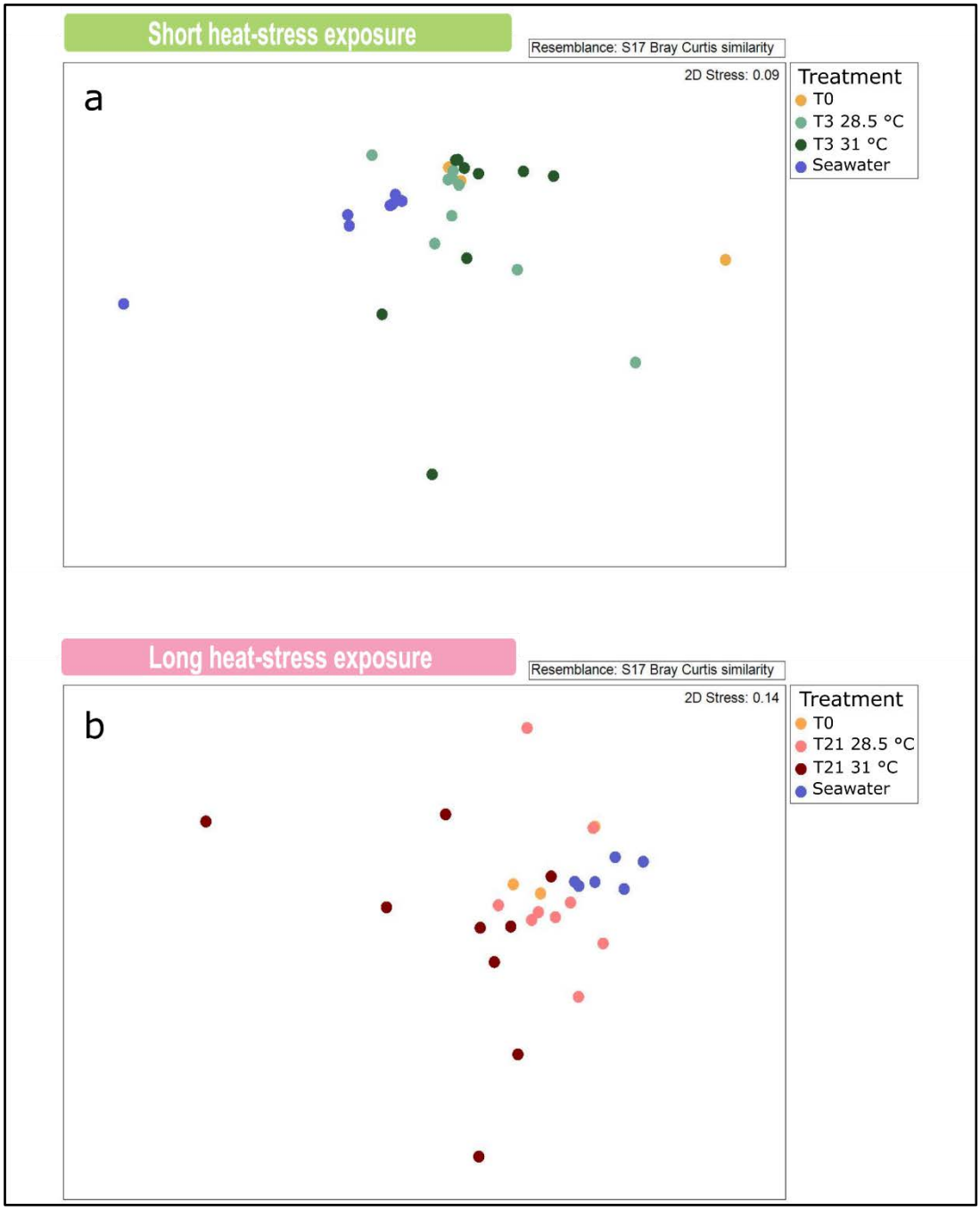

Figure 4.2 Non-metric multidimensional scaling plot based on Bray-Curtis similarity of genus-level taxonomic assignment for predicted genes, based on viral RefSeq BLASTP taxonomic assignment. Ordination displays similarities in the viral communities of *C. foliascens* exposed to two temperatures (28.5° C and 31° C) for a (a) 3 day and (b) 21 day heat-stress exposure. Samples were taken at day 0 (T0) for both experimental set-ups and at day 3 (T3) and day 21, (T21) respectively. Control seawater samples were also taken for each tank at day 0 (T0).

Mvabund analysis identified an enrichment of *Inovirus* matches and a decline of tailed bacteriophages as drivers of difference between control and thermally stressed samples in the 21 d experiment (Fig. 4.3).

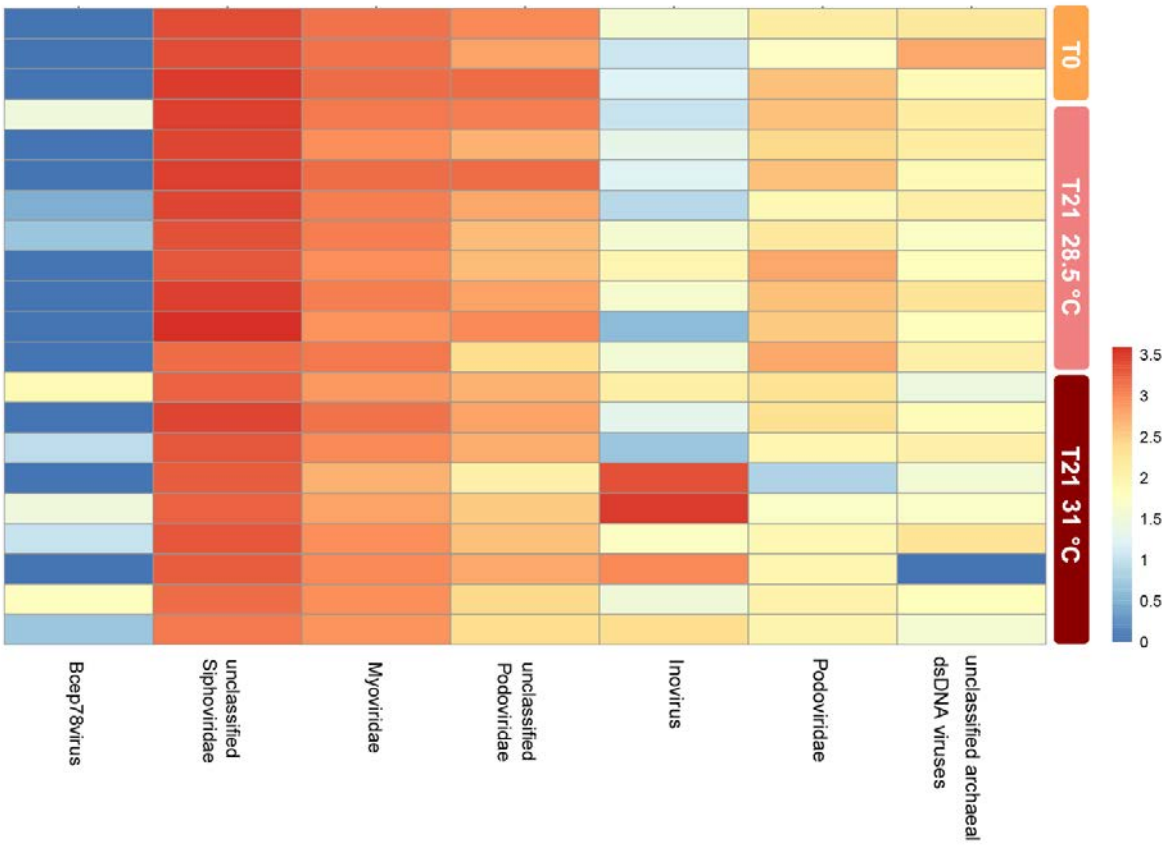

Figure 4.3 Heatmap of viral communities associated with *C. foliascens* following a 21 d heat-stress exposure, showing significant differences between treatments (*p-value* <0.05) according to mvabund analysis summarised on genus-level based MEGAN6 LCA taxonomic assignment using parameters defined in Laffy *et al.*, 2016. Mvabund analysis was used to identify the drivers of difference between samples at day zero (T0), after 21 days exposure to ambient temperature (T21 28.5 °C) and to sublethal temperature (T21 31 °C).

Similarity percentage analysis (SIMPER) of species-level taxonomic assignments showed that the *Inoviridae* representative, *Pseudomonas phage* pf3, primarily contributed to the dissimilarity between ambient and sub-lethal conditions (Table 4.3), accounting for 0.9 % of the total dissimilarity. This *Inovirus* representative species was six times more abundant in *C. foliascens* at 31 °C.

Table 4.3 Similarity percentage analysis (SIMPER) of differences in *C. foliascens* viral metagenomes in individuals exposed to 28.5 °C and 31 °C, based on Bray-Curtis similarity of species-level taxonomic assignment of predicted genes. The columns two and three identify the average abundance of viral taxa within each temperature treatment, the fourth and fifth columns represent the Bray Curtis dissimilarity metric between both temperatures and its standard deviation, respectively. The sixth column shows the percentage of dissimilarity contribution explained by that phylum and the seventh column shows the cumulative Bray Curtis dissimilarity metric for the phylum.

Species	Average Abundance 28.5 °C	Average Abundance 31 °C	Average dissimilarity	Dissimilarity standard deviation	% Contribution	Cumulative %
Pseudomonas phage Pf3	1.77	10.82	0.46	0.6	0.9	0.9
Gordonia phage Orchid	9.26	1.33	0.38	1.17	0.74	1.64
Bacillus virus G	22.68	27.58	0.38	1.32	0.74	2.38
Loktanella phage pCB2051-A	4.44	9.15	0.37	0.6	0.71	3.09
Eel River basin pequenovirus	7.65	4.49	0.36	1.05	0.69	3.78
Burkholderia virus Bcep22	6.95	8.85	0.33	1.39	0.64	4.42
Ralstonia phage RS603	0.94	7.14	0.33	0.64	0.64	5.06
Mycobacterium phage Dori	13.31	8.82	0.3	1.11	0.59	5.65
Vibrio phage douglas 12A4	8.15	4.92	0.28	1.15	0.53	6.18
Ectocarpus siliculosus virus 1	8.88	9.11	0.27	1.18	0.52	6.7
Xylella phage Xfas53	6.76	1.58	0.26	1.1	0.51	7.21
Ostreococcus lucimarinus virus 1	9.45	5.4	0.26	1.33	0.5	7.72
Trichoplusiani ascovirus 2c	8.74	9.59	0.25	1.36	0.48	8.19
Staphylococcus phage phiIPLA-C1C	0.12	4.74	0.24	0.41	0.46	8.66
Brucella phage Tb	5.78	1.38	0.23	1.1	0.45	9.11
Verrucomicrobia phage P8625	5.74	2.57	0.23	1.06	0.45	9.56
Aureococcus anophagefferens virus	14.92	14.96	0.23	1.28	0.45	10.01

4.4.3. Viral community profile in bleached and necrosed sponges

The impact of elevated temperature on *C. foliascens* was evident by the occurrence of morpho-physiological anomalies, specifically bleaching and tissue necrosis, in several of the thermally stressed individuals from the longer-term exposure experiment (Fig. 4.4; Table 4.1). Ordination and variance analyses performed at the genus-level on the viral taxonomic assignments showed no significant distinction in viral community composition across visibly healthy and bleached/necrotic sponges (Table 4.4; Fig. 4.5). However, analysis using mvabund identified drivers of significant difference between non-stressed samples, thermally stressed samples with no signs of bleaching/necrosis and stressed individuals with visible signs of

bleaching/necrosis (Fig. 4.6). A higher proportion of *Inovirus* matches were evident in bleached individuals compared to non-bleached ones (Fig. 4.6a). While the *Circoviridae* and *Gokushovirinae* matches in bleached individuals were comparable to non-stressed individuals, there was an increase in the number of matches to these taxa in the non-bleached samples at 31 °C. Similarly, while matches to *P1 virus*, *Andromedavirus* and *Tavenvirinae* were largely absent from visibly unaffected samples at 31 °C, they were observed in both control samples at 28.5 °C and bleached samples at 31 °C (Fig. 4.6a). Mvabund analysis performed to assess drivers of difference between 28.5 °C healthy individuals, 31 °C visibly unaffected individuals and 31 °C necrosed individuals, identified that matches to the viral subfamily *Autographivirinae* were largely absent from most samples, but were prominent in three quarters of the necrotic heat stressed samples (Fig 4.5b). Additionally, matches to *Herpersviridae*, *Gammaherpesvirinae*, *Muvirus* and *Betabaculovirus* in necrosed individuals at 31 °C was comparable to healthy samples at 28.5 °C, but reduced in visibly unaffected samples at 31 °C. Similarly, matches to *Lymphocystivirus* were comparable between necrosed samples at 31 °C and healthy samples at 28.5 °C, but higher in visibly unaffected samples at 31 °C (Fig 4.5b).

Table 4.4 PERMANOVA pairwise comparisons of predicted viral genes from *C. foliascens* based on viral RefSeq taxonomic assignments (genus level) from long heat-stress exposure experiment. Multivariate permutational analysis of variance (PERMANOVA) (Primer6/PERMANOVA+ v1.0.2, Plymouth, UK) was used to compare taxonomic differences in the viral communities in bleached/necrotic and visibly healthy individuals amongst all experimental samples and within thermally stressed (31 °C) samples. Samples with significant *p*-values from pairwise tests (≤0.05) are highlighted with an asterix (*). Student t-tests are indicated by the letter "t" and "Unique perms" indicates how many unique-values of the test statistic were obtained under permutation.

Assignment	Factors	Groups	t	p	Unique perms
Taxonomic	Bleaching	Bleached - Non-bleached	1.282	0.082	993
	Bleaching (within 31 °C)	Bleached - Non-bleached	0.703	0.948	84
	Necrosis	Necrosed – Non-necrosed	0.881	0.652	925
	Necrosis (within 31 °C)	Necrosed – Non-necrosed	0.968	0.565	126
Functional	Bleaching	Bleached - Non-bleached	0.8958	0.619	988
	Bleaching (within 31 °C)	Bleached - Non-bleached	1.559	0.013*	84
	Necrosis	Necrosed – Non-necrosed	1.106	0.216	126
	Necrosis (within 31 °C)	Necrosed – Non-necrosed	0.771	0.879	919

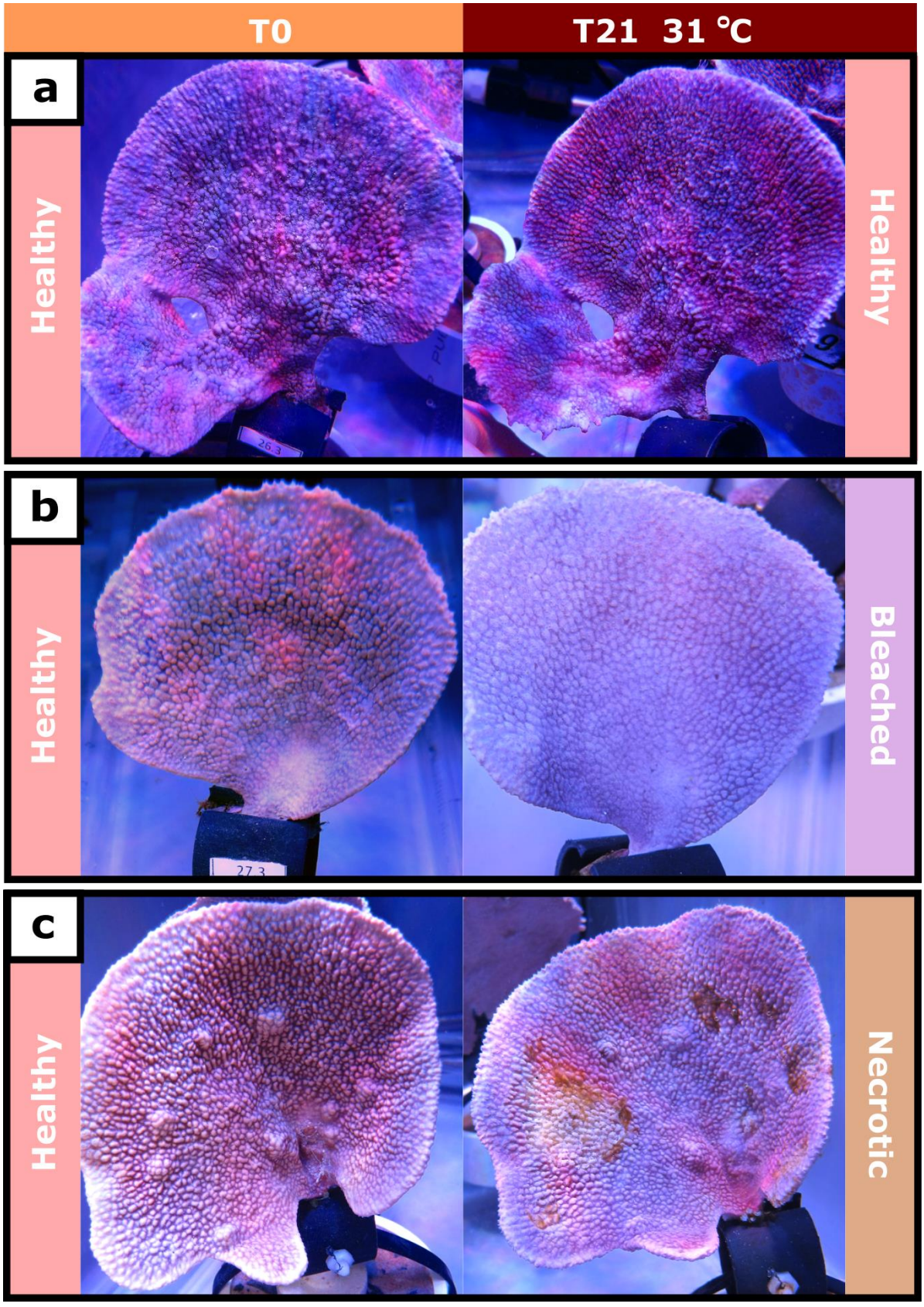

Figure 4.4 Health state representation of three *C. foliascens* individuals photographed at day zero (T0), and after 21 d exposed to 31 °C (T21 31 °C), exemplifying the sponges that (a) kept the initial visibly heathy, (b) bleached, or (c) necrosed morphotypes after exposed to the heat-stress treatment.

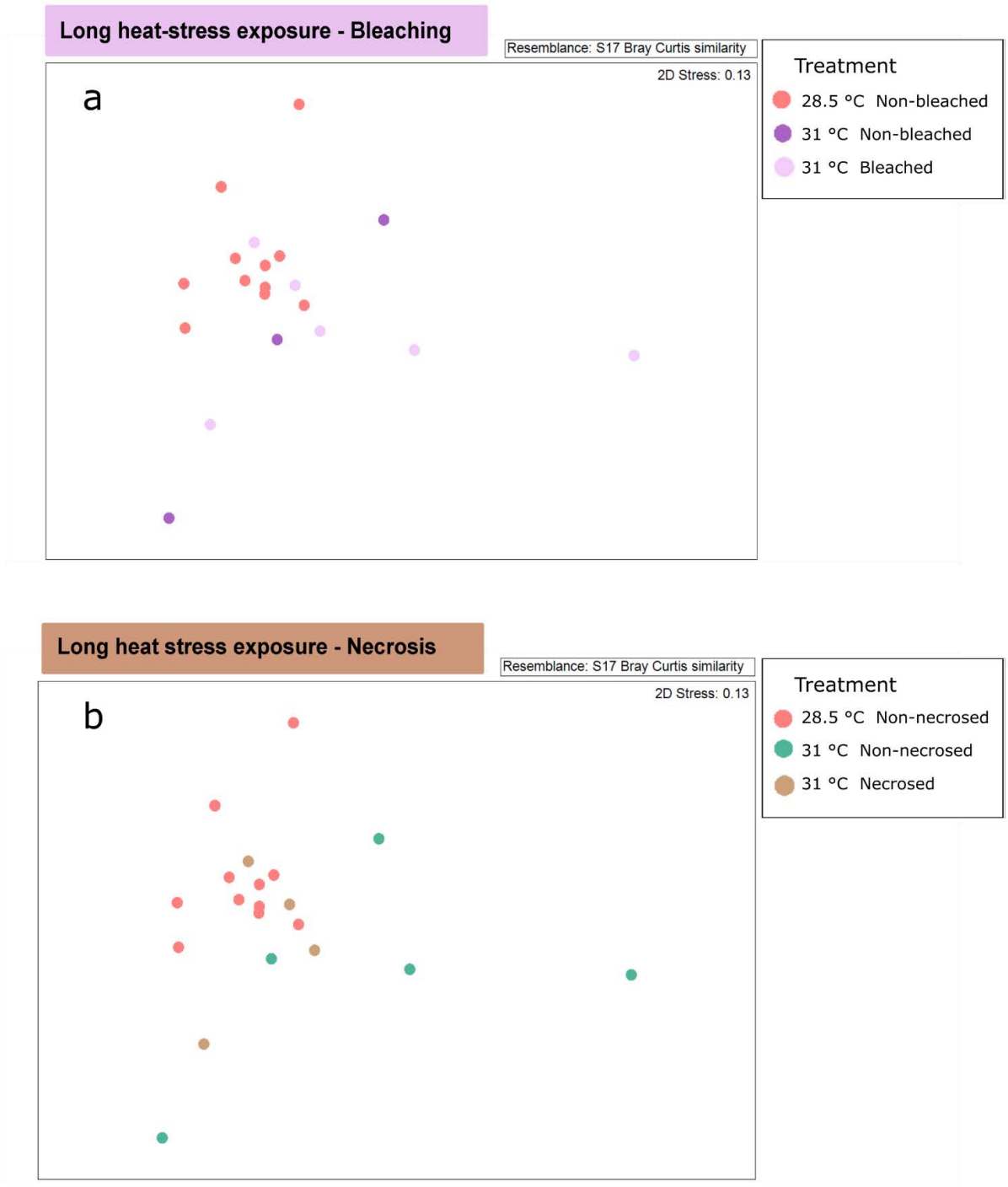

Figure 4.5 Non-metric multidimensional scaling plot based on Bray-Curtis similarity of genus-level viral taxonomic assignment for predicted genes from *C. foliascens* individuals exposed to temperature treatments for 21 days. Ordination displays similarities in the viral communities of (a) i) 28.5 °C healthy, ii) 31 °C visibly unaffected and iii) 31 °C bleached individuals and (b) between i) 28.5 °C healthy, ii) 31 °C visibly unaffected and iii) 31 °C necrotic individuals.

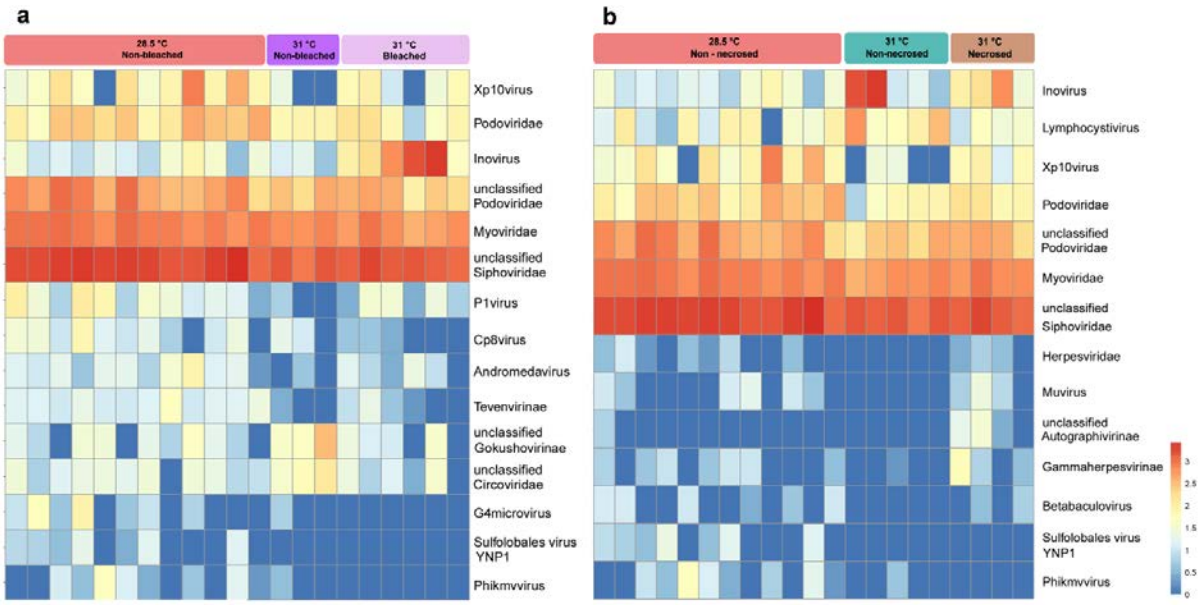

Figure 4.6 Heatmap of the metaviromic communities associated with *C. foliascens* following 21 days experimental exposure to elevated temperature. Heatmap shows significant differences between samples (p-value <0.05) according to PERMANOVA tests performed using the mvabund package, summarised at the genus level based on MEGAN6 LCA assignment using parameters defined in Laffy et al., 2016. Mvabund analysis was used to identify the drivers of difference between (a) i) 28.5 °C healthy, ii) 31 °C visibly unaffected and iii) 31 °C bleached individuals and (b) between i) 28.5 °C healthy, ii) 31 °C visibly unaffected and 31 °C necrotic individuals.

Canonical Correspondence Analysis (CCA) (Fig. 4.7) was carried out to determine which viral taxa contributed most to the dissimilarities between experimental samples according to temperature, bleaching and necrosis (Table 4.3). The first two axes of the CCA biplot accounted for 89 % and 10 % of the total community variation, respectively, with temperature and bleaching the most correlated factors with the first axis (Temperature (axis 1: -0.51, axis 2: 0.25); Bleaching (axis 1: 0.56, axis 2: -0.26)) and necrosis mostly correlated with axis 2 (axis 1: -0.1, axis 2: -0.46), showing minimal impact on the viral community structuring (Fig. 4.7).

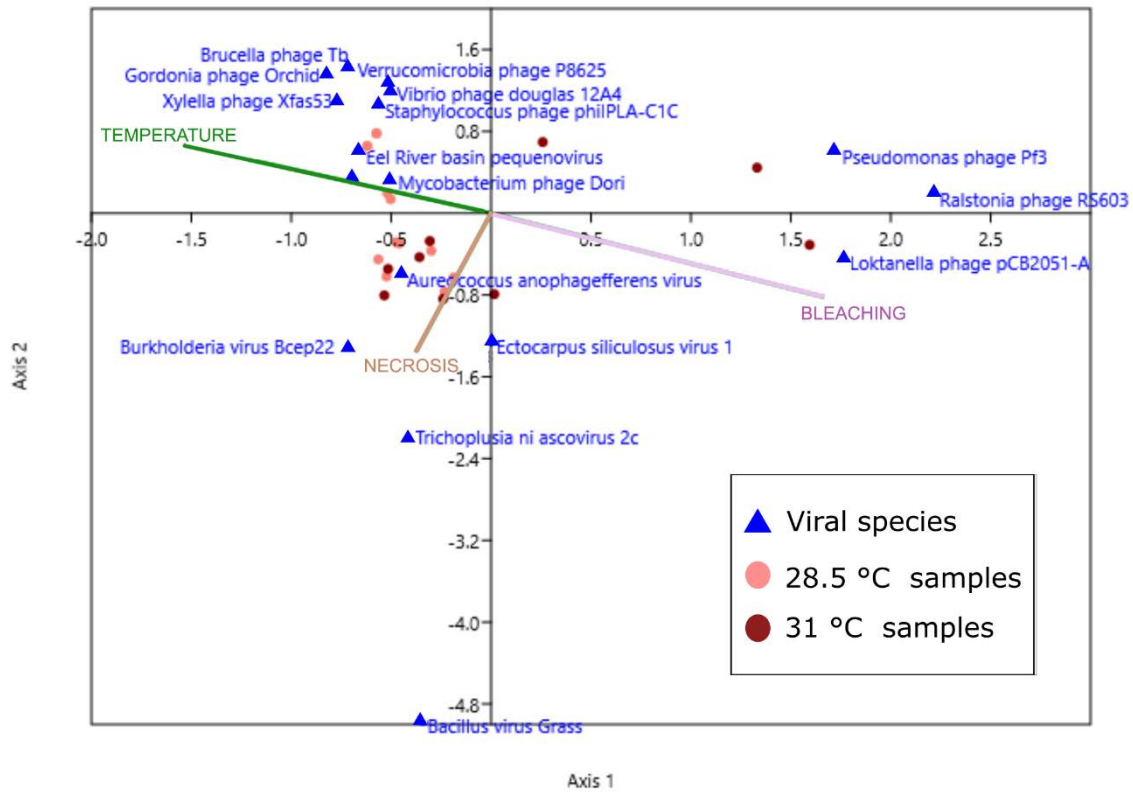

Figure 4.7 Canonical correspondence analysis (CCA) biplot correlating the occurrence of morpho-physiological anomalies in *C. foliascens* exposed to a 21 d heat stress experiment, with the viral community profile represented by the species that contribute with over 0.45% of the represent the Bray Curtis dissimilarity metric between stressed and non-stressed samples according SIMPER analysis (Table 4.3) and the parameters temperature, occurrence of bleaching and necrosis.

4.4.4. Analysis of overall functional profile of virome

Comparing the 50 most abundant Swissprot keywords within the metaviromic data sets showed differences and similarities in viral function between treatment, control and seawater samples after 3 and 21 days of exposure (Fig. 4.8). The functional keywords 'tonB box', 'flagellar rotation', 'transposition', 'restriction system', 'two-component regulatory system', 'iron transport', 'transcription antitermination' were consistently present across all samples in the short-exposure experiment (Fig. 4.8), while 'transposition', 'transposable element' and 'transcription antitermination' were enriched in all samples from the longer-exposure experiment (Fig. 4.8). The functional profile of *C. foliascens* was consistent with the observed functional profile from environmentally sampled individuals (Fig. 4.8 and Chapter 3, Fig. 3.5). For example, *C. foliascens* from environmental and experimental conditions share 54 % of their 50 most enriched keywords, where 'tonB box', 'transposition', 'transposable element'

and ‘restriction system’ were enriched in every sample. The keywords ‘limb-girdle muscular dystrophy’, ‘cardiomyopathy’, ‘viral extrusion’, ‘respiratory chain’, ‘RNA-directed DNA polymerase’, ‘kelch-repeat’, ‘calmodulin-binding’, ‘metachromatic leukodystrophy’, ‘viral latency’, ‘mucopolysaccharidosis’, ‘TPR repeat’, ‘Kartagener syndrome’, ‘immunoglobulin domain’ were exclusively enriched in sponge samples. Most of these keywords are related to a suite of auxiliary metabolic genes, and amongst them, the keywords limb-girdle muscular dystrophy and cardiomyopathy were more abundant in samples from the ambient temperature treatment. The keywords ‘degradation of lipopolysaccharide during viral entry’, ‘viral DNA replication’ and ‘viral tail tube protein’ were exclusively detected in seawater samples from the short-term exposure. Ordinate and variance analysis based on Bray-Curtis similarity of the overall functional profile of the *C. foliascens* virome showed no significant difference between ambient and sublethal temperature treatments following short or longer term exposure to 31 °C (Fig. 4.9; Table 4.5).

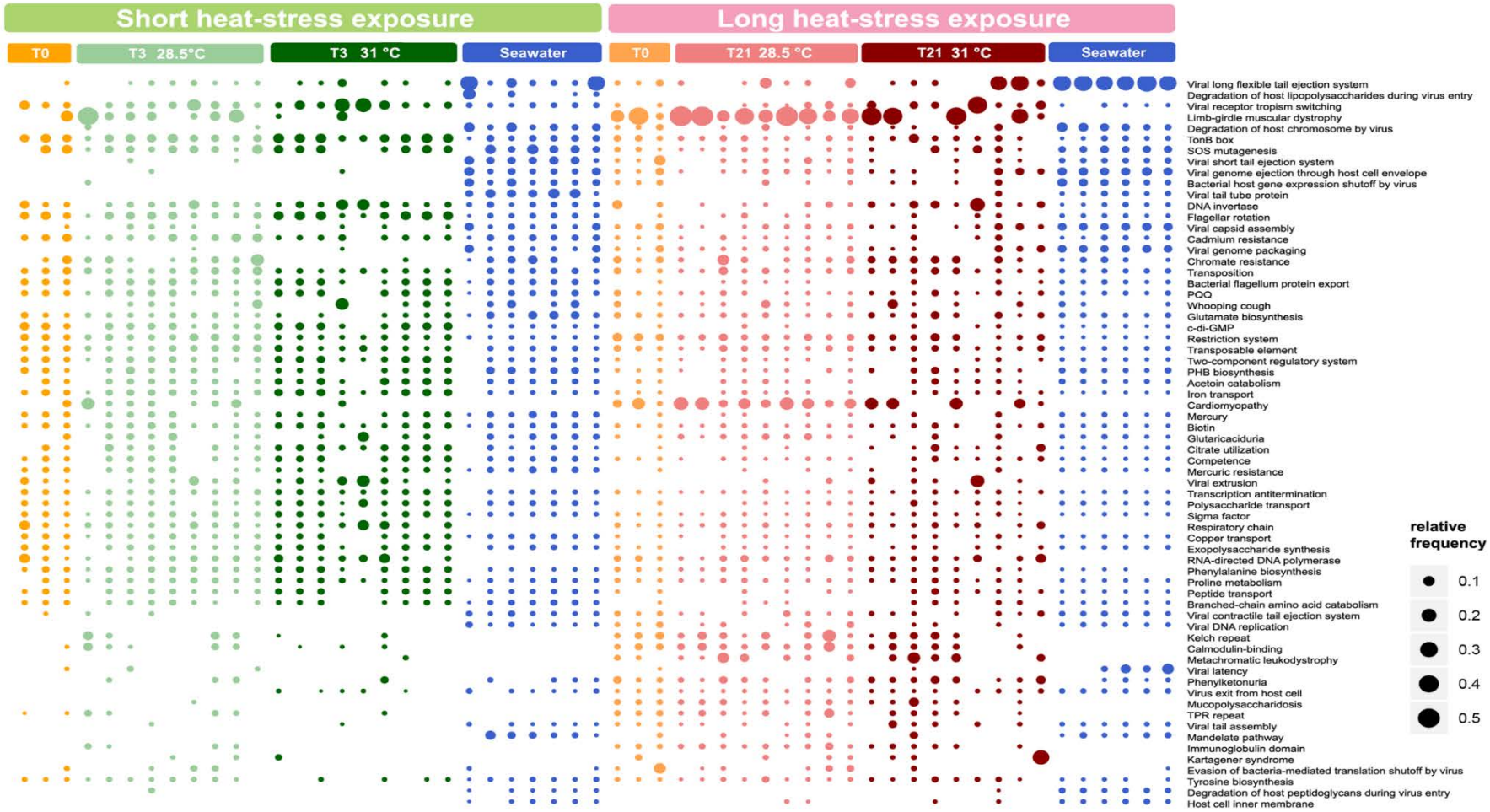

Figure 4.8 Swiss-Prot functional keyword assignment to predicted genes associated with *C. foliascens*, normalised according to keyword frequency within the SwissProt database and read coverage of the source contig within the presented virome. The 50 most abundant keywords across all datasets were identified based on UniProt-KB BLAST analysis of sponge metaviromes and an *e*-value cutoff of $1e^{-10}$. Samples are labelled with experimental information (short heat-stress exposure (3 days) and long heat-stress exposure (21 days), number of days of treatment exposure (T0, T3, and T21), the temperature (28.5 °C and 31 °C) and seawater control samples).

Figure 4.9 Non-metric multidimensional scaling plot based on Bray-Curtis similarity of Swiss-Prot functional keyword assignment for predicted genes. Ordination displays similarities in the viral functions of *C. foliascens* subjected to (a) a short heat-stress exposure (3 days) and (b) a long heat-stress exposure (21 days). The associated figure legends denote the differences in treatment exposure (T0, T3, and T21 days), temperature exposure (28.5 °C and 31 °C) and seawater control samples.

Table 4.5 PERMANOVA pairwise comparisons of functional assignment of viral contigs based on Swiss-Prot keyword abundance data from *C. foliascens* in the short heat-stress exposure (3 days) and long heat-stress exposure (21 days), each exposed to ambient (28.5 °C) and sublethal (31 °C) temperatures. Multivariate permutational analysis of variance (PERMANOVA) (Primer6/PERMANOVA+ v1.0.2, Plymouth, UK) was used to compare functional differences from different tanks, time and temperature treatments. For each heat-stress treatment there were three tanks at 28.5 °C (A1, A2 and A3) and three tanks at 31 °C (S1, S2, and S3), each containing three sponge replicates. Temporal differences between day zero (T0), day 3 (T3) and day 21 (T21) were also measured within ambient conditions. Student t-tests are indicated by the letter "t" and "Unique perms" indicates how many unique-values of the test statistic were obtained under permutation.

Experiment	Factors	Groups	t	p	Unique perms
Short heat-stress exposure	Tank (within 28.5 °C)	A1-A2	0.925	0.601	10
		A1-A3	0.702	0.907	10
		A2-A3	1.042	0.203	10
	Tank (within 31 °C)	S1-S2	1.99	0.098	10
		S1-S3	0.864	0.502	10
		S2-S3	2.045	0.094	10
	Time (within 28.5 °C)	T0-T3	0.782	0.778	59
	Temperature	28.5 °C-31 °C	1.039	0.376	10
Long heat-stress exposure	Tank (within 28.5 °C)	A1-A2	0.899	0.529	463
		A1-A3	1.108	0.339	471
		A2-A3	1.174	0.255	463
	Tank (within 31 °C)	S1-S2	0.851	0.692	10
		S1-S3	1.081	0.273	10
		S2-S3	0.937	0.708	10
	Time (within 28.5 °C)	T0-T21	1.107	0.384	59
	Temperature	28.5 °C-31 °C	1.511	0.113	10

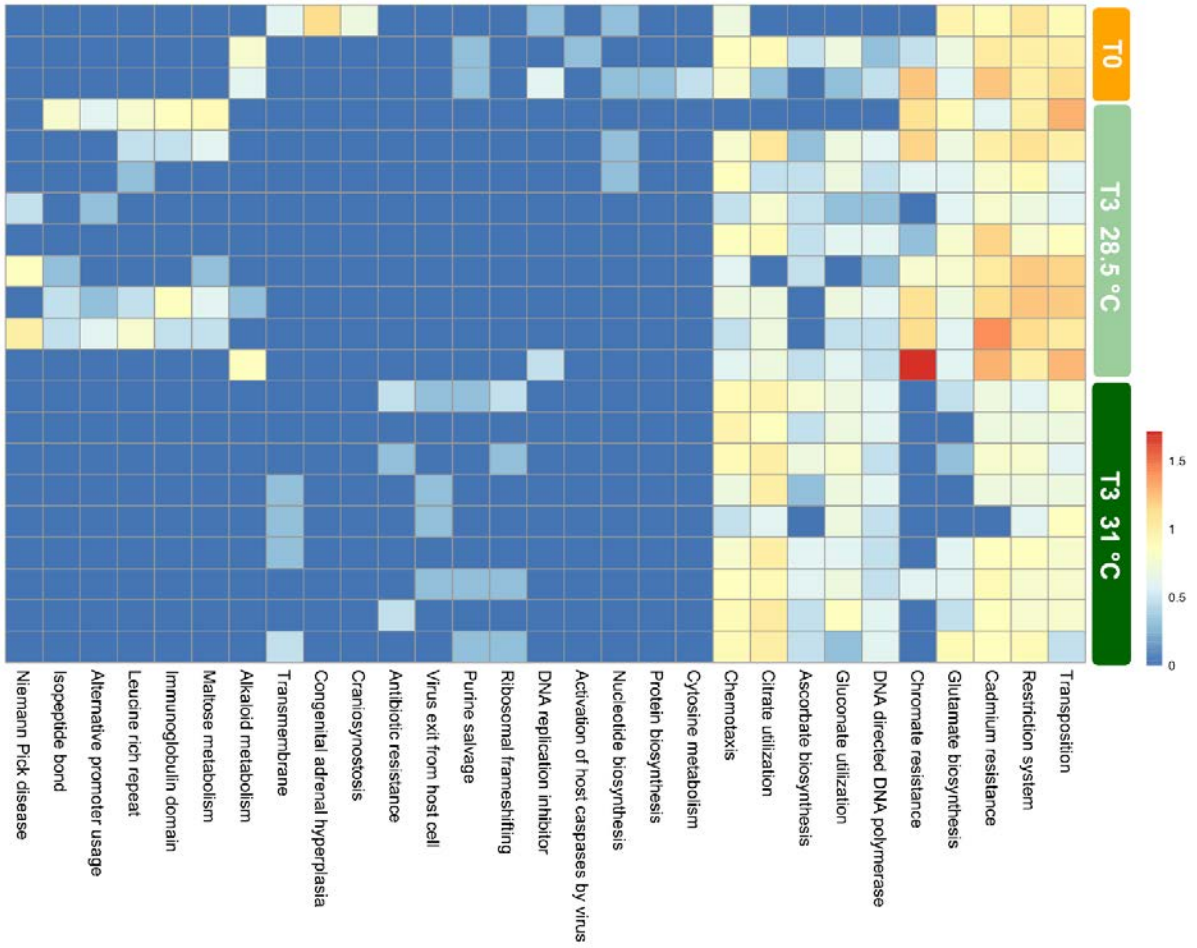

Figure 4.10 Heatmap of the viral functions associated with *C. foliascens* samples following 3 days experimental exposure to elevated temperature. Heatmap shows significant differences between samples (*p*-value <0.05) according to PERMANOVA tests performed using the mvabund package summarised at the Swiss-Prot keyword abundance data using parameters defined in Laffy *et al.*, 2016. Mvabund analysis was used to identify the drivers of difference between individuals sampled at day zero (T0), after 3 days exposure to ambient temperature (T3, 28.5 °C) and to sublethal temperature (T3, 31 °C).

Mvabund analysis performed with data from the 21 d temperature exposure revealed no significant difference in the relative abundance of antibiotic resistance genes between 28 and 31 °C exposed samples (Fig. 4.11). The keyword 'tyrosine catabolism' was considered a driver of variation between 28 and 31 °C exposed samples, being exclusively detected in samples at 31 °C. A total of 53 % of contigs containing tyrosine catabolism genes were taxonomically assigned, matching members of the bacteriophage Family *Myoviridae* (Supplementary Table 4.2).

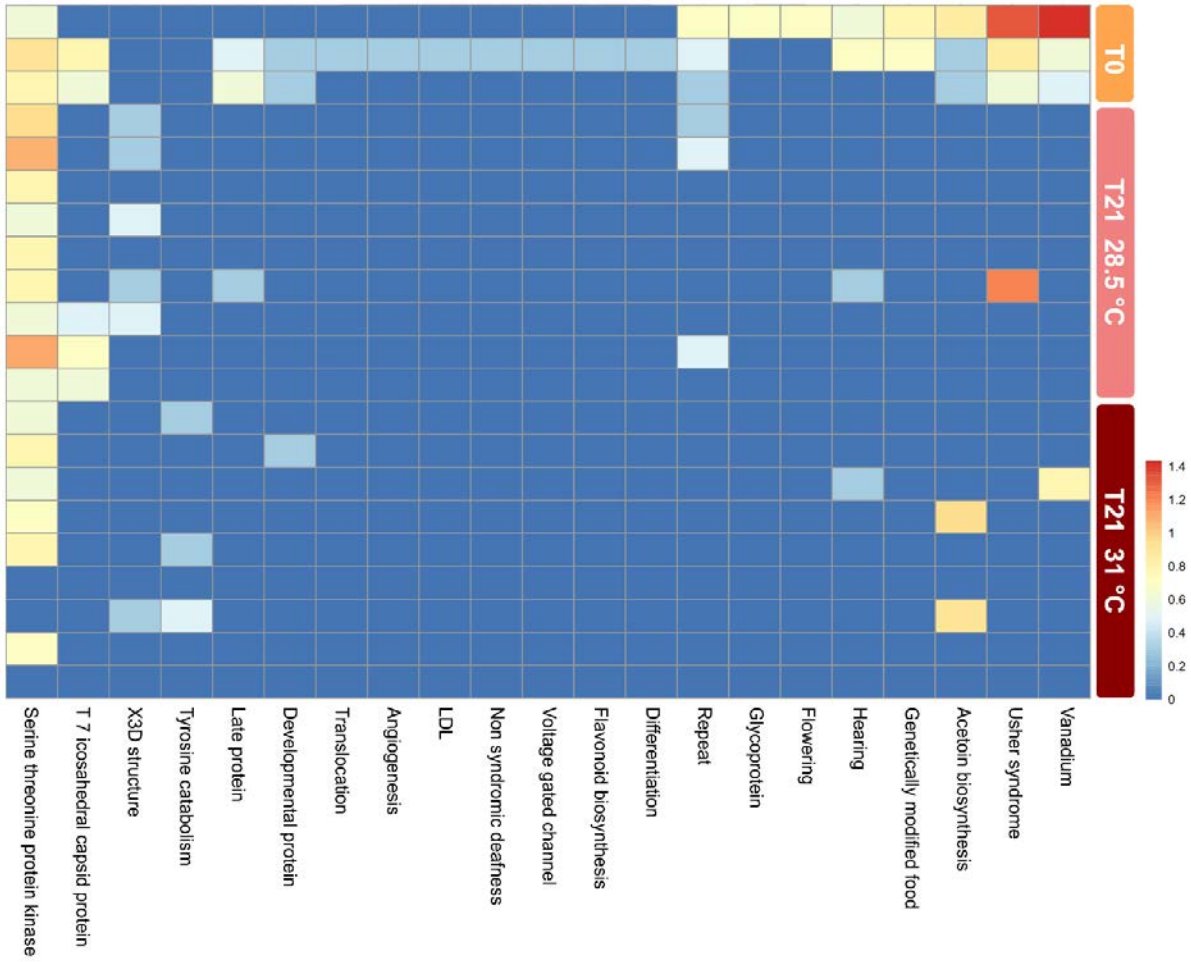

Figure 4.11 Heatmap of the viral functions associated with *C. foliascens* samples following 21 days experimental exposure to elevated temperature. Heatmap shows significant differences between samples (p-value <0.05) according to PERMANOVA tests performed using the mvabund package summarised at the Swiss-Prot keyword abundance data using parameters defined in Laffy *et al.*, 2016. Mvabund analysis was used to identify the drivers of difference between individuals sampled at day zero (T0), after 21 days exposure to ambient temperature (T21, 28.5 °C) and to sublethal temperature (T21, 31 °C).

4.4.5. Functional profile in bleached and necrosed sponges

Comparison of enriched Swiss-Prot keywords associated with visually stressed and healthy sponges viromes, revealed variations in the functional profiles of sponges with distinct morphophysiological responses to heat-stress. Ordination and variance analyses performed at genus-level on the relative frequency of Swiss-Prot keywords showed a significant difference in the viral functions between bleached and non-bleached sponges at 31 °C (Table 4.4; Fig. 4.12a). In contrast, no functional variation was noted between necrosed and healthy sponge viromes (Table 4.4; Fig. 4.12b).

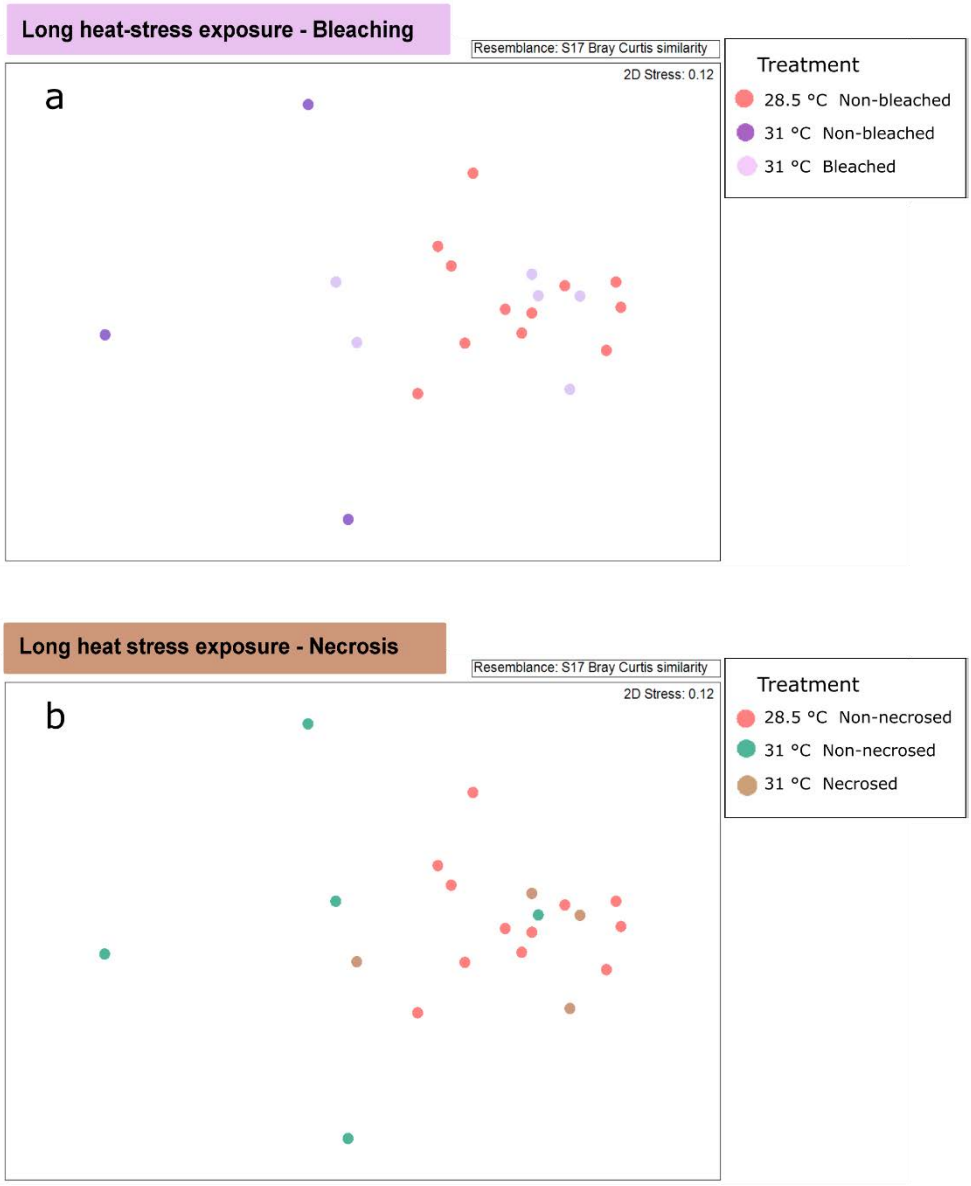

Figure 4.12 Non-metric multidimensional scaling plot based on Bray-Curtis similarity of Swiss-Prot functional keyword assignment for predicted genes from *C. foliascens* individuals exposed to temperature treatments for 21 days. Ordination displays similarities in the viral functions of (a) i) 28.5 °C healthy, ii) 31 °C visibly unaffected and iii) 31 °C bleached individuals and (b) between i) 28.5 °C healthy, ii) 31 °C visibly unaffected and 31 °C necrotic individuals.

Mvabund analysis identified several significant differences between control samples at 28.5 °C, visibly unaffected samples at 31 °C and bleached / necrotic samples at 31 °C (Fig. 4.13). The keywords 'galactose metabolism' and 'alternative promoter usage' were identified as drivers of functional difference between bleached and healthy sponges (Fig. 4.13). The genes assigned the keyword 'galactose metabolism' were found on 98 contigs, 47 % of which were

taxonomically assigned as unclassified dsDNA viruses and 30 % matched *Myoviridae* bacteriophage (Supplementary Table 4.2). Genes coding for UDP-glucose 4-epimerase (UgeA) represented two thirds of all genes associated with the keyword 'galactose metabolism'. The functional keyword 'alternative promoter usage', was enriched in bleached sponges, and identified on 33 viral contigs, of which 45 % were taxonomically assigned to the bacteriophage order Caudovirales. Half of the genes associated with this keyword assignment were classified as transposase genes.

Amongst the functional variations observed between healthy and necrotic individuals after 21 days of heat exposure, genes assigned the functional keywords 'tissue remodelling' and 'citrate utilization' were shown to be drivers of difference in necrotic heat-stressed sponges (Fig. 4.13). Fifty percent of the genes assigned to the tissue remodelling keyword matched known chondroitin sulphate proteoglycan 4 (CSPG4) genes (Supplementary Table 4.2).

Figure 4.13 Heatmap of the viral functions associated with *C. foliascens* samples following 21 days experimental exposure to elevated temperature. Heatmap shows significant differences between samples (p-value <0.05) according to PERMANOVA tests performed using the mvabund package summarised at the Swiss-Prot keyword abundance data using parameters defined in Laffy *et al.*, 2016. Mvabund analysis was used to identify the drivers of difference (a) between i) 28.5 °C healthy, ii) 31 °C visibly unaffected and 31 °C bleached individuals and (b) between i) 28.5 °C healthy, ii) 31 °C visibly unaffected and iii) 31 °C necrotic individuals.

4.5. DISCUSSION

Despite viruses being acknowledged as critical components of marine ecosystems (Suttle, 2007; Breitbart *et al.*, 2018), their role in coral reef organisms, threatened by environmental disturbances, including ocean warming (OW) are still poorly described (Thurber et al., 2009b; Littman, Willis & Bourne, 2011; Laffy et al., 2019). In the first study to test the effect of OW on the viral community of a phototrophic coral reef sponge, the taxonomy and function of viruses associated with *C. foliascens* in response to elevated seawater temperature was described. The overall viral community profile in *C. foliascens* followed a similar structure to what had been previously described for this species (Chapter3), with communities dominated by bacteriophages, including members of the Caudovirales and *Inoviridae*, although NCLDV viral families were also represented in all samples (Fig. 3.2 and Fig. 4.1). The predominance of matches to bacteriophage is likely reflective of the high abundance of microbial symbionts associated with *C. foliascens*. This abundance was also seen in TEM images and microbial descriptions presented in Appendix 1 (Figs. A1.2d, A1.3a-e, A1.6a-b; Table A1.1), and is also in accordance with the current classification of *C. foliascens* as a high microbially abundant (HMA) sponge species (Moitinho-Silva *et al.*, 2017). The high proportion of matches to members of the bacteriophage family *Myoviridae*, which includes the predominant viruses that infect the cyanobacterium *Synechococcus* (Breitbart, 2012), reflects the characteristic association between *C. foliascens* and *Synechococcus* (Gao et al., 2014b, 2015; Luter et al., 2015). Amongst the NCLDV viruses observed, the dominance of *Phycodnaviridae* and *Mimiviridae* followed a similar pattern to what has been observed in other sponge species (Chapter 3; Laffy *et al.*, 2018, 2019). Matches to these two viral families may reflect the presence of a novel eukaryotic viral family, or may be indicative of the sponge-association with eukaryotic algae and protists, natural hosts of *Phycodnaviridae* and *Mimiviridae*, respectively (Laffy *et al.*, 2018).

The viral community profile of *C. foliascens* did not change when sponges were exposed to 31 °C for 3 days (Fig. 4.2; Table 4.2). These results differ to a previous investigation into viruses in thermally stressed marine sponge *R. odorabile* which showed a significant difference in viral community composition after 12 h of exposure to 32 °C (Laffy *et al.*, 2019). These findings are

likely a reflection of *C. foliascens* ecological niche, since this species typically inhabits shallow reefs and lagoons (Wilkinson & Evans, 1989) and is therefore exposed to periodic, acute but short temperature fluctuations (McCabe *et al.*, 2010). However, a shift in viral community composition was evident in *C. foliascens* exposed to 31 °C for 21 days. This shift comprised an increase in sequences matching *Inovirus* and a decrease in tailed bacteriophages (Fig. 4.3). Inoviruses are filamentous bacteriophages with multiple groups of bacteria serving as natural hosts (Ploss & Kuhn, 2010). They are considered temperate phages, whose infection doesn't result in immediate cell death, but instead, establishes a chronic infection by continuously releasing virions without inducing cell lysis (Bayer & Bayer, 1986; Addy *et al.*, 2012; Roux *et al.*, 2019). The increase in *Inovirus* is consistent with a previously described trend where lysogenic viruses increase in response to stress exposure (Howard-Varona *et al.*, 2017). Inoviruses are also distinguished by their lysogenic conversions, where they coexist with the host in a dormant state for several host generations, either remaining integrated within host chromosomes as prophages or in a free episomal state (Bayer & Bayer, 1986; Howard-Varona *et al.*, 2017; Roux *et al.*, 2019). The induction of a reproductive cycle in dormant viruses, a process known as reactivation, can occur spontaneously or be induced by exposure to an environmental stressor, such as changes in temperature, pH and nutrients (Howard-Varona et al., 2017). The reactivation mechanism in herpesviruses, for instance, often requires disabling repressive chromatin marks, facilitating the viral gene expression and translation (Bloom, Giordani & Kwiatkowski, 2010; Avgousti & Weitzman, 2015). Although the mechanisms underpinning the gene translation are not fully understood, it is known that epigenetic regulation and stress-inducing compounds can induce viral reactivation, highlighting the key roles host metabolic pathways play in the viral life cycle (Wilson & Mohr, 2012). For example, heat-shock has been demonstrated to trigger reactivation of herpes simplex virus in latently infected mice neurons after detecting infectious viruses and as a result of raising the core body temperature to 43 °C for 10 min (Sawtell & Thompson, 1992).". Yet, the increase in abundance of Inoviruses in thermally stressed sponges (Fig 4.3) suggests that a viral reactivation is occurring as a response to prolonged thermal stress. The increase of lysogenic virus matches after a heat-stress event has previously been reported for marine sponges, where representatives of the viral family *Retroviridae* increased in *R. odorabile* after exposure to 32 °C for 12 hours (Laffy *et al.*, 2019). Although both sponge species showed an increase in lysogenic viruses, these viruses belong to different families. While Inoviruses are

prokaryotic viruses which likely target specific sponge microbial symbionts, retrotranscribing viruses target eukaryotes, suggesting they infect either the sponge host, or an associated eukaryotic symbiont. The identification of an *Inovirus* representative, *Pseudomonas phage* pf3, as the taxa that contributed most to the dissimilarity across temperature treatments (Table 4.3) was further supported by mvabund analysis which indicated that *Inovirus* distribution was a major driver of the differences between ambient and sublethal temperatures. However, *Pseudomonas phage* pf3 contributed to less than 30 % of the total variation, indicating a multi-species response to heat stress.

A higher relative abundance of *Inovirus* matches in sponges at 31 °C was also one of the main drivers of variation between healthy and bleached samples (Fig. 4.6). Bleaching events have been previously reported for *C. foliascens* exposed to heat stress (Bennett *et al.*, 2017). The bleaching process in phototrophic sponges is often associated with the loss of photosynthetic symbiont communities, such as cyanobacteria (Thacker, 2005; Whalan, 2018). The correlation between bleaching occurrence and *Inovirus* enrichment suggests that the cyanobacterial symbiont of *C. foliascens* plays host to Inoviruses, which are increasing in abundance as they leave their host cell in anticipation of host death. Even though Inoviruses are yet to be isolated from *C. foliascens* cyanobacteria, *Inoviridae*-like particles have been observed associated with *C. foliascens* cyanobacteria symbionts (Pascelli *et al.*, 2018) and *Inovirus*-like sequences have been identified from cyanobacterial genomes (Roux *et al.*, 2019).

It is important to note that the heat stress response in *C. foliascens* viral and microbial assemblages may also be influenced by the sponge hosts innate immune response. For example, prolonged exposure to warmer waters has been showed to alter immune responses in abalone by increasing antiviral activity while decreasing antibiotic activity (Dang, Speck & Benkendorff, 2012). In sponges, exposure of *Haliclona tubifera* to thermal stress activates immune response related genes, including toll-like receptors (TLRs) (Guzman & Conaco, 2016). TLRs are important mediators of the innate response in sponges, providing signalling pathways of the antimicrobial host-defence system (Wiens et al., 2006) (Yuen, Bayes & Degnan, 2014). TLRs are also known to play important roles in mediating the antiviral immune responses of metazoans, by recognizing viral infections, activating signalling pathways and inducing the production of antiviral proteins (Xagorari & Chlichlia, 2008; Green & Speck, 2018). Moreover, sublethal temperature stress in sponges can also up regulate heat-shock

protein (Hsp90) genes (Guzman & Conaco, 2016), which has been demonstrated to interact with viral proteins and mediate apoptotic pathways in vertebrates (Zhang et al., 2011). Despite the understanding that immune receptors play key roles in antiviral responses in aquatic organisms (Rauta et al., 2014), there is a critical knowledge gap regarding antiviral immune responses in sponges. Therefore, to better understand viral dynamics in stressed or diseased sponges, further studies must investigate signalling pathways of immune genes and pathogen recognition pathways in healthy versus stressed sponges.

In the *C. foliascens* virome, keywords related to a suite of auxiliary metabolic genes, such as limb-girdle muscular dystrophy and cardiomyopathy were abundant in control samples (Fig. 4.8). Although these keywords describe human dysfunctions, the specific genes assigned to these keywords were associated with the biosynthesis and degradation of collagen (Jokela *et al.*, 2019), an important component of the sponges skeletal structure (Simpson, 2011). Until recently, collagen was considered an animal-exclusive protein (Morris, 1993). However, recent work characterising giant Mimiviruses has identified that collagen plays a key role in envelope structure and collagenase genes are contained within Mimivirus genomes (Luther *et al.*, 2011). Although there are varied cellular mechanisms associated with collagen biosynthesis (Kavitha & Thampan, 2008), the enrichment of limb-girdle muscular dystrophy and cardiomyopathy keywords in sponge associated viromes suggests viruses may utilize sponge collagen as a resource for their own metabolic pathways.

The overall functional profile of the *C. foliascens* virome did not vary significantly when exposed to 31 °C (Table 4.5), although mvabund analysis identified specific keywords as significant drivers of variation between healthy and stressed individuals (Figs. 4.10, 4.11). After 3 days exposure to 31 °C, genes associated with cadmium and chromate resistance were significantly reduced at 31 °C (Fig. 4.10). In microorganisms, mechanisms related to both resistance systems include a reduction in cellular uptake and a promotion of an efflux transport of heavy metal molecules (Summers, 1985; Silver, 1996). These resistance genes are naturally enriched in *C foliascens* and have been proposed to improve the viral hosts' resistance to heavy metal contamination (Chapter 3). If the resistance genes function in this way, a reduction in their relative abundance in thermally stressed sponges could indicate that increased temperature interferes with the ability of the sponge holobiont to resist the effects

of marine pollutants. However, further studies employing methods that assess variation in gene expression are needed to test this hypothesis.

After 3 days at 31 °C, a significant increase in the frequency of the SwissProt functional keyword 'antibiotic resistance' was observed in the sponge viromes (Fig. 4.10). Antibiotic resistance genes are naturally present in microbial communities (Allen *et al.*, 2010). Besides providing defence against specific therapeutic manipulated compounds (Davies & Davies, 2010), antibiotic resistance genes are also associated with self-protection mechanisms, including inhibition of competitors growth through the production of bioactive compounds (Martinez, 2008; Neeno-Eckwall, Kinkel & Schottel, 2011) and regulation of biosynthesis pathways (Tahlan *et al.*, 2007). Antibiotic resistance genes in microbes can be transmitted through viral infection, and this has been shown to improve their hosts survival under strong antibiotic selection pressures (Haaber *et al.*, 2016). Considering that sponges naturally harbour dense communities of microbial symbionts (Cuvelier et al., 2014) which play important roles in their biological functions (Webster & Taylor, 2012), the enrichment of antibiotic resistance genes in sponge viruses indicates that viruses could play roles in mediating self-protection mechanisms within specific microbial groups in the sponge holobiont. Genes coding for antibiotic resistance in the *C. foliascens* virome were mostly found on contigs taxonomically assigned to *Myoviridae* sequences (Supplementary Table 4.2). The increase in antibiotic resistance genes in *Myoviridae*-assigned contigs in sponges at 31 °C may suggest an initial viral-mediated defence mechanism in *C. foliascens.*

An increase in the frequency of the SwissProt functional keyword denoting tyrosine catabolism in the virome dataset of sponges exposed to 31 °C for 21 days is indicative of a viral mediated response to heat stress (Fig. 4.11). Most viral contigs containing tyrosine catabolism genes were taxonomically assigned to known *Myoviridae* sequences (Supplementary Table 4.2). Genes assigned this keyword are commonly associated with the degradation of the aromatic amino acid tyrosine (Dixon & Edwards, 2006). Tyrosine synthesis and degradation pathways are involved in regulatory mechanisms in bacteria, interfering with physiology, virulence, stress response and changes to DNA metabolism (Grangeasse, Nessler & Mijakovic, 2012). Most genes associated with this keyword were functionally identified as 4-hydroxyphenylpyruvate dioxygenase (4-HPPD) gene homologues, which have been proposed to influence bacterial survival in the natural environment (Steinert *et al.*, 2001) as

well as contributing to microbial virulence and self-defence mechanisms (Liang *et al.*, 2018). It remains unclear whether the introduction of viral tyrosine catabolism genes contributes to increased host survival and fitness in heat-stressed *C. foliascens*. Identification of 4-HPPD genes in thermally stressed sponge viromes may point to the appearance of pathogenic species within thermally stressed sponges, although further work is required to confirm this.

The enrichment of "leucine rich repeat" (LRR) genes in *C. foliascens* virome (Fig. 4.10) likely indicates a viral interaction with host-associated immune responses. LRRs integrate the Nod-like receptors (NLRs) or nucleotide-binding oligomerization domain receptors family, which are important intracellular sensors in the in innate immune systems of metazoans (Ting et al., 2008). NLRs play key roles on the differentiation between self from non-self-molecules and are capable of detecting microbial- or pathogen-associated molecular patterns (MAMPs/PAMPs) (Boller & Felix, 2009), mediating animal–bacterial interactions (Franchi et al., 2012; Robertson & Girardin, 2013). Marine sponges are notable for holding a highly abundant and diverse NLRs immune receptors genes (Yuen, Bayes & Degnan, 2014), which have been proposed to intercede in the complex interactions between sponges and microbial symbionts (Degnan, 2015). A distinct NLR-like proteins domain, the ankyrin repeat, has been discovered and expressed in sponge viruses, confirming that immunomodulatory viral protein can mediate microbe-sponge interaction (Jahn et al., 2019). Yet, during the short term heat-stress experiment, it was noted significant difference on the LRR genes enrichment between ambient and sublethal temperatures, with LRR genes exclusively enriched in non-stressed sponges (Fig. 4.10). This result indicates that heat stress potentially interferes with the immunomodulatory viral response in sponges. In order to confirm the viral contribution to the adaptive immunity in sponges further studies must focus on the expression of LRR sponge viral genes across multiple stress levels.Significant functional differences in the sponge virome were also evident between control and bleached individuals, in comparison to visibly unaffected sponges at 31 °C (Table 4.4; Fig. 4.12a). Increases in galactose catabolism and alternative promoter usage genes in bleached sponges were amongst the primary drivers of functional variations between bleached and non-bleached sponges (Fig. 4.13a). Most genes associated with the galactose metabolism keyword pertained to enzyme UDP-glucose 4-epimerase (UgeA) homologues, and these genes have previously been associated with cell wall biosynthesis (Rösti *et al.*, 2007). UgeA genes are also involved in the synthesis of

lipooligosaccharide, characteristic of virulence factors in pathogenic bacteria (Lee *et al.*, 1999). The functional keyword 'alternative promoter usage', also enriched in bleached sponges, was assigned to genes present within contigs taxonomically assigned to Caudovirales. Half of the genes associated with this keyword were functionally identified as Transposases for transposon Tn5, a gene characterised by its ability to insert into several sites within host genomes, and transposase elements which may be involved in transmitting antibiotic resistance genes to their hosts (Berg & Berg, 1983). Tn5-induced mutations can also interfere with the virulence and pathogenicity of some bacterial groups (Weiss *et al.*, 1983; Cuppels, 1986). Transposable elements can facilitate viral integration into bacterial chromosomes during lysogeny (Harshey, 2014). Genes associated with an increase in tissue remodelling were also identified as drivers of functional variation between control and necrotic sponges, with an elevated relative abundance in necrotic sponges at 31 °C. Most genes associated with this keyword were identified as sulphate proteoglycan 4 (CSPG4) homologues (Supplementary Table 4.2). In bacteria, CSPG4 can be involved in receptor-mediated endocytosis of toxins and virulence factors secreted by pathogenic bacteria (Yuan *et al.*, 2015; Gupta *et al.*, 2017), and the presence of these genes in the viromes of necrosed sponges suggests that viruses containing these genes may be contributing to cell mortality and tissue degradation in sponges. No genes on contigs associated with this function were taxonomically assigned, and it remains to be seen whether this process, if occurring, is viral-mediated.

These results, combined with a previous report of sponge viral responses to heat stress (Laffy *et al.*, 2019), suggest that while thermal stress does not cause a significant change in the overall functional composition of the viral community, elevated temperature can drive specific variations related to heavy metal resistance, antibiotics and virulence. Nevertheless, physiological responses in the holobiont, such as bleaching and necrosis, do correlate with functional variations in the sponge virome. The multi-species viral response to bleaching suggests that there is no single viral mediated driver of bleaching in sponges.

4.6. CONCLUSION

This chapter drew upon the comprehensive knowledgebase of sponge viral ecology established in Chapters 2 and 3 to provide an improved understanding of how sponge-viral

dynamics will respond to ocean warming. The main conclusions from this study are that 1) the *C. foliascens* viral community does not change in response to short term (3 days) heat-stress; 2) inoviruses increased after longer term heat-stress (21 days), which correlates with *C. foliascens* bleaching; 3) bleaching correlates with shifts in the functional capacity of the *C. foliascens* viral metagenome; and 4) specific functional differences between control and heat-stressed samples include a reduction in genes associated with heavy metal resistance and an increase of virulence related genes in the viral communities of sponges exposed to 31 °C. From these results, it appears that thermal sensitivity affects susceptibility to viral infections in *C. foliascens*, particularly in sponges displaying a phenotypic bleaching response. Future studies should aim to characterise the switch from lysogenic to active viral life cycles in thermally stressed sponges, and to identify specific *Inovirus* hosts within the sponge holobiont in order to characterise the mechanisms associated with the bleaching phenotype and endeavour to confirm the expression of viral resistance and virulence genes in *C. foliascens* at elevated seawater temperature.

Chapter 5. GENERAL DISCUSSION

5.1. SYNTHESIS OF RESULTS

This research was inspired by a knowledge gap regarding the role of viruses in coral reef sponges. My dissertation has provided important insights into the taxonomic and functional diversity of viruses in sponges, using morphological and metagenomic approaches to identify 50 viral morphotypes, over 25 viral families and several auxiliary metabolic genes (AMGs), including those associated with herbicide resistance, heavy metal resistance, nylon degradation and antimicrobial activity, associated with 15 sponge species from two distinct biogeographic regions. This research provided visual evidence that viruses are important members of coral reef sponges, associating with the eukaryotic and prokaryotic components of the sponge holobiont. In addition, it presented compelling evidence that the sponge-viral community and function are structured by biogeographic variation and influenced by sponge-holobiont symbiotic strategies, including microbial abundance and the presence of photosymbionts. Furthermore, it demonstrated that the viral community associated with *Carteriospongia foliascens* is impacted by elevated seawater temperature, with an increase in temperate viruses occurring after 21 days exposure to 31 °C. Furthermore, *C. foliascens* that exhibited thermal bleaching were enriched in Inoviruses compared to visually healthy sponges. This research greatly advances what is currently known about the roles viruses play in sponges, and more broadly in coral reef invertebrates.

5.2. DIVERSITY AND FUNCTION OF VIRUSES IN CORAL REEF SPONGES

Viruses are the most abundant biological entities in the marine environment (Danovaro et al., 2011), infecting all living organisms (Fuhrman, 1999; Rohwer & Thurber, 2009), and although viruses were first observed within sponges more than forty years ago (Vacelet & Donadey, 1977), this thesis is the first follow up study visualizing VLPs in sponges (Pascelli et al., 2018). Chapter 2 shows a diverse array of VLPs associated with different components of the sponge holobiont. To visualize viruses and associated microorganisms inside sponges, three Transmission Electron Microscopy (TEM) techniques were combined. Although most VLPs observed inside the sponges were considered rare (visualized less than 5 times per sample during 1 h of searching), select morphotypes were found in high abundance, in dense

aggregates, e.g., associated with archaeocytes in *Xestospongia testudinaria* and in cyanobacteria associated with *Amphimedon ochracea* (Figs. 2.4. j-l, 2.5. d-g; Appendix 2 Table A2.1). This is supportive of with the "virus bank model", which suggests that although most viruses are widely distributed in low abundance, only a fraction are active at any one point in time, a d the majority remain rare and inactive., This phenomenon has been compared to seed-banks in plant populations (Breitbart & Rohwer, 2005). The high diversity and low frequency of viral morphotypes in sponges further suggests that the sponge holobiont also behaves as a viral bank, where specific environmental factors could trigger shifts in the viral communities in these ecosystems.

Most of the observed viral morphotypes were exclusively detected in just one host species (Figs. 2.1-5, Appendix 2 Table A2.1). This observation was supported by the metagenomic data, which revealed that the viral community in sponges was species-specific (Figs 3.3a). Marine sponges are filter-feeders capable of retaining viral particles from seawater (Hadas et al., 2006). Thus, variation in viral community composition across sponge species may be partially attributed to their differential ability to filter seawater particles. The sponge filtration ability is associated with its morphological characteristics, such as body plan, mesohyl density, aquiferous systems complexity / dimensions and oscular behaviour, as these parameters determine the water density and pumping rates and subsequent filtration efficiency (Weisz, Lindquist & Martens, 2008; Strehlow et al., 2016). This hypothesis is supported by analysis presented in Appendix 3 (Table A3.2), which shows a significant correlation between sponge morphotypes and viral community structure, indicating that sponge morphology may play roles in determining the viral composition.

Sponge microbial associations also play key roles in structuring the sponge virome. Morphological and metagenomic approaches (Chapters 2 and 3) both highlighted bacteriophages as the dominant viral group across all sponge species (Figs. 2.1-5, 3.2), suggesting that the microbial and viral consortia are interconnected with the sponge holobiont. The clear delineation in viral communities observed between high (HMA) and low microbial abundance (LMA) sponges, combined with observed viral community differentiation between sponges with and without photosymbionts (Fig. 3.3b) supports the argument that the sponge-viral community is greatly influenced by sponge associated microbial symbionts. A dominance of bacteriophages has been previously reported in marine

invertebrate viromes (Patten, Harrison & Mitchell, 2008; Wood-Charlson et al., 2015; Correa et al., 2016; Weynberg et al., 2017a; Thurber et al., 2017; Laffy et al., 2018), which is consistent with the current theoretical proposal that all multicellular organisms form a holobiont, encompassing multiple symbiotic associations, including a wide range of microorganisms (Morris, 2018). The premise that sponge microbes are key elements influencing viral community structure within sponges is further supported by reports that distinct sponge species maintain a highly uniform and specific association with microorganisms (Hentschel et al., 2002; Webster et al., 2013a).

Although bacteriophages are likely the major players in the sponge holobiont, eukaryotic viruses were also part of the core sponge virome (Fig. 3.2) as was observed via TEM analysis (Figs. 2.1. a, 2.3. k-l, 2.4. j-l, 2.5. h). Observed eukaryotic viruses included the nucleocytoplasmic large DNA viruses (NCLDV) families, a collection of known viral families that infect a range of eukaryotic organisms including protists, algae, and animals (Wegley et al., 2007; Thurber & Correa, 2011; Grasis et al., 2014; Wood-Charlson et al., 2015; Leigh et al., 2018; Laffy et al., 2018). The presence of these viruses in sponges may indicate that these viral groups are either targeting sponge cells or other multicellular representatives of the sponge holobiont, such as macroalgae or other associated invertebrates. Yet, their occurrence might not be strictly related with the presence of a host, they could have been assimilated during sponge filtration (Hadas et al., 2006), or trapped within sponge canals. However, it is notable that sponges have the capacity to shape and maintain their viral communities, as individual sponge viromes are significantly different from surrounding seawater viromes (Laffy et al., 2018). Giant viruses, including Mimiviridae and Marseilleviridae, are members of the NCLDV observed within sponge-associated viromes (Chapters 3 and 4). It has previously been suggested that sponges may be a potential marine host for giant viruses (Claverie et al., 2009), and although giant viruses were consistently identified in the sponge viromes (Fig. 3.2), no viral morphology consistent with giant viruses was observed through TEM analysis. However, the observation of VLPs could have been hindered by the TEM preparation methods, since tissue sectioning commonly restricts observations to a relatively small host area and filtering and centrifuging can potentially eliminate or damage larger viral particles.

A major goal of this research was to understand the mechanisms through which viruses interact with their hosts. For instance, sponge viruses are likely mediating cellular mortality (eukaryotic or prokaryotic) in sponges, which is suggested by the observation of burst viral infected cells (Fig. 2.4 j-l; Figs 3e and 5e) as well as by the occurrence of obligately lytic viruses, such as the T4 bacteriophages (Hobbs & Abedon, 2016), amongst the sponge virome (Appendix 3 Table 3.2). Viral-induced cellular mortality in sponges may be partially contributing to Darwin's paradox, explaining how ecosystems with low nutrient input can sustain high biodiversity (Darwin, 2013). In a process termed the "sponge-loop", sponges have been shown to cycle dissolved organic matter (DOM), making it available to other reef species via rapid cellular turnover and expulsion of detritus (de Goeij et al., 2013a). It is also possible that sponge viruses play a role in this microbial loop by transforming the DOM (microbial food source) incorporated as bacterial biomass into cellular detritus, or particulate organic matter (POM) via the lysis of their host/microbial cells, especially considering that viruses are responsible for killing 20 – 40% of oceanic bacteria per day (Suttle, 1994). Although part of this organic matter would be trapped in an internal loop (viral shunt, (Suttle, 2005)), it is possible that a portion of the cellular material that is lysed by members of the sponge virome would produce detritus that would subsequently be expelled by the sponge and further incorporated by other coral reef organisms, thereby impacting coral reef food webs and biogeochemical cycles.

Viral-induced cellular mortality was not the only role identified for viruses in the sponge holobiont. Results presented in Chapter 3 showed that sponge viruses contain genes that can manipulate their host transcription through expression of auxiliary metabolic genes (AMGs). Core viral functions were consistently identified within the sponge viromes, in contrast with AMGs, which varied across sponge species (Fig. 3.5). Previous research demonstrated the specificity of AMGs in sponge and coral holobionts (Laffy et al., 2018), and the findings presented in Chapter 3 further expand our understanding of how viral functional profiles are correlated to host nutritional strategy, microbial abundance and geographic location (Chapter 3). For instance, functional profiling revealed that genes associated with photosynthesis were enriched in phototrophic sponges, nitrogen metabolism genes were enriched in HMA sponges, and antibiotic synthesis genes were enriched in LMA sponges (Figs. 3.8-9). Additionally, geographic location (or the specific environmental conditions of each site)

contributed to the metaviromic functional profiles, with an enrichment of heavy metal resistance genes observed in the viromes of Red Sea sponges and herbicide resistance genes observed in GBR sponge viral metagenomes (Fig. 3.7). These functional differences may be reflecting the elevated levels of heavy metal contamination in the Red Sea (Badr et al., 2009) in comparison with the generally low levels in the GBR Marine Park (Haynes & Johnson, 2000), as well as reflecting the impact of agricultural runoff on the GBR (Jones & Kerswell, 2003; Lewis et al., 2009).

Considering the variability of the sponge viral metagenomes in accordance with their host species, geographic location and microbial association strategies (HMA/LMA and presence/absence of photosymbionts) (Chapter 3), the last component of this research (Chapter 4) investigated how the sponge viral metagenomes responded to changing environmental conditions, specifically short (3 days) and long-term (21 days) exposure to elevated seawater temperature. Significant differences were observed in the *Carteriospongia foliascens*-associated viral metagenomes after long-term exposure to elevated seawater temperature, although these communities remained stable for the first three days of exposure. These findings are likely a consequence of the ecological niche occupied by this host species, as *C. foliascens* typically inhabits shallow reefs and lagoons (Wilkinson & Evans, 1989) and is, therefore, often exposed to periodic and acute temperature fluctuations (McCabe et al., 2010). However, longer term heat-exposure resulted in a significant increase in the relative abundance of temperate bacteriophages from the genus *Inovirus* (Fig. 4.3). This increase may be attributed to a switching of Inoviruses from a dormant lysogenic stage to an active stage, trigged by heat-stress, as has been previously proposed for temperate viruses (Howard-Varona et al., 2017). Interestingly, the only other study describing sponge-viral responses to heat-stress also showed a significant increase in temperate viruses in heat-stressed GBR sponge *Rhopaloiedes odorabile* (Laffy et al., 2019). Laffy et al. (2019) identified that these temperate viruses belonged to the *Retroviridae*, and although also lysogenic, this viral family typically infects eukaryotic cells, suggesting that the lysogenic/ active switching response in thermally stressed sponges involves both prokaryotic and eukaryotic viruses. Viral communities within marine organisms other than sponge have been shown to exhibit varying responses to heat-stress, including an increase in *Herpesviridae* in the coral *Porites compressa* (Thurber et al., 2008) and a decrease of *Inoviridae* in *Hydra vulgaris* (Grasis et al., 2014).

Knowledge regarding host-viral interactions in coral reef communities is still very limited, and Chapter 4 of this thesis provides a solid base from which to expand our understanding of virome community dynamics in marine holobiont systems exposed to heat stress. Chapter 4 also identified a correlation between bleaching and increased *Inovirus* in heat stressed *C. foliascens* (Fig. 4.6). As a bleaching phenotype in *C. foliascens* is likely the result of a decrease in the abundance of cyanobacteria (Thacker, 2005; Whalan, 2018), the associated rise in *Inovirus* in bleached sponges suggests a host-virus interaction between *Inovirus* and cyanobacterial symbionts. As a result of this correlation, I hypothesize that *C. foliascens* cyanobacteria associated inoviruses increase in abundance as a result of dormant viruses being induced to reproduce prior to the death of the sponge, although additional validation is needed to confirm this.

In addition to highlighting how the sponge viral community responds to heat stress, experiments described in Chapter 3 detected functional variations in the virome of *C. foliascens* at elevated seawater temperature. Significant differences in the assigned functional keywords were found between bleached and non-bleached sponge viromes following thermal stress (Table 4.4.; Fig. 4.11.a). Analysis of the drivers of difference between these phenotypes showed that viral genes characteristic of microbial virulence and pathogenicity were enriched in bleached sponges compared to visibly healthy individuals. This functional response in the virome may be a result of an increase in microbial pathogenicity within bleached sponges, suggesting that viruses may potentially interfere with the sponge-microbial infection or defence ability during a heat-stress event. Although the functional variations were clearly related with this physiological condition, heat-stress did not result in a significant difference in the *C. foliascens* virome functional profile. The overall functional stability of heat-stressed viromes suggests that the observed viral taxonomic shift did not contribute to a metabolic advantage within the sponge holobiont system. This result is comparable to the observed functional stability of the *R. odorabile* virome under heat stress (Laffy et al., 2019).

5.3. FUTURE DIRECTIONS FOR SPONGE HOLOBIONT-VIRAL STUDIES

Our knowledge of the roles viruses play in marine holobionts is still in its infancy. While the number of studies exploring viral interactions with coral reef organisms has grown

substantially in recent years, almost all of these focused on hard coral species (Seymour et al., 2005; Wilson et al., 2005; Davy et al., 2006; Davy & Patten, 2007; Cervino et al., 2008; Patten, Harrison & Mitchell, 2008; Thurber & Correa, 2011; Pollock et al., 2014; Soffer et al., 2014; Wood-Charlson et al., 2015; Correa et al., 2016; Brüwer et al., 2017; Weynberg et al., 2017a; Thurber et al., 2017; Mahmoud & Jose, 2017; Weynberg, 2018). In contrast, studies that investigate viral roles in marine sponge have been very scarce (Pascelli et al., 2018; Laffy et al., 2018, 2019; Jahn et al., 2019). The findings of this thesis greatly expand this field by visually cataloguing VLPs and characterising viral communities and their associated and functions within 15 sponge species from distinct biogeographic regions, thereby establishing a robust baseline that will inform future studies aimed at understanding the role of viruses in sponge holobiont biology.

This PhD research showed that sponges host several viral groups that typically infect a diverse array of macro and microorganisms. This knowledge sets the scene for future studies to focus on identifying specific hosts for individual viruses within the sponge holobiont. This could be achieved by sorting specific cell types within the sponge holobiont prior to viral purification, using techniques including macro and micromanipulation (Fröhlich & König, 2005), fluorescence-activated cell sorting (FACS) (Worden, Dupont & Allen, 2011) and immunomagnetic cell separation (Clarke & Davies, 2003). Utilising cell culture techniques may also facilitate the targeting of specific viral groups within the sponge holobiont, a strategy that has been successfully applied for other marine invertebrate systems (Rinkevich, 2005). Allied to these methods, other technologies could be used to characterize specific viral or host group within the sponge holobiont, including fluorescent *in situ* hybridization (FISH) (Liehr, 2016) and single molecule, real-time (SMRT) sequencing (Eid et al., 2009). As an example, FISH can be used to detect and localize specific viral/microbial sequences, providing new insights into the abundance, distribution and interactions of viruses or specific viral genes within the sponge holobiont (Li et al., 2006). Additionally, SMRT technology could be used to sequence independently longer strands of the viral and host genomes and generate full-length transcripts, providing a more accurate classification of these viruses as well as their functions (Boldogkői et al., 2019).

Another gap in this research is the lack of characterization of virus integration into host microbial genomes, as the purification method used in this thesis specifically targeted viral

particles, and did not account for the identification of prophage (inserted into host genome) signatures within host genomes. The results presented in Chapter 4 suggest that the increase in *Inovirus* in thermal stressed sponges is related to the switching of *Inovirus* from dormant lysogeny to an active life stage, trigged by heat-stress. In order to test this hypothesis, the experiment must be expanded, quantifying and comparing lysogeny across treatments in order to verify the *Inovirus* infection strategy. This could be achieved by isolating the microbial genome associated with the sponges and incorporating an additional verification of viral signatures in microbial sequence data, using specific bioinformatic pipelines, including VirSorter, a tool to detect viral signals in different types of microbial sequence data (Lima-Mendez et al., 2008; Roux et al., 2015a). Moreover, investigating the presence of viruses or prophages in the sponge gametes and any vertically transmitted microbes (which comprise a large part of the microbiome of many sponge species, (Gloeckner et al., 2014; Cuvelier et al., 2014)) would elucidate viral transmission strategies (Gaino et al., 2006). Additionally, in order to understand the viral community dynamics within the sponge host, and more precisely understand the sponge efficiency in selectively removing viruses from seawater, viral standard experiments could be conducted to investigate the viral composition and concentration among the sponge inhalant canal, chambers and exhalant canals as well as correlating these results with sponge features like species affiliation, morphological complexity and symbiotic association.

Methodology used in this thesis captured extensive viral diversity associated with coral reef sponges (Chapters 3 and 4) by focussing on visualising and sequencing the viral communities. However, sequencing efforts exclusively targeted DNA viruses because efforts to capture informative sequences from RNA viruses were constrained by a lack of homologous sequences in existing databases (Steward et al., 2013) and difficulty in assembling RNA virus contigs (Marz et al., 2014). Considering that prokaryotic symbionts comprise up to half of the sponge volume (Cuvelier et al., 2014), and that RNA viruses are largely absent from prokaryotic communities (Culley, Mueller & Belcaid, 2014), it is expected that DNA viruses are responsible for the largest part of the overall community and functional composition in sponge viromes. However, since new techniques have been developed to isolate, assemble and annotate RNA viral genes (Bruinsma et al., 2016; Wolf et al., 2018) and metatranscriptomic approaches have improved the description of host-RNA virus interaction

(Shi et al., 2017, 2018), future studies on sponge viromes should also consider the roles RNA viruses play in the sponge holobiont. This may uncover new insights into sponge viral associations, highlighting interactions between viruses and the eukaryotic component of the sponge holobiont.

Findings from this thesis suggest that viral communities in sponges can be influenced by environmental factors including location and water quality (Chapters 3 and 4). As sponges are key benthic taxa occupying polar to tropical regions, shallow, deep water and other distinct ecosystems (Bell, 2008; Van Soest et al., 2012), a more comprehensive descriptive study targeting sponge species from varied habitats, depth and latitudes would help us to understand the stability of sponge-viral associations and provide a better understanding of how the surrounding environment influences these biological associations. In addition, future studies should investigate whether viruses play specific roles in modulating specific sponge ecological traits. For instance, it is known that most diseases reported for marine sponges lack a specific etiological agent (Maldonado, Sánchez-Tocino & Navarro, 2010; Angermeier et al., 2012; Luter & Webster, 2017; Slaby et al., 2019), and while many diseases in marine organisms have been shown to be virally-mediated (Sánchez-Paz, 2010; Crane & Hyatt, 2011; Soffer et al., 2014; Petton et al., 2015), the role of viruses in sponge diseases has been poorly explored (Slaby et al., 2019). Disease occurrence in marine organisms can also be associated with dysbiosis, or an imbalance of the microbial symbiotic consortia (Egan & Gardiner, 2016; Pita et al., 2018b). Thus, in order to investigate whether viruses play a causative role in sponge disease, or are involved in the onset of dysbiosis, comparative studies must be conducted to characterize the viral community of healthy versus diseased sponges using a variety of approaches, including metagenomics (Laffy et al., 2016), viral enumeration (FCM) (Marie et al., 1999), isolation of the etiological agent (Middelboe, Chan & Bertelsen, 2010) and bioinformatics methodologies that search for viral-induced microbiome alteration (Roux et al., 2015a).

Our methodology used amplification techniques to produce sufficient material for sequencing and also relied on relative abundance data derived from sequencing reads to characterize each viral group or function associated with each distinct sponge species. A more accurate quantitative description of viral functions is now needed to test the specific hypotheses generated by this thesis. For instance, Chapters 3 and 4 highlight the potential roles of viral

AMGs in the holobiont, including enrichment of heavy metal resistance genes in sponges at the Red Sea site and enrichment of herbicide and insecticide resistance genes in GBR sponge viral metagenomes. These findings are indicative of heavy metal contamination in the Red Sea and agricultural runoff affecting the GBR. Previous work has indicated that it is unlikely that viruses would maintain redundant or random genes within their genomes, as maintenance of larger genomes result in a putative fitness cost (Mahmoudabadi, Milo & Phillips, 2017). This suggests that the occurrence of AMGs are a result of specific selective pressures (Breitbart et al., 2007; Rosario & Breitbart, 2011; Crummett et al., 2016). Future studies exposing distinct sponge species to controlled environmental conditions, including various levels of pollutants, nutrients, temperature, pH, UV radiation or sedimentation may elucidate whether viral AMGs play an active role in manipulating host metabolic processes, as has been proposed in this thesis. Future research should also undertake a more accurate description of viral community dynamics using quantitative approaches. Flow cytometry (FCM) and quantitative real-time PCR (qPCR) are amongst the techniques that could be used to better quantify viruses in marine sponges (Brussaard, 2004b; Albinana-Gimenez et al., 2009), as these tools have been effectively used to count microbes and VLPs in other coral reef organisms (Patten, Seymour & Mitchell, 2006; Bourne, Muirhead & Sato, 2011; Weynberg et al., 2017b).

The effect of future climate scenarios predicted for coral reef ecosystems (IPCC, 2014) must be studied in the context of viral-sponge holobiont associations. Environmental stresses including ocean warming and acidification, sedimentation, light attenuation, nutrient availability, salinity variation and pollutant exposure have all been shown to impact the fitness of sponges and their associated microbial communities (Pineda et al., 2016, 2017; Bennett et al., 2017; Gantt, López-Legentil & Erwin, 2017; Watson et al., 2017; Glasl et al., 2018). The role viruses play in these stress responses remains largely uncharacterized in marine sponges, despite studies in other systems highlighting the capacity for viruses to manipulate their hosts (Breitbart et al., 2018; Roux et al., 2019), contributing to acclimation (Llave, 2016), survival (Karpf et al., 1997) and evolution (Villarreal, 1999). Chapter 4 builds on existing work (Laffy et al., 2019) that has started to investigate the sponge holobiont-viral response to heat-stress, an important step towards understanding the role that viruses play in sponge response to a changing world. It has been suggested that sponges may dominate some coral reefs under

future climate scenarios (Bell et al., 2018), hence additional experimental work is needed to assess sponge-viral responses to a range of environmental pressures, including shifts in ocean temperature, pCO_2, nutrients, pollutants and a combination of these factors. Additional studies must me grounded in forecasted future climate scenarios, to better understand the roles that viruses will play in reef community restructuring. Similarly, an understanding of the thresholds that mediate viral functional contributions to heavy metal, plastic and herbicide contaminations and associated dose response relationships should be generated, in order to implement the best possible management strategies and mitigate the effects of these contaminants on reef communities.

Additionally, the enrichment of important Nod-like receptor genes in the sponge virome, as well as their distinct thermal stress responses (Fig. 4.10) are possible indicators of a viral modulation of the sponge immune system. To elucidate whether and how viruses communicate with the sponge immune system and respond to environmental stress future studies must consider the sponge innate immune system while investigating the host response. This could be achieved by accessing changes in expression of signalling and immunity pathways within control and stressed individuals.

5.4. FINAL CONCLUSIONS

This PhD research has shown that viruses are a diverse component of the sponge holobiont in all 15 species investigated. TEM and metagenomic analyses revealed that sponge associated viral communities are dominated by bacteriophages, and the composition of these communities is primarily influenced by the composition of the sponge associated microbiome. Additionally, multiple eukaryotic viral groups were identified within the sponge holobiont, likely targeting sponge cells or a eukaryotic symbiont in the holobiont. This research has greatly expanded upon previous findings highlighting the species-specificity of the sponge-viral community (Laffy et al., 2018), and also shows that sponge viromes are influenced by host strategies for symbiosis, including microbial abundance and the presence of photosymbionts. Sponge viral community composition is also influenced by environmental factors, including geographic location and seawater temperature. Finally, this study revealed that the functional profiles of sponge viromes vary significantly between species and sites, involving differential representation of auxiliary metabolic genes (AMGs), including those

associated with herbicide resistance, heavy metal resistance and nylon degradation. Findings from this PhD have greatly expanded our understanding of sponge-viral interactions and improved our knowledge of sponge ecology, revealing putatively important roles for viruses in the sponge holobiont.

REFERENCES

Abdullah A., Ramli R., Ridzuan MSM., Murni M., Hashim S., Sudirwan F., Abdullah SZ., Mansor NN., Amira S., Saad MZ., Amal MNA. 2017. The presence of Vibrionaceae, Betanodavirus and Iridovirus in marine cage-cultured fish: Role of fish size, water physicochemical parameters and relationships among the pathogens. *Aquaculture Reports* 7:57–65. DOI: 10.1016/j.aqrep.2017.06.001.

Ackermann H., Kropinski AM. 2007. Curated list of prokaryote viruses with fully sequenced genomes. *Research in Microbiology* 158:555–566. DOI: 10.1016/j.resmic.2007.07.006.

Addy HS., Askora A., Kawasaki T., Fujie M., Yamada T. 2012. Utilization of Filamentous Phage φRSM3 to Control Bacterial Wilt Caused by Ralstonia solanacearum . *Plant Disease* 96:1204–1209. DOI: 10.1094/pdis-12-11-1023-re.

Alavandi S V., Poornima M. 2012. Viral metagenomics: A tool for virus discovery and diversity in aquaculture. *Indian Journal of Virology* 23:88–98. DOI: 10.1007/s13337-012-0075-2.

Albinana-Gimenez N., Miagostovich MP., Calgua B., Huguet JM., Matia L., Girones R. 2009. Analysis of adenoviruses and polyomaviruses quantified by qPCR as indicators of water quality in source and drinking-water treatment plants. *Water Research* 43:2011–2019. DOI: 10.1016/j.watres.2009.01.025.

Allen GR. 2008. Conservation hotspots of biodiversity and endemism for Indo-Pacific coral reef fishes. *Aquatic Conservation: Marine and Freshwater Ecosystems* 18:541–556. DOI: 10.1002/aqc.880.

Allen HK., Donato J., Wang HH., Cloud-Hansen KA., Davies J., Handelsman J. 2010. Call of the wild: Antibiotic resistance genes in natural environments. *Nature Reviews Microbiology* 8:251–259. DOI: 10.1038/nrmicro2312.

Allers E., Moraru C., Duhaime MB., Beneze E., Solonenko N., Barrero-Canosa J., Amann R., Sullivan MB. 2013. Single-cell and population level viral infection dynamics revealed by phageFISH, a method to visualize intracellular and free viruses. *Environmental Microbiology* 15:2306–2318. DOI: 10.1111/1462-2920.12100.

Andreakis N., Luter HM., Webster NS. 2012. Cryptic speciation and phylogeographic relationships in the elephant ear sponge Ianthella basta (Porifera, Ianthellidae) from northern Australia. *Zoological Journal of the Linnean Society* 166:225–235. DOI: 10.1111/j.1096-3642.2012.00848.x.

Angermeier H., Glöckner V., Pawlik JR., Lindquist NL., Hentschel U. 2012. Sponge white patch disease affecting the Caribbean sponge Amphimedon compressa. *Diseases of Aquatic Organisms* 99:95–102. DOI: 10.3354/dao02460.

Angly FE., Felts B., Breitbart M., Salamon P., Edwards R a., Carlson C., Chan AM., Haynes M., Kelley S., Liu H., Mahaffy JM., Mueller JE., Nulton J., Olson R., Parsons R., Rayhawk S., Suttle C a., Rohwer F. 2006. The marine viromes of four oceanic regions. *PLoS biology* 4:e368. DOI: 10.1371/journal.pbio.0040368.

Arillo A., Bavestrello G., Burlando B., Sarà M. 1993. Metabolic integration between symbiotic

cyanobacteria and sponges: a possible mechanism. *Marine Biology* 117:159–162. DOI: 10.1007/BF00346438.

Arzul I., Corbeil S., Morga B., Renault T. 2017. Viruses infecting marine molluscs. *Journal of Invertebrate Pathology* 147:118–135. DOI: 10.1016/j.jip.2017.01.009.

Atabekov JG. 2011. Host specificity of plant viruses. *Annual Review of Phytopathology* 13:127–145.

Auguet JC., Montanié H., Lebaron P. 2006. Structure of Virioplankton in the Charente Estuary (France): Transmission Electron Microscopy versus Pulsed Field Gel Electrophoresis. *Microbial Ecology* 51:197–208. DOI: 10.1007/s00248-005-0043-0.

Avgousti DC., Weitzman MD. 2015. Stress flips a chromatin switch to wake up latent virus. *Cell Host & Microbe* 18:639–641. DOI: 10.1016/j.chom.2015.11.011.

Azam F., Fenchel T., Field J. 1983. The ecological role of water-column microbes in the sea. *Marine ecology …* 10:257–263.

Baalkhuyur FM., Bin Dohaish E-JA., Elhalwagy MEA., Alikunhi NM., AlSuwailem AM., Røstad A., Coker DJ., Berumen ML., Duarte CM. 2018. Microplastic in the gastrointestinal tract of fishes along the Saudi Arabian Red Sea coast. *Marine Pollution Bulletin* 131:407–415. DOI: 10.1016/j.marpolbul.2018.04.040.

Badr NBE., El-Fiky AA., Mostafa AR., Al-Mur BA. 2009. Metal pollution records in core sediments of some Red Sea coastal areas, Kingdom of Saudi Arabia. *Environmental Monitoring and Assessment* 155:509–526. DOI: 10.1007/s10661-008-0452-x.

Bai CM., Li YN., Chang PH., Jiang JZ., Xin LS., Li C., Wang JY., Wang CM. 2019. Susceptibility of two abalone species, Haliotis diversicolor supertexta and Haliotis discus hannai, to Haliotid herpesvirus 1 infection. *Journal of Invertebrate Pathology* 160:26–32. DOI: 10.1016/j.jip.2018.11.008.

Bandín I., Dopazo CP. 2011. Host range, host specificity and hypothesized host shift events among viruses of lower vertebrates. *Veterinary Research* 42:67. DOI: 10.1186/1297-9716-42-67.

Barnes DKA. 1999. High diversity of tropical intertidal zone sponges in temperature, salinity and current extremes. *African Journal of Ecology* 37:424–434. DOI: 10.1046/j.1365-2028.1999.00197.x.

Bayer ME., Bayer MH. 1986. Effects of bacteriophage fd infection on Escherichia coli HB11 envelope: a morphological and biochemical study. *Journal of virology* 57:258–66.

Bell JJ. 2008. The functional roles of marine sponges. *Estuarine, Coastal and Shelf Science* 79:341–353. DOI: 10.1016/j.ecss.2008.05.002.

Bell JJ., Bennett HM., Rovellini A., Webster NS. 2018. Sponges to be winners under near-future climate scenarios. *BioScience* 68:955–968. DOI: 10.1093/biosci/biy142.

Bell JJ., Davy SK., Jones T., Taylor MW., Webster NS., Leininger S., Adamski M., Bergum B., Guder C., Liu J., Laplante M., Bråte J., Hoffmann F., Fortunato S., Jordal S., Rapp HT., Adamska M., Lôbo-hajdu G., Muricy G., Maldonado M., Ribes M., van Duyl FC., Paul JH.,

Rose JB., Jiang SC., Kellogg CA., Dickson L., Rozenblatt-Rosen O., Deo RC., Padi M., Adelmant G., Calderwood M a., Rolland T., Grace M., Dricot A., Askenazi M., Tavares M., Pevzner SJ., Abderazzaq F., Byrdsong D., Carvunis A-R., Chen A a., Cheng J., Correll M., Duarte M., Fan C., Feltkamp MC., Ficarro SB., Franchi R., Garg BK., Gulbahce N., Hao T., Holthaus AM., James R., Korkhin A., Litovchick L., Mar JC., Pak TR., Rabello S., Rubio R., Shen Y., Singh S., Spangle JM., Tasan M., Wanamaker S., Webber JT., Roecklein-Canfield J., Johannsen E., Barabási A-L., Beroukhim R., Kieff E., Cusick ME., Hill DE., Münger K., Marto J a., Quackenbush J., Roth FP., DeCaprio J a., Vidal M., Soler N., Krupovic M., Marguet E., Forterre P., Sciences B., Science M., Carolina N., Thomassen S., Riisgdrd HU., Pollock FJ., Wood-charlson EM., Oppen MJH Van., Bourne DG., Willis BL., Weynberg KD., Edgeworth J., Freemont P., Hogg N., Cuvelier ML., Blake E., Mulheron R., McCarthy PJ., Blackwelder P., Thurber RLV., Lopez J V., Gili JMM., Coma R., Schmitt S., Tsai P., Bell JJ., Fromont J., Ilan M., Lindquist N., Perez T., Rodrigo A., Schupp PJ., Vacelet J., Webster NS., Hentschel U., Taylor MW., Perdicaris S., Vlachogianni T., Valavanidis A., Proctor LM., Fuhrman J a., Sandaa R., Short SM., Schroeder DC., Goeij JM De., Oevelen D Van., Vermeij MJ a., Osinga R., Middelburg JJ., Goeij AFPM De., Admiraal W. 2014. Assessing the complex sponge microbiota: core, variable and species-specific bacterial communities in marine sponges. *Nature* 5:114. DOI: 10.1126/science.1241981.

Bell JJ., McGrath E., Biggerstaff A., Bates T., Bennett H., Marlow J., Shaffer M. 2015. Sediment impacts on marine sponges. *Marine Pollution Bulletin* 94:5–13. DOI: 10.1016/j.marpolbul.2015.03.030.

Belzile N., Chen Y-W. 2015. Tellurium in the environment: a critical review focused on natural waters, soils, sediments and airborne particles. *Applied Geochemistry* 63:83–92. DOI: 10.1016/j.apgeochem.2015.07.002.

Bennett HM., Altenrath C., Woods L., Davy SK., Webster NS., Bell JJ. 2017. Interactive effects of temperature and pCO2on sponges: from the cradle to the grave. *Global Change Biology* 23:2031–2046. DOI: 10.1111/gcb.13474.

Berg DE., Berg CM. 1983. The Prokaryotic Transposable Element Tn5. *Bio/Technology* 1:417–435. DOI: 10.1038/nbt0783-417.

Bergh O., Yngve Borsheim K., Bratbak G., Heldal M. 1989. High abundance of viruses found in aquatic environments. *Nature* 340:467–468.

Berthold RJ., Borowitzka MA., Mackay MA. 1982. The ultrastructure of Oscillatoria spongeliae, the blue-green algal endosymbiont of the sponge Dysidea herbacea. *Phycol* 21:327–335.

Bettarel Y., Sime-Ngando T., Amblard C., Laveran H. 2000. A comparison of methods for counting viruses in aquatic systems. *Applied and Environmental Microbiology* 66:2283–2289. DOI: 10.1128/AEM.66.6.2283-2289.2000.

Bir J., Howlader P., Ray S., Sultana S., Khalil SMI., Banu GR. 2017. A critical review on white spot syndrome virus (WSSV): A potential threat to shrimp farming in Bangladesh and some Asian countries. *International Journal of Microbiology and Mycology* 6:39–48.

Blanquer A., Uriz MJ., Cebrian E., Galand PE. 2016. Snapshot of a bacterial microbiome shift during the early symptoms of a massive sponge die-offin the western Mediterranean. *Frontiers in Microbiology* 7:1–10. DOI: 10.3389/fmicb.2016.00752.

Bloom DC., Giordani N V., Kwiatkowski DL. 2010. Epigenetic regulation of latent HSV-1 gene expression. *Biochimica et Biophysica Acta - Gene Regulatory Mechanisms* 1799:246–256. DOI: 10.1016/j.bbagrm.2009.12.001.

Boex-Fontvieille E., Davanture M., Jossier M., Zivy M., Hodges M., Tcherkez G. 2014. Photosynthetic activity influences cellulose biosynthesis and phosphorylation of proteins involved therein in Arabidopsis leaves. *Journal of Experimental Botany* 65:4997–5010. DOI: 10.1093/jxb/eru268.

Boldogkői Z., Moldován N., Balázs Z., Snyder M., Tombácz D. 2019. Long-Read Sequencing – A Powerful Tool in Viral Transcriptome Research. *Trends in Microbiology* 27:578–592. DOI: 10.1016/j.tim.2019.01.010.

Boller T., Felix G. 2009. A Renaissance of Elicitors: Perception of Microbe-Associated Molecular Patterns and Danger Signals by Pattern-Recognition Receptors. *Annual Review of Plant Biology* 60:379–406. DOI: 10.1146/annurev.arplant.57.032905.105346.

Bollback JP., Huelsenbeck JP. 2001. Phylogeny, genome evolution, and host specificity of single-stranded RNA bacteriophage (family Leviviridae). *Journal of Molecular Evolution* 52:117–128. DOI: 10.1007/s002390010140.

Boriová K., Čerňanský S., Matúš P., Bujdoš M., Šimonovičová A. 2014. Bioaccumulation and biovolatilization of various elements using filamentous fungus Scopulariopsis brevicaulis. *Letters in Applied Microbiology* 59:217–223. DOI: 10.1111/lam.12266.

Borsheim KY., Bratbak G., Heldal M. 1990. Enumeration and biomass estimation of planktonic bacteria and viruses by transmission electron microscopy. *Applied and Environmental Microbiology* 56:352–356.

Bosch TCG., McFall-Ngai MJ. 2011. Metaorganisms as the new frontier. *Zoology* 114:185–190. DOI: 10.1016/j.zool.2011.04.001.

Bourne DG., Muirhead A., Sato Y. 2011. Changes in sulfate-reducing bacterial populations during the onset of black band disease. *ISME Journal* 5:559–564. DOI: 10.1038/ismej.2010.143.

Bouvier T., Del Giorgio P a. 2007. Key role of selective viral-induced mortality in determining marine bacterial community composition. *Environmental Microbiology* 9:287–297. DOI: 10.1111/j.1462-2920.2006.01137.x.

Bowser PR., Casey JW. 1993. Retroviruses of fish. *Annual Review of Fish Diseases* 3:209–224. DOI: 10.1016/0959-8030(93)90035-A.

Boyer M., Yutin N., Pagnier I., Barrassi L., Fournous G., Espinosa L., Robert C., Azza S., Sun S., Rossmann MG., Suzan-Monti M., La Scola B., Koonin E V., Raoult D. 2009. Giant Marseillevirus highlights the role of amoebae as a melting pot in emergence of chimeric microorganisms. *Proceedings of the National Academy of Sciences of the United States of America* 106:21848–21853. DOI: 10.1073/pnas.0911354106.

Bracht AJ., Brudek RL., Ewing RY., Manire CA., Burek KA., Rosa C., Beckmen KB., Maruniak JE., Romero CH. 2006. Genetic identification of novel poxviruses of cetaceans and pinnipeds. *Archives of Virology* 151:423–438. DOI: 10.1007/s00705-005-0679-6.

Bratbak G., Heldal M., Thingstad TF., Tuomi P. 1996. Dynamics of virus abundance in coastal seawater. *FEMS Microbiology Ecology* 19:263–269. DOI: 10.1016/0168-6496(96)00023-2.

Bratbak G., Thingstad F., Heldal M. 1994. Viruses and the microbial loop. *Microbial Ecology* 28:209–221. DOI: 10.1007/BF00166811.

Breitbart M. 2012. Marine viruses: truth or dare. *Annual Review of Marine Science* 4:425–448. DOI: 10.1146/annurev-marine-120709-142805.

Breitbart M., Bonnain C., Malki K., Sawaya NA. 2018. Phage puppet masters of the marine microbial realm. *Nature Microbiology* 3:754–766. DOI: 10.1038/s41564-018-0166-y.

Breitbart M., Felts B., Kelley S., Mahaffy JM., Nulton J., Salamon P., Rohwer F. 2004. Diversity and population structure of a near-shore marine-sediment viral community. *Proceedings. Biological sciences / The Royal Society* 271:565–574. DOI: 10.1098/rspb.2003.2628.

Breitbart M., Miyake JH., Rohwer F. 2004. Global distribution of nearly identical phage-encoded DNA sequences. *FEMS Microbiology Letters* 236:249–256. DOI: 10.1016/j.femsle.2004.05.042.

Breitbart M., Rohwer F. 2005. Here a virus, there a virus, everywhere the same virus? *Trends in Microbiology* 13:278–284. DOI: 10.1016/j.tim.2005.04.003.

Breitbart M., Salamon P., Andresen B., Mahaffy JM., Segall AM., Mead D., Azam F., Rohwer F. 2002. Genomic analysis of uncultured marine viral communities. *Proceedings of the National Academy of Sciences of the United States of America* 99:14250–14255. DOI: 10.1073/pnas.202488399.

Breitbart M., Thompson L., Suttle C., Sullivan M. 2007. Exploring the Vast Diversity of Marine Viruses. *Oceanography* 20:135–139. DOI: 10.5670/oceanog.2007.58.

Brentlinger KL., Hafenstein S., Novak CR., Fane BA., Borgon R., McKenna R., Agbandje-McKenna M. 2002. Microviridae, a family divided: Isolation, characterization, and genome sequence of ϕMH2K, a bacteriophage of the obligate intracellular parasitic bacterium Bdellovibrio bacteriovorus. *Journal of Bacteriology* 184:1089–1094. DOI: 10.1128/jb.184.4.1089-1094.2002.

Van Bressem MF., Van Waerebeek K., Raga JA. 1999. A review of virus infections of cetaceans and the potential impact of morbilliviruses, poxviruses and papillomaviruses on host population dynamics. *Diseases of Aquatic Organisms* 38:53–65. DOI: 10.3354/dao038053.

Broecker WS., Takahashi T., Simpson HJ., Peng T-H. 1979. Fate of Fossil Fuel Carbon Dioxide and the Global Carbon Budget. *Science* 206:409–418. DOI: 10.1126/science.206.4417.409.

Bruinsma RF., Comas-Garcia M., Garmann RF., Grosberg AY. 2016. Equilibrium self-assembly of small RNA viruses. *Physical Review E* 93:1–14. DOI: 10.1103/PhysRevE.93.032405.

Brum JR., Ignacio-Espinoza JC., Roux S., Doulcier G., Acinas SG., Alberti A., Chaffron S., Cruaud C., de Vargas C., Gasol JM., Gorsky G., Gregory AC., Guidi L., Hingamp P., Iudicone D., Not

F., Ogata H., Pesant S., Poulos BT., Schwenck SM., Speich S., Dimier C., Kandels-Lewis S., Picheral M., Searson S., Bork P., Bowler C., Sunagawa S., Wincker P., Karsenti E., Sullivan MB. 2015. Patterns and ecological drivers of ocean viral communities. *Science* 348:1261498. DOI: 10.1126/science.1261498.

Brum JR., Schenck RO., Sullivan MB. 2013. Global morphological analysis of marine viruses shows minimal regional variation and dominance of non-tailed viruses. *The ISME Journal* 7:1738–1751. DOI: 10.1038/ismej.2013.67.

Brussaard CPD. 2004a. Viral Control of Phytoplancton Populations. *The Journal of Eukariootc Microbiology* 51:125–138. DOI: 10.1111/j.1550-7408.2005.000vol-cont.x.

Brussaard CPD. 2004b. Optimization of Procedures for Counting Viruses by Flow Cytometry. *Applied and Environmental Microbiology* 70:1506–1513. DOI: 10.1128/AEM.70.3.1506-1513.2004.

Buller RM., Palumbo GJ. 1991. Poxvirus pathogenesis. *Microbiological reviews* 55:80–122.

Butina TV., Potapov SA., Belykh OI., Belikov SI. 2015. Genetic diversity of cyanophages of the myoviridae family as a constituent of the associated community of the Baikal sponge Lubomirskia baicalensis. *Russian Journal of Genetics* 51:313–317. DOI: 10.1134/S1022795415030011.

Byers MJ., Avery RJ., Boaz J., Kohne DE. 1979. Presence of virus-specific DNA sequences in murine type C viruses. *Journal of General Virology* 43:611–621. DOI: 10.1099/0022-1317-43-3-611.

Capon RJ., Elsbury K., Butler MS., Lu CC., Hooper JNA., Rostas JAP., O'Brien KJ., Mudge L-M., Sim ATR. 1993. Extraordinary levels of cadmium and zinc in a marine sponge,Tedania charcoti Topsent: inorganic chemical defense agents. *Experientia* 49:263–264. DOI: 10.1007/BF01923536.

Carballo JL., Bautista E., Nava H., Cruz-Barraza JA., Chávez JA. 2013. Boring sponges, An increasing threat for coral reefs affected by bleaching events. *Ecology and Evolution* 3:872–886. DOI: 10.1002/ece3.452.

Carballo JL., Bell JJ. 2017. *Climate Change, Ocean Acidification and Sponges*. Cham: Springer International Publishing. DOI: 10.1007/978-3-319-59008-0.

Carballo JL., Naranjo SA., García-Gómez JC. 1996. Use of marine sponges as stress indicators in marine ecosystems at Algeciras Bay (southern Iberian Peninsula). *Marine Ecology Progress Series* 135:109–122. DOI: 10.3354/meps135109.

Casjens SR. 2005. Comparative genomics and evolution of the tailed-bacteriophages. *Current Opinion in Microbiology* 8:451–458. DOI: 10.1016/j.mib.2005.06.014.

Cebrian E., Uriz MJ., Garrabou J., Ballesteros E. 2011. Sponge mass mortalities in a warming mediterranean sea: Are cyanobacteria-harboring species worse off? *PLoS ONE* 6. DOI: 10.1371/journal.pone.0020211.

Chastel C., Main AJ., Guiguen C., le Lay G., Quillien MC., Monnat JY., Beaucournu JC. 1985. The isolation of Meaban virus, a new Flavivirus from the seabird tick Ornithodoros (Alectorobius) maritimus in France. *Archives of Virology* 83:129–140. DOI:

10.1007/BF01309911.

Cheville NF., Stasko J. 2014. Techniques in Electron Microscopy of Animal Tissue. *Veterinary Pathology* 51:28–41. DOI: 10.1177/0300985813505114.

Choudhury JD., Pramanik A., Webster NS., Llewellyn LE., Gachhui R., Mukherjee J. 2015. The Pathogen of the Great Barrier Reef Sponge Rhopaloeides odorabile Is a New Strain of Pseudoalteromonas agarivorans Containing Abundant and Diverse Virulence-Related Genes. *Marine Biotechnology* 17:463–478. DOI: 10.1007/s10126-015-9627-y.

Chow C-ET., Kim DY., Sachdeva R., Caron DA., Fuhrman JA. 2014. Top-down controls on bacterial community structure: microbial network analysis of bacteria, T4-like viruses and protists. *The ISME Journal* 8:816–829. DOI: 10.1038/ismej.2013.199.

Clark KF. 2016. Nimaviruses of Crustaceans. In: *Aquaculture Virology*. Elsevier, 397–413. DOI: 10.1016/B978-0-12-801573-5.00026-7.

Clarke C., Davies S. 2003. Immunomagnetic Cell Separation. In: *Metastasis Research Protocols*. New Jersey: Humana Press, 017–023. DOI: 10.1385/1-59259-137-X:017.

Claverie J-M., Grzela R., Lartigue A., Bernadac A., Nitsche S., Vacelet J., Ogata H., Abergel C. 2009. Mimivirus and Mimiviridae: giant viruses with an increasing number of potential hosts, including corals and sponges. *Journal of Invertebrate Pathology* 101:172–180. DOI: 10.1016/j.jip.2009.03.011.

Cochlan WP., Wikner J., Steward GF., Smith DC. 1993. Spatial distribution of viruses, bacteria and chlorophyll a in neritic, oceanic and estuarine environments. *Marine Ecology Progress Series* 92:77–87.

Colegrove KM., Wellehan JFX., Rivera R., Moore PF., Gulland FMD., Lowenstine LJ., Nordhausen RW., Nollens HH. 2010. Polyomavirus Infection in a Free-Ranging California Sea Lion (Zalophus Californianus) with Intestinal T-Cell Lymphoma. *Journal of Veterinary Diagnostic Investigation* 22:628–632. DOI: 10.1177/104063871002200422.

Colombet J., Sime-Ngando T., Cauchie HM., Fonty G., Hoffmann L., Demeure G. 2006. Depth-Related Gradients of Viral Activity in Lake Pavin. *Applied and Environmental Microbiology* 72:4440–4445. DOI: 10.1128/AEM.00021-06.

Colombo S., Arioli S., Neri E., Della Scala G., Gargari G., Mora D. 2017. Viromes as genetic reservoir for the microbial communities in aquatic environments: a focus on antimicrobial-resistance genes. *Frontiers in Microbiology* 8:1095. DOI: 10.3389/fmicb.2017.01095.

Correa AMS., Ainsworth TD., Rosales SM., Thurber AR., Butler CR., Vega Thurber RL. 2016. Viral outbreak in corals associated with an in situ bleaching event: atypical herpes-like viruses and a new megavirus infecting Symbiodinium. *Frontiers in microbiology* 7:127. DOI: 10.3389/fmicb.2016.00127.

Correa AMS., Welsh RM., Vega Thurber RL. 2013. Unique nucleocytoplasmic dsDNA and +ssRNA viruses are associated with the dinoflagellate endosymbionts of corals. *The ISME Journal* 7:13–27. DOI: 10.1038/ismej.2012.75.

Coutinho FH., Silveira CB., Gregoracci GB., Thompson CC., Edwards RA., Brussaard CPD., Dutilh

BE., Thompson FL. 2017. Marine viruses discovered via metagenomics shed light on viral strategies throughout the oceans. *Nature Communications* 8:1–12. DOI: 10.1038/ncomms15955.

Crane M., Hyatt A. 2011. Viruses of fish: An overview of significant pathogens. *Viruses* 3:2025–2046. DOI: 10.3390/v3112025.

Crummett LT., Puxty RJ., Weihe C., Marston MF., Martiny JBH. 2016. The genomic content and context of auxiliary metabolic genes in marine cyanomyoviruses. *Virology* 499:219–229. DOI: 10.1016/j.virol.2016.09.016.

Culley AI., Mueller JA., Belcaid M. 2014. The Characterization of RNA Viruses in Tropical Seawater Using Targeted PCR and Metagenomics. DOI: 10.1128/mBio.01210-14.Editor.

Cuppels DA. 1986. Generation and Characterization of Tn5 Insertion Mutations in Pseudomonas syringae pv. tomato. *Applied and environmental microbiology* 51:323–7.

Cuvelier ML., Blake E., Mulheron R., McCarthy PJ., Blackwelder P., Thurber RLV., Lopez J V. 2014. Two distinct microbial communities revealed in the sponge Cinachyrella. *Frontiers in Microbiology* 5:1–12. DOI: 10.3389/fmicb.2014.00581.

Danovaro R., Corinaldesi C., Dell'Anno A., Fuhrman JA., Middelburg JJ., Noble RT., Suttle CA. 2011. Marine viruses and global climate change. *FEMS Microbiology Reviews* 35:993–1034. DOI: 10.1111/j.1574-6976.2010.00258.x.

Dang VT., Speck P., Benkendorff K. 2012. Influence of elevated temperatures on the immune response of abalone, Haliotis rubra. *Fish and Shellfish Immunology* 32:732–740. DOI: 10.1016/j.fsi.2012.01.022.

Danovaro R., Corinaldesi C., Filippini M., Fischer UR., Gessner MO., Jacquet S., Magagnini M., Velimirov B. 2008. Viriobenthos in freshwater and marine sediments: A review. *Freshwater Biology* 53:1186–1213. DOI: 10.1111/j.1365-2427.2008.01961.x.

Darwin C. 2013. *The Structure and Distribution of Coral Reefs: Being the First Part of the Geology of the Voyage of the Beagle, under the Command of Capt. Fitzroy, R.N. during the Years 1832 to 1836.* Cambridge: Cambridge University Press. DOI: 10.1017/CBO9781107325098.

Davy S., Burchett S., Dale A., Davies P., Davy J., Muncke C., Hoegh-Guldberg O., Wilson W. 2006. Viruses: agents of coral disease? *Diseases of Aquatic Organisms* 69:101–110. DOI: 10.3354/dao069101.

Davy JE., Patten NL. 2007. Morphological diversity of virus-like particles within the surface microlayer of scleractinian corals. *Aquatic Microbial Ecology* 47:37–44. DOI: 10.3354/ame047037.

Degnan SM. 2015. The surprisingly complex immune gene repertoire of a simple sponge, exemplified by the NLR genes: A capacity for specificity? *Developmental and Comparative Immunology* 48:269–274. DOI: 10.1016/j.dci.2014.07.012.

Dell'Anno A., Corinaldesi C., Danovaro R. 2015. Virus decomposition provides an important contribution to benthic deep-sea ecosystem functioning. *Proceedings of the National Academy of Sciences* 112:E2014–E2019. DOI: 10.1073/pnas.1422234112.

Delmer DP., Haigler CH. 2002. The regulation of metabolic flux to cellulose, a major sink for carbon in plants. *Metabolic Engineering* 4:22–28. DOI: 10.1006/mben.2001.0206.

Delwart E., Li L. 2012. Rapidly expanding genetic diversity and host range of the Circoviridae viral family and other Rep encoding small circular ssDNA genomes. *Virus Research* 164:114–121. DOI: 10.1016/j.virusres.2011.11.021.

Denayer S., Matthijs S., Cornelis P. 2007. Pyocin S2 (Sa) kills Pseudomonas aeruginosa strains via the FpvA type I ferripyoverdine receptor. *Journal of Bacteriology* 189:7663–7668. DOI: 10.1128/JB.00992-07.

Diaz MC., Rützler K. 2001. Sponges: An essential component of Caribbean coral reefs. *Bulletin of Marine Science* 69:535–546.

Díez-Vives C., Moitinho-Silva L., Nielsen S., Reynolds D., Thomas T. 2017. Expression of eukaryotic-like protein in the microbiome of sponges. *Molecular Ecology* 26:1432–1451. DOI: 10.1111/mec.14003.

Doan QK., Vandeputte M., Chatain B., Morin T., Allal F. 2017. Viral encephalopathy and retinopathy in aquaculture: a review. *Journal of Fish Diseases* 40:717–742. DOI: 10.1111/jfd.12541.

Doney SC., Ruckelshaus M., Emmett Duffy J., Barry JP., Chan F., English C a., Galindo HM., Grebmeier JM., Hollowed AB., Knowlton N., Polovina J., Rabalais NN., Sydeman WJ., Talley LD. 2012. Climate Change Impacts on Marine Ecosystems. *Annual Review of Marine Science* 4:11–37. DOI: 10.1146/annurev-marine-041911-111611.

Drake JW. 1993. Rates of spontaneous mutation among RNA viruses. *Proceedings of the National Academy of Sciences* 90:4171–4175. DOI: 10.1073/pnas.90.9.4171.

Duffy S., Burch CL., Turner PE. 2007. Evolution of host specificity drives reproductive isolation among RNA viruses. *Evolution* 61:2614–2622. DOI: 10.1111/j.1558-5646.2007.00226.x.

Dunlap DS., Ng TFF., Rosario K., Barbosa JG., Greco AM., Breitbart M., Hewson I. 2013. Molecular and microscopic evidence of viruses in marine copepods. *Proceedings of the National Academy of Sciences* 110:1375–1380. DOI: 10.1073/pnas.1216595110.

Dutova N V., Drucker V V. 2013. Viral community of biofilms forming on different substrates under natural conditions of Lake Baikal. *Doklady Biological Sciences* 451:238–240. DOI: 10.1134/S0012496613030113.

Dyson ZA., Tucci J., Seviour RJ., Petrovski S. 2015. Lysis to Kill: Evaluation of the Lytic Abilities, and Genomics of Nine Bacteriophages Infective for Gordonia spp. and Their Potential Use in Activated Sludge Foam Biocontrol. *PLOS ONE* 10:e0134512. DOI: 10.1371/journal.pone.0134512.

Eakin CM., Sweatman HPA., Brainard RE. 2019. The 2014–2017 global-scale coral bleaching event: insights and impacts. *Coral Reefs* 38:539–545. DOI: 10.1007/s00338-019-01844-2.

Edwards R., Rohwer F. 2005. Viral Metagenomics. *Nature Reviews Microbiology* 3:504–510. DOI: 10.1002/9781118010549.ch2.

Egan S., Gardiner M. 2016. Microbial dysbiosis: Rethinking disease in marine ecosystems. *Frontiers in Microbiology* 7:1–8. DOI: 10.3389/fmicb.2016.00991.

Eid J., Fehr A., Gray J., Luong K., Lyle J., Otto G., Peluso P., Rank D., Baybayan P., Bettman B., Bibillo A., Bjornson K., Chaudhuri B., Christians F., Cicero R., Clark S., Dalal R., DeWinter A., Dixon J., Foquet M., Gaertner A., Hardenbol P., Heiner C., Hester K., Holden D., Kearns G., Kong X., Kuse R., Lacroix Y., Lin S., Lundquist P., Ma C., Marks P., Maxham M., Murphy D., Park I., Pham T., Phillips M., Roy J., Sebra R., Shen G., Sorenson J., Tomaney A., Travers K., Trulson M., Vieceli J., Wegener J., Wu D., Yang A., Zaccarin D., Zhao P., Zhong F., Korlach J., Turner S. 2009. Real-Time DNA Sequencing from Single Polymerase Molecules. *Science* 323:133–138. DOI: 10.1126/science.1162986.

El-Moselhy KM., Othman AI., Abd El-Azem H., El-Metwally MEA. 2014. Bioaccumulation of heavy metals in some tissues of fish in the Red Sea, Egypt. *Egyptian Journal of Basic and Applied Sciences* 1:97–105. DOI: 10.1016/j.ejbas.2014.06.001.

El-Naggar M., Al-Amoudi O. 1989. Heavy metal levels in several species of marine algae from the Red Sea of Saudi Arabia. *Journal of King Abdulaziz University-Science* 1:5–13. DOI: 10.4197/Sci.1-1.1.

Erwin PM., Thacker RW. 2007. Phylogenetic analyses of marine sponges within the order Verongida: A comparison of morphological and molecular data. *Invertebrate Biology* 126:220–234. DOI: 10.1111/j.1744-7410.2007.00092.x.

Fan L., Liu M., Simister R., Webster NS., Thomas T. 2013. Marine microbial symbiosis heats up: the phylogenetic and functional response of a sponge holobiont to thermal stress. *The ISME Journal* 7:991–1002. DOI: 10.1038/ismej.2012.165.

Fan L., Reynolds D., Liu M., Stark M., Kjelleberg S., Webster NS., Thomas T. 2012. PNAS Plus: Functional equivalence and evolutionary convergence in complex communities of microbial sponge symbionts. *Proceedings of the National Academy of Sciences* 109:E1878–E1887. DOI: 10.1073/pnas.1203287109.

Fichtner D., Philipps A., Groth M., Schmidt-Posthaus H., Granzow H., Dauber M., Platzer M., Bergmann SM., Schrudde D., Sauerbrei A., Zell R. 2013. Characterization of a Novel Picornavirus Isolate from a Diseased European Eel (Anguilla anguilla). *Journal of Virology* 87:10895–10899. DOI: 10.1128/jvi.01094-13.

Finke JF., Hunt BPV., Winter C., Carmack EC., Suttle CA. 2017. Nutrients and other environmental factors influence virus abundances across oxic and hypoxic marine environments. *Viruses* 9:1–15. DOI: 10.3390/v9060152.

Fischetti VA. 2005. Bacteriophage lytic enzymes: novel anti-infectives. *Trends in Microbiology* 13:491–496. DOI: 10.1016/j.tim.2005.08.007.

Flombaum P., Gallegos JL., Gordillo R a., Rincon J., Zabala LL., Jiao N., Karl DM., Li WKW., Lomas MW., Veneziano D., Vera CS., Vrugt J a., Martiny a C. 2013. Present and future global distributions of the marine Cyanobacteria Prochlorococcus and Synechococcus. *Proceedings of the National Academy of Sciences* 110:9824–9829. DOI: 10.1073/pnas.1307701110.

Flores CO., Meyer JR., Valverde S., Farr L., Weitz JS. 2011. Statistical structure of host – phage

interactions. *Proceedings of the National Academy of Sciences* 108:E288–E297. DOI: 10.1073/pnas.1101595108/-/DCSupplemental.www.pnas.org/cgi/doi/10.1073/pnas.1101595108.

Flores CO., Valverde S., Weitz JS. 2013. Multi-scale structure and geographic drivers of cross-infection within marine bacteria and phages. *The ISME Journal* 7:520–532. DOI: 10.1038/ismej.2012.135.

Flowers EM., Johnson AF., Aguilar R., Schott EJ. 2018. Prevalence of the pathogenic crustacean virus Callinectes sapidus reovirus 1 near flow-through blue crab aquaculture in Chesapeake Bay, USA. *Diseases of Aquatic Organisms* 129:135–144. DOI: 10.3354/dao03232.

Forterre P., Soler N., Krupovic M., Marguet E., Ackermann H-W. 2013. Fake virus particles generated by fluorescence microscopy. *Trends in Microbiology* 21:1–5. DOI: 10.1016/j.tim.2012.10.005.

Franchi L., Kamada N., Nakamura Y., Burberry A., Kuffa P., Suzuki S., Shaw MH., Kim YG., Núñez G. 2012. NLRC4-driven production of IL-1β discriminates between pathogenic and commensal bacteria and promotes host intestinal defense. *Nature Immunology* 13:449–456. DOI: 10.1038/ni.2263.

Freeman CJ., Thacker RW. 2011. Complex interactions between marine sponges and their symbiotic microbial communities. *Limnology and Oceanography* 56:1577–1586. DOI: 10.4319/lo.2011.56.5.1577.

Fröhlich J., König H. 2005. Micromanipulation Techniques for the Isolation of Single Microorganisms. In: *Intestinal Microorganisms of Termites and Other Invertebrates*. Berlin/Heidelberg: Springer-Verlag, 425–437. DOI: 10.1007/3-540-28185-1_18.

Fuhrman JA. 1999. Marine viruses and their biogeochemical and ecological effects. *Nature* 399:541–548. DOI: 10.1038/21119.

Fuhrman J., Suttle C. 1993. Viruses in Marine Planktonic Systems. *Oceanography* 6:51–63. DOI: 10.5670/oceanog.1993.14.

Fuhrmann M., Petton B., Quillien V., Faury N., Morga B., Pernet F. 2016. Salinity influences disease-induced mortality of the oyster Crassostrea gigas and infectivity of the ostreid herpesvirus 1 (OsHV-1). *Aquaculture Environment Interactions* 8:543–552. DOI: 10.3354/aei00197.

Gaino E., Sciscioli M., Lepore E., Rebora M., Corriero G. 2006. Association of the sponge Tethya orphei (Porifera, Demospongiae) with filamentous cyanobacteria. *Invertebrate Biology* 125:281–287. DOI: 10.1111/j.1744-7410.2006.00061.x.

Gantt SE., López-Legentil S., Erwin PM. 2017. Stable microbial communities in the sponge Crambe crambe from inside and outside a polluted Mediterranean harbor. *FEMS Microbiology Letters* 364:1–7. DOI: 10.1093/femsle/fnx105.

Gao Z-M., Wang Y., Lee OO., Tian R-M., Wong YH., Bougouffa S., Batang Z., Al-Suwailem A., Lafi FF., Bajic VB., Qian P-Y. 2014a. Pyrosequencing reveals the microbial communities in the Red Sea Sponge Carteriospongia foliascens and their impressive shifts in abnormal tissues. *Microbial Ecology* 68:621–632. DOI: 10.1007/s00248-014-0419-0.

Gao Z-M., Wang Y., Tian R-M., Lee OO., Wong YH., Batang ZB., Al-Suwailem A., Lafi FF., Bajic VB., Qian P-Y. 2015. Pyrosequencing revealed shifts of prokaryotic communities between healthy and disease-like tissues of the Red Sea sponge Crella cyathophora. *PeerJ* 3:e890. DOI: 10.7717/peerj.890.

Gao Z-M., Wang Y., Tian R-M., Wong YH., Batang ZB., Al-Suwailem AM., Bajic VB., Qian P-Y. 2014b. Symbiotic adaptation drives genome streamlining of the cyanobacterial sponge symbiont "Candidatus Synechococcus spongiarum." *mBio* 5:1–11. DOI: 10.1128/mBio.00079-14.

Gelderblom HR. 1996. Structure and Classification of Viruses. In: S B ed. *Medical Microbiology*. University of Texas Medical Branch at Galveston,.

Giles EC., Kamke J., Moitinho-Silva L., Taylor MW., Hentschel U., Ravasi T., Schmitt S. 2013. Bacterial community profiles in low microbial abundance sponges. *FEMS Microbiology Ecology* 83:232–241. DOI: 10.1111/j.1574-6941.2012.01467.x.

Glasl B., Smith CE., Bourne DG., Webster NS. 2018. Exploring the diversity-stability paradigm using sponge microbial communities. *Scientific Reports* 8:1–9. DOI: 10.1038/s41598-018-26641-9.

Glazebrook JS., Heasman MP., Beer SW. 1990. Picorna-like viral particles associated with mass mortalities in larval barramundi, Lates calcarifer Bloch. *Journal of Fish Diseases* 13:245–249. DOI: 10.1111/j.1365-2761.1990.tb00780.x.

Gloeckner V., Wehrl M., Moitinho-Silva L., Gernert C., Schupp P., Pawlik JR., Lindquist NL., Erpenbeck D., Wörheide G., Hentschel U. 2014. The HMA-LMA dichotomy revisited: an electron microscopical survey of 56 sponge species. *The Biological Bulletin* 227:78–88. DOI: 10.1086/BBLv227n1p78.

Glynn PW., Ault JS. 2000. A biogeographic analysis and review of the far eastern Pacific coral reef region. *Coral Reefs* 19:1–23. DOI: 10.1007/s003380050220.

de Goeij JM., van Oevelen D., Vermeij MJ a., Osinga R., Middelburg JJ., de Goeij AFPM., Admiraal W. 2013a. Surviving in a marine desert: the sponge loop retains resources within coral reefs. *Science (New York, N.Y.)* 342:108–10. DOI: 10.1126/science.1241981.

de Goeij JM., van Oevelen D., Vermeij MJA., Osinga R., Middelburg JJ., de Goeij AFPM., Admiraal W. 2013b. Surviving in a Marine Desert: The Sponge Loop Retains Resources Within Coral Reefs. *Science* 342:108–110. DOI: 10.1126/science.1241981.

Goncharoff P., Saadi S., Chang CH., Saltman LH., Figurski DH. 1991. Structural, molecular, and genetic analysis of the *kilA* operon of broad-host-range plasmid RK2. *Journal of Bacteriology* 173:3463–3477.

Grangeasse C., Nessler S., Mijakovic I. 2012. Bacterial tyrosine kinases: Evolution, biological function and structural insights. *Philosophical Transactions of the Royal Society B: Biological Sciences* 367:2640–2655. DOI: 10.1098/rstb.2011.0424.

Grasis JA., Lachnit T., Anton-Erxleben F., Lim YW., Schmieder R., Fraune S., Franzenburg S., Insua S., Machado G., Haynes M., Little M., Kimble R., Rosenstiel P., Rohwer FL., Bosch TCG. 2014. Species-specific viromes in the ancestral holobiont hydra. *PLoS ONE* 9:e109952. DOI: 10.1371/journal.pone.0109952.

Green TJ., Montagnani C., Benkendorff K., Robinson N., Speck P. 2014. Ontogeny and water temperature influences the antiviral response of the Pacific oyster, Crassostrea gigas. *Fish and Shellfish Immunology* 36:151–157. DOI: 10.1016/j.fsi.2013.10.026.

Green TJ., Speck P. 2018. Antiviral defense and innate immune memory in the oyster. *Viruses* 10:1–11. DOI: 10.3390/v10030133.

Gregory A., Zayed A., Conceição-Neto N., Temperton B., Bolduc B., Alberti A., Ardyna M., Arkhipova K., Carmicheal M., Cruaud C., Dimier C., Dominguez-Huerta G., Ferland J., Kandels S., Liu Y., Marec C., Pesant S., Picheral M., Pisarev S., Poulain J., Tremblay J-É., Vik D., Coordinators TO., Babin M., Bowler C., Culley A., de Vargas C., Dutilh B., Iudicone D., Karp-Boss L., Roux S., Sunagawa S., Wincker P., Sullivan M. 2019. Marine DNA viral macro-and micro-diversity from pole to pole. *SSRN Electronic Journal*:1–15. DOI: 10.2139/ssrn.3319797.

Di Guardo G., Marruchella G., Agrimi U., Kennedy S. 2005. Morbillivirus infections in aquatic mammals: A brief overview. *Journal of Veterinary Medicine Series A: Physiology Pathology Clinical Medicine* 52:88–93. DOI: 10.1111/j.1439-0442.2005.00693.x.

Gudenkauf BM., Hewson I. 2016. Comparative metagenomics of viral assemblages inhabiting four phyla of marine invertebrates. *Frontiers in Marine Science* 3:1–12. DOI: 10.3389/fmars.2016.00023.

Gupta P., Zhang Z., Sugiman-Marangos SN., Tam J., Raman S., Julien JP., Kroh HK., Lacy DB., Murgolo N., Bekkari K., Therien AG., Hernandez LD., Melnyk RA. 2017. Functional defects in Clostridium difficile TcdB toxin uptake identify CSPG4 receptor-binding determinants. *Journal of Biological Chemistry* 292:17290–17301. DOI: 10.1074/jbc.M117.806687.

Guzman C., Conaco C. 2016. Gene Expression Dynamics Accompanying the Sponge Thermal Stress Response. *PLOS ONE* 11:e0165368. DOI: 10.1371/journal.pone.0165368.

Haaber J., Leisner JJ., Cohn MT., Catalan-Moreno A., Nielsen JB., Westh H., Penadés JR., Ingmer H. 2016. Bacterial viruses enable their host to acquire antibiotic resistance genes from neighbouring cells. *Nature Communications* 7. DOI: 10.1038/ncomms13333.

Hadas E., Marie D., Shpigel M., Ilan M. 2006. Virus predation by sponges is a new nutrient-flow pathway in coral reef food webs. *Limnology and Oceanography* 51:1548–1550. DOI: 10.4319/lo.2006.51.3.1548.

Haller SL., Peng C., McFadden G., Rothenburg S. 2014. Poxviruses and the evolution of host range and virulence. *Infection, Genetics and Evolution* 21:15–40. DOI: 10.1016/j.meegid.2013.10.014.

Harrison HB., Álvarez-Noriega M., Baird AH., Heron SF., MacDonald C., Hughes TP. 2018. Back-to-back coral bleaching events on isolated atolls in the Coral Sea. *Coral Reefs*:713–719. DOI: 10.1007/s00338-018-01749-6.

Harshey RM. 2014. Transposable Phage Mu. *Microbiology spectrum* 2:669–691. DOI: 10.1128/microbiolspec.MDNA3-0007-2014.

Haynes D., Johnson JE. 2000. Organochlorine, heavy metal and polyaromatic hydrocarbon pollutant concentrations in the Great Barrier Reef (Australia) environment: a review. *Marine Pollution Bulletin* 41:267–278. DOI: 10.1016/S0025-326X(00)00134-X.

Hentschel U., Hopke J., Horn M., Friedrich AB., Wagner M., Hacker J., Moore BS. 2002. Molecular evidence for a uniform microbial community in sponges from different oceans. *Applied and Environmental Microbiology* 68:4431–4440. DOI: 10.1128/AEM.68.9.4431-4440.2002.

Hentschel U., Usher KM., Taylor MW. 2006. Marine sponges as microbial fermenters. *FEMS Microbiology Ecology* 55:167–177. DOI: 10.1111/j.1574-6941.2005.00046.x.

Herbst LH., Lenz J., Van Doorslaer K., Chen Z., Stacy BA., Wellehan JFX., Manire CA., Burk RD. 2009. Genomic characterization of two novel reptilian papillomaviruses, Chelonia mydas papillomavirus 1 and Caretta caretta papillomavirus 1. *Virology* 383:131–135. DOI: 10.1016/j.virol.2008.09.022.

Hewson I., Button JB., Gudenkauf BM., Miner B., Newton AL., Gaydos JK., Wynne J., Groves CL., Hendler G., Murray M., Fradkin S., Breitbart M., Fahsbender E., Lafferty KD., Kilpatrick a M., Miner CM., Raimondi P., Lahner L., Friedman CS., Daniels S., Haulena M., Marliave J., Burge C a., Eisenlord ME., Harvell CD. 2014. Densovirus associated with sea-star wasting disease and mass mortality. *Proceedings of the National Academy of Sciences* 111:17278–17283. DOI: 10.1073/pnas.1416625111.

Hewson I., Fuhrman J a. 2007. Covariation of viral parameters with bacterial assemblage richness and diversity in the water column and sediments. *Deep-Sea Research Part I: Oceanographic Research Papers* 54:811–830. DOI: 10.1016/j.dsr.2007.02.003.

Hinde R., Pironet F., Borowitzka MA. 1994. Isolation of Oscillatoria spongeliae, the filamentous cyanobacterial symbiont of the marine sponge Dysidea herbacea. *Marine Biology* 119:99–104. DOI: 10.1007/BF00350111.

Hingamp P., Grimsley N., Acinas SG., Clerissi C., Subirana L., Poulain J., Ferrera I., Sarmento H., Villar E., Lima-Mendez G., Faust K., Sunagawa S., Claverie J-M., Moreau H., Desdevises Y., Bork P., Raes J., de Vargas C., Karsenti E., Kandels-Lewis S., Jaillon O., Not F., Pesant S., Wincker P., Ogata H. 2013. Exploring nucleo-cytoplasmic large DNA viruses in Tara Oceans microbial metagenomes. *The ISME journal* 7:1678–95. DOI: 10.1038/ismej.2013.59.

Hobbs Z., Abedon ST. 2016. Diversity of phage infection types and associated terminology: the problem with "Lytic or lysogenic." *FEMS microbiology letters* 363:1–8. DOI: 10.1093/femsle/fnw047.

Hoegh-Guldberg O. 2011. Coral reef ecosystems and anthropogenic climate change. *Regional Environmental Change* 11:215–227. DOI: 10.1007/s10113-010-0189-2.

Hoegh-Guldberg O., Bruno JF. 2010. The impact of climate change on the world's marine ecosystems. *Science* 328:1523–1528. DOI: 10.1126/science.1189930.

Hoffmann F., Larsen O., Thiel V., Rapp HT., Pape T., Michaelis W., Reitner J. 2005. An Anaerobic World in Sponges. *Geomicrobiology Journal* 22:1–10. DOI: 10.1080/01490450590922505.

Holmfeldt K., Middelboe M., Nybroe O., Riemann L. 2007. Large variabilities in host strain susceptibility and phage host range govern interactions between lytic marine phages and their Flavobacterium hosts. *Applied and Environmental Microbiology* 73:6730–6739.

DOI: 10.1128/AEM.01399-07.

Hooper JNA., Kennedy JA., Quinn RJ. 2002. Biodiversity “hotspots”, patterns of richness and endemism, and taxonomic affinities of tropical Australian sponges (Porifera). *Biodiversity and Conservation* 11:851–885. DOI: 10.1023/A:1015370312077.

Hooper JNA., Van Soest RWM. 2002. Systema Porifera. A Guide to the Classification of Sponges. *Invertebrate Systematics* 18:233–234. DOI: http://dx.doi.org/10.1007/978-1-4615-0747-5_1.

Howard-Varona C., Hargreaves KR., Abedon ST., Sullivan MB. 2017. Lysogeny in nature: Mechanisms, impact and ecology of temperate phages. *ISME Journal* 11:1511–1520. DOI: 10.1038/ismej.2017.16.

Hughes TP. 2003. Climate change, human impacts, and the resilience of coral reefs. *Science* 301:929–933. DOI: 10.1126/science.1085046.

Hughes TP., Anderson KD., Connolly SR., Heron SF., Kerry JT., Lough JM., Baird AH., Baum JK., Berumen ML., Bridge TC., Claar DC., Eakin CM., Gilmour JP., Graham NAJ., Harrison H., Hobbs JPA., Hoey AS., Hoogenboom M., Lowe RJ., McCulloch MT., Pandolfi JM., Pratchett M., Schoepf V., Torda G., Wilson SK. 2018. Spatial and temporal patterns of mass bleaching of corals in the Anthropocene. *Science* 359:80–83. DOI: 10.1126/science.aan8048.

Hughes TP., Kerry JT., Álvarez-Noriega M., Álvarez-Romero JG., Anderson KD., Baird AH., Babcock RC., Beger M., Bellwood DR., Berkelmans R., Bridge TC., Butler IR., Byrne M., Cantin NE., Comeau S., Connolly SR., Cumming GS., Dalton SJ., Diaz-Pulido G., Eakin CM., Figueira WF., Gilmour JP., Harrison HB., Heron SF., Hoey AS., Hobbs JPA., Hoogenboom MO., Kennedy E V., Kuo CY., Lough JM., Lowe RJ., Liu G., McCulloch MT., Malcolm HA., McWilliam MJ., Pandolfi JM., Pears RJ., Pratchett MS., Schoepf V., Simpson T., Skirving WJ., Sommer B., Torda G., Wachenfeld DR., Willis BL., Wilson SK. 2017. Global warming and recurrent mass bleaching of corals. *Nature* 543:373–377. DOI: 10.1038/nature21707.

Hurwitz BL., Brum JR., Sullivan MB. 2015. Depth-stratified functional and taxonomic niche specialization in the “core” and “flexible” Pacific Ocean Virome. *The ISME Journal* 9:472–484. DOI: 10.1038/ismej.2014.143.

Hurwitz BL., Deng L., Poulos BT., Sullivan MB. 2013. Evaluation of methods to concentrate and purify ocean virus communities through comparative, replicated metagenomics. *Environmental Microbiology* 15:1428–1440. DOI: 10.1111/j.1462-2920.2012.02836.x.

Hurwitz BL., Westveld AH., Brum JR., Sullivan MB. 2014. Modeling ecological drivers in marine viral communities using comparative metagenomics and network analyses. *Proceedings of the National Academy of Sciences* 111:10714–10719. DOI: 10.1073/pnas.1319778111.

Huson DH., Mitra S., Ruscheweyh H., Weber N., Schuster SC. 2011. Integrative analysis of environmental sequences using MEGAN4. *Genome Research* 21:1552–1560. DOI: 10.1101/gr.120618.111.

Ibrahim AMM., Abdelmenam MA. 2015. Heavy metals in Suez Canal and Red Sea Gulfs, review article. *Blue Biotechnology Journal* 2:157–183.

Ilan M., Gugel J., Van Soest R. 2004. Taxonomy, reproduction and ecology of new and known Red Sea sponges. *Sarsia* 89:388–410. DOI: 10.1080/00364820410002659.

Iyer LM., Aravind L., Koonin E V. 2001. Common origin of four diverse families of large eukaryotic DNA viruses. *Journal of Virology* 75:11720–11734. DOI: 10.1128/JVI.75.23.11720-11734.2001.

Jackson EW., Bistolas KSI., Button JB., Hewson I. 2016. Novel circular single-stranded DNA viruses among an asteroid, echinoid and holothurian (Phylum: Echinodermata). *PLoS ONE* 11:1–9. DOI: 10.1371/journal.pone.0166093.

Jacquet S., Bratbak G. 2003. Effects of ultraviolet radiation on marine virus-phytoplankton interactions. *FEMS Microbiology Ecology* 44:279–289. DOI: 10.1016/S0168-6496(03)00075-8.

Jahn MT., Arkhipova K., Markert SM., Stigloher C., Lachnit T., Pita L., Kupczok A., Ribes M., Stengel ST., Rosenstiel P., Dutilh BE., Hentschel U. 2019. A phage protein aids bacterial symbionts in eukaryote immune evasion. *Cell Host & Microbe* 26:542–550.e5. DOI: 10.1016/j.chom.2019.08.019.

Jiang SC., Paul JH. 1998. Gene transfer by transduction in the marine environment. *Applied and environmental microbiology* 64:2780–7.

Jokela M., Lehtinen S., Palmio J., Saukkonen AM., Huovinen S., Vihola A., Udd B. 2019. A novel COL6A2 mutation causing late-onset limb-girdle muscular dystrophy. *Journal of Neurology* 266:1649–1654. DOI: 10.1007/s00415-019-09307-y.

Jones K., Ariel E., Burgess G., Read M. 2016. A review of fibropapillomatosis in Green turtles (Chelonia mydas). *Veterinary Journal* 212:48–57. DOI: 10.1016/j.tvjl.2015.10.041.

Jones R., Kerswell A. 2003. Phytotoxicity of Photosystem II (PSII) herbicides to coral. *Marine Ecology Progress Series* 261:149–159. DOI: 10.3354/meps261149.

Jover LF., Effler TC., Buchan A., Wilhelm SW., Weitz JS. 2014. The elemental composition of virus particles: Implications for marine biogeochemical cycles. *Nature Reviews Microbiology* 12:519–528. DOI: 10.1038/nrmicro3289.

Juhnke S., Peitzsch N., Hübener N., Große C., Nies DH. 2002. New genes involved in chromate resistance in Ralstonia metallidurans strain CH34. *Archives of Microbiology* 179:15–25. DOI: 10.1007/s00203-002-0492-5.

Kakudo S., Negoro S., Urabe I., Okada H. 1993. Nylon oligomer degradation gene, nylC, on plasmid pOAD2 from a Flavobacterium strain encodes endo-type 6-aminohexanoate oligomer hydrolase: Purification and characterization of the nylC gene product. *Applied and Environmental Microbiology* 59:3978–3980. DOI: 10.1128/aem.59.11.3978-3980.1993.

Karpf AR., Lenches E., Strauss EG., Strauss JH., Brown DT. 1997. Superinfection exclusion of alphaviruses in three mosquito cell lines persistently infected with Sindbis virus. *Journal of virology* 71:7119–23.

Kauffman KM., Hussain FA., Yang J., Arevalo P., Brown JM., Chang WK., VanInsberghe D., Elsherbini J., Sharma RS., Cutler MB., Kelly L., Polz MF. 2018. A major lineage of non-

tailed dsDNA viruses as unrecognized killers of marine bacteria. *Nature* 554:118–122. DOI: 10.1038/nature25474.

Kavitha O., Thampan RV. 2008. Factors influencing collagen biosynthesis. *Journal of Cellular Biochemistry* 104:1150–1160. DOI: 10.1002/jcb.21728.

Kelmo F., Bell JJ., Attrill MJ. 2013. Tolerance of Sponge Assemblages to Temperature Anomalies: Resilience and Proliferation of Sponges following the 1997-8 El-Niño Southern Oscillation. *PLoS ONE* 8. DOI: 10.1371/journal.pone.0076441.

Keren R., Mayzel B., Lavy A., Polishchuk I., Levy D., Fakra SC., Pokroy B., Ilan M. 2017. Sponge-associated bacteria mineralize arsenic and barium on intracellular vesicles. *Nature Communications* 8:14393. DOI: 10.1038/ncomms14393.

Kieselbach T., Hagman Å., Andersson B., Schröder WP. 1998. The thylakoid lumen of chloroplasts. *Journal of Biological Chemistry* 273:6710–6716. DOI: 10.1074/jbc.273.12.6710.

Kim A., Terzian C., Santamaria P., Pelisson A., Purd'homme N., Bucheton A. 1994. Retroviruses in invertebrates: the gypsy retrotransposon is apparently an infectious retrovirus of Drosophila melanogaster. *Proceedings of the National Academy of Sciences* 91:1285–1289. DOI: 10.1073/pnas.91.4.1285.

Kim M-S., Whon TW., Bae J-W. 2013. Comparative Viral Metagenomics of Environmental Samples from Korea. *Genomics & Informatics* 11:121. DOI: 10.5808/GI.2013.11.3.121.

Kinoshita S., Negoro S., Muramatsu M., Bisaria VS., Sawada S., Okada H. 1977. 6-aminohexanoic acid cyclic dimer hydrolase. A new cyclic amide hydrolase produced by Acromobacter guttatus KI72. *European Journal of Biochemistry* 80:489–495. DOI: 10.1111/j.1432-1033.1977.tb11904.x.

Kitamura SI., Tomaru Y., Kawabata Z., Suzuki S. 2002. Detection of marine birnavirus in the Japanese pearl oyster Pinctada fucata and seawater from different depths. *Diseases of Aquatic Organisms* 50:211–217. DOI: 10.3354/dao050211.

Kriss AE., Rukina EA. 1947. Bacteriophages in the sea. *Dokl Akad Nauk SSR* 57:833–836.

Kumar M., Turner S. 2015. Plant cellulose synthesis: CESA proteins crossing kingdoms. *Phytochemistry* 112:91–99. DOI: 10.1016/j.phytochem.2014.07.009.

Laffy PW., Botté ES., Wood-Charlson EM., Weynberg KD., Rattei T., Webster NS. 2019. Thermal stress modifies the marine sponge virome. *Environmental Microbiology Reports* 0:1758–2229.12782. DOI: 10.1111/1758-2229.12782.

Laffy PW., Wood-Charlson EM., Turaev D., Jutz S., Pascelli C., Botté ES., Bell SC., Peirce TE., Weynberg KD., van Oppen MJH., Rattei T., Webster NS. 2018. Reef invertebrate viromics: diversity, host specificity and functional capacity. *Environmental Microbiology* 20:2125–2141. DOI: 10.1111/1462-2920.14110.

Laffy PW., Wood-Charlson EM., Turaev D., Weynberg KD., Botté ES., Van Oppen MJH., Webster NS., Rattei T. 2016. HoloVir: a workflow for investigating the diversity and function of viruses in invertebrate holobionts. *Frontiers in Microbiology* 7:1–15. DOI: 10.3389/fmicb.2016.00822.

Lara E., Arrieta JM., Garcia-Zarandona I., Boras JA., Duarte CM., Agustí S., Wassmann PF., Vaqué D. 2013. Experimental evaluation of the warming effect on viral, bacterial and protistan communities in two contrasting Arctic systems. *Aquatic Microbial Ecology* 70:17–32. DOI: 10.3354/ame01636.

Lawrence JE., Steward GF. 2010. Purification of viruses by centrifugation. In: Wilhelm SW, Weinbauer MG, Suttle CA eds. *Manual of Aquatic Viral Ecology*. American Society of Limnology and Oceanography, 166–181. DOI: 10.4319/mave.2010.978-0-9845591-0-7.166.

Lawrence S., Wilkinson S., Davy J., Arlidge W., Williams G., Wilson W., Aeby G., Davy S. 2015. Influence of local environmental variables on the viral consortia associated with the coral Montipora capitata from Kaneohe Bay, Hawaii, USA. *Aquatic Microbial Ecology* 74:251–262. DOI: 10.3354/ame01743.

Leaper R., Cooke J., Trathan P., Reid K., Rowntree V., Payne R. 2006. Global climate drives southern right whale (Eubalaena australis) population dynamics. *Biology Letters* 2:289–292. DOI: 10.1098/rsbl.2005.0431.

Lebarbenchon C., Jaeger A., Feare C., Bastien M., Dietrich M., Larose C., Lagadec E., Rocamora G., Shah N., Pascalis H., Boulinier T., Le Corre M., Stallknecht DE., Dellagi K. 2015. Influenza A Virus on Oceanic Islands: Host and Viral Diversity in Seabirds in the Western Indian Ocean. *PLoS Pathogens* 11:1–17. DOI: 10.1371/journal.ppat.1004925.

Lee FKN., Gibson BW., Melaugh W., Zaleski A., Apicella MA. 1999. Relationship between UDP-glucose 4-epimerase activity and oligoglucose glycoforms in two strains of Neisseria meningitidis. *Infection and Immunity* 67:1405–1414.

Lehahn Y., Koren I., Schatz D., Frada M., Sheyn U., Boss E., Efrati S., Rudich Y., Trainic M., Sharoni S., Laber C., Ditullio GR., Coolen MJL., Martins AM., Van Mooy BAS., Bidle KD., Vardi A. 2014. Decoupling physical from biological processes to assess the impact of viruses on a mesoscale algal bloom. *Current Biology* 24:2041–2046. DOI: 10.1016/j.cub.2014.07.046.

Leigh BA., Djurhuus A., Breitbart M., Dishaw LJ. 2018. The gut virome of the protochordate model organism, Ciona intestinalis subtype A. *Virus Research* 244:137–146. DOI: 10.1016/j.virusres.2017.11.015.

Lemloh M., Fromont J., Brümmer F., Usher KM. 2009. Diversity and abundance of photosynthetic sponges in temperate Western Australia. *BMC Ecology* 9:4. DOI: 10.1186/1472-6785-9-4.

Lemoine NP., Buell N., Hill A., Hill M. 2007. Assessing the utility of sponge microbial symbiont communities as models to study global climate change: a case study with Halichondria bowerbanki. In: Custodio MR, Lobo-Hajdu G, Hajdu E MG ed. *Porifera Research: Biodiversity, Innovation and Sustainability*. Rio de Janeiro: Museu Nacional, 419–426.

Leruste A., Bouvier T., Bettarel Y. 2012. Enumerating Viruses in Coral Mucus. *Applied and Environmental Microbiology* 78:6377–6379. DOI: 10.1128/AEM.01141-12.

Lesser MP., Fiore C., Slattery M., Zaneveld J. 2016. Climate change stressors destabilize the microbiome of the Caribbean barrel sponge, Xestospongia muta. *Journal of Experimental*

Marine Biology and Ecology 475:11–18. DOI: 10.1016/j.jembe.2015.11.004.

Levin RA., Voolstra CR., Weynberg KD., Van Oppen MJH. 2017. Evidence for a role of viruses in the thermal sensitivity of coral photosymbionts. *ISME Journal* 11:808–812. DOI: 10.1038/ismej.2016.154.

Levitus S., Antonov J., Boyer T. 2005. Warming of the world ocean, 1955-2003. *Geophysical Research Letters* 32:1–4. DOI: 10.1029/2004GL021592.

Lewis SE., Brodie JE., Bainbridge ZT., Rohde KW., Davis AM., Masters BL., Maughan M., Devlin MJ., Mueller JF., Schaffelke B. 2009. Herbicides: a new threat to the Great Barrier Reef. *Environmental Pollution* 157:2470–2484. DOI: 10.1016/j.envpol.2009.03.006.

Leys SP., Eerkes-Medrano DI. 2006. Feeding in a calcareous sponge: particle uptake by pseudopodia. *The Biological Bulletin* 211:157–171. DOI: 10.2307/4134590.

Li L., Kapoor A., Slikas B., Bamidele OS., Wang C., Shaukat S., Masroor MA., Wilson ML., Ndjango J-BN., Peeters M., Gross-Camp ND., Muller MN., Hahn BH., Wolfe ND., Triki H., Bartkus J., Zaidi SZ., Delwart E. 2010. Multiple diverse circoviruses infect farm animals and are commonly found in human and chimpanzee feces. *Journal of Virology* 84:1674–1682. DOI: 10.1128/JVI.02109-09.

Liang W., Zhang W., Shao Y., Zhao X., Li C. 2018. Dual functions of a 4-hydroxyphenylpyruvate dioxygenase for Vibrio splendidus survival and infection. *Microbial Pathogenesis* 120:47–54. DOI: 10.1016/j.micpath.2018.04.055.

Li S., Ou T., Zhang Q. 2013. Two virus-like particles that cause lytic infections in freshwater cyanobacteria. *Virologica Sinica* 28:303–305. DOI: 10.1007/s12250-013-3339-0.

Li C., Shields JD., Small HJ., Reece KS., Hartwig CL., Cooper RA., Ratzlaff RE. 2006. Detection of Panulirus argus Virus 1 (PaV1) in the Caribbean spiny lobster using fluorescence in situ hybridization (FISH). *Diseases of Aquatic Organisms* 72:185–192. DOI: 10.3354/dao072185.

Liehr T. 2016. *Fluorescence In Situ Hybridization (FISH) Application Guide Second Edition*.

Lima-Mendez G., Van Helden J., Toussaint A., Leplae R. 2008. Prophinder: A computational tool for prophage prediction in prokaryotic genomes. *Bioinformatics* 24:863–865. DOI: 10.1093/bioinformatics/btn043.

Lindell D., Jaffe JD., Coleman ML., Futschik ME., Axmann IM., Rector T., Kettler G., Sullivan MB., Steen R., Hess WR., Church GM., Chisholm SW. 2007. Genome-wide expression dynamics of a marine virus and host reveal features of co-evolution. *Nature* 449:83–86. DOI: 10.1038/nature06130.

Lindell D., Sullivan MB., Johnson ZI., Tolonen AC., Rohwer F., Chisholm SW. 2004. Transfer of photosynthesis genes to and from Prochlorococcus viruses. *Proceedings of the National Academy of Sciences of the United States of America* 101:11013–11018. DOI: 10.1073/pnas.0401526101.

Linden H., Sandmann G., Chamovitz D., Hirschberg J., Böger P. 1990. Biochemical characterization of Synechococcus mutants selected against the bleaching herbicide norflurazon. *Pesticide Biochemistry and Physiology* 36:46–51. DOI: 10.1016/0048-

3575(90)90019-X.

La Linn M., Gardner J., Warrilow D., Darnell GA., McMahon CR., Field I., Hyatt AD., Slade RW., Suhrbier A. 2001. Arbovirus of Marine Mammals: a New Alphavirus Isolated from the Elephant Seal Louse, Lepidophthirus macrorhini. *Journal of Virology* 75:4103–4109. DOI: 10.1128/jvi.75.9.4103-4109.2001.

Littman R., Willis BL., Bourne DG. 2011. Metagenomic analysis of the coral holobiont during a natural bleaching event on the Great Barrier Reef. *Environmental Microbiology Reports* 3:651–660. DOI: 10.1111/j.1758-2229.2010.00234.x.

Llave C. 2016. Dynamic cross-talk between host primary metabolism and viruses during infections in plants. *Current Opinion in Virology* 19:50–55. DOI: 10.1016/j.coviro.2016.06.013.

Lohr JE., Chen F., Hill RT. 2005. Genomic Analysis of Bacteriophage JL001: Insights into Its Interaction with a Sponge-Associated Alpha-Proteobacterium. *Applied and Environmental Microbiology* 71:1598–1609. DOI: 10.1128/AEM.71.3.1598-1609.2005.

López-Legentil S., Song B., McMurray SE., Pawlik JR. 2008. Bleaching and stress in coral reef ecosystems: hsp70 expression by the giant barrel sponge Xestospongia muta. *Molecular ecology* 17:1840–9. DOI: 10.1111/j.1365-294X.2008.03667.x.

Lurgi M., Thomas T., Wemheuer B., Webster NS., Montoya JM. 2019. Modularity and predicted functions of the global sponge-microbiome network. *Nature Communications* 10:992. DOI: 10.1038/s41467-019-08925-4.

Luter HM., Bannister RJ., Whalan S., Kutti T., Pineda MC., Webster NS. 2017. Microbiome analysis of a disease affecting the deep-sea sponge Geodia barretti. *FEMS microbiology ecology* 93:1–6. DOI: 10.1093/femsec/fix074.

Luter HM., Webster NS. 2017. Sponge Disease and Climate Change. In: *Climate Change, Ocean Acidification and Sponges*. Cham: Springer International Publishing, 411–428. DOI: 10.1007/978-3-319-59008-0_9.

Luter HM., Whalan S., Webster NS. 2010. Exploring the Role of Microorganisms in the Disease-Like Syndrome Affecting the Sponge Ianthella basta. *Applied and Environmental Microbiology* 76:5736–5744. DOI: 10.1128/AEM.00653-10.

Luter HM., Widder S., Botté ES., Abdul Wahab M., Whalan S., Moitinho-Silva L., Thomas T., Webster NS. 2015. Biogeographic variation in the microbiome of the ecologically important sponge, Carteriospongia foliascens. *PeerJ* 3:e1435. DOI: 10.7717/peerj.1435.

Luther KB., Hülsmeier AJ., Schegg B., Deuber SA., Raoult D., Hennet T. 2011. Mimivirus Collagen Is Modified by Bifunctional Lysyl Hydroxylase and Glycosyltransferase Enzyme. *Journal of Biological Chemistry* 286:43701–43709. DOI: 10.1074/jbc.M111.309096.

Lvov DK., Zdanov VM., Sazonov AA., Braude NA., Vladimirtceva EA., Agafonova L V., Skljanskaja EI., Kaverin N V., Reznik VI., Pysina T V., Oserovic AM., Berzin AA., Mjasnikova IA., Podcernjaeva RY., Klimenko SM., Andrejev VP., Yakhno MA. 1978. Comparison of influenza viruses isolated from man and from whales. *Bulletin of the World Health Organization* 56:923–930.

Lyman JM., Good SA., Gouretski V V., Ishii M., Johnson GC., Palmer MD., Smith DM., Willis JK. 2010. Robust warming of the global upper ocean. *Nature* 465:334–337. DOI: 10.1038/nature09043.

Mahmoudabadi G., Milo R., Phillips R. 2017. Energetic cost of building a virus. *Proceedings of the National Academy of Sciences* 114:E4324–E4333. DOI: 10.1073/pnas.1701670114.

Maldonado M. 2007. Intergenerational transmission of symbiotic bacteria in oviparous and viviparous demosponges, with emphasis on intracytoplasmically-compartmented bacterial types. *Journal of the Marine Biological Association of the UK* 87:1701–1713. DOI: 10.1017/S0025315407058080.

Maldonado M., Sánchez-Tocino L., Navarro C. 2010. Recurrent disease outbreaks in corneous demosponges of the genus Ircinia: Epidemic incidence and defense mechanisms. *Marine Biology* 157:1577–1590. DOI: 10.1007/s00227-010-1431-7.

Malki K., Kula A., Bruder K., Sible E., Hatzopoulos T., Steidel S., Watkins SC., Putonti C. 2015. Bacteriophages isolated from Lake Michigan demonstrate broad host-range across several bacterial phyla. *Virology Journal* 12:164. DOI: 10.1186/s12985-015-0395-0.

Margulis L. 1981. *Symbiosis in Cell Evolution*. New York: W. H. Freeman & Co.

Margulis L., Fester R. 1991. *Symbiosis as a source of evolutionary innovation : speciation and morphogenesis*. MIT Press.

Marie D., Brussaard CPD., Thyrhaug R., Bratbak G., Vaulot D. 1999. Enumeration of marine viruses in culture and natural samples by flow cytometry. *Applied and Environmental Microbiology* 65:45–52.

Marlow J., Davy SK., Shaffer M., Haris A., Bell JJ. 2018. Bleaching and recovery of a phototrophic bioeroding sponge. *Coral Reefs* 37:565–570. DOI: 10.1007/s00338-018-1680-3.

Martelli A., Rousselet E., Dycke C., Bouron A., Moulis JM. 2006. Cadmium toxicity in animal cells by interference with essential metals. *Biochimie* 88:1807–1814. DOI: 10.1016/j.biochi.2006.05.013.

Martí E., Martin C., Cózar A., Duarte CM. 2017. Low abundance of plastic fragments in the surface waters of the red sea. *Frontiers in Marine Science* 4:333. DOI: 10.3389/fmars.2017.00333.

Martinez JL. 2008. Antibiotics and Antibiotic Resistance Genes in Natural Environments. *Science* 321:365–367. DOI: 10.1126/science.1159483.

Marz M., Beerenwinkel N., Drosten C., Fricke M., Frishman D., Hofacker IL., Hoffmann D., Middendorf M., Rattei T., Stadler PF., Töpfer A. 2014. Challenges in RNA virus bioinformatics. *Bioinformatics* 30:1793–1799. DOI: 10.1093/bioinformatics/btu105.

Massaro AJ., Weisz JB., Hill MS., Webster NS. 2012. Behavioral and morphological changes caused by thermal stress in the Great Barrier Reef sponge Rhopaloeides odorabile. *Journal of Experimental Marine Biology and Ecology* 416–417:55–60. DOI: 10.1016/j.jembe.2012.02.008.

Mayzel B., Aizenberg J., Ilan M. 2014. The elemental composition of Demospongiae from the Red Sea, Gulf of Aqaba. *PLoS ONE* 9:e95775. DOI: 10.1371/journal.pone.0095775.

McCabe RM., Estrade P., Middleton JH., Melville WK., Roughan M., Lenain L. 2010. Temperature variability in a shallow, tidally isolated coral reef lagoon. *Journal of Geophysical Research: Oceans* 115:1–17. DOI: 10.1029/2009JC006023.

McDaniel L., Houchin LA., Williamson SJ., Paul JH. 2002. Lysogeny in marine Synechococcus. *Nature* 415:496–496. DOI: 10.1038/415496a.

McMurray SE., Blum JE., Leichter JJ., Pawlik JR. 2011. Bleaching of the giant barrel sponge Xestospongia muta in the Florida Keys. *Limnology and Oceanography* 56:2243–2250. DOI: 10.4319/lo.2011.56.6.2243.

Meselson M., Stahl FW., Vinograd J. 1957. Equilibrium sedimentation of macromolecules in density gradients. *Proceedings of the National Academy of Sciences of the United States of America* 43:581–8. DOI: 10.1073/pnas.43.7.581.

Meyers TR. 1979. A Reo-like Virus Isolated from Juvenile American Oysters (Crassostrea virginica). *Journal of General Virology* 43:203–212. DOI: 10.1099/0022-1317-43-1-203.

Meyers TR. 1981. Endemic diseases of cultured shellfish of Long Island, New York: Adult and juvenile American oysters (Crassostrea virginica) and hard clams (Mercenaria mercenaria). *Aquaculture* 22:305–330. DOI: 10.1016/0044-8486(81)90158-7.

Meyers TR., Burton T., Evans W., Starkey N. 2010. Detection of viruses and virus-like particles in four species of wild and farmed bivalve molluscs in Alaska, USA, from 1987 to 2009. *Diseases of Aquatic Organisms* 88:1–12. DOI: 10.3354/dao02154.

Middelboe M., Chan AM., Bertelsen SK. 2010. Isolation and life cycle characterization of lytic viruses infecting heterotrophic bacteria and cyanobacteria. In: *Manual of Aquatic Viral Ecology*. American Society of Limnology and Oceanography, 118–133. DOI: 10.4319/mave.2010.978-0-9845591-0-7.118.

Middelboe M., Lyck PG. 2002. Regeneration of dissolved organic matter by viral lysis in marine microbial communities. *Aquatic Microbial Ecology* 27:187–194. DOI: 10.3354/ame027187.

Mizuno CM., Rodriguez-Valera F., Kimes NE., Ghai R. 2013. Expanding the Marine Virosphere Using Metagenomics. *PLoS Genetics* 9. DOI: 10.1371/journal.pgen.1003987.

Mochizuki T., Krupovic M., Pehau-Arnaudet G., Sako Y., Forterre P., Prangishvili D. 2012. Archaeal virus with exceptional virion architecture and the largest single-stranded DNA genome. *Proceedings of the National Academy of Sciences* 109:13386–13391. DOI: 10.1073/pnas.1203668109.

Mohamed SA., Elshal MF., Kumosani TA., Mal AO., Ahmed YM., Almulaiky YQ., Asseri AH., Zamzami MA. 2016. Heavy metal accumulation is associated with molecular and pathological perturbations in liver of Variola louti from the Jeddah coast of Red Sea. *International Journal of Environmental Research and Public Health* 13:1–11. DOI: 10.3390/ijerph13030342.

Moitinho-Silva L., Steinert G., Nielsen S., Hardoim CCP., Wu Y-C., McCormack GP., López-

Legentil S., Marchant R., Webster N., Thomas T., Hentschel U. 2017. Predicting the HMA-LMA Status in Marine Sponges by Machine Learning. *Frontiers in Microbiology* 8:752. DOI: 10.3389/fmicb.2017.00752.

Mojica KD a., Brussaard CP. 2014. Factors affecting virus dynamics and microbial host-virus interactions in marine environments. *FEMS microbiology ecology* 89:1–21. DOI: 10.1111/1574-6941.12343.

Monier A., Claverie J-M., Ogata H. 2008. Taxonomic distribution of large DNA viruses in the sea. *Genome Biology* 9:R106. DOI: 10.1186/gb-2008-9-7-r106.

Moran D., Reaka M. 1988. Bioerosion and availability of shelter for benthic reef organisms. *Marine Ecology Progress Series* 44:249–263. DOI: 10.3354/meps044249.

Mori T., Cahn JKB., Wilson MC., Meoded RA., Wiebach V., Martinez AFC., Helfrich EJN., Albersmeier A., Wibberg D., Dätwyler S., Keren R., Lavy A., Rückert C., Ilan M., Kalinowski J., Matsunaga S., Takeyama H., Piel J. 2018. Single-bacterial genomics validates rich and varied specialized metabolism of uncultivated Entotheonella sponge symbionts. *Proceedings of the National Academy of Sciences* 115:1718–1723. DOI: 10.1073/pnas.1715496115.

Mori KI., Nakai T., Muroga K., Arimoto M., Mushiake K., Furusawa I. 1992. Properties of a new virus belonging to nodaviridae found in larval striped jack (Pseudocaranx dentex) with nervous necrosis. *Virology* 187:368–371. DOI: 10.1016/0042-6822(92)90329-N.

Morris PJ. 1993. The developmental role of the extracellular matrix suggests a monophyletic origin of the kingdom Animalia. *Evolution* 47:152–165. DOI: 10.1111/j.1558-5646.1993.tb01206.x.

Morris JJ. 2018. What is the hologenome concept of evolution? *F1000Research* 7:1–9. DOI: 10.12688/f1000research.14385.1.

Mosavi LK., Cammett TJ., Desrosiers DC., Peng Z. 2004. The ankyrin repeat as molecular architecture for protein recognition. *Protein Science* 13:1435–1448. DOI: 10.1110/ps.03554604.

Moss B. 2012. Poxvirus Cell Entry: How Many Proteins Does it Take? *Viruses* 4:688–707. DOI: 10.3390/v4050688.

Mouchka ME., Hewson I., Harvell CD. 2010. Coral-associated bacterial assemblages: Current knowledge and the potential for climate-driven impacts. *Integrative and Comparative Biology* 50:662–674. DOI: 10.1093/icb/icq061.

Müller W., Batel R., Lacorn M., Steinhart H., Simat T., Lauenroth S., Hassanein H., Schröder H. 1998. Accumulation of cadmium and zinc in the marine sponge Suberites domuncula and its potential consequences on single-strand breaks and on expression of heat-shock protein:a natural field study. *Marine Ecology Progress Series* 167:127–135. DOI: 10.3354/meps167127.

Neeno-Eckwall EC., Kinkel LL., Schottel JL. 2011. Competition and antibiosis in the biological control of potato scab. *Canadian Journal of Microbiology* 47:332–340. DOI: 10.1139/w01-010.

Negoro S., Kakudo S., Urabe I., Okada H. 1992. A new nylon oligomer degradation gene (nylC) on plasmid pOAD2 from a Flavobacterium sp. *Journal of Bacteriology* 174:7948–7953. DOI: 10.1128/jb.174.24.7948-7953.1992.

Negoro S., Ohki T., Shibata N., Mizuno N., Wakitani Y., Tsurukame J., Matsumoto K., Kawamoto I., Takeo M., Higuchi Y. 2005. X-ray crystallographic analysis of 6-aminohexanoate-dimer hydrolase: molecular basis for the birth of a nylon oligomer-degrading enzyme. *Journal of Biological Chemistry* 280:39644–39652. DOI: 10.1074/jbc.M505946200.

Negri A., Burns K., Boyle S., Brinkman D., Webster N. 2006. Contamination in sediments, bivalves and sponges of McMurdo Sound, Antarctica. *Environmental Pollution* 143:456–467. DOI: 10.1016/j.envpol.2005.12.005.

Neves G., Omena E. 2003. Influence of sponge morphology on the composition of the polychaete associated fauna from Rocas Atoll, northeast Brazil. *Coral Reefs* 22:123–129. DOI: 10.1007/s00338-003-0295-4.

Ng TFF., Miller MA., Kondov NO., Dodd EM., Batac F., Manzer M., Ives S., Saliki JT., Deng X., Delwart E. 2015. Oral papillomatosis caused by Enhydra lutris papillomavirus 1 (ELPV-1) in southern sea otters (Enhydra lutris nereis) in California, USA. *Journal of Wildlife Diseases* 51:446–453. DOI: 10.7589/2014-06-152.

Nguyen T V., Alfaro AC., Merien F. 2018. Omics approaches to investigate host–pathogen interactions in mass mortality outbreaks of Crassostrea gigas. *Reviews in Aquaculture*:1–17. DOI: 10.1111/raq.12294.

Nguyen KDT., Morley SA., Lai CH., Clark MS., Tan KS., Bates AE., Peck LS. 2011. Upper temperature limits of tropical marine ectotherms: Global warming implications. *PLoS ONE* 6:6–13. DOI: 10.1371/journal.pone.0029340.

Nies A., Nies DH., Silver S. 1990. Nucleotide sequence and expression of a plasmid-encoded chromate resistance determinant from Alcaligenes eutrophus. *Journal of Biological Chemistry* 265:5648–5653.

Noble RT., Fuhrman J a. 1998. Use of SYBR Green I for rapid epifluorescence counts of marine viruses and bacteria. *Aquatic Microbial Ecology* 14:113–118. DOI: 10.3354/ame014113.

Nobles DR., Romanovicz DK., Brown RM. 2001. Cellulose in cyanobacteria. Origin of vascular plant cellulose synthase? *Plant Phisiology* 127:529–542. DOI: 10.1104/pp.010557.

Noguchi H., Taniguchi T., Itoh T. 2008. MetaGeneAnnotator: detecting species-specific patterns of ribosomal binding site for precise gene prediction in anonymous prokaryotic and phage genomes. *DNA Research* 15:387–396. DOI: 10.1093/dnares/dsn027.

O'Mahony J., Simes R., Redhill D., Heaton K., Atkinson C., Hayward E., Nguyen M. 2017. *At what price? The economic, social and icon value of the Great Barrier Reef*. Sydney: Delloite Access Economics.

Oliveira H., Melo LDR., Santos SB., Nóbrega FL., Ferreira EC., Cerca N., Azeredo J., Kluskens LD. 2013. Molecular aspects and comparative genomics of bacteriophage endolysins. *Journal of virology* 87:4558–70. DOI: 10.1128/JVI.03277-12.

Ollivier PRL., Bahrou AS., Marcus S., Cox T., Church TM., Hanson TE. 2008. Volatilization and precipitation of tellurium by aerobic, tellurite-resistant marine microbes. *Applied and Environmental Microbiology* 74:7163–7173. DOI: 10.1128/AEM.00733-08.

Olson JB., Mccarthy PJ. 2005. Associated bacterial communities of two deep-water sponges. *Aquatic Microbial Ecology* 39:47–55.

Pan K., Lee OO., Qian P-Y., Wang W-X. 2011. Sponges and sediments as monitoring tools of metal contamination in the eastern coast of the Red Sea, Saudi Arabia. *Marine Pollution Bulletin* 62:1140–1146. DOI: 10.1016/j.marpolbul.2011.02.043.

Parsons RJ., Breitbart M., Lomas MW., Carlson C a. 2012. Ocean time-series reveals recurring seasonal patterns of virioplankton dynamics in the northwestern Sargasso Sea. *The ISME Journal* 6:273–284. DOI: 10.1038/ismej.2011.101.

Pascelli C., Laffy PW., Kupresanin M., Ravasi T., Webster NS. 2018. Morphological characterization of virus-like particles in coral reef sponges. *PeerJ* 6:e5625. DOI: 10.7717/peerj.5625.

Patel B., Balani MC., Patel S. 1985. Sponge “sentinel” of heavy metals. *Science of The Total Environment* 41:143–152. DOI: 10.1016/0048-9697(85)90184-6.

Patten NL., Harrison PL., Mitchell JG. 2008. Prevalence of virus-like particles within a staghorn scleractinian coral (Acropora muricata) from the Great Barrier Reef. *Coral Reefs* 27:569–580. DOI: 10.1007/s00338-008-0356-9.

Patten NL., Seymour JR., Mitchell JG. 2006. Flow cytometric analysis of virus-like particles and heterotrophic bacteria within coral-associated reef water. *Journal of the Marine Biological Association of the UK* 86:563. DOI: 10.1017/S0025315406013476.

Patterson MR., Chernykh VI., Fialkov VA., Savarese M. 1997. Trophic effects of sponge feeding within Lake Baikal’s littoral zone. 1. Insitu pumping rates. *Limnology and Oceanography* 42:171–178. DOI: 10.4319/lo.1997.42.1.0171.

Paul JH. 2008. Prophages in marine bacteria: dangerous molecular time bombs or the key to survival in the seas? *The ISME journal* 2:579–589. DOI: 10.1038/ismej.2008.35.

Pearson WR. 2013. An introduction to sequence and series (“homology”) searching. *Curr Protoc bioinformatics* 1:1286–1292. DOI: 10.1002/0471250953.bi0301s42.An.

Pen HC., Shu TK., San HL., Hong SY., Yun YT., Ching LH., Hon CC. 2005. Herpes-like virus infection causing mortality of cultured abalone Haliotis diversicolor supertexta in Taiwan. *Diseases of Aquatic Organisms* 65:23–27. DOI: 10.3354/dao065023.

Perdicaris S., Vlachogianni T., Valavanidis A. 2013. Bioactive Natural Substances from Marine Sponges: New Developments and Prospects for Future Pharmaceuticals. *Natural Products Chemistry & Research* 1:114.

Perez Sepulveda B., Redgwell T., Rihtman B., Pitt F., Scanlan DJ., Millard A. 2016. Marine phage genomics: The tip of the iceberg. *FEMS Microbiology Letters* 363:1–8. DOI: 10.1093/femsle/fnw158.

Peters KJ., Amsler CD., McClintock JB., Baker BJ. 2010. Potential chemical defenses of

Antarctic sponges against sympatric microorganisms. *Polar Biology* 33:649–658. DOI: 10.1007/s00300-009-0741-z.

Petton B., Bruto M., James A., Labreuche Y., Alunno-Bruscia M., Le Roux F. 2015. Crassostrea gigas mortality in France: the usual suspect, a herpes virus, may not be the killer in this polymicrobial opportunistic disease. *Frontiers in Microbiology* 6:1–10. DOI: 10.3389/fmicb.2015.00686.

Pile AJ., Young CM. 2006. The natural diet of a hexactinellid sponge: Benthic–pelagic coupling in a deep-sea microbial food web. *Deep Sea Research Part I: Oceanographic Research Papers* 53:1148–1156. DOI: 10.1016/j.dsr.2006.03.008.

Pineda MC., Strehlow B., Duckworth A., Doyle J., Jones R., Webster NS. 2016. Effects of light attenuation on the sponge holobiont-implications for dredging management. *Scientific Reports* 6:1–13. DOI: 10.1038/srep39038.

Pineda MC., Strehlow B., Sternel M., Duckworth A., Haan J Den., Jones R., Webster NS. 2017. Effects of sediment smothering on the sponge holobiont with implications for dredging management. *Scientific Reports* 7:1–15. DOI: 10.1038/s41598-017-05243-x.

Pirtle EC., Beran GW. 1991. Virus survival in the environment. *Revue scientifique et technique (International Office of Epizootics)* 10:733–748. DOI: 10.20506/rst.10.3.570.

Pita L., Rix L., Slaby BM., Franke A., Hentschel U. 2018a. The sponge holobiont in a changing ocean: from microbes to ecosystems. *Microbiome* 6:46. DOI: 10.1186/s40168-018-0428-1.

Pita L., Rix L., Slaby BM., Franke A., Hentschel U. 2018b. The sponge holobiont in a changing ocean: from microbes to ecosystems. *Microbiome* 6:46. DOI: 10.1186/s40168-018-0428-1.

Ploss M., Kuhn A. 2010. Kinetics of filamentous phage assembly. *Physical Biology* 7:45002. DOI: 10.1088/1478-3975/7/4/045002.

Pollard PC. 2012. Enumerating Viruses by Using Fluorescence and the Nature of the Nonviral Background Fraction. *Applied and Environmental Microbiology* 78:6615–6618. DOI: 10.1128/AEM.01268-12.

Pollock F., Wood-Charlson E., van Oppen M., Bourne D., Willis B., Weynberg K. 2014. Abundance and morphology of virus-like particles associated with the coral Acropora hyacinthus differ between healthy and white syndrome-infected states. *Marine Ecology Progress Series* 510:39–43. DOI: 10.3354/meps10927.

Prangishvili D., Forterre P., Garrett R a. 2006. Viruses of the Archaea: a unifying view. *Nature reviews. Microbiology* 4:837–848. DOI: 10.1038/nrmicro1527.

Proctor LM. 1997. Advances in the study of marine viruses. *Microscopy Research and Technique* 37:136–161. DOI: 10.1002/(SICI)1097-0029(19970415)37:2<136::AID-JEMT3>3.0.CO;2-M.

Proctor LM., Fuhrman J a. 1990. Viral mortality of marine bacteria and cyanobacteria. *Nature* 343:60–62. DOI: 10.1038/343060a0.

Pruitt KD., Tatusova T., Maglott DR. 2007. NCBI reference sequences (RefSeq): a curated non-redundant sequence database of genomes, transcripts and proteins. *Nucleic Acids Research* 35:D61–D65. DOI: 10.1093/nar/gkl842.

Przeslawski R., Ahyong S., Byrne M., Wörheide G., Hutchings P. 2008. Beyond corals and fish: the effects of climate change on noncoral benthic invertebrates of tropical reefs. *Global Change Biology* 14:2773–2795. DOI: 10.1111/j.1365-2486.2008.01693.x.

Rädecker N., Pogoreutz C., Voolstra CR., Wiedenmann J., Wild C. 2015. Nitrogen cycling in corals: The key to understanding holobiont functioning? *Trends in Microbiology* 23:490–497. DOI: 10.1016/j.tim.2015.03.008.

Rasmussen LPD. 1986. Virus-associated granulocytomas in the marine mussel, Mytilus edulis, from three sites in Denmark. *Journal of Invertebrate Pathology* 48:117–123. DOI: 10.1016/0022-2011(86)90150-3.

Rauta PR., Samanta M., Dash HR., Nayak B., Das S. 2014. Toll-like receptors (TLRs) in aquatic animals: Signaling pathways, expressions and immune responses. *Immunology Letters* 158:14–24. DOI: 10.1016/j.imlet.2013.11.013.

Reaka-Kudla ML. 2005. Biodiversity of Caribbean Coral Reefs. In: Miloslavich P, Klein E eds. *Caribbean Marine Biodiversity*. Lancaster, PA: Des Tech Publishers, 259–276.

Reiswig HM. 1981. Partial carbon and energy budgets of the bacteriosponge Verongia fistularis (Porifera: Demospongiae) in Barbados. *Marine Ecology* 2:273–293. DOI: 10.1111/j.1439-0485.1981.tb00271.x.

Renault T., Novoa B. 2004. Viruses infecting bivalve molluscs. *Aquatic Living Resources* 17:397–409. DOI: 10.1051/alr:2004049.

Reynolds D., Thomas T. 2016. Evolution and function of eukaryotic-like proteins from sponge symbionts. *Molecular Ecology* 25:5242–5253. DOI: 10.1111/mec.13812.

Ribes M., Coma R., Gili JM. 1999. Natural diet and grazing rate of the temperate sponge Dysidea avara (Demospongiae, Dendroceratida) throughout an annual cycle. *Marine Ecology Progress Series* 176:179–190. DOI: 10.3354/meps176179.

Richelle-Maurer E., Degoudenne Y., Van De Vyver G., Dejonghe L. 1994. Some aspects of heavy metal tolerance in freshwater sponges. *Sponges in time and space: Biology, chemistry, paleontology*:351–354.

Rinkevich B. 2005. Marine invertebrate cell cultures: New millennium trends. *Marine Biotechnology* 7:429–439. DOI: 10.1007/s10126-004-0108-y.

Rivera R., Nollens HH., Venn-Watson S., Gulland FMD., Wellehan JFX. 2010. Characterization of phylogenetically diverse astroviruses of marine mammals. *Journal of General Virology* 91:166–173. DOI: 10.1099/vir.0.015222-0.

Roberts PC., Compans RW. 1998. Host cell dependence of viral morphology. *Proceedings of the National Academy of Sciences of the United States of America* 95:5746–5751. DOI: 10.1073/pnas.95.10.5746.

Roberts DE., Davis AR. 1996. Patterns in sponge (Porifera) assemblages on temperate coastal

reefs off Sydney, Australia. *Marine and Freshwater Research* 47:897–906. DOI: 10.1071/MF9960897.

Robertson SJ., Girardin SE. 2013. Nod-like receptors in intestinal host defense: Controlling pathogens, the microbiota, or both? *Current Opinion in Gastroenterology* 29:15–22. DOI: 10.1097/MOG.0b013e32835a68ea.

Rohwer F., Edwards R. 2002. The phage proteomic tree: A genome-based taxonomy for phage. *Journal of Bacteriology* 184:4529–4535. DOI: 10.1128/JB.184.16.4529-4535.2002.

Rohwer F., Thurber RV. 2009. Viruses manipulate the marine environment. *Nature* 459:207–212. DOI: 10.1038/nature08060.

Rosario K., Breitbart M. 2011. Exploring the viral world through metagenomics. *Current Opinion in Virology* 1:289–297. DOI: 10.1016/j.coviro.2011.06.004.

Rosenberg E., Koren O., Reshef L., Efrony R., Zilber-Rosenberg I. 2007. The role of microorganisms in coral health, disease and evolution. *Nature reviews. Microbiology* 5:355–362. DOI: 10.1038/nrmicro1635.

Rösti J., Barton CJ., Albrecht S., Dupree P., Pauly M., Findlay K., Roberts K., Seifert GJ. 2007. UDP-Glucose 4-Epimerase Isoforms UGE2 and UGE4 Cooperate in Providing UDP-Galactose for Cell Wall Biosynthesis and Growth of Arabidopsis thaliana . *The Plant Cell* 19:1565–1579. DOI: 10.1105/tpc.106.049619.

Roux S. 2019. A Viral Ecogenomics Framework To Uncover the Secrets of Nature's "Microbe Whisperers." *mSystems* 4:1–5. DOI: 10.1128/msystems.00111-19.

Roux S., Brum JR., Dutilh BE., Sunagawa S., Duhaime MB., Loy A., Poulos BT., Solonenko N., Lara E., Poulain J., Pesant S., Kandels-Lewis S., Dimier C., Picheral M., Searson S., Cruaud C., Alberti A., Duarte CM., Gasol JM., Vaqué D., Bork P., Acinas SG., Wincker P., Sullivan MB. 2016. Ecogenomics and potential biogeochemical impacts of globally abundant ocean viruses. *Nature* 537:689–693. DOI: 10.1038/nature19366.

Roux S., Enault F., Hurwitz BL., Sullivan MB. 2015a. VirSorter: mining viral signal from microbial genomic data. *PeerJ* 3:e985. DOI: 10.7717/peerj.985.

Roux S., Hallam SJ., Woyke T., Sullivan MB. 2015b. Viral dark matter and virus–host interactions resolved from publicly available microbial genomes. *eLife* 4:1–20. DOI: 10.7554/eLife.08490.

Roux S., Krupovic M., Daly RA., Borges AL., Nayfach S., Schulz F., Cheng J-F., Ivanova NN., Bondy-Denomy J., Wrighton KC., Woyke T., Visel A., Kyrpides N., Eloe-Fadrosh EA. 2019. Cryptic inoviruses are pervasive in bacteria and archaea across Earth's biomes. *bioRxiv*:548222. DOI: 10.1101/548222.

Roux S., Krupovic M., Poulet A., Debroas D., Enault F. 2012. Evolution and diversity of the microviridae viral family through a collection of 81 new complete genomes assembled from virome reads. *PLoS ONE* 7:1–12. DOI: 10.1371/journal.pone.0040418.

Rubio-Portillo E., Izquierdo-Muñoz A., Gago JF., Rosselló-Mora R., Antón J., Ramos-Esplá AA. 2016. Effects of the 2015 heat wave on benthic invertebrates in the Tabarca Marine

Protected Area (southeast Spain). *Marine Environmental Research* 122:135–142. DOI: 10.1016/j.marenvres.2016.10.004.

Russel M. 1991. Filamentous phage assembly. *Molecular microbiology* 5:1607–13.

Sánchez-Paz A. 2010. White spot syndrome virus: An overview on an emergent concern. *Veterinary Research* 41. DOI: 10.1051/vetres/2010015.

Sauvage C., Pépin JF., Lapègue S., Boudry P., Renault T. 2009. Ostreid herpes virus 1 infection in families of the Pacific oyster, Crassostrea gigas, during a summer mortality outbreak: Differences in viral DNA detection and quantification using real-time PCR. *Virus Research* 142:181–187. DOI: 10.1016/j.virusres.2009.02.013.

Sawtell NM., Thompson RL. 1992. Rapid in vivo reactivation of herpes simplex virus in latently infected murine ganglionic neurons after transient hyperthermia. *Journal of Virology* 66:2150–2156. DOI: 10.1128/JVI.66.4.2150-2156.1992.

Schmitt S., Tsai P., Bell J., Fromont J., Ilan M., Lindquist N., Perez T., Rodrigo A., Schupp PJ., Vacelet J., Webster N., Hentschel U., Taylor MW. 2012. Assessing the complex sponge microbiota: core, variable and species-specific bacterial communities in marine sponges. *The ISME Journal* 6:564–576. DOI: 10.1038/ismej.2011.116.

Schönberg CHL. 2015. Self-cleaning surfaces in sponges. *Marine Biodiversity* 45:623–624. DOI: 10.1007/s12526-014-0302-8.

Schroeder DC., Oke J., Malin G., Wilson WH. 2002. Coccolithovirus (Phycodnaviridae): Characterisation of a new large dsDNA algal virus that infects Emiliania huxleyi. *Archives of Virology* 147:1685–1698. DOI: 10.1007/s00705-002-0841-3.

Scola B La. 2003. A giant virus in Amoebae. *Science* 299:2033–2033. DOI: 10.1126/science.1081867.

Shah N., Hulsmeier AJ., Hochhold N., Neidhart M., Gay S., Hennet T. 2014. Exposure to mimivirus collagen promotes arthritis. *Journal of Virology* 88:838–845. DOI: 10.1128/JVI.03141-13.

Shapiro HM. 2003. *Practical Flow Cytometry*. New York: Wiley. DOI: 10.1002/0471722731.

Sharon I., Battchikova N., Aro E-M., Giglione C., Meinnel T., Glaser F., Pinter RY., Breitbart M., Rohwer F., Béjà O. 2011. Comparative metagenomics of microbial traits within oceanic viral communities. *The ISME journal* 5:1178–1190. DOI: 10.1038/ismej.2011.2.

Shelford EJ., Middelboe M., Møller EF., Suttle CA. 2012. Virus-driven nitrogen cycling enhances phytoplankton growth. *Aquatic Microbial Ecology* 66:41–46. DOI: 10.3354/ame01553.

Shi M., Lin XD., Chen X., Tian JH., Chen LJ., Li K., Wang W., Eden JS., Shen JJ., Liu L., Holmes EC., Zhang YZ. 2018. The evolutionary history of vertebrate RNA viruses. *Nature* 556:197–202. DOI: 10.1038/s41586-018-0012-7.

Shi M., Neville P., Nicholson J., Eden J-S., Imrie A., Holmes EC. 2017. High-Resolution Metatranscriptomics Reveals the Ecological Dynamics of Mosquito-Associated RNA Viruses in Western Australia. *Journal of Virology* 91:1–17. DOI: 10.1128/jvi.00680-17.

Shieh WY., Lin YM. 1994. Association of heterotrophic nitrogen-fixing bacteria with a marine sponge of Halichondria sp. *Bulletin of Marine Science* 54:557–564.

Silver S. 1996. Bacterial resistances to toxic metal ions - a review. *Gene* 179:9–19. DOI: 10.1016/S0378-1119(96)00323-X.

Simpson TL. 2011. *The Cell Biology of Sponges*. New York, NY: Springer, New York.

Singh D., Khattar J., Kaur G., Singh Y. 2016. Toxicological impact of herbicides on cyanobacteria. *Annual Research & Review in Biology* 9:1–39. DOI: 10.9734/ARRB/2016/22614.

Skirving WJ., Heron SF., Marsh BL., Liu G., De La Cour JL., Geiger EF., Eakin CM. 2019. The relentless march of mass coral bleaching: a global perspective of changing heat stress. *Coral Reefs* 38:547–557. DOI: 10.1007/s00338-019-01799-4.

Slaby BM., Franke A., Rix L., Pita L., Bayer K., Jahn MT., Hentschel U. 2019. Marine Sponge Holobionts in Health and Disease. In: *Symbiotic Microbiomes of Coral Reefs Sponges and Corals*. Dordrecht: Springer Netherlands, 81–104. DOI: 10.1007/978-94-024-1612-1_7.

Tahlan K., Ahn SK., Sing A., Bodnaruk TD., Willems AR., Davidson AR., Nodwell JR. 2007. Initiation of actinorhodin export in Streptomyces coelicolor. *Molecular Microbiology* 63:951–961. DOI: 10.1111/j.1365-2958.2006.05559.x.

Tsuchiya K., Fukuyama S., Kanzaki N., Kanagawa K., Negoro S., Okada H. 1989. High homology between 6-aminohexanoate-cyclic-dimer hydrolases of Flavobacterium and Pseudomonas strains. *Journal of Bacteriology* 171:3187–3191. DOI: 10.1128/jb.171.6.3187-3191.1989.

Van Soest RWM., Boury-Esnault N., Vacelet J., Dohrmann M., Erpenbeck D., De Voogd NJ., Santodomingo N., Vanhoorne B., Kelly M., Hooper JNA. 2012. Global diversity of sponges (Porifera). *PloS one* 7:e35105. DOI: 10.1371/journal.pone.0035105.

Soffer N., Brandt ME., Correa AMS., Smith TB., Thurber RV. 2014. Potential role of viruses in white plague coral disease. *The ISME journal* 8:271–83. DOI: 10.1038/ismej.2013.137.

Sonnewald M., El-Sherbiny MM. 2017. Editorial: Red Sea biodiversity. *Marine Biodiversity* 47:991–993. DOI: 10.1007/s12526-017-0648-9.

Steindler L., Beer S., Ilan M. 2002. Photosymbiosis in intertidal and subtidal tropical sponges. *Symbiosis* 33:263–273.

Steinert M., Flügel M., Schuppler M., Helbig JH., Supriyono A., Proksch P., Lück PC. 2001. The Lly protein is essential for p-hydroxyphenylpyruvate dioxygenase activity in Legionella pneumophila. *FEMS Microbiology Letters* 203:41–47. DOI: 10.1016/S0378-1097(01)00331-7.

Steward GF., Culley AI., Mueller J a., Wood-Charlson EM., Belcaid M., Poisson G. 2013. Are we missing half of the viruses in the ocean? *The ISME journal* 7:672–9. DOI: 10.1038/ismej.2012.121.

Steward GF., Culley AI., Wood-Charlson EM. 2013. *Marine Viruses*. Elsevier Ltd. DOI: 10.1016/B978-0-12-384719-5.00401-9.

Strand R., Whalan S., Webster NS., Kutti T., Fang JKH., Luter HM., Bannister RJ. 2017. The response of a boreal deep-sea sponge holobiont to acute thermal stress. *Scientific Reports* 7:1–12. DOI: 10.1038/s41598-017-01091-x.

Strehlow BW., Jorgensen D., Webster NS., Pineda MC., Duckworth A. 2016. Using a thermistor flowmeter with attached video camera for monitoring sponge excurrent speed and oscular behaviour. *PeerJ* 2016:1–21. DOI: 10.7717/peerj.2761.

Stuart-Smith RD., Brown CJ., Ceccarelli DM., Edgar GJ. 2018. Ecosystem restructuring along the Great Barrier Reef following mass coral bleaching. *Nature* 560:92–96. DOI: 10.1038/s41586-018-0359-9.

Sullivan MB., Coleman ML., Weigele P., Rohwer F., Chisholm SW. 2005. Three Prochlorococcus cyanophage genomes: Signature features and ecological interpretations. *PLoS Biology* 3:0790–0806. DOI: 10.1371/journal.pbio.0030144.

Summers AO. 1985. Bacterial resistance to toxic elements. *Trends in Biotechnology* 3:122–125. DOI: 10.1016/0167-7799(85)90127-1.

Sun G., Xiao J., Wang H., Gong C., Pan Y., Yan S., Wang Y. 2014. Efficient purification and concentration of viruses from a large body of high turbidity seawater. *MethodsX* 1:197–206. DOI: 10.1016/j.mex.2014.09.001.

Suttle CA. 1994. The significance of viruses to mortality in aquatic microbial communities. *Microbial Ecology* 28:237–243. DOI: 10.1007/BF00166813.

Suttle CA. 2005. Viruses in the sea. *Nature* 437:356–361. DOI: 10.1038/nature04160.

Suttle CA. 2007. Marine viruses — major players in the global ecosystem. *Nature Reviews Microbiology* 5:801–812. DOI: 10.1038/nrmicro1750.

Suttle CA., Chan AM. 1993. Marine cyanophages infecting oceanic and coastal strains of Synechococcus: abundance, morphology, cross-infectivity and growth characteristics. *Marine Ecology Progress Series* 92:99–109. DOI: 10.3354/meps092099.

Sweet M., Bythell J. 2017. The role of viruses in coral health and disease. *Journal of Invertebrate Pathology* 147:136–144. DOI: 10.1016/j.jip.2016.12.005.

Swierts T., Cleary DFR., de Voogd NJ. 2018. Prokaryotic communities of Indo-Pacific giant barrel sponges are more strongly influenced by geography than host phylogeny. *FEMS Microbiology Ecology* 94:1–12. DOI: 10.1093/femsec/fiy194.

Tahlan K., Ahn SK., Sing A., Bodnaruk TD., Willems AR., Davidson AR., Nodwell JR. 2007. Initiation of actinorhodin export in Streptomyces coelicolor. *Molecular Microbiology* 63:951–961. DOI: 10.1111/j.1365-2958.2006.05559.x.

Tanaka M., Arakaki A., Staniland SS., Matsunaga T. 2010. Simultaneously discrete biomineralization of magnetite and tellurium nanocrystals in magnetotactic bacteria. *Applied and Environmental Microbiology* 76:5526–5532. DOI: 10.1128/AEM.00589-10.

Taylor MW., Hill RT., Piel J., Thacker RW., Hentschel U. 2007a. Soaking it up: the complex lives of marine sponges and their microbial associates. *The ISME journal* 1:187–90. DOI: 10.1038/ismej.2007.32.

Taylor MW., Radax R., Steger D., Wagner M. 2007b. Sponge-associated microorganisms: evolution, ecology, and biotechnological potential. *Microbiology and molecular biology reviews : MMBR* 71:295–347. DOI: 10.1128/MMBR.00040-06.

Tchounwou PB., Yedjou CG., Patlolla AK., Sutton DJ. 2012. Heavy metal toxicity and the environment. *Springer* 101:133–164. DOI: 10.1007/978-3-7643-8340-4_6.

Thacker RW. 2005. Impacts of Shading on Sponge-Cyanobacteria Symbioses: A Comparison between Host-Specific and Generalist Associations. *Integrative and Comparative Biology* 45:369–376. DOI: 10.1093/icb/45.2.369.

Thacker R., Starnes S. 2003. Host specificity of the symbiotic cyanobacterium Oscillatoria spongeliae in marine sponges , Dysidea spp . *Marine Biology* 142:643–648. DOI: 10.1007/s00227-002-0971-x.

Thomas T., Moitinho-Silva L., Lurgi M., Björk JR., Easson C., Astudillo-García C., Olson JB., Erwin PM., López-Legentil S., Luter H., Chaves-Fonnegra A., Costa R., Schupp PJ., Steindler L., Erpenbeck D., Gilbert J., Knight R., Ackermann G., Victor Lopez J., Taylor MW., Thacker RW., Montoya JM., Hentschel U., Webster NS. 2016. Diversity, structure and convergent evolution of the global sponge microbiome. *Nature Communications* 7:11870. DOI: 10.1038/ncomms11870.

Thomas T., Rusch D., DeMaere MZ., Yung PY., Lewis M., Halpern A., Heidelberg KB., Egan S., Steinberg PD., Kjelleberg S. 2010. Functional genomic signatures of sponge bacteria reveal unique and shared features of symbiosis. *ISME Journal* 4:1557–1567. DOI: 10.1038/ismej.2010.74.

Thomassen S., Riisgård H. 1995. Growth and energetics of the sponge Halichondria panicea. *Marine Ecology Progress Series* 128:239–246. DOI: 10.3354/meps128239.

Thompson JR. 2002. Heteroduplexes in mixed-template amplifications: formation, consequence and elimination by "reconditioning PCR." *Nucleic Acids Research* 30:2083–2088. DOI: 10.1093/nar/30.9.2083.

Thompson LR., Zeng Q., Kelly L., Huang KH., Singer AU., Stubbe J., Chisholm SW. 2011. Phage auxiliary metabolic genes and the redirection of cyanobacterial host carbon metabolism. *Proceedings of the National Academy of Sciences* 108:E757–E764. DOI: 10.1073/pnas.1102164108.

Thurber RLV., Barott KL., Hall D., Liu H., Rodriguez-Mueller B., Desnues C., Edwards R a., Haynes M., Angly FE., Wegley L., Rohwer FL. 2008. Metagenomic analysis indicates that stressors induce production of herpes-like viruses in the coral Porites compressa. *Proceedings of the National Academy of Sciences of the United States of America* 105:18413–18418. DOI: 10.1073/pnas.0808985105.

Thurber RLV., Correa AMS. 2011. Viruses of reef-building scleractinian corals. *Journal of Experimental Marine Biology and Ecology* 408:102–113. DOI: 10.1016/j.jembe.2011.07.030.

Thurber R V., Haynes M., Breitbart M., Wegley L., Rohwer F. 2009a. Laboratory procedures to generate viral metagenomes. *Nature Protocols* 4:470–483. DOI: 10.1038/nprot.2009.10.

Thurber RV., Payet JP., Thurber AR., Correa AMS. 2017. Virus–host interactions and their roles

in coral reef health and disease. *Nature Reviews Microbiology* 15:205–216. DOI: 10.1038/nrmicro.2016.176.

Thurber RV., Willner-Hall D., Rodriguez-Mueller B., Desnues C., Edwards R a., Angly F., Dinsdale E., Kelly L., Rohwer F. 2009b. Metagenomic analysis of stressed coral holobionts. *Environmental Microbiology* 11:2148–2163. DOI: 10.1111/j.1462-2920.2009.01935.x.

Ting JPY., Lovering RC., Alnemri ES., Bertin J., Boss JM., Davis BK., Flavell RA., Girardin SE., Godzik A., Harton JA., Hoffman HM., Hugot J-P., Inohara N., MacKenzie A., Maltais LJ., Nunez G., Ogura Y., Otten LA., Philpott D., Reed JC., Reith W., Schreiber S., Steimle V., Ward PA. 2008. The NLR gene family: a standard nomenclature. *Immunity* 28:285–287. DOI: 10.1016/j.immuni.2008.02.005.

Traavik T., Mehl R., Kjeldsberg E. 1977. "Runde" virus, a coronavirus-like agent associated with seabirds and ticks. *Archives of Virology* 55:25–38. DOI: 10.1007/BF01314476.

Trevors JT., Stratton GW., Gadd GM. 1986. Cadmium transport, resistance, and toxicity in bacteria, algae, and fungi. *Canadian Journal of Microbiology* 32:447–464. DOI: 10.1139/m86-085.

Tsao Y-F., Taylor VL., Kala S., Bondy-Denomy J., Khan AN., Bona D., Cattoir V., Lory S., Davidson AR., Maxwell KL. 2018. Phage Morons Play an Important Role in Pseudomonas aeruginosa Phenotypes . *Journal of Bacteriology* 200:1–15. DOI: 10.1128/jb.00189-18.

Tsuchiya K., Fukuyama S., Kanzaki N., Kanagawa K., Negoro S., Okada H. 1989. High homology between 6-aminohexanoate-cyclic-dimer hydrolases of Flavobacterium and Pseudomonas strains. *Journal of Bacteriology* 171:3187–3191. DOI: 10.1128/jb.171.6.3187-3191.1989.

Tuulaikhuu BA., Romaní AM., Guasch H. 2015. Arsenic toxicity effects on microbial communities and nutrient cycling in indoor experimental channels mimicking a fluvial system. *Aquatic Toxicology* 166:72–82. DOI: 10.1016/j.aquatox.2015.07.005.

UniProt Consortium. 2015. UniProt: a hub for protein information. *Nucleic Acids Research* 43:D204–D212. DOI: 10.1093/nar/gku989.

Vacelet J., Boury-Esnault N. 1995. Carnivorous sponges. *Nature* 373:333–335. DOI: 10.1038/373333a0.

Vacelet J., Gallissian M-F. 1978. Virus-like particles in cells of the sponge Verongia cavernicola (demospongiae, dictyoceratida) and accompanying tissues changes. *Journal of Invertebrate Pathology* 31:246–254. DOI: 10.1016/0022-2011(78)90014-9.

Varsani A., Kraberger S., Jennings S., Porzig EL., Julian L., Massaro M., Pollard A., Ballard G., Ainley DG. 2014. A novel papillomavirus in Adélie penguin (Pygoscelis adeliae) faeces sampled at the Cape Crozier colony, Antarctica. *Journal of General Virology* 95:1352–1365. DOI: 10.1099/vir.0.064436-0.

Vicente VP. 1990. Response of sponges with autotrophic endosymbionts during the coral-bleaching episode in Puerto Rico. *Coral Reefs* 8:199–202. DOI: 10.1007/BF00265011.

Villarreal LP. 1999. DNA Virus Contribution to Host Evolution. In: *Origin and Evolution of*

Viruses. Elsevier, 391–420. DOI: 10.1016/B978-012220360-2/50016-7.

Walters KD., Pawlik JR. 2005. Is there a trade-off between wound-healing and chemical defenses among Caribbean reef sponges? *Integrative and comparative biology* 45:352–358. DOI: 10.1093/icb/45.2.352.

Wang L., Jeon B., Sahin O., Zhang Q. 2009. Identification of an arsenic resistance and arsenic-sensing system in Campylobacter jejuni. *Applied and Environmental Microbiology* 75:5064–5073. DOI: 10.1128/AEM.00149-09.

Wang Y., Naumann U., Wright ST., Warton DI. 2012. mvabund - an R package for model-based analysis of multivariate abundance data. *Methods in Ecology and Evolution* 3:471–474. DOI: 10.1111/j.2041-210X.2012.00190.x.

Warwick-Dugdale J., Buchholz HH., Allen MJ., Temperton B. 2019. Host-hijacking and planktonic piracy: How phages command the microbial high seas. *Virology Journal* 16:1–13. DOI: 10.1186/s12985-019-1120-1.

Watson JR., Krömer JO., Degnan BM., Degnan SM. 2017. Seasonal changes in environmental nutrient availability and biomass composition in a coral reef sponge. *Marine Biology* 164:1–13. DOI: 10.1007/s00227-017-3167-0.

Webster NS., Botté ES., Soo RM., Whalan S. 2011. The larval sponge holobiont exhibits high thermal tolerance. *Environmental Microbiology Reports* 3:756–762. DOI: 10.1111/j.1758-2229.2011.00296.x.

Webster NS., Cobb RE., Negri AP. 2008. Temperature thresholds for bacterial symbiosis with a sponge. *The ISME journal* 2:830–42. DOI: 10.1038/ismej.2008.42.

Webster NS., Hill RT. 2001. The culturable microbial community of the Great Barrier Reef sponge Rhopaloeides odorabile is dominated by an α-Proteobacterium. *Marine Biology* 138:843–851. DOI: 10.1007/s002270000503.

Webster NS., Luter HM., Soo RM., Botté ES., Simister RL., Abdo D., Whalan S. 2013a. Same, same but different: symbiotic bacterial associations in GBR sponges. *Frontiers in Microbiology* 3:1–11. DOI: 10.3389/fmicb.2012.00444.

Webster NS., Negri AP., Webb RI., Hill RT. 2002. A spongin-boring α-proteobacterium is the etiological agent of disease in the Great Barrier Reef sponge Rhopaloeides odorabile. *Marine Ecology Progress Series* 232:305–309. DOI: 10.3354/meps232305.

Webster N., Pantile R., Botté E., Abdo D., Andreakis N., Whalan S. 2013b. A complex life cycle in a warming planet: Gene expression in thermally stressed sponges. *Molecular Ecology* 22:1854–1868. DOI: 10.1111/mec.12213.

Webster NS., Reusch TBH. 2017. Microbial contributions to the persistence of coral reefs. *ISME Journal* 11:2167–2174. DOI: 10.1038/ismej.2017.66.

Webster NS., Taylor MW. 2012. Marine sponges and their microbial symbionts: love and other relationships. *Environmental Microbiology* 14:335–346. DOI: 10.1111/j.1462-2920.2011.02460.x.

Webster NS., Thomas T. 2016. The sponge hologenome. *mBio* 7:e00135-16. DOI:

10.1128/mBio.00135-16.

Wegley L., Edwards R., Rodriguez-Brito B., Liu H., Rohwer F. 2007. Metagenomic analysis of the microbial community associated with the coral Porites astreoides. *Environmental Microbiology* 9:2707–2719. DOI: 10.1111/j.1462-2920.2007.01383.x.

Weinbauer MG. 2004. Ecology of prokaryotic viruses. *FEMS Microbiology Reviews* 28:127–181. DOI: 10.1016/j.femsre.2003.08.001.

Weinbauer MG., Suttle C a. 1997. Comparison of epifluorescence and transmission electron microscopy for counting viruses in natural marine waters. *Aquatic Microbial Ecology* 13:225–232. DOI: 10.3354/ame013225.

Weiner JA., DeLorenzo ME., Fulton MH. 2004. Relationship between uptake capacity and differential toxicity of the herbicide atrazine in selected microalgal species. *Aquatic Toxicology* 68:121–128. DOI: 10.1016/j.aquatox.2004.03.004.

Weiss AA., Hewlett EL., Myers GA., Falkow S. 1983. Tn5-induced mutations affecting virulence factors of Bordetella pertussis. *Infection and immunity* 42:33–41.

Weisz JB., Lindquist N., Martens CS. 2008. Do associated microbial abundances impact marine demosponge pumping rates and tissue densities? *Oecologia* 155:367–376. DOI: 10.1007/s00442-007-0910-0.

Weitz JS., Poisot T., Meyer JR., Flores CO., Valverde S., Sullivan MB., Hochberg ME. 2013. Phage-bacteria infection networks. *Trends in Microbiology* 21:82–91. DOI: 10.1016/j.tim.2012.11.003.

Weitz J., Wilhelm S. 2012. Ocean viruses and their effects on microbial communities and biogeochemical cycles. *F1000 Biology Reports* 8:2–9. DOI: 10.3410/B4-17.

Weynberg KD. 2018. *Viruses in Marine Ecosystems: From Open Waters to Coral Reefs*. Elsevier Inc. DOI: 10.1016/bs.aivir.2018.02.001.

Weynberg KD., Laffy PW., Wood-Charlson EM., Turaev D., Rattei T., Webster NS., van Oppen MJH. 2017a. Coral-associated viral communities show high levels of diversity and host auxiliary functions. *PeerJ* 5:e4054. DOI: 10.7717/peerj.4054.

Weynberg KD., Neave M., Clode PL., Voolstra CR., Brownlee C., Laffy P., Webster NS., Levin RA., Wood-Charlson EM., van Oppen MJH. 2017b. Prevalent and persistent viral infection in cultures of the coral algal endosymbiont Symbiodinium. *Coral Reefs* 36:773–784. DOI: 10.1007/s00338-017-1568-7.

Weynberg KD., Wood-Charlson EM., Suttle CA., van Oppen MJH. 2014. Generating viral metagenomes from the coral holobiont. *Frontiers in Microbiology* 5:1–11. DOI: 10.3389/fmicb.2014.00206.

Whalan S. 2018. Not just corals - sponges are bleaching too! *Frontiers in Ecology and the Environment* 16:471–471. DOI: 10.1002/fee.1957.

Whalan S., Webster NS. 2014. Sponge larval settlement cues: The role of microbial biofilms in a warming ocean. *Scientific Reports* 4:28–32. DOI: 10.1038/srep04072.

Wiebe WJ., Johannes RE., Webb KL. 1975. Nitrogen Fixation in a Coral Reef Community.

Science 188:257–259. DOI: 10.1126/science.188.4185.257.

Wiens M., Korzhev M., Perovic-Ottstadt S., Luthringer B., Brandt D., Klein S., Muller WEG. 2006. Toll-like receptors are part of the innate immune defense system of sponges (Demospongiae: Porifera). *Molecular Biology and Evolution* 24:792–804. DOI: 10.1093/molbev/msl208.

Wilkinson CR. 1978. Microbial associations in sponges. II. Numerical analysis of sponge and water bacterial populations. *Marine Biology* 49:169–176. DOI: 10.1007/BF00387116.

Wilkinson CR. 1980. Nutrient translocation from green algal symbionts to the freshwater sponge Ephydatia fluviatilis. *Hydrobiologia* 75:241–250. DOI: 10.1007/BF00006488.

Wilkinson CR., Evans E. 1989. Sponge distribution across Davies Reef, Great Barrier Reef, relative to location, depth, and water movement. *Coral Reefs* 8:1–7. DOI: 10.1007/BF00304685.

Wilkinson CR., Fay P. 1979. Nitrogen fixation in coral reef sponges with symbiotic cyanobacteria. *Nature* 279:527–529. DOI: 10.1038/279527a0.

Williams T. 2008. Natural invertebrate hosts of iridoviruses (Iridoviridae). *Neotropical Entomology* 37:615–632. DOI: 10.1590/S1519-566X2008000600001.

Williamson SJ., McLaughlin MR., Paul JH. 2001. Interaction of the ΦHSIC Virus with Its Host: Lysogeny or Pseudolysogeny? *Applied and Environmental Microbiology* 67:1682–1688. DOI: 10.1128/AEM.67.4.1682-1688.2001.

Willner D., Furlan M., Haynes M., Schmieder R., Angly FE., Silva J., Tammadoni S., Nosrat B., Conrad D., Rohwer F. 2009. Metagenomic analysis of respiratory tract DNA viral communities in cystic fibrosis and non-cystic fibrosis individuals. *PLoS ONE* 4:e7370. DOI: 10.1371/journal.pone.0007370.

Willner D., Hugenholtz P. 2013. From deep sequencing to viral tagging: Recent advances in viral metagenomics. *BioEssays* 35:436–442. DOI: 10.1002/bies.201200174.

Wilson WH., Chapman DM. 2001. Observation of virus-like particles in thin sections of the plumose anemone, Metridium senile. *Journal of the Marine Biological Association of the UK* 81:879–880. DOI: 10.1017/S0025315401004726.

Wilson WH., Dale AL., Davy JE., Davy SK. 2005. An enemy within? Observations of virus-like particles in reef corals. *Coral Reefs* 24:145–148. DOI: 10.1007/s00338-004-0448-0.

Wilson WH., Van Etten JL., Allen MJ. 2009. The Phycodnaviridae: The Story of How Tiny Giants Rule the World. In: 1–42. DOI: 10.1007/978-3-540-68618-7_1.

Wilson AC., Mohr I. 2012. A cultured affair: HSV latency and reactivation in neurons. *Trends in Microbiology* 20:604–611. DOI: 10.1016/j.tim.2012.08.005.

Wilson MC., Mori T., Rückert C., Uria AR., Helf MJ., Takada K., Gernert C., Steffens U a E., Heycke N., Schmitt S., Rinke C., Helfrich EJN., Brachmann AO., Gurgui C., Wakimoto T., Kracht M., Crüsemann M., Hentschel U., Abe I., Matsunaga S., Kalinowski J., Takeyama H., Piel J. 2014. An environmental bacterial taxon with a large and distinct metabolic repertoire. *Nature* 506:58–62. DOI: 10.1038/nature12959.

Winget DM., Wommack KE. 2008. Randomly amplified polymorphic DNA PCR as a tool for assessment of marine viral richness. *Applied and Environmental Microbiology* 74:2612–2618. DOI: 10.1128/AEM.02829-07.

Wolf YI., Kazlauskas D., Iranzo J., Lucía-Sanz A., Kuhn JH., Krupovic M., Dolja V V., Koonin E V. 2018. Origins and evolution of the global RNA virome. *mBio* 9:1–31. DOI: 10.1128/mBio.02329-18.

Wolf K., Snieszko SF., Dunbar CE., Pyle E. 1960. Virus Nature of Infectious Pancreatic Necrosis in Trout. *Experimental Biology and Medicine* 104:105–108. DOI: 10.3181/00379727-104-25743.

Wommack KE., Bhavsar J., Ravel J. 2008. Metagenomics: Read length matters. *Applied and Environmental Microbiology* 74:1453–1463. DOI: 10.1128/AEM.02181-07.

Wommack KE., Colwell RR. 2000. Virioplankton: viruses in aquatic ecosystems. *Microbiology and molecular biology reviews : MMBR* 64:69–114. DOI: 10.1128/MMBR.64.1.69-114.2000.

Wommack KE., Hill RT., Kessel M., Russek-Cohen E., Colwell RR. 1992. Distribution of viruses in the Chesapeake Bay. *Applied and environmental microbiology* 58:2965–70.

Wommack KE., Sime-Ngando T., Winget DM., Jamindar S., Helton RR. 2010. Filtration-based methods for the collection of viral concentrates from large water samples. In: *Manual of Aquatic Viral Ecology*. American Society of Limnology and Oceanography, 110–117. DOI: 10.4319/mave.2010.978-0-9845591-0-7.110.

Wood-Charlson EM., Weynberg KD., Suttle CA., Roux S., van Oppen MJH. 2015. Metagenomic characterization of viral communities in corals: mining biological signal from methodological noise. *Environmental Microbiology* 17:3440–3449. DOI: 10.1111/1462-2920.12803.

Worden AZ. 2006. Picoeukaryote diversity in coastal waters of the Pacific Ocean. *Aquatic Microbial Ecology* 43:165–175. DOI: 10.3354/ame043165.

Worden AZ., Dupont C., Allen AE. 2011. Genomes of uncultured eukaryotes: sorting FACS from fiction. *Genome Biology* 12:117. DOI: 10.1186/gb-2011-12-6-117.

Wörheide G., Dohrmann M., Erpenbeck D., Larroux C., Maldonado M., Voigt O., Borchiellini C., Lavrov DV. 2012. Deep Phylogeny and Evolution of Sponges (Phylum Porifera). *Advances in Marine Biology* 61:1–78. DOI: 10.1016/B978-0-12-387787-1.00007-6.

Worm B., Lotze HK., Jubinville I., Wilcox C., Jambeck J. 2017. Plastic as a persistent marine pollutant. *Annual Review of Environment and Resources* 42:1–26. DOI: 10.1146/annurev-environ-102016-060700.

Xagorari A., Chlichlia K. 2008. Toll-Like Receptors and Viruses: Induction of Innate Antiviral Immune Responses. *The Open Microbiology Journal* 2:49–59. DOI: 10.2174/1874285800802010049.

Yahel G., Sharp JH., Marie D., Häse C., Genin A. 2003. In situ feeding and element removal in the symbiont-bearing sponge Theonella swinhoei: Bulk DOC is the major source for carbon. *Limnology and Oceanography* 48:141–149. DOI: 10.4319/lo.2003.48.1.0141.

Yau S., Lauro FM., DeMaere MZ., Brown M V., Thomas T., Raftery MJ., Andrews-Pfannkoch C., Lewis M., Hoffman JM., Gibson JA., Cavicchioli R. 2011. Virophage control of antarctic algal host-virus dynamics. *Proceedings of the National Academy of Sciences* 108:6163–6168. DOI: 10.1073/pnas.1018221108.

Yuan P., Zhang H., Cai C., Zhu S., Zhou Y., Yang X., He R., Li C., Guo S., Li S., Huang T., Perez-Cordon G., Feng H., Wei W. 2015. Chondroitin sulfate proteoglycan 4 functions as the cellular receptor for Clostridium difficile toxin B. *Cell Research* 25:157–168. DOI: 10.1038/cr.2014.169.

Yuen B., Bayes JM., Degnan SM. 2014. The characterization of sponge nlrs provides insight into the origin and evolution of this innate immune gene family in animals. *Molecular Biology and Evolution* 31:106–120. DOI: 10.1093/molbev/mst174.

Yung PY., Burke C., Lewis M., Kjelleberg S., Thomas T. 2011. Novel antibacterial proteins from the microbial communities associated with the sponge Cymbastela concentrica and the green alga Ulva australis. *Applied and Environmental Microbiology* 77:1512–1515. DOI: 10.1128/AEM.02038-10.

Yvan B., Bouvier T., Nguyen HK., Thu PT. 2014. The versatile nature of coral-associated viruses. *Environmental microbiology*:1–7. DOI: 10.1111/1462-2920.12579.

Zaki AE. 2003. Plant retroviruses: structure, evolution and future applications. *African Journal of Biotechnology* 2:136–139. DOI: 10.5897/AJB2003.000-1027.

Zeltins A. 2013. Construction and characterization of virus-like particles: a review. *Molecular Biotechnology* 53:92–107. DOI: 10.1007/s12033-012-9598-4.

Zhang C., Yang Y., Zhou X., Yang Z., Liu X., Cao Z., Song H., He Y., Huang P. 2011. The NS1 protein of influenza a virus interacts with heat shock protein Hsp90 in human alveolar basal epithelial cells: Implication for virus-induced apoptosis. *Virology Journal* 8:181. DOI: 10.1186/1743-422X-8-181.

Zhao C., Li Z., Li T., Zhang Y., Bryant DA., Zhao J. 2015. High-yield production of extracellular type-I cellulose by the cyanobacterium Synechococcus sp. PCC 7002. *Cell Discovery* 1:15004. DOI: 10.1038/celldisc.2015.4.

Zozaya-Valdes E., Egan S., Thomas T. 2015. A comprehensive analysis of the microbial communities of healthy and diseased marine macroalgae and the detection of known and potential bacterial pathogens. *Frontiers in Microbiology* 6:1–9. DOI: 10.3389/fmicb.2015.00146.

APPENDIX 1

This dataset presents the morphological characterization of prokaryotes associated with coral reef sponges from the Red Sea and the GBR as described in Chapter 2.

Sponge-associated prokaryotes

TEM analysis revealed high variability in the microbial morphotypes, abundance and distribution associated with the different sponge species. Gram-positive and Gram-negative bacteria were observed and morphologically characterized as coccus; diplococci; rod; Star-cross section-oriented rod and spore. Gram-negative was the dominant bacterial group, which was represented mostly by rod shaped cells in the RS sponges and coccus shaped cells in the GBR sponges (Fig. A1.1).

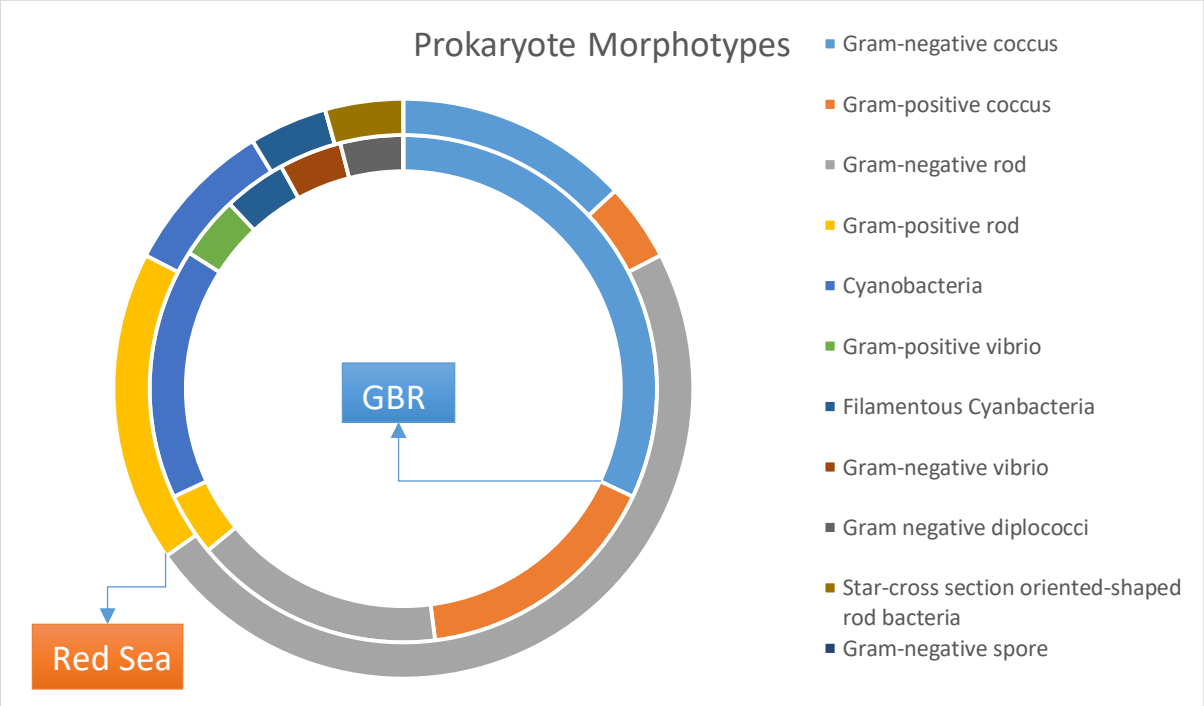

Figure A1.1 Proportion of prokaryote morphotypes in the Great Barrier Reef (internal circle) and Read Sea (external circle) sponges described in Table 2.1.

TEM sections also revealed that most of the sponge-associated bacteria were spread into the intercellular spaces, distributed across the mesohyl. In total, fifty prokaryote morphotypes where identified and enumerated as M-I to M-L (Fig. 2-6; Table 2). Microbial cells were found

isolated or aggregated with other bacteria from the same (Figure 2A, D) and different morphotypes (Figure 2B, C). Aggregations of similar morphotypes were observed in *Carteriospongia foliascens* and *Echinochalina isaaci*, while aggregations of multiple morphotypes were observed in *Xestospongia testudinaria* and *Hyrtios erectus.* Aggregations were often observed in the sponge mesohyl matrix with high amounts of particulate organic matter, usually located between sponge collagen fibrils.

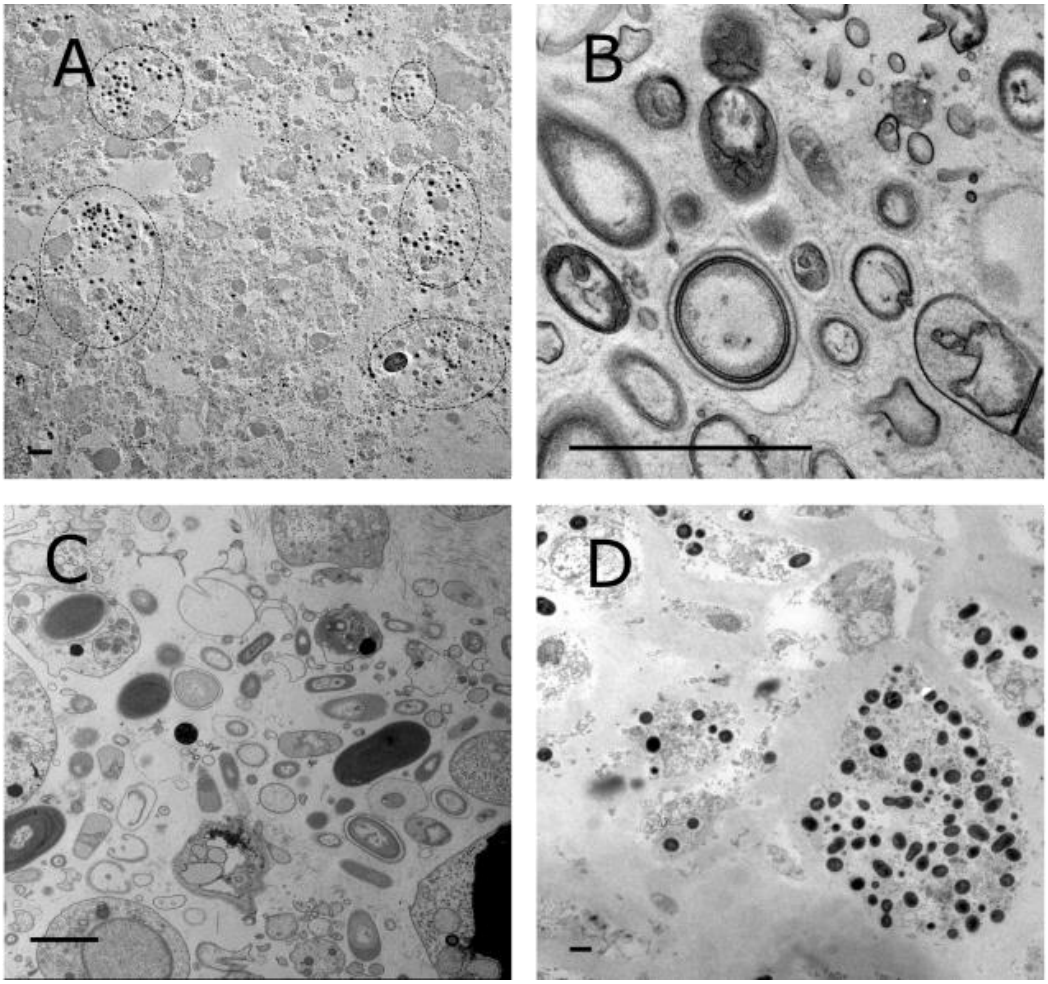

Figure A1.2 Examples of Microbial aggregations in ultrathin sections of (A) *Echinochalina isaaci*, (B) *Hyrtios erectus*, (C) *Xestospongia testudinaria* and (D) *Carteriospongia foliascens*. Scale bar= 2µm.

The number of observed prokaryotic morphotypes associated with each sponge species varied from one, in *Cymbastela marshae, Lamellodysidea herbacea* (GBR) and *Amphimedon* sp., *Mycale* sp. (RS) to six, in *Stylissa carteri* (GBR) and *Xestospongia testudinaria (*RS). Cyanobacteria were frequently observed in the sponges *C. foliascens* (GBR and RS)*, X. testudinaria* (RS) and *C. marshae*. Cyanobacteria were the dominant bacterial morphotype

associated with *C. foliascens* from both the GBR and RS (Figs. A1.3 A-E; A1.6 A-B), however morphotypes from both locations were clearly distinct. The RS morphotype was notably smaller and presented a thicker and lobate cell wall. Filamentous cyanobacteria were found associated with *L. herbacea* (GBR) (Fig. A1.4 I) and *Amphimedon ochracea* (GBR) (Figs. A1.8 D-G). The number of cells per filament observed in the sponge sections were six in *A. ochracea,* and three in *L. herbacea*, although this number may be biased by the tissue sectioning methodology. In *A. ochracea* each cell presented radially organized thylakoid membranes, dense bodies resembling polyphosphate granules and stellar bodies, which have been noted before in this sponge species (Berthold et al 1982). In the *L. herbacea* cyanobacteria, the thylakoid membranes were also concentrically arranged within the cells, peripherally distributed, with an electron translucent cell core. A filamentous Cyanobacterium identified as *Oscillatoria spongeliae* has been previously isolated from *L. herbacea*, cited as *Dysidea herbacea* (Berthold, Borowitzka & Mackay, 1982; Hinde, Pironet & Borowitzka, 1994; Thacker & Starnes, 2003). However, the cyanobacteria in *L. herbacea* from the present study are distinctly thinner (5.5-6.5 µm width; 3.0-4.3 µm long) than *O. spongeliae* associated with the same sponge species from a previous study (6·0-8·0 µm width; 3·0-4·0 µm long) (Berthold, Borowitzka & Mackay, 1982). In addition, it did not presented Stellar bodies, abundant structure in *O. spongeliae.* However, the thylakoid structure, homogeneously spaced and oriented in right angles to the outer cell wall, seemed to be similar amongst both Cyanobacteria.

A very rare microbial morphotype, the star cross section shaped rod, was found associated with the sponge *Niphates rowi* (Figure A1.7 I). These cells were about 1.5 µm long and their star-shaped cross section measured 500 nm in diameter with eight radial protrusions. A similar morphotype has been observed associated with the larva of the sponge *Haliclona caerulea* (Maldonado, 2007). However, the *N. rowi* associated bacterium apparently have eight radial protrusions, do not present a thick outer peptideoglycan layer and were found exclusively extracellularly. In comparison, the *H caerulea* bacteria have strictly nine protrusions, a thick peptideoglycan layer and are observed within sponge cells.

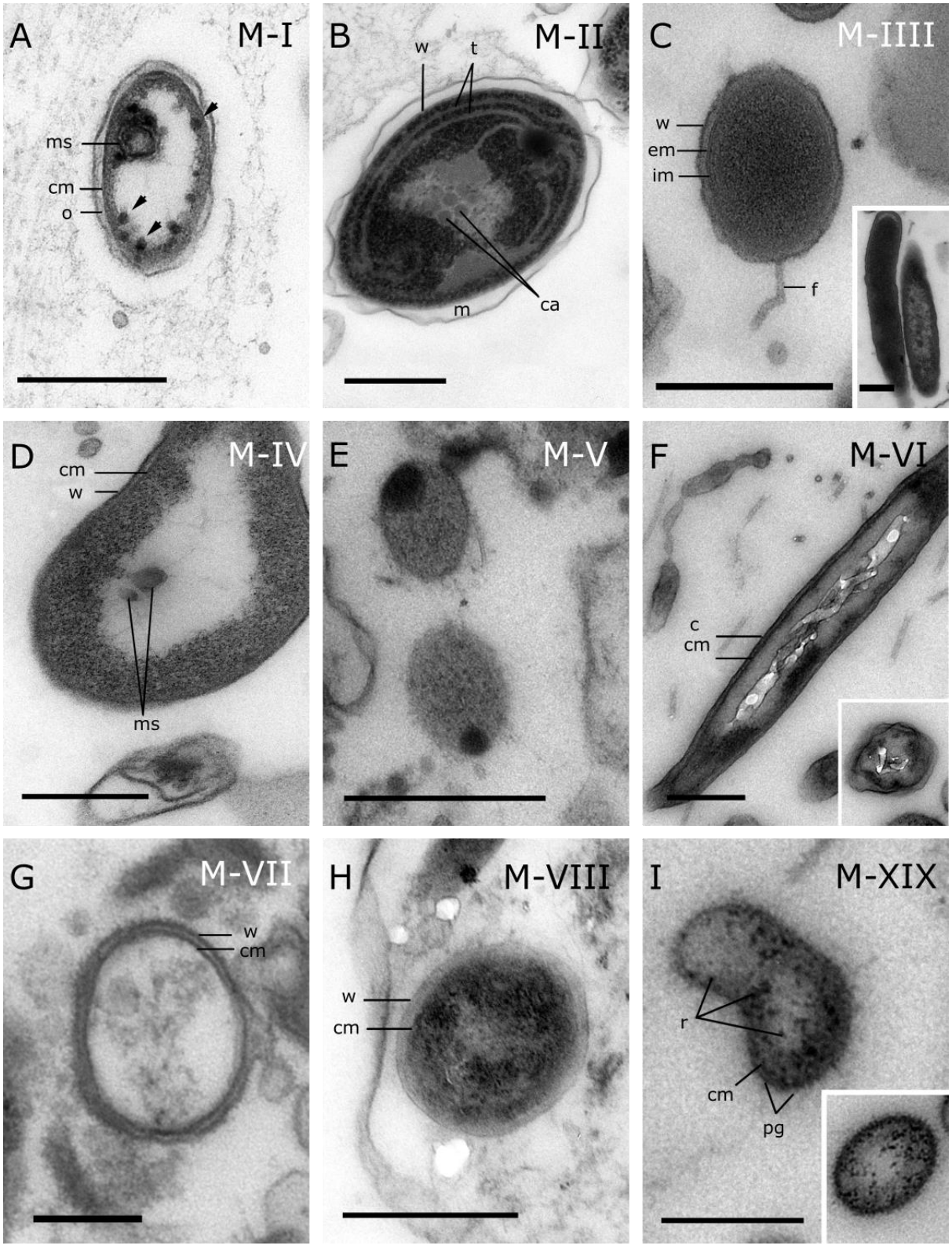

Figure A1.3 Prokaryote morphotypes associated with the GBR sponges: (A-E) *Carteriospongia foliascens*, (F-I) *Stylissa carteri* in (A-B; C in detail D-I) longitudinal section and (C; F & I in detail) transversal section. Scale bar= 500 nm. cm: cytoplasmic membrane; c: capsule, w: cell wall; ms: mesossome structure; t: thylakoid membrane; ca: carboxisome; em: external membrane; im: internal membrane; f: flagellum; r: ribosome; pg: peptidoglycan.

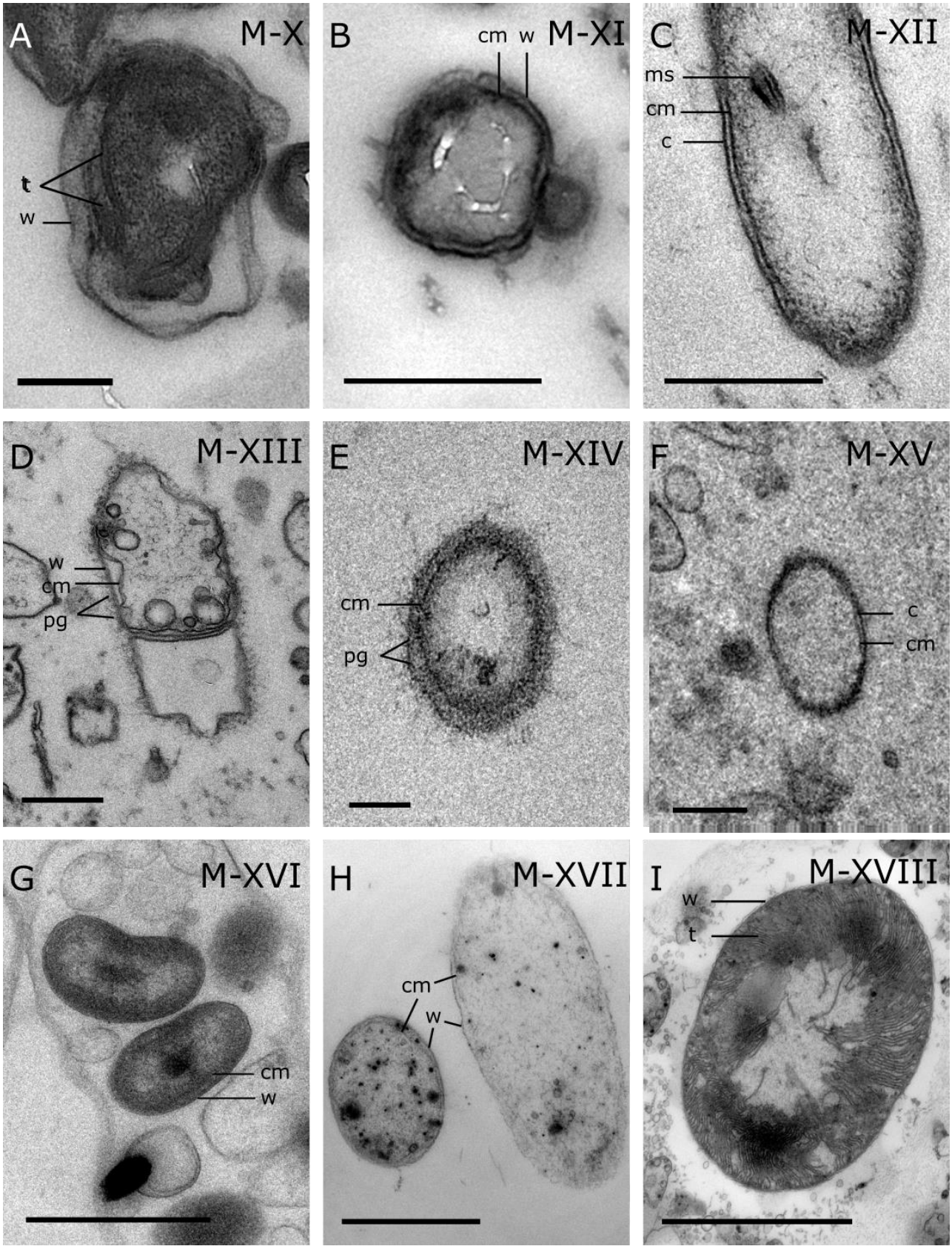

Figure A1.4 Prokaryote morphotypes associated with the GBR sponges: (A-B) *Stylissa carteri*, (C-F) *Xestospongia testudinaria*, (G-H) *Pipestela candelabra*, (I) *Lamellodysidea herbacea* in (A-H) longitudinal section and transversal (I) section. Scale bar= 500 nm (A-G) and 5 µm (I). cm: cytoplasmic membrane; c: capsule, w: cell wall; ms: mesossome structure; t: thylakoid membrane; pg: peptidoglycan.

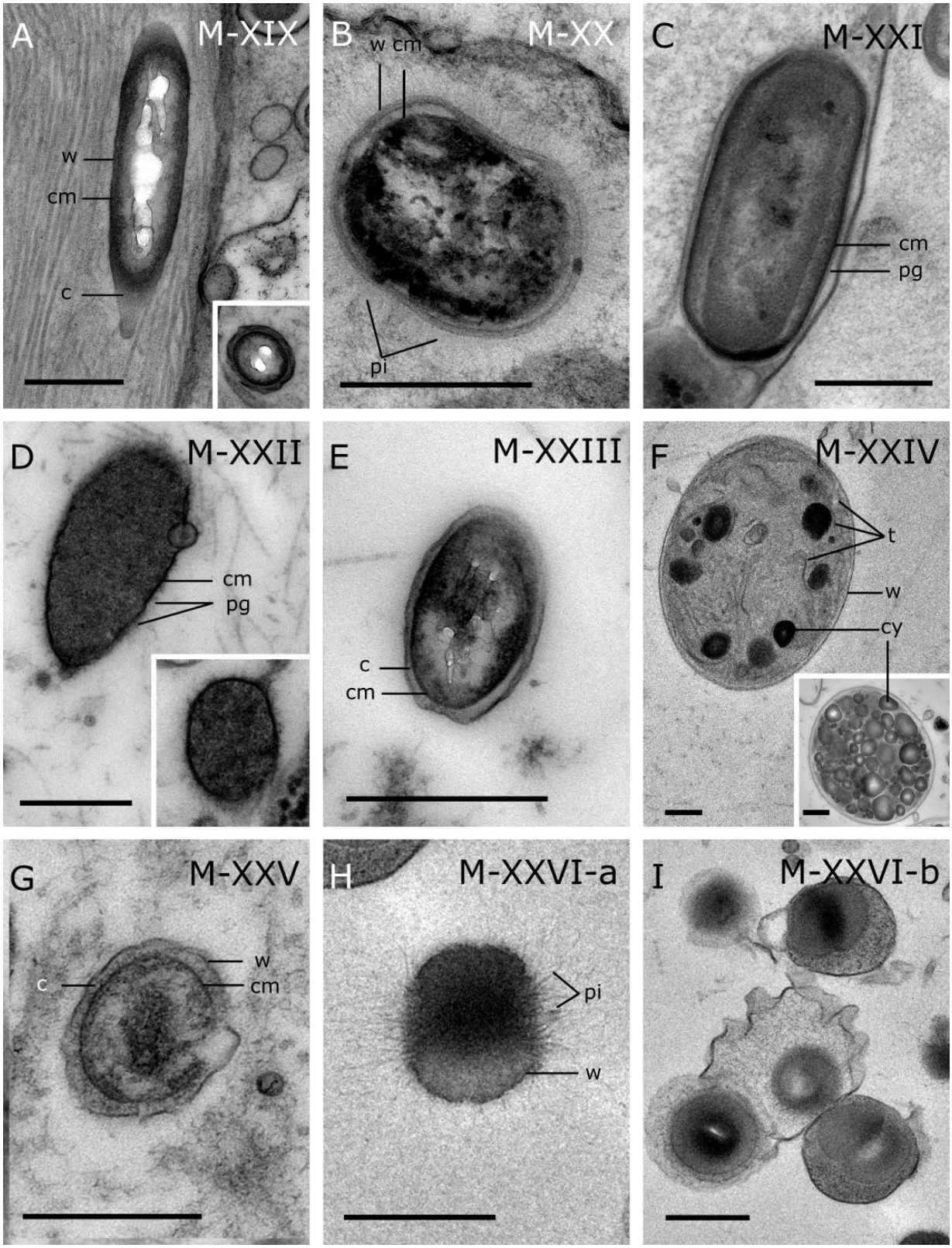

Figure A1.5 Prokaryote morphotypes associated with the GBR sponges: (A-C) *Cinachyrella schulzei*, (D-E) *Ianthella basta*, (F) *Cymbastela marshae*, (G-I) *Echinochalina isaaci* in (A-I) longitudinal section and (A, D, F in detail) transversal section. Scale bar= 500 nm. cm: cytoplasmic membrane; c: capsule, w: cell wall; ms: mesossome structure; t: thylakoid membrane; om: outer membrane; pi: pili; pg: peptidoglycan; cy: cyanosome.

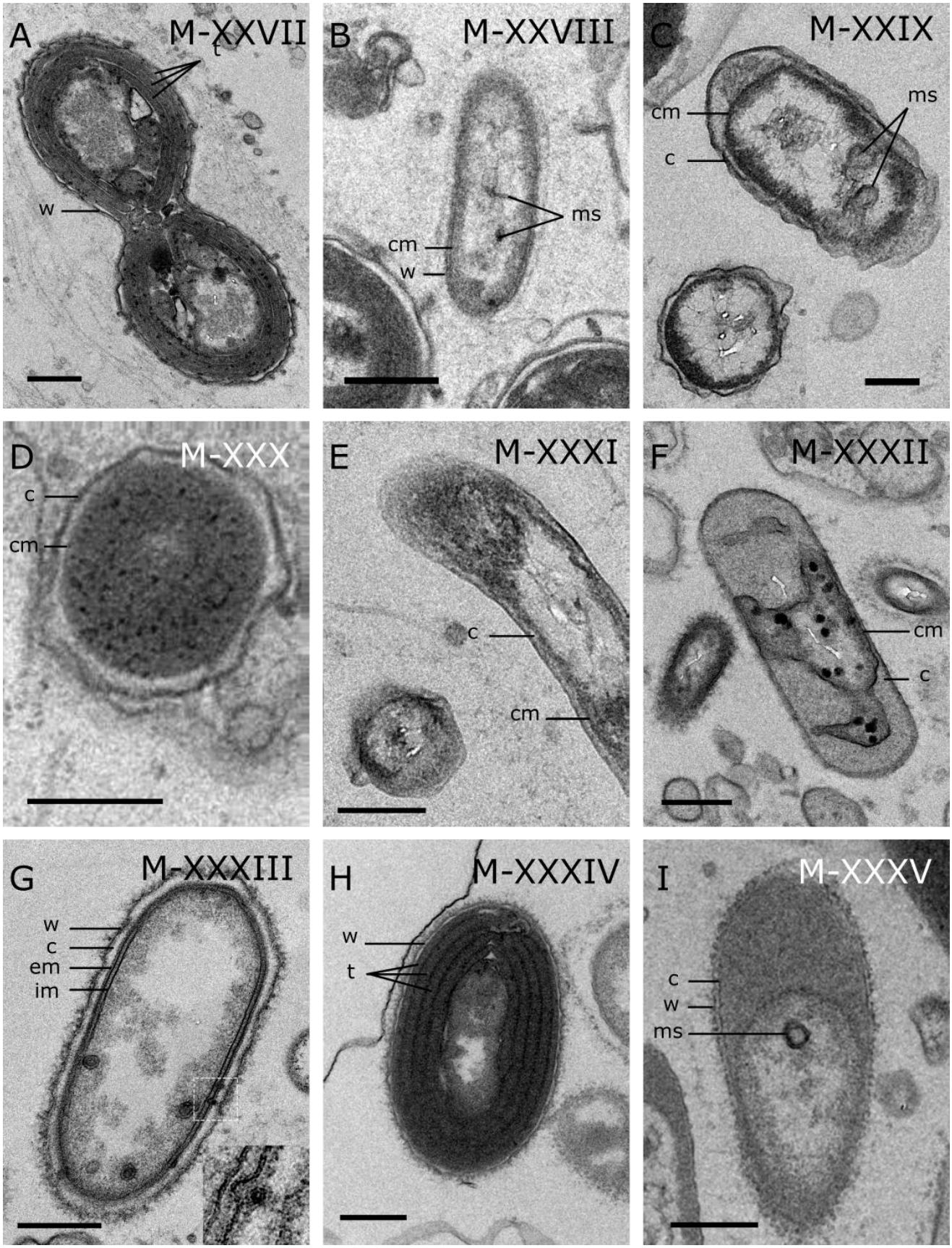

Figure A1.6 Prokaryote morphotypes associated with the RS sponges: (A-B) *Carteriospongia foliascens*, (C-E) *Stylissa carteri,* (F-I) *Xestospongia testudinaria,* in (A-I) longitudinal section and (C in detail) transversal section. Scale bar= 500 nm. cm: cytoplasmic membrane; c: capsule, w: cell wall; ms: mesossome structure; t: thylakoid membrane; em: external membrane; im: internal membrane. White arrows indicate Inclusion bodies.

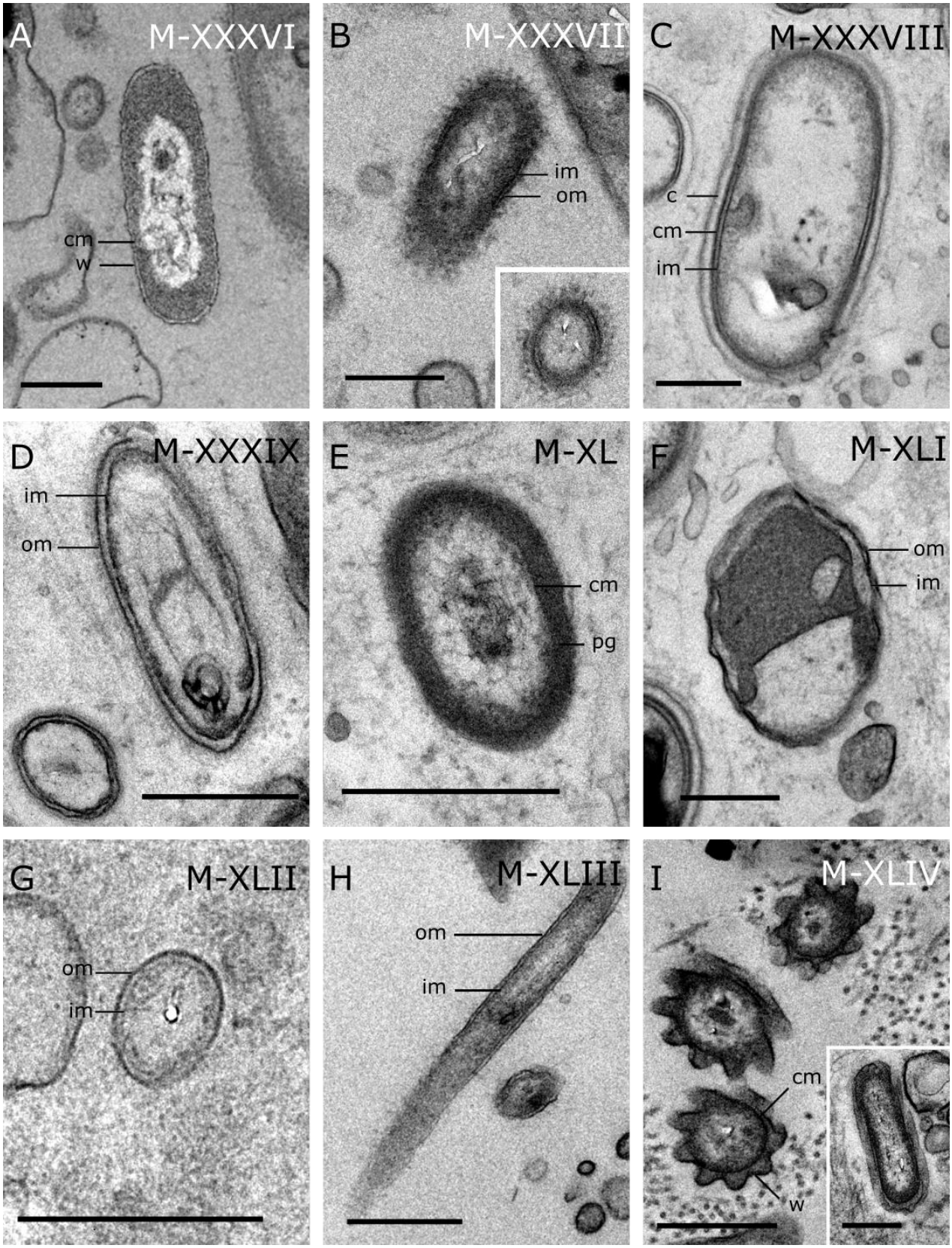

Figure A1.7 Prokaryote morphotypes associated with the RS sponges: (A-B) *Xestospongia testudinaria*, (C-F) *Hyrtios erectus*, (G) *Mycale* sp., (H-I) *Niphates rowi* in (A-H, I in detail) longitudinal section and (I; B & D in detail) transversal section. Scale bar= 500 nm. cm: cytoplasmic membrane; c: capsule, w: cell wall; ms: mesossome structure; t: thylakoid membrane; ca: carboxisome; om: outer membrane; im: internal membrane; pg: peptidoglycan.

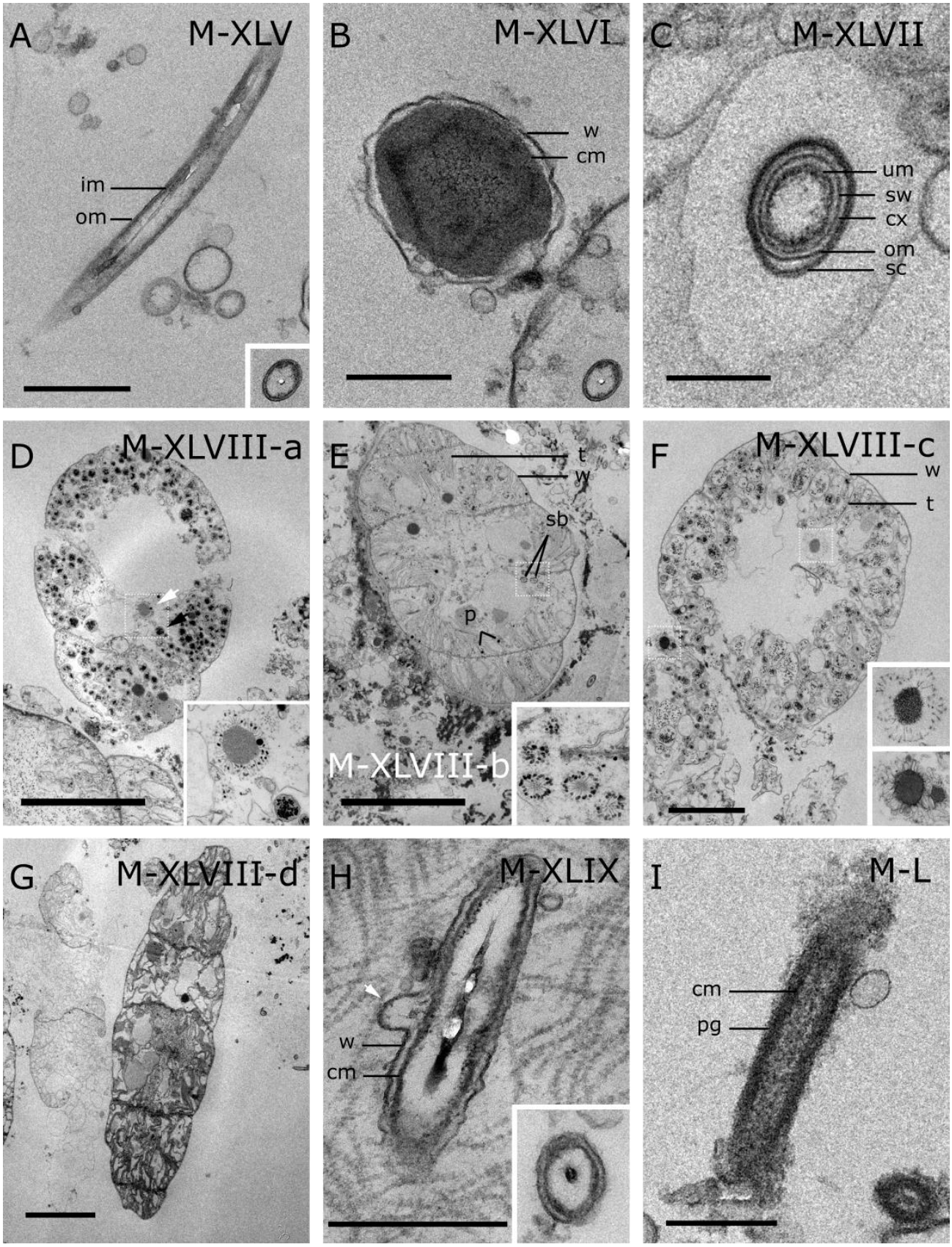

Figure A1.8 Prokaryote morphotypes associated with the RS sponges: (A-H) *Amphimedon ochracea*, (I) *Amphimedon* sp, in (A-E, G-I) longitudinal section and (F; A, H, I in detail) transversal section. Scale bar= 500 nm. cm: cytoplasmic membrane; w: cell wall; t: thylakoid membrane; om: outer membrane; im: internal membrane; bodies; sb: stellar sw: spore wall; cx: cortex; sc: spore coat; r: ribosome; pg: peptidoglycan.

Table A1.1 GBR and RS sponge-associate prokaryote morphotype characterization represented from the figures A1.3-8. The abundance was classified in high: more than 15 individuals; moderate: between 5-15 individual and low: less than 5 individual per sampling time (1h).

Prokaryote morphotype	Site	Associated sponge specie	Classification	Size range	Abundance	Additional comments
M-I	GBR	*Carteriospongia foliascens*	Ovoid-shaped Gram-negative coccus	700-800 nm long and 400-500 nm wide	High	
M-II	GBR	*Carteriospongia foliascens*	Ovoid-shaped Cyanobacteria	2-2.5 µm long, 1.5-1.7 µm wide	High	Presented evident photosynthetic thylakoid membranes present (3-4 layers), often peripheral and concentric. This morphotype was very abundant and broadly distributed across the mesohyle and often clustered arranged individualized by collagen fibrils bundles in areas with notable high concentration of vesicles and particulate organic matter and where other bacteria types are present.
M-III	GBR	*Carteriospongia foliascens*	Flagellate Gram-negative rod	3.8-4 µm long. 500-600 nm wide	Moderate	Present filamentous similar with flagellum.
M-IV	GBR	*Carteriospongia foliascens*	Gram-negative coccus	1.2-1.4 µm diameter	Low	

M-V	GBR	*Carteriospongia foliascens*	Ovoid-shaped Gram-positive coccus	320-340 nm long, 240-250 nm wide	Moderate	
M-VI	GBR	*Stylissa carteri*	Elongated Gram-negative rod	1.5-2 µm long, 200-300 nm wide	Moderate	
M-VII	GBR	*Stylissa carteri*	Ovoid-shaped Gram-negative coccus	425-450 nm long, 320-325 nm wide	Low	
M-VIII	GBR	*Stylissa carteri*	Gram-negative coccus/Cyanobacteria?	500-550 nm radius	Low	Resemble a cyanobacteria, although the electrodense core and presence of ribosomes prevents the thylakoid observation
M-IX	GBR	*Stylissa carteri*	Gram-positive vibrio	280-300 nm long, 125-150 nm wide	Moderate	High number of ribosomes in cytoplasm.
M-X	GBR	*Stylissa carteri*	Amorphous Cyanobacteria	600-700 nm long, 500-550 nm wide	Low	Present a pair of concentric thylakoid membranes.
M-XI	GBR	*Stylissa carteri*	Gram-negative coccus	400-420 nm radius	Low	

M-XII	GBR	*Xestospongia testudinaria*	Gram-negative rod	1.5 µm long, 500 nm wide	Low	A single individual was observed.
M-XIII	GBR	*Xestospongia testudinaria*	Square-shaped gram-positive coccobacilli	1.7 µm long, 700 nm wide	Low	A single individual was observed.
M-XIV	GBR	*Xestospongia testudinaria*	Ovoid-shaped Gram-positive coccus	700-850 nm long, 500-550 nm wide	High	
M-XV	GBR	*Xestospongia testudinaria*	Ovoid-shaped Gram-negative coccus	1-1.2 µm long, 600-650 nm wide	Low	
M-XVI	GBR	*Pipestela candelabra*	Bean-shaped Gram-negative vibrio	430-450 nm long 300 nm wide	Low	
M-XVII	GBR	*Pipestela candelabra*	Gram-negative rod	1-1.25 µm long, 500-560 nm wide	Low	
M-XVIII	GBR	*Lamellodyside a herbacea*	Filamentous cyanobacteria	5,5-6.5 µm wide 3-4,3 µm long	Low	Cyanobacteria with thylakoids radially arranged similar with *Annamia toxica* and *Oscillatoria spongeliae* also previously described *for L. herbacea*

M-XIX	GBR	*Cinachyrella schulzei*	Gram-negative rod	1.4-1.6 µm long, 400-500 nm wide	High	
M-XX	GBR	*Cinachyrella schulzei*	Gram-negative coccus / Archaea-like	700 nm long 500 nm wide	Low	The high presence of a thin pili/ hili suggests that it can be part of the Archaea domain
M-XXI	GBR	*Cinachyrella schulzei*	Gram-positive Rod	1.2-1.3 µm long, 500-550 nm wide	Moderate	This morphotype is commonly found in aggregations of 5-6 bacteria inside a capsule/ vacuole.
M-XXII	GBR	*Ianthella basta*	Ovoid-shaped Gram-positive coccus	900 nm- 1 µm long, 500-520 nm wide	Moderate	
M-XXIII	GBR	*Ianthella basta*	Ovoid-shaped gram negative	530-550 nm long, 350-360 n wide	Moderate	
M-XXIV	GBR	*Cymbastela marshae*	Rounded-shaped Cyanobacteria	3-3.5 µm long 2.2-2.7 µm wide	High	A single prokaryote morphotype dominated in Cymbastela

M-XXV	GBR	*Echinochalina isaaci*	Ovoid-shaped Gram-negative coccus	550-570 nm long, 450-460 nm wide	Moderate	
M-XXVI	GBR	*Echinochalina isaaci*	Gram-negative diplococci with long lateral pili	450-500 nm long 400-410 nm wide	High	The bacteria structure is Similar with the gammaproteobacteria morphotype like Proteus mirabilis. These bacteria was mostly observed forming spores.
M-XXVII	RS	*Carteriospongia foliascens*	Ovoid-shaped Cyanobacteria	1.7-2 µm long, 1.4-1.5 µm wide	High	Shows evident photosynthetic thylakoid membranes present (3-4 layers), often peripheral and concentric. Presents a thick and lobate cell wall. This type was observed broadly distributed across the mesohyle.
M-XXVIII	RS	*Carteriospongia foliascens*	Gram-negative rod	1-1.3 µm long, 300-600nm wide	High	Thick cell wall. Clear distinction and wide separation of internal and external cytoplasmic membrane.
M-XXIX	RS	*Stylissa carteri*	Gram-negative rod	1-1.2 µm long, 400-500 nm wide	Low	

M-XXX	RS	*Stylissa carteri*	Gram-negative coccus/Cyanobacteria?	500 nm radius	Moderate	This bacteria shape resembles cyanobacteria, besides present a thick capsule and apparent concentric ribosome orientation. Its dark core could potentially hide a possible thylakoid membrane.
M-XXXI	RS	*Stylissa carteri*	Gram-negative rod	About 1.25 µm long, 250-300 nm wide	Moderate	Similar with type VI, from the GBR S. carteri.
M-XXXII	RS	*Xestospongia testudinaria*	Gram-positive rod	2.3-2.5 µm long, 700-750 nm wide	Moderate	It was observed about 50 nm electrodense particles inside the cytoplasm.
M-XXXIII	RS	*Xestospongia testudinaria*	Gram-negative rod	2-2.2 µm long, 850-900 nm wide	High	This morphotype often presents invagination bodies peripherally arranged in the cytoplasm. It strongly resembles with M-XXXVIII from *H. erectus*, however this doesn't show invagination bodies.
M-XXXIV	RS	*Xestospongia testudinaria*	Ovoid-shaped Cyanobacteria	1.8-2 µm long, 1.2-1.3 µm wide	High	Presents 5 thick layers of peripheral concentric Thylakoid membranes. Slightly lobate cell wall and covered by a thin layer of peptidoglycan. This morphotype strongly resembles with the clade Candidatus *Synechococcus spongiarum.*
M-XXXV	RS	*Xestospongia testudinaria*	Triangular-shaped Gram-positive rod	2-2.1 µm long, 1 µm wide	High	

M-XXXVI	RS	*Xestospongia testudinaria*	Gram-negative rod	1.4-1.6 µm long, 500-550 nm wide	Moderate	Presents a slightly lobate cell wall and a distinct peripheral electrodense core in the cytoplasm.
M-XXXVII	RS	*Xestospongia testudinaria*	Gram-positive rod	800-950 nm long, 300-400 nm wide	Moderate	
M-XXXVIII	RS	*Hyrtios erectus*	Gram-negative-rod	1.9-2.1 µm long, 800 nm-1 µm wide	High	Very abundant and widely distributed across the sponge mesohyle.
M-XXXIX	RS	*Hyrtios erectus*	Gram-negative-rod	1-1.1 µm long, 390-410 nm wide	High	
M-XL	RS	*Hyrtios erectus*	Ovoid-shaped Gram-positive coccus	500-600 nm long, 420-450 nm wide	Moderate	This type presents a very thick external peptidoglycan layer
M-XLI	RS	*Hyrtios erectus*	Ovoid-shaped Gram-negative coccus	1-1.3 µm long, 750-850 nm wide	High	

M-XLII	RS	*Mycale sp*	Ovoid-shaped Gram-negative coccus	300-340 nm long, 200-225 nm wide	High	
M-XLIII	RS	*Niphates rowi*	Elongate Gram-negative Rod	2-2.3 µm long 200-220 nm wide	Low	
M-XLIV	RS	*Niphates rowi*	Star-cross section oriented-shaped rod bacteria	1.3-1.5 µm long, 450-550 nm wide	High	Rod bacteria characterized by a star-shaped cross section with 8/9 radial protrusions.
M-XLV	RS	*Amphimedon ochracea*	Elongate Gram-negative Rod	2.6-2.8 µm long, 160-180 nm wide	Low	
M-XLVI	RS	*Amphimedon ochracea*	Ovoid-shaped Gram-negative coccus	950 nm-1.5 µm long 800-850 nm wide	Low	

M-XLVII	RS	*Amphimedon ochracea*	Gram-negative spore	650-700 nm long 400-500 nm wide	Low	
M-XLVIII	RS	*Amphimedon ochracea*	Filamentous Cyanobacteria	7-9 µm wide.	High	Filamentous cyanobacteria with radial organized parallel thylakoids (t), dense bodies resembling polyphosphate granules (p) and stellar bodies (sb). In a few cyanobacteria, a Geminiviridae VLP composed of two spherical subunits are visible in the cytoplasm, thylakoid lumina or even inside vesicles (Fig). The microscopy section allowed the visualization of maximum 6 cells.
M-XLIX	RS	*Amphimedon ochracea*	Gram-negative rod	1-1.5 µm long, 250-350 nm wide	high	Often observed surrounding the filamentous cyanobacteria.
M-L	RS	*Amphimedon sp*	Gram-positive rod	1.3-1.5 µm long, 350-400 nm wide	Moderate	

APPENDIX 2

Figure A2.1 Sponge species where the VLPs were investigated. Red Sea sponge species: (a) Amphimedon ochracea, (b) Xestospongia testudinaria, (c) Crella cyathophora, (d) Hyrtios erectus, (e) Mycale sp. GBR and Red Sea sponge species: (f) Stylissa carteri, (g) Carteriospongia foliascens. GBR sponge species: (h) Echinochalina isaaci, (i) Cymbastella marshae, (j), Cinachyrella schulzei, (k), Lamellodysidea herbacea, (l), Pipestela candelabra, (m) Xestospongia sp.. Scale bar = 10 cm. Photos by Cecília Pascelli.

The concept of Virus-like particle (VLP).

The terminology virus-like particle (VLP) used in chapters 2 and 3 is in accordance with the ecological concept defined by Forterre and colleagues (Forterre et al., 2013), where VLP is a general term that a priori covers true virions, gene transfer agents (GTAs), and membrane vesicles (MVs). This terminology was preferentially used to encompass the distinct particles that morphologically resemble viruses, considering that microscopy images may not distinguish between true virion or resembling non-virion particles. Nevertheless, it is important to consider the term VLP has been previously used to define non-infectious viral resembling molecules, composed of an empty structural capsid (without genetic material) (Zeltins, 2013).

Table A2.1 GBR and RS sponge-associate VLP morphotype characterization represented in the figures 2.1 – 2.5. The VLP abundance was classified in **h**igh: more than 15 **individuals**; moderate: between 5-15 individual and **l**ow: less than 5 individual per sampling time (1h).

VLP Morphotype	Site	Associated sponge specie	Classification	Abundance	Size range	Details
M-I	GBR	*Carteriospongia foliascens*	Tailed (short) non-enveloped, spherical-shaped VLP (icosahedral symmetry), with electron-dense core.	Low	210 nm in diameter, core with 194 nm in diameter, tail with 25 nm long and wide.	Observed in the cellular lumen of sponge archaeocytes. The icosahedral structure and the short tail are characteristic of the *Podoviridae*.
M-II	GBR	*Xestospongia* sp.	Tailed (short), non-enveloped VLP, with icosahedral symmetry.	Low	Capsid with 52 nm diameter, core with 40 nm in diameter. Tail with 48/21 nm long/wide.	Observed in sponge mucus.
M-III	GBR	*Echinochalina isaaci*	Tailed (short), non-enveloped VLP, with icosahedral symmetry.	Low	Head measuring 50 nm in diameter. Tail measuring 14 nm long, 11 nm wide.	Observed in sponge mucus.
M-IV	RS	*Stylissa carteri*	Tailed (short), non-enveloped VLP, with icosahedral symmetry.	Low	Capsid with 75-78 nm diameter and tail with 24-25 nm long/wide.	Observed in sponge mucus and characteristic of Podoviridae family
M-V	GBR	*Cinachyrella schulzei*	Non-enveloped tailed bacteriophage	Moderate	150 nm in total length, with symmetric hexagonal head measuring 55 nm in	Observed in sponge mucus.

			with symmetric icosahedral head.		diameter and an elongated tail measuring 95 nm in length and 10 nm in width.	
M-VI	GBR	*Echinochalina isaaci*	Non-enveloped tailed bacteriophage with symmetric icosahedral head.	Low	260 nm in total length, with symmetric hexagonal head measuring 90 nm in diameter and an elongated tail measuring 160 nm in length and 1nm in width.	Observed in sponge mucus.
M-VII	GBR	*Echinochalina isaaci*	Filamentous VLP with electron-dense core.	Low	200 nm in total length, with elongated head measuring 95 nm in length and 70 nm in width and an elongated tail measuring 105 nm in length and 22.5 nm in width.	Observed in sponge mucus.
M-VIII	RS	*Stylissa carteri*	Non-enveloped T4-like bacteriophage.	Low	283 nm in total length, with elongated hexagonal head measuring 128 nm in length and 84 nm in width and tail measuring 155 nm in length and 26,6 nm in width.	Observed in sponge mucus and strong resemblance to Myoviridae.
M-IX	RS	*Amphimedon ochracea*	Non-enveloped tailed bacteriophage with symmetric icosahedral head.	Low	142 nm long, head measuring 59.8 nm in diameter with electron-dense core with 36.4 nm in diameter. Tail measuring 82 nm long, 12 nm wide.	Observed in the sponge mucus. The VLP features are characteristic of Siphoviridae.
M-X	GBR	*Carteriospongia foliascens*	Non-enveloped, icosahedral symmetry VLP, with electron-dense core.	Low	150 nm in diameter; core with 122 nm in diameter.	Observed in sponge mesohyl.

M-XI	GBR	*Carteriospongia foliascens*	Non-enveloped, icosahedral symmetry VLP, with electron-dense core.	Moderate	140-150 nm in diameter, core with 90-100 nm in diameter.	Observed in sponge mesohyl and the cellular lumen of sponge archaeocytes.
M-XII	GBR	*Carteriospongia foliascens*	Non-enveloped VLP with spherical/icosahedral symmetry and electron-dense core.	Low	103 nm in diameter, core with 81 nm in diameter.	Observed in sponge mucus.
M-XIII	GBR	*Carteriospongia foliascens*	Icosahedral symmetry VLP, with electron-dense core.	Low	56 nm in diameter, core with 41 nm in diameter.	Observed in sponge mucus.
M-XIV	GBR	*Stylissa carteri*	Enveloped VLP with spherical/icosahedral symmetry.	High	90-100 nm of diameter.	Purified from sponge tissue via density gradient ultracentrifugation.
M-XV	GBR	*Stylissa carteri*	Icosahedral symmetry VLP, with electron-dense core.	Moderate	89 +- 4 nm in diameter, core with 74 nm +- 7 nm in diameter.	Observed in sponge mucus.
M-XVI	GBR	*Xestospongia* sp.	Non-enveloped, icosahedral symmetry VLP, with electron-dense core.	Low	70 nm in diameter, core with 37 nm in diameter.	Purified from sponge tissue via density gradient ultracentrifugation.

M-XVII	GBR	*Pipestela candelabra*	Enveloped VLP with spherical/icosahedral symmetry.	Low	180-205 nm in diameter.	Purified from sponge tissue via density gradient ultracentrifugation.
M-XVIII	GBR	*Pipestela candelabra*	Non-enveloped VLP with spherical/icosahedral symmetry and electron-dense core.	Low	138 nm in diameter, core with 35 nm in diameter.	Purified from sponge tissue via density gradient ultracentrifugation.
M-XIX	GBR	*Pipestela candelabra*	Non-enveloped VLP with spherical/icosahedral symmetry and electron-dense core.	Moderate	180-200 nm in diameter, core with 120-124 nm in diameter.	Observed within gram-negative bacteria.
M-XX	GBR	*Pipestela candelabra*	Non-enveloped VLP with spherical/icosahedral symmetry and electron-dense core.	Low	100 nm in diameter, core with 69 nm in diameter.	Observed in sponge mucus.
M-XXI	GBR	*Lamellodysidea herbacea*	Geminate VLP.	Low	135 nm in diameter. Comprise 2 quasi-isometric particles with 72 nm in diameter each with a dese core with 57 nm in diameter.	Observed in sponge mucus.
M-XXII	GBR	*Lamellodysidea herbacea*	Non-enveloped VLP with	Low	118 nm in diameter, core with 91 nm in diameter.	Observed in sponge mucus.

			spherical/icosahedral symmetry and electron-dense core.			
M-XXIII	GBR	*Lamellodysidea herbacea*	Non-enveloped VLP with spherical symmetry and electron-dense core.	Low	111 nm in diameter, core with 81 nm in diameter.	Observed in sponge mucus.
M-XXIV	GBR	*Cinachyrella schulzei*	Non-enveloped VLP with spherical/icosahedral symmetry and electron-dense core.	High	70-85 nm in diameter, core with 35-45 nm in diameter.	Purified from sponge tissue via density gradient ultracentrifugation.
M-XXV	GBR	*Cinachyrella schulzei*	Non-enveloped electron-dense VLP with icosahedral symmetry.	Low	135 nm in diameter, core with 95 nm in diameter.	Observed in sponge mucus.
M-XXVI	GBR	*Cymbastella marshae*	Non-enveloped, icosahedral symmetry VLP, with electron-dense core.	Low	74 nm in diameter, core with 42 nm in diameter.	Observed in sponge mucus.
M-XXVII	RS	*Carteriospongia foliascens*	Non-enveloped electron-dense VLP with icosahedral symmetry.	Moderate	60-65 nm in diameter. core with 32-35 nm in diameter.	Observed within Gram-negative bacteria.

M-XXVIII	RS	*Carteriospongia foliascens*	Non-enveloped VLP with icosahedral symmetry and electron-dense core.	Moderate	100-110 nm in diameter.	Observed in sponge mesohyl and inside a lysed cyanobacterial cell.
M-XXIX	RS	*Stylissa carteri*	Non-enveloped VLP with spherical/icosahedral symmetry and electron-dense core.	Low	81 nm in diameter, core of 56 nm diameter.	Observed in sponge mucus.
M-XXX	RS	*Stylissa carteri*	Non-enveloped VLP with spherical/icosahedral symmetry.	High	163-175 nm in diameter.	Observed in sponge mucus.
M-XXXI	RS	*Stylissa carteri*	Non-enveloped VLP with icosahedral symmetry.	Low	60 nm in diameter, core of 42 nm diameter.	Observed in sponge mucus.
M-XXXII	RS	*Xestospongia testudinaria*	Non-enveloped VLP with icosahedral symmetry and electron-dense core.	Moderate	140-150 nm in diameter, core of 120-125 nm diameter.	Observed in the sponge mesohyl.
M-XXXIII	RS	*Hyrtios erectus*	Non-enveloped VLP with icosahedral symmetry and electron-dense core.	Low	85 nm in diameter, core with 53 nm in diameter.	Single VLP observed inside sponge cell.

M-XXXIV	RS	*Hyrtios erectus*	Enveloped VLP with icosahedral symmetry and electron-dense core.	Moderate	110-128 nm in diameter, ovoid-shaped core with 50-80 nm in diameter.	Observed within vacuole in the sponge mesohyle matrix and sitting on top of the sponge cell.
M-XXXV	RS	*Mycale* sp.	Non-enveloped VLP with icosahedral symmetry and electron-dense core.	Moderate	71-85 nm in diameter, core with 54-70 nm in diameter.	Observed in sponge mucus.
M-XXXVI	GBR	*Carteriospongia foliascens*	Ovoid-shaped VLP with electron-dense core.	Low	118 nm long, 85 nm wide, core 82 nm long, 59 nm wide.	Observed in sponge mucus.
M-XXXVII	GBR	*Xestospongia* sp.	Rod-shaped Filamentous VLP	High	120-130 nm long, 18 nm wide.	Purified from sponge tissue via density gradient ultracentrifugation.
M-XXXVIII	GBR	*Xestospongia* sp.	Rod-shaped Filamentous VLP	Low	171 nm long, 28 nm wide. Core with157 nm long, 23 nm wide.	Observed in sponge mucus.
M-XXXIX	GBR	*Cinachyrella schulzei*	Filamentous VLP with electron-dense core.	Low	400 nm in length and 25 nm in width. With an electrodense core measuring 7.5 nm in diameter.	Observed in sponge mucus.
M-XL	RS	*Carteriospongia foliascens*	Filamentous VLP, non-electron-dense core.	High	100-130 nm long, 50-60 nm wide	Observed sitting on top of the Cyanobacteria and in the sponge mesohyl.

M-XLI	RS	*Stylissa carteri*	Filamentous VLP with electron-translucent core.	Low	520-600 nm long 12-15 nm wide.	Observed in sponge mucus.
M-XLII	RS	*Stylissa carteri*	Rod-shaped filamentous VLP with electron-translucent core.	Low	230 nm long, 19 nm wide.	Observed in sponge mucus.
M-XLIII	RS	*Xestospongia testudinaria*	Filamentous VLP with electron-translucent core.	High	340-1300 nm long, 15-30 nm wide.	Observed in sponge mesohyl and in sponge archaeocytes.
M-XLIV	RS	*Crella cyathophora*	Filamentous VLP.	Moderate	150-154 nm long, 22-25 nm wide.	Observed in the sponge mucus. This VLP tube-like structure resembles Paramyxovridae morphology.
M-XLV	RS	*Crella cyathophora*	Non-enveloped VLP with geminate icosahedral capsid and an electron-dense core.	Low	221 nm long, formed of two hexagonally symmetric portions with 110 nm in diameter. Core measuring 83-90 nm in diameter.	Observed inside a vacuole in the sponge mesohyl.
M-XLVI	GBR	*Lamellodysidea herbacea*	Geminate VLP.	Low	135 nm in diameter. Comprise 2 quasi-isometric particles with 72 nm in diameter each with a dese core with 57 nm in diameter.	Observed in sponge mucus.

M-XLVII	RS	*Amphimedon ochracea*	Geminate VLP.	High	81-95 nm long, 37-48 nm wide. Comprise 2 quasi-isometric particles with 34-45 nm long each.	Observed in the sponge mucus as well as in association with filamentous Cyanobacteria. VLP was observed inside cell vacuoles, between thylakoid membranes and around stellar bodies.
M-XLVIII	RS	*Crella cyathophora*	Enveloped brick-shaped VLP with electron-dense lateral bodies.	Low	Envelope 230-252 nm in diameter, core 169-178 nm in diameter.	Observed in the sponge mesohyl. This VLP was characteristic of the Poxviridae morphology.
M-XLIX	GBR	*Carteriospongia foliascens*	Beaded filamentous VLP.	Low	340 nm long, with each bead measuring 30-35 nm in diameter.	Observed in sponge mesohyl.
M-L	RS	*Hyrtios erectus*	Beaded filamentous VLP.	Moderate	80-350 nm long. 15-23 nm wide. Composed of 2-8 aligned beads with 36-42 nm in longest diameter.	Observed inside vacuole of a sponge archaeocyte and in the sponge mesohyl as either a free VLP or attached to extracellular vacuole membranes.

APPENDIX 3

In order to understand how specific sponge features structure the viral communities in sponges, Principal Coordinate Analysis (PCoA) was performed at the sample level over the Hellinger-transformed data and fitted variables describing sponge host features were identified. The variables (i.e. sponge features) tested were: 1-microbial symbiont strategy, classified as high microbial abundance (HMA) or low microbial abundance (LMA) sponge; 2-host nutritional mode, classified by the presence or absence of photosymbionts and 3- sponge morphology, classified as massive, cup-like, erect and encrusting (Table A3.1). PCoA was performed using the function cmdscale from the stats package in R, while the fitting of sponge features to this ordination was done using the envfit function from the vegan library. To support these analyses, permutational multivariate analysis of variance was performed using the R package mvabund.

Fitting of sponge features to the PCoA ordination revealed that all tested features were able to explain variability among samples, although to different extents (Table A3.2). Microbial abundance category and sponge morphology are the best predictors of viral community composition, accounting for 40% ($p<0.001$) and 47% ($p<0.001$) of the variability in the data, respectively. The presence of photosymbionts is also a good predictor of viral composition, although to a lesser extent ($R2 = 0.125$, $p = 0.023$). These results provide support for our conclusion that sponge-viral community are primarily driven by the associated microbial community, responding to both microbial abundance and composition. Likewise, the correlation between the viral community and sponge morphology may reflect the host-symbiont association, as microbial symbiont composition has been shown to vary with sponge morphology (Neves & Omena, 2003) . Additionally, morphology can influence the pumping rate in sponges, and although a more detailed study describing the mechanisms of selective filtration in sponges is still required, this could in turn affect the composition of microbial/viral communities within them.

Table A3.1 Summary of sponge features classified according to: i) microbial symbiont strategy as high microbial abundancy (HMA) or low microbial abundancy (LMA) sponge; ii) host nutritional mode, classified by the presence or absence of photosymbionts and iii) sponge morphology, classified as massive, cup-like, erect and encrusting. The sponge morphology was classified according Schoenberg and Fromont (2014).

Host species	**# replicates**	**Collection site**	**Hosts Photosymbionts**	**Microbial Abundance**	**Morphotype***	**References**
Callyspongia sp.	3	Orpheus Island, GBR	Yes	LMA	Erect	Thomas et al 2016; Moitinho-Silva et al 2017
Carteriospongia foliascens	3	Orpheus Island, GBR	Yes	HMA	Cup-like	Luter et al 2015
Cinachyrella schulzei	3	Orpheus Island, GBR	No	HMA	Massive	Thomas et al 2016
Cymbastela marshae	3	Orpheus Island, GBR	Yes	HMA	Cup-like	Thomas et al 2016
Echinochalina isaaci	3	Orpheus Island, GBR	na	na	Erect	
Ianthella basta	3	Orpheus Island, GBR	No	LMA	Erect	Luter et al 2010
Lamellodysidea herbacea	3	Orpheus Island, GBR	Yes	LMA	Encrusting	Flatt et al 2015
Pipestela candelabra	3	Orpheus Island, GBR	na	na	Erect	
Stylissa carteri	2	Orpheus Island, GBR	No	LMA	Erect	Moitinho-Silva et al 2017; Giles et al 2012
Amphimedon ochracea	3	Al Fahal Reef, Red Sea	Yes	LMA	Erect	Radwan et al 2009
Carteriospongia foliascens	3	Al Fahal Reef, Red Sea	Yes	HMA	Cup-like	Gao et al 2015
Crella cyathophora	3	Al Fahal Reef, Red Sea	Yes	LMA	Massive	Gao et al 2015; Giles et al 2012
Hyrtios erectus	2	Al Fahal Reef, Red Sea	No	HMA	Erect	Lee et al., 2011
Mycale sp.	3	Al Fahal Reef, Red Sea	na	na	Encrusting	
Niphates rowi	2	Al Fahal Reef, Red Sea	na	na	Encrusting	
Xestospongia testudinaria	2	Al Fahal Reef, Red Sea	Yes	HMA	Cup-like	Ryu et al 2016; Thomas et al 2016

Table A3.2 Fitting of sponge features to PCoA ordination classified according: i) microbial symbiont strategy as high microbial abundancy (HMA) or low microbial abundancy (LMA) sponge; ii) host nutritional mode, classified by the presence or absence of photosymbionts and iii) sponge morphology, classified as massive, cup-like, erect and encrusting, according Table A.3.1.

Sponge features	Classification	Goodness of fit		Centroid	
		r2 Pr(>r)	p-value	Dim 1	Dim 2
Microbial symbiosis strategy	HMA	0.402	0.001	0.1183	0.0239
	LMA			-0.0852	-0.0186
Host nutritional mode	Photosymbionts present	0.125	0.023	0.0330	-0.0308
	No photosymbionts present			-0.0313	0.0776
Sponge morphology	Massive	0.37	0.001	0.0981	0.0773
	Cup-like			0.1393	0.0112
	Erect			-0.0569	0.0192
	Encrusting			-0.0602	-0.0775

APPENDIX 4

Considering that the marker evaluation identified an average of 1.3% of contigs generated from the thermal-stress experiment containing cellular marker matches, a filtration step was implemented in order to evaluate the inferences of the cellular contamination on the viral community. During this step the major cellular contaminant was identified (*Marinomonas* sp.) and all contigs mapping to this group were removed. Comparative analyses were applied between the least contaminated samples and the most contaminated samples using marker genes and with *Marinomonas* sp. contigs, with and without the filtering step, checking for variations in gene prediction (Table 4A.1) and contig assembly (Fig. 4A.1).

Table A4.1 Summary of assembly statistics evaluation of virome datasets with and without a contigs filtration step. This table shows a subsample of the thermal stress virome dataset, representing the three samples highest contaminated with marker genes (H), highest contaminated with Marinomonas sp. assembled contigs (M) and less contaminated with marker genes (L) samples.

Contigs filtration	Contamination level	Samples	N50	# raw reeds	# contigs	Longest contig
Non filtrated	H	**E1_T0_1-1_43**	398	4041947	6125	17212
	H	**E1_T0_1-2_39**	611	4736967	6041	218069
	H	**E1_T72_1-4_17**	478	10604377	18388	27146
	M	**E1_T72_1-1_7**	1046	2066936	5219	50164
	M	**E1_T72_1-4_24**	540	3367742	8288	17034
	M	**E1_T72_3-2_4**	466	5034752	8462	12238
	L	**E2_T0_1-4_D64**	583	5994626	23637	70431
	L	**E2_T3W_3-2_D24**	566	4512308	19013	76225
	L	**SW_E2_T0_1-1**	939	3734748	16288	102801
Filtrated	H	**E1_T0_1-1_43**	386	3928205	5328	8354
	H	**E1_T0_1-2_39**	553	4333806	7133	35069
	H	**E1_T72_1-4_17**	464	10279047	18367	22905
	M	**E1_T72_1-1_7**	743	3659869	5806	15912
	M	**E1_T72_1-4_24**	491	3222783	8087	16052
	M	**E1_T72_3-2_4**	352	4993361	1789	17055
	L	**E2_T0_1-4_D64**	575	5851611	22603	70427
	L	**E2_T3W_3-2_D24**	568	4425918	18823	84056
	L	**SW_E2_T0_1-1**	621	3532864	17592	85266

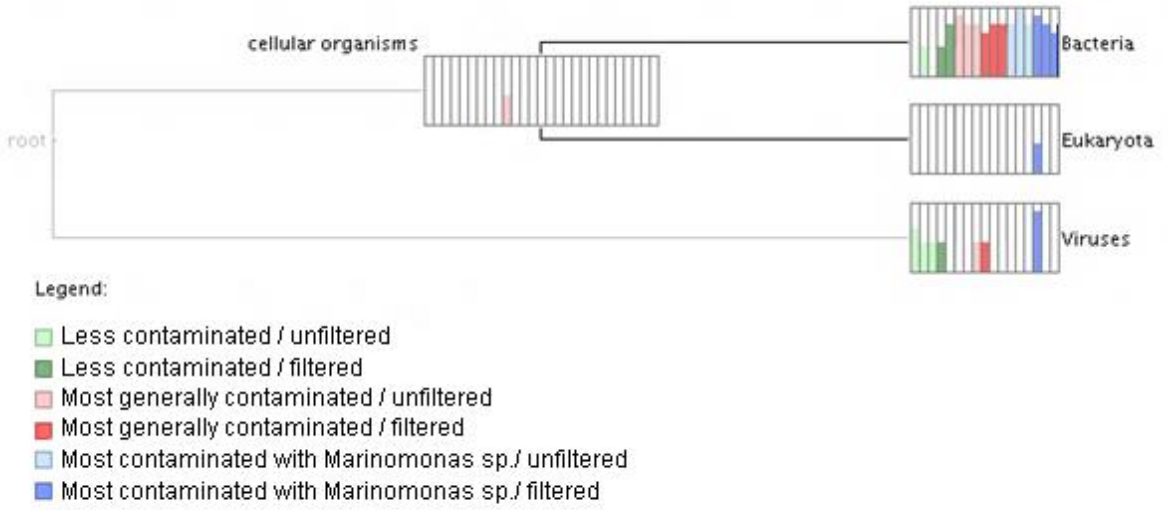

Figure A4.1 Gene-centric comparison of the taxonomic composition of cellular marker genes based on two reference databases of phylogenetic markers, a ribosomal RNA database (SILVA, release 115) (Quast et al., 2013) and an in-house database of universally conserved proteins found in EggNOG 4.0 (Powell et al., 2014). Output is based on BLAST analysis of MetaGeneAnnotator predicted genes using parameters defined in Laffy *et al.*, 2016. The green colours represent the less contaminated samples, the red colours represent the highest contaminated with marker genes and the blue colours represent the highest contaminated samples with *Marinomonas* sp., while the light colours represent Marinomonas unfiltered samples and the darker colours represent the samples which contigs assigned to *Marinomonas* sp. were removed.